

Christian Schlosser reviews

Dear Christian Schlosser and Editor,

The reviewers are thanked for their insightful comments; these have helped to improve the manuscript considerably. Please see our detailed answers to the referees' comments below. Line numbers refer to the new version.

All the answers are attached as a supplementary file.

Best regards,

Tonnard et al.,

Abstract

Please, note that we added François Lacan as a co-author.

Line 29ff: Air-sea interactions responsible for deep winter convection – Did you mean special cooling!

→ We have changed the sentence "Air-sea interactions were suspected to be responsible for the increase in DFe concentrations within subsurface waters of the Irminger Sea due to deep convection occurring the previous winter..." by "Enhanced air-sea interactions were suspected to be responsible for the increase in DFe concentrations within subsurface waters of the Irminger Sea due to deep convection occurring the previous winter..."

Introduction

Page 2 Line 4: I would also include oxygen, the whole ventilation and redox state of the deep ocean depends on deep water formation in the North Atlantic and Weddell Sea

→ We removed this sentence.

Page 2 Line 6: "stores" is maybe the wrong term; I would rather go with "accumulates"

→ We have modified this part based on your comment and Reviewer#2 comment.

Page 2 Lines 2-33 Page 3 Lines 1-25: The North Atlantic Ocean is known for its pronounced spring phytoplankton blooms (Henson et al., 2009; Longhurst, 2007). Phytoplankton blooms induce the capture of aqueous carbon dioxide through photosynthesis, and conversion into particulate organic carbon (POC). This POC is then exported into deeper waters through the production of sinking biogenic particles and ocean currents. Via these processes, and in conjunction with the physical carbon pump, the North Atlantic Ocean is the largest oceanic sink of anthropogenic CO₂ (Pérez et al., 2013), despite covering only 15% of global ocean area (Humphreys et al., 2016; Sabine et al., 2004) and is therefore crucial for Earth's climate.

Indeed, phytoplankton must obtain, besides light and inorganic carbon, chemical forms of essential elements, termed nutrients to be able of photosynthesis. Indeed, Fe is a key element for a number of metabolic processes (e.g. Morel et al., 2008). The availability of these nutrients in the upper ocean frequently limits the activity and abundance of these organisms together with light conditions

Formatted: Normal

Formatted: French (France)

Formatted: Normal

Formatted: Normal

Formatted: List Paragraph, Bulleted + Level: 1 +
Aligned at: 0.63 cm + Indent at: 1.27 cm

Deleted: <#>¶

Deleted: <#>¶

Formatted: List Paragraph, Bulleted + Level: 1 +
Aligned at: 0.63 cm + Indent at: 1.27 cm

(Moore et al., 2013). In particular, winter nutrient reserves in surface waters set an upper limit for biomass accumulation during the annual spring-to-summer bloom and will influence the duration of the bloom (Follows and Dutkiewicz, 2001; Henson et al., 2009; Moore et al., 2013; 2008). Hence, nutrient depletion due to biological consumption is considered as a major factor in the decline of blooms (Harrison et al., 2013).

The extensive studies conducted in the North Atlantic Ocean through the Continuous Plankton Recorder (CPR) have highlighted the relationship between the strength of the westerlies and the displacement of the subarctic front (SAF), (which corresponds to the North Atlantic Oscillation (NAO) index (Bersch et al., 2007)), and the phytoplankton dynamics of the central North Atlantic Ocean (Barton et al., 2003). Therefore, the SAF not only delineates the subtropical gyre from the subpolar gyre but also two distinct systems in which phytoplankton limitations are controlled by different factors. In the North Atlantic Ocean, spring phytoplankton growth is largely light-limited within the subpolar gyre. Light levels are primarily set by freeze-thaw cycles of sea ice and the high-latitude extremes in the solar cycle (Longhurst, 2007). Simultaneously, intense winter mixing supplies surface waters with high concentrations of nutrients. In contrast, within the subtropical gyre, the spring phytoplankton growth is less impacted by the light regime and has been shown to be N and P-co-limited (e.g. Harrison et al., 2013; Moore et al., 2008). This is principally driven by Ekman downwelling with an associated export of nutrients out of the euphotic zone (Oschlies, 2002). Thus, depending on the location of the SAF, phytoplankton communities from the central North Atlantic Ocean will be primarily light or nutrient limited.

However, once the water column stratifies and phytoplankton are released from light limitation, seasonal high-nutrient, low chlorophyll (HNLC) conditions were reported at the transition zone between the gyres, especially in the Irminger Sea and Iceland Basin (Sanders et al., 2005). In these HNLC zones, trace metals are most likely limiting the biological carbon pump. Among all the trace metals, Fe has been recognized as the prime limiting element of North Atlantic primary productivity (e.g. Boyd et al., 2000; Martin et al., 1994; 1988; 1990). However, the phytoplankton community has been shown to become N and/or Fe-(co)-limited in the Iceland Basin and the Irminger Sea (e.g. Nielsdóttir et al., 2009; Painter et al., 2014; Sanders et al., 2005).

In the North Atlantic Ocean, dissolved Fe (DFe) is delivered through multiple pathways such as ice-melting (e.g. Klunder et al., 2012; Tovar-Sanchez et al., 2010), atmospheric inputs (Achterberg et al., 2018; Baker et al., 2013; Shelley et al., 2015; 2017), coastal runoff (Rijkenberg et al., 2014), sediment inputs (Hatta et al., 2015), hydrothermal inputs (Achterberg et al., 2018; Conway and John, 2014) and by water mass circulation (vertical and lateral advections, e.g. Laes et al., 2003). Dissolved Fe can be regenerated through biological recycling (microbial loop, zooplankton grazing, e.g. Boyd et al., 2010; Sarthou et al., 2008). Iron is removed from the dissolved phase by biological uptake, export and scavenging along the water column and precipitation (itself a function of salinity, pH of seawater and ligand concentrations).

Although many studies investigated the distribution of DFe in the North Atlantic Ocean, much of this work was restricted to the upper layers (< 1000 m depth) or to one basin. Therefore, uncertainties

Formatted: English (Australia)

Formatted: English (Australia)

Field Code Changed

Field Code Changed

remain on the large-scale distribution of DFe in the North Atlantic Ocean and more specifically within the subpolar gyre where few studies have been undertaken, and even fewer in the Labrador Sea. In this biogeochemically important area, high-resolution studies are still lacking for understanding the processes influencing the cycle of DFe.

The aim of this paper is to elucidate the sources and sinks of DFe, its distribution regarding water masses and assesses the links with biological activity along the GEOVIDE (GEOTRACES-GA01) transect. This transect spanned several biogeochemical provinces including the West European Basin, the Iceland Basin, the Irminger and the Labrador Seas (Fig. 1). In doing so we hope to constrain the potential long-range transport of DFe through the Deep Western Boundary Current (DWBC) via the investigation of the local processes effecting the DFe concentrations within the three main water masses that constitute it: Iceland Scotland Overflow Water (ISOW), Denmark Strait Overflow Water (DSOW) and Labrador Sea Water (LSW).

MM

Page 3 Line 11: Remove “the” from “. . .aboard the N/O. . .”

→ We have modified this part as suggested

Page 3 Line 24ff: Two different filtration techniques were applied, 0.2 and 0.45 μm . Did you test that both approaches deliver the same result? I know water is restricted and sometimes sampling techniques need to be changed, however, please indicate why you did this and that swapping between both filtration techniques did not cause problems (offset, etc.)!

Deleted: ¶

→ We have added precision as suggested. Please note that there was no station where both filtration techniques were used.

Formatted: List Paragraph, Bulleted + Level: 1 + Aligned at: 0.63 cm + Indent at: 1.27 cm

Page 4 Lines 10-14: Samples were either taken from the filtrate of particulate samples (collected on polyethersulfone filters, 0.45 μm supor[®], see Gourain et al., this issue) or after filtration using 0.2 μm filter cartridges (Sartorius SARTOBRAN[®] 300) due to water budget restriction (Table 1). No significant difference was observed between DFe values filtered through 0.2 μm and 0.45 μm filters (p-value > 0.2, Wilcoxon test) for most stations. Differences were only observed between profiles of stations 11 and 13 and, 13 and 15.

Page 3 Line 26: exchange “on” by “using”. By the way, did you apply pressured air to the Go-Flo’s to filter your samples. If so, please state that!

Deleted: ¶

→ We have added precision as suggested

Page 3 Line 30: You did you use 0.2% HCl to acidify your water, or? It reads like that! I assume you used concentrated HCl and the dilution with the seawater was than 0.2%.

Deleted: ¶

→ We have modified the text for clarification

Page 4 Lines 17-18: Samples were then acidified to ~ pH 1.7 with HCl (Ultrapur[®] Merck, 2 % v/v) under a class 100 laminar flow hood inside the clean container.

Page 4 Line 2: The first sentence does not fit here; first you preconcentrated your sample using a SeaFAST system. Then the eluent was introduced via a PFA nebulizer and cyclonic spray chamber into your instrument (please indicate what kind of instrument you used, Element?). Please clarify!

→ We have modified this part as suggested

Page 4 Lines 27-30: Seawater samples were preconcentrated using a SeaFAST-pico™ (ESI, Elemental Scientific, USA) and the eluent was directly introduced via a PFA-ST nebulizer and a cyclonic spray chamber in an Element XR Sector Field Inductively Coupled Plasma Mass Spectrometry (Element XR SF-ICP-MS, Thermo Fisher Scientific Inc., Omaha, NE), following the protocol of Lagerström et al. (2013).

Note that we have also changed part of the reagent text, as we found out there were mistakes.

Page 4 Lines 31-33, Page 5 Lines 1-4: High-purity grade solutions and water (Milli-Q) were used to prepare the following reagents: the acetic acid-ammonium acetate buffer (CH_3COO^- and NH_4^+) was made of 140 mL acetic acid (> 99% NORMATOM® - VWR chemicals) and ammonium hydroxide (25%, Merck Suprapur®) in 500 mL PTFE bottles and was adjusted to pH 6.0 ± 0.2 for the on-line pH adjustment of the samples. The eluent was made of 1.4 M nitric acid (HNO_3 , Merck Ultrapur®) in Milli-Q water by a 10-fold dilution and spiked with $1 \mu\text{g L}^{-1}$ ^{115}In (SCP Science calibration standards) to allow for drift correction. Autosampler and column rinsing solutions were made of HNO_3 2.5% (v/v) (Merck Suprapur®) in Milli-Q water. The carrier solution driven by the syringe pumps to move the sample and buffer through the flow injection system was made in the same way.

Page 4 Line 11: gravimetrically is perhaps not the right word, you used a balance, right!

→ We did not changed our sentence here since gravimetrically means by weighting the standards.

Page 4 Line 13ff: please include "...in-house standard seawater..", was this seawater acidified in the same way?

→ We have modified this part as suggested and added at the end of section 2.1 the precision on the sampling and acidification methods of the in-house standard seawater.

In section 2.1:

Page 4 lines 20-25: Large volumes of seawater sample (referred hereafter as the in-house standard seawater) were also collected using a towed fish at around 2-3 m deep and filtered in-line inside a clean container through a $0.2 \mu\text{m}$ pore size filter capsule (Sartorius SARTOBAN® 300) and was stored unacidified in 20-30 L LDPE carboys (Nalgene™). All the carboys were cleaned following the guidelines of the GEOTRACES Cookbook (Cutter et al., 2017). This in-house standard seawater was used for calibration on the SeaFAST-pico™ - SF-ICP-MS (see Section 2.2) and was acidified to \sim pH 1.7 with HCl (Ultrapur® Merck, 2 % v/v) at least 24h prior to analysis.

Page 4 Line 16ff: Please include the analytical precision, the blank, detection limit of the analytical method. And how many samples did you run normally and how much samples were between each calibration curve? Please also include, how you calculated your errors, standard deviation of the three slopes? Or just the s.d. of the Element?

→ We have added precision as suggested.

Page 5 Lines 11-20: Data were blank-corrected by subtracting an average acidified Milli-Q blank that was pre-concentrated on the SeaFAST-pico™ in the same way as the samples and seawater

Deleted: ¶

Formatted: List Paragraph, Bulleted + Level: 1 + Aligned at: 0.63 cm + Indent at: 1.27 cm

Moved down [1]: And how many samples did you run normally and how much samples were between each calibration curve?

Formatted: Normal, No bullets or numbering

Deleted: ¶

Moved (insertion) [1]

Deleted: ¶

Formatted: List Paragraph, Bulleted + Level: 1 + Aligned at: 0.63 cm + Indent at: 1.27 cm

standards. Each analytical session consisted of about fifty samples and two calibrations, one at the beginning and another one at the end of each analytical session. The errors associated to each sample were calculated as the standard deviation for five measurements of low-Fe seawater samples. The mean Milli-Q blank was equal to $0.08 \pm 0.09 \text{ nmol L}^{-1}$ ($n = 17$). The detection limit, calculated for a given run as 3 times the standard deviation of the Milli-Q blanks, was on average $0.05 \pm 0.05 \text{ nmol L}^{-1}$ ($n = 17$). Reproducibility was assessed through the standard deviation of replicate samples (every 10th sample was a replicate) and the average of the in-house standard seawater, and was equal to 17% ($n = 84$). Accuracy was determined from the analysis of consensus (SAFE S, GSP) and certified (NASS-7) seawater matrices (see Table 2) and in-house standard seawater ($D_{Fe} = 0.42 \pm 0.07 \text{ nmol L}^{-1}$, $n = 84$).

Page 4 Line 21: The CTD sensors were deployed on a stainless steel rosette. Correct? Please indicate and correct throw-out the rest of the text.

→ We have modified this part as suggested

Page 6 Lines 11-15: Potential temperature (θ), Salinity (S), dissolved oxygen (O_2) and beam attenuation data were retrieved from the CTD sensors (CTD SBE911 equipped with a SBE-43) that were deployed on a stainless steel rosette. Nutrient and pigment samples were obtained from the stainless steel rosette casts and analysed according to Aminot and Kerouel (2007) and Ras et al. (2008), respectively. We used the data from the stainless steel rosette casts that were deployed immediately before or after our TMR casts. All these data are/will be available on the LEFE/CYBER database (<http://www.obs-vlfr.fr/proof/php/geovide/geovide.php>).

Deleted: ¶

Formatted: Normal, No bullets or numbering

Page 4 Line 28: Name the parameter $\Delta\sigma$

▪ We have added this precision (Page 6 Line 18): "...where Z_m is defined as an absolute change in the density of seawater at a given temperature ($\Delta\sigma_p \geq 0.125 \text{ kg m}^{-3}$)..."

Formatted: List Paragraph, Justified, Line spacing: 1.5 lines, Bulleted + Level: 1 + Aligned at: 0.63 cm + Indent at: 1.27 cm

Page 4 Line 30: What do you mean with perturbation, at which depth, please indicate in Table 1, for which station this was the case.

Formatted: Font: Bold, Complex Script Font: Bold

Formatted: Subscript

→ We have changed the word "perturbation" by "disturbance" for clarification. In addition, we have reported in Table 1 the precision on whether temperature and salinity profiles were uniform or disturbed with an asterisk symbol next to stations where profiles were not uniform and we added the following sentence in the legend of Table 1: "Note that the asterisk next to station numbers refers to disturbed temperature and salinity profiles as opposed to uniform profiles."

Formatted: Bulleted + Level: 1 + Aligned at: 0.63 cm + Indent at: 1.27 cm

Page 5 Line 2ff: Please indicate for which data you applied statistics on?

Formatted: Normal

→ We have modified the text as suggested.

Formatted: Bulleted + Level: 1 + Aligned at: 0.63 cm + Indent at: 1.27 cm

Page 6 Lines (23-24): All statistical approaches, namely the comparison between the pore size used for filtration, correlations and Principal Component Analysis (PCA), were performed using the R statistical software (R development Core Team 2012).

Formatted: Normal

Page 5 Line 3: You did not measure the p-value, you maybe determined or calculated the value.

→ We have modified this part as suggested (Page 6 Line 25),

Formatted: List Paragraph, Bulleted + Level: 1 + Aligned at: 0.63 cm + Indent at: 1.27 cm

Page 5 Line 15: Include "...540 data points. . .

Deleted: ¶

→ We have modified this part as suggested (Page 7 Lines 8-9).

Page 5 Line 19: Exchange “The complete relational database. . .” by “The complete data set. . .”

→ We have modified this part as suggested (Page 7 Line 12)

Results

Page 5 Line 27: I would swap the two sentences “For a schematic of water masses, currents and pathways, see Danialt et al. (2016).” and “Hereafter we summarise the main features (Fig. 1 and 2).”

→ We have modified this part as suggested (Page 7 Lines 19-20)

Page 6 Line 1: Give a depth range of the “Upper waters (0 – 800 m)” or so! Please also include this to the Intermediate and Deep waters.

→ We have added precisions as suggested.

Page 6 Line 5: Did you mean with central water the Subarctic intermediate water (SAIW). Please clarify! Please also increase the letter size in Fig. 2. It is really hard to see on a normal A4 print out! There are no currents in Fig. 2, either you somehow include them or remove the caption.

→ By central waters, we meant ENACW as defined in the first sentence of the paragraph and therefore changed “Cnetral Waters” by “ENACW”. We have removed the currents from the figure caption in Fig. 2 and we have increased the font size.

Page 6 Line 18: Please rewrite “..Labrador Sea Water (LSW).

→ We have modified this part as suggested (Page 8 Line 9)

Page 6 Line 29ff: I do not understand the sentence, starting with “During GA01,. . .”

→ We have rewritten this part

Page 8 Lines 19-20: During GEOVIDE, LSW formed by deep convection the previous winter was found at several stations from the Labrador Sea (68, 69, 71 and 77).

Page 6 Line 30ff, I am not sure about, explaining the different flow paths, It is really hard to follow without any drawing. Other question, is it really important, since you are just interested in water masses and their DFe signal, and not about currents! I would remove that!

→ We have modified this part to make it shorter.

Page 8 Lines 20-22: After convecting, LSW splits into three main branches with two main cores separated by the Reykjanes Ridge (stations 1-32, West European and Iceland Basins; stations 40-60, Irminger Sea), and the last one entering the West European Basin (Zunino et al., 2017).

Page 7 Line 8: I do not see any silicic acid and nitrate data, please indicate concentrations and where they can be found.

→ We have added the averages and SD for silicic acid and nitrate concentrations (Page 8, Line 26) and the reference where data can be found.

Page 8 Lines 24-27: North East Atlantic Deep Water (NEADW, $1.98 < \theta < 2.50^{\circ}\text{C}$, $34.895 < S < 34.940$) was the dominant water mass in the West European Basin at stations 1-29 from 2000 m depth to the

Deleted: ¶

Formatted: List Paragraph, Bulleted + Level: 1 +
Aligned at: 0.63 cm + Indent at: 1.27 cm

Formatted: List Paragraph, Bulleted + Level: 1 +
Aligned at: 0.63 cm + Indent at: 1.27 cm

Formatted: List Paragraph, Bulleted + Level: 1 +
Aligned at: 0.63 cm + Indent at: 1.27 cm

Formatted: List Paragraph, Bulleted + Level: 1 +
Aligned at: 0.63 cm + Indent at: 1.27 cm

Deleted: ¶

Deleted: <#>¶

Formatted: List Paragraph, Bulleted + Level: 1 +
Aligned at: 0.63 cm + Indent at: 1.27 cm

Formatted: Normal, No bullets or numbering

Deleted: ¶

Formatted: List Paragraph, Bulleted + Level: 1 +
Aligned at: 0.63 cm + Indent at: 1.27 cm

Deleted: Danialt et al., 2016¶

Formatted: List Paragraph, Bulleted + Level: 1 +
Aligned at: 0.63 cm + Indent at: 1.27 cm

bottom and is characterized by high silicic acid ($42 \pm 4 \mu\text{mol L}^{-1}$), nitrate ($21.9 \pm 1.5 \mu\text{mol L}^{-1}$) concentrations and lower oxygen concentration ($\text{O}_2 \approx 252 \mu\text{mol kg}^{-1}$) (see Sarthou et al., 2018).

Page 7 Line 9ff: It is hard to understand what you mean with "PIW is in contact with the atmosphere once a year (?) during the time of winter convection.." All together there is a lot of water mass information, that can be found elsewhere in the special issue, I would rather shorten that part of the result section.

→ We have modified this part to make it shorter

Page 8 Lines 28-32: Polar Intermediate Water (PIW, $\theta \approx 0^\circ\text{C}$, $S \approx 34.65$) is a ventilated, dense, low-salinity water intrusion to the deep overflows within the Irminger and Labrador Seas that is formed at the Greenland shelf. PIW represents only a small contribution to the whole water mass pool (up to 27%) and was observed over the Greenland slope at stations 53 and 61 as well as in surface waters from station 63 (from 0 to ~ 200 m depth), in intermediate waters of stations 49, 60 and 63 (from ~ 500 to ~ 1500 m depth) and in bottom waters of stations 44, 68, 69, 71 and 77 with a contribution higher than 10%.

Page 7 Line 30: Cannot check if this is correct! No nitrate data available.

→ The location of these data was already precised "Sarthou et al. (this issue)". However, we have changed this reference by the accurate one and added the reference of the SEANOE data base and associated paper: García-Ibáñez et al., 2018; Pérez et al., 2018; Sarthou et al., 2018 Please note that in this manuscript, Nitrate data are changed for RFe/N data, therefore we did not added the nitrate data.

Page 8 Line 11-12: This is school book knowledge, that is why we are using sensors! Remove the two sentences! However this entire section 3.2.2 needs an overhaul.

→ We have removed this part as suggested.

Page 9 Lines 24-28: Overall, most of the phytoplankton biomass was localised above 100 m depth with lower total chlorophyll-*a* (TChl-*a*) concentrations South of the Subarctic Front and higher at higher latitudes (Fig. 3). While comparing TChl-*a* maxima considering all stations, the lowest value (0.35 mg m^{-3}) was measured within the West European Basin (station 19, 50 m depth) while the highest values were measured at the Greenland (up to 4.9 mg m^{-3} , 30 m depth, station 53 and up to 6.6 mg m^{-3} , 23 m depth, station 61) and Newfoundland (up to 9.6 mg m^{-3} , 30 m depth, station 78) margins.

Page 8 Line 20ff: You can delete the first three sentences, they do not contain any important data!

→ We have removed this part as suggested

Page 8 Line 29: Also station 61 and 78 are high, at least this is shown by your plot!

→ We were talking about enhanced DFe at the surface compared to deeper DFe values, and this is only the case for stations 2, 4 and 56.

And replace "...were around..." by "...ranged from..."

→ We have modified the text as suggested.

Generally, I would merge section 3.3, 3.3.1 and 3.3.2.

Deleted: ¶

Formatted: List Paragraph, Bulleted + Level: 1 + Aligned at: 0.63 cm + Indent at: 1.27 cm

Deleted: ¶

Formatted: List Paragraph, Justified, Bulleted + Level: 1 + Aligned at: 0.63 cm + Indent at: 1.27 cm

Formatted: List Paragraph

Deleted: n

Formatted: List Paragraph, Bulleted + Level: 1 + Aligned at: 0.63 cm + Indent at: 1.27 cm

Deleted: ¶

Formatted: List Paragraph, Bulleted + Level: 1 + Aligned at: 0.63 cm + Indent at: 1.27 cm

→ We have modified the text as suggested.

Figure 4: Are you sure that single elevated values at site 40 (1500m) and at site 44 (500m) are correct. They just seem like outliers to me! Do we really need Fig.5 and 6, we see everything already in Fig. 4.

→ These enhanced DFe concentrations are consistent with high ligand concentrations measured during this study. In addition, these samples were analysed during 3 separated analytical sessions on the seaFAST SF-ICP-MS. Regarding Figs 5 and 6, we agree that Fig. 6 is repetitive and therefore we removed it from the ms and included it into the supplementary material. However, we think Fig. 5 is helpful to understand the section 4.2.2 on high latitudes meteoric water and sea-ice processes.

Page 9 Line 1ff: rewrite sentence, hard to read!

→ We have rewritten the sentence

Page 10 Lines 7-9: Considering the four oceanic basins, mean vertical profiles (supplementary material Fig. S2) showed increasing DFe concentrations down to 3000 m depth followed by decreasing DFe concentrations down to the bottom. Among deep-water masses, the lowest DFe concentrations were measured in the West European Basin.

Page 9 Line 6ff: Please provide numbers for surface waters.

→ We have added this precision.

Page 10 Lines 12-14: Overall, surface DFe concentrations were higher ($0.36 \pm 0.18 \text{ nmol L}^{-1}$) in the North Atlantic Subpolar gyre (above 52°N) than in the North Atlantic Subtropical gyre ($0.17 \pm 0.05 \text{ nmol L}^{-1}$).

Page Line 9ff: But also at station 21 the DFe value is high. I do not think they are significantly different from the others, s.d. is $\pm 20\%$ and higher.

→ We agree with you and removed this sentence.

Page 9 Line 17: NEADW was very similar to the median GEOVIDE voyage but compared to test of deep waters lower, please rewrite! But the DSOW in the Labrador Sea was similar.

→ We have modified the text accordingly

Page 11 Lines 8-11: The DFe concentrations in the NEADW were relatively similar to the DFe median value of the GEOVIDE voyage (median DFe = 0.75 nmol L^{-1} , Figs. 4 and 7) with an average value of $0.74 \pm 0.16 \text{ nmol L}^{-1}$ ($n=18$) and presented relatively low median DFe concentrations (median DFe = 0.71 nmol L^{-1}) compared to other deep water masses.

I am not sure Fig. 7 is really required. It just comprises what we already see in Fig. 4. And apart from some outliers (hydrothermal? Any Mn data), surface waters, NADW and waters from the Labrador Sea, concentrations are around 1nM. And as numerous times shown, it is impossible to fingerprint water masses with DFe.

→ We agree with this suggestion and Figure 7 was removed from the MS and added to supplementary material.

Page 10 Line 9: Others showed also elevated concentrations, for instance, station 44. However I understand why the authors decided to explain both station! For myself station 1 is not a problem, it

Formatted: List Paragraph, Bulleted + Level: 1 +
Aligned at: 0.63 cm + Indent at: 1.27 cm

Deleted: a

Formatted: List Paragraph, Bulleted + Level: 1 +
Aligned at: 0.63 cm + Indent at: 1.27 cm

Formatted: List Paragraph, Bulleted + Level: 1 +
Aligned at: 0.63 cm + Indent at: 1.27 cm

Formatted: List Paragraph, Bulleted + Level: 1 +
Aligned at: 0.63 cm + Indent at: 1.27 cm

Formatted: List Paragraph, Bulleted + Level: 1 +
Aligned at: 0.63 cm + Indent at: 1.27 cm

Formatted: List Paragraph, Bulleted + Level: 1 +
Aligned at: 0.63 cm + Indent at: 1.27 cm

Formatted: List Paragraph, Bulleted + Level: 1 +
Aligned at: 0.63 cm + Indent at: 1.27 cm

is very close to the continental margin and influenced by lateral water mass transport than the other stations farther off-shore. However, site 17 is a bit more tricky. Did you reanalyze that station, that would confirm that the analysis was alright and you do not face just a strange offset. Anyway, I would discuss station 17, but please rephrase some sentences, it was really hard to grasp the issue you wanted to bring across. From the first sentence it should be clear what the issue is, than explain (eg. Concentrations are irregularly high).

→ We have modified the text as suggested

Page 11 Lines 20-28: Considering the entire section, two stations (stations 1 and 17) showed irregularly high DFe concentrations ($> 1 \text{ nmol L}^{-1}$) throughout the water column, thus suggesting analytical issues. However, these two stations were analysed twice and provided similar results, therefore discarding any analytical issues. This means that these high values originated either from genuine processes or from contamination issues. If there had been contamination issues, one would expect a more random distribution of DFe concentrations and less consistence throughout the water column. It thus appears that contamination issues were unlikely to happen. Similarly, the influence of water masses to explain these distributions was discarded as the observed high homogenized DFe concentrations were restricted to these two stations. Station 1, located at the continental shelf-break of the Iberian Margin, also showed enhanced PFe concentrations from lithogenic origin suggesting a margin source (Gourain et al., 2018).

Page 10 Line 23ff: Please provide the numbers from the other studies. Would it be possible to plot the surface DFe concentration and put the graph in the sup material. Than you can relate to that!

→ We have provided the numbers from other studies, updated Table 3 with the DFe values from Achterberg et al., 2018 and we added the following plot to the supplementary material:

Formatted: List Paragraph, Bulleted + Level: 1 + Aligned at: 0.63 cm + Indent at: 1.27 cm

Deleted: a

Formatted: List Paragraph, Bulleted + Level: 1 + Aligned at: 0.63 cm + Indent at: 1.27 cm

Formatted: Indent: Before: 0.63 cm

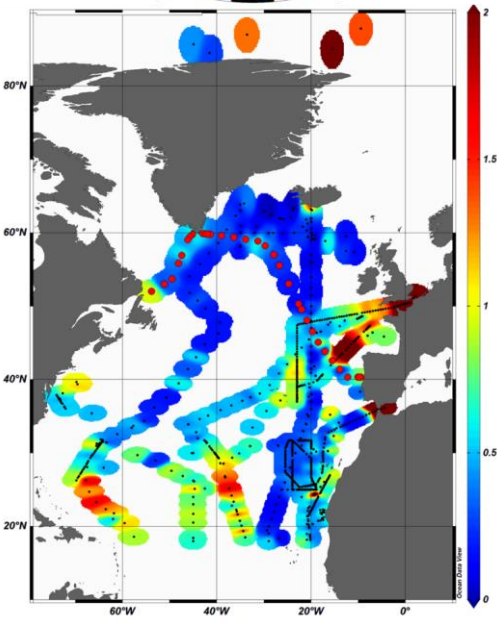
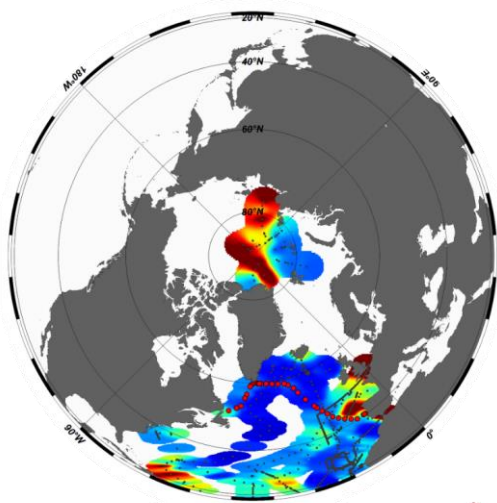


Figure S4: Surface layer of DFe concentrations, new measurements are shown in red dots (GEOVIDE voyage), while previous studies are displayed in black (Achterberg et al., 2018; Bergquist et al., 2007; Blain et al., 2004; Boye et al., 2006, 2003; de Jong et al., 2007; Gledhill et al., 1998; Hatta et al., 2015; Klunder et al., 2012; Laës et al., 2003; Martin et al., 1993; Measures et al., 2008; Mills et al., 2008; Mohamed et al., 2011; Nédélec et al., 2007; Nielsdóttir et al., 2009; Pohl et al., 2011; Rijkenberg et al., 2014; Sarthou et al., 2007, 2003; Sedwick et al., 2005; Ussher et al., 2013; Witter and Luther III, 1998; Wu and Boyle, 2002; Wu and Luther III, 1996, 1994; Wu et al., 2001).

Formatted: Indent: First line: 0 cm

Field Code Changed

Formatted: French (France)

Deleted: Achterberg et al., 2018

Formatted: French (France)

Formatted: French (France)

→ We also changed the text as we made a mistake in this section. Indeed, low DFe concentrations were previously measured in the central Irminger Sea. When we first wrote this part we considered stations that were closed to land likely impacted by sea-ice melting.

Formatted: English (Australia)

Formatted: List Paragraph, Bulleted + Level: 1 +
Aligned at: 0.63 cm + Indent at: 1.27 cm

Formatted: English (Australia)

Page 12 Lines 3-7: Among the four distinct basins described in this paper, the Irminger Sea exhibited the highest DFe concentrations within the surface waters (from 0 to 250 m depth) with values ranging from 0.23 to 1.3 nmol L⁻¹ for open-ocean stations. Conversely, low DFe concentrations were previously reported in the central Irminger Sea by Rijkenberg et al. (2014) (April-May, 2010) and Achterberg et al. (2018) (April-May and July-August, 2010) with DFe concentrations ranging from 0.11 to 0.15 and from ~ 0 to 0.14 nmol L⁻¹, respectively (see supplementary material Fig. S4 and Table S2).

Page 10 Line 29: Please include an opening sentence, what you think is the reason (something similar to the last sentence). It is quite a step from Fe distribution to the original of water mass mixing.

→ We have added an opening sentence

Formatted: List Paragraph, Bulleted + Level: 1 +
Aligned at: 0.63 cm + Indent at: 1.27 cm

Page 12 Lines 9-11: Indeed, enhanced surface DFe concentrations measured during GEOVIDE in the Irminger Sea could be due to intense wind forcing events that would deepen the winter Z_m down to the core of the Fe-rich LSW.

Page 11 Line 5: Explain what tip jets are!

→ We have added a definition

Deleted: ¶

Formatted: List Paragraph, Bulleted + Level: 1 +
Aligned at: 0.63 cm + Indent at: 1.27 cm

Page 12 Lines 19-22: Moore (2003) and Piron et al. (2016) described low-level westerly jets centred northeast of Cape Farewell, over the Irminger Sea, known as tip jet events, whose structure depends upon the splitting occurring as the flow encounter the orographic features from Cape Farewell, and that are strong enough to induce deep convective mixing (Bacon et al., 2003; Pickart et al., 2003).

Page 11 Line 10ff: This process is called winter entrainment (Tagliabue et al. 2014). Rephrase sentence and delete the last one (You just repeat yourself).

→ We have modified the text as suggested

Formatted: List Paragraph, Bulleted + Level: 1 +
Aligned at: 0.63 cm + Indent at: 1.27 cm

Page 12 Lines 26-28: Such winter entrainment was likely the process involved in the vertical supply of DFe within surface waters fuelling the spring phytoplankton bloom with DFe values close to those found in LSW.

Page 11 Line 16: Also contaminated waters are introduced!

→ Yes, we completely agree. However, since this section is dedicated to atmospheric deposition we did not specify this.

Formatted: List Paragraph, Bulleted + Level: 1 +
Aligned at: 0.63 cm + Indent at: 1.27 cm

Page 11 Line 18: What is a stratification period? Be preciss!

→ We have changed the text

Deleted: ¶

Formatted: List Paragraph, Bulleted + Level: 1 +
Aligned at: 0.63 cm + Indent at: 1.27 cm

Page 12 Line 32: "During the summer, when thermal stratification occurs, ..."

Page 11 Line 218ff: You can not compare the Mediterranean surface waters with MOW. Rewrite! DAI and DFe behave entirely different in the water column (residence time, organic complexation,

concentrations, etc.), but both of them are likely to be scavenged from particles. So when a dust storm hits, both elements should decrease, do they actually do this in the water column of the Mediterranean sea. However, I am not too much surprised to see no DFe signal in the MOW. However, I suggest you have a look for DFe literature values from deep Mediterranean waters (GA04 is not available, a pity).

→ Yes, we agree that DAI and DFe behave differently in the water column depending on organic complexation and that they are both likely to be scavenged from particles. However, DAI and DFe originating from dust deposition are not scavenged by the same type of particles. Indeed, Wuttig et al. (2013) reported that after a single dust deposition event DAI loss rates was highly affected by the concentrations of biogenic particles while DFe was removed by sinking dust particles. The same authors highlighted that the following dust deposition event were likely inducing the dissolution of Fe from dust particles depending on the amounts of Fe-binding organic ligands. Therefore, both elements should not necessarily decrease.

→ We have changed the text as suggested

Page 13 Lines 2-14: After atmospheric deposition, the fate of Fe will depend on the nature of aerosols, vertical mixing, biological uptake and scavenging processes (Bonnet and Guieu, 2006; Wuttig et al., 2013). During GEOVIDE, MOW was observed from stations 1 to 29 between 1000 and 1200 m depth and associated with high dissolved aluminium (DAI, Menzel Barraqueta et al., 2018) concentrations (up to 38.7 nmol L⁻¹), confirming the high atmospheric deposition in the Mediterranean region. In contrast to Al, no DFe signature was associated with MOW (Figs. 2 and 3). This feature was also reported in some studies (Hatta et al., 2015; Thuróczy et al., 2010), while others measured higher DFe concentrations in MOW (Gerringa et al., 2017; Sarthou et al., 2007). However, MOW coincides with the maximum Apparent Oxygen Utilization (AOU) and it is not possible to distinguish the MOW signal from the remineralisation one (Sarthou et al., 2007). On the other hand, differences between studies are likely originating from the intensity of atmospheric deposition and the nature of aerosols. Indeed, Wagener et al. (2010) highlighted that large dust deposition events can accelerate the export of Fe from the water column through scavenging. As a result, in seawater with high DFe concentrations and where high dust deposition occurs, a strong individual dust deposition event could act as a sink for DFe. It thus becomes less evident to observe a systematic high DFe signature in MOW despite dust inputs.

Page 12 Line 1: The entire section 4.1.3 is highly speculative. I agree elevated DFe in the Irminger Basin needs to come from somewhere, however, just looking at your Chl a data it is a very productive site, so presumably PFe concentrations are elevated as well, if so you should mention that, than it is just elevated remineralization and intense deep mixing during winter time that is responsible. However, you need to rewrite that section, to make it less speculative, look for existing data!

→ We have changed the text as suggested.

Page 13 Lines 16-33 and Page 14 Lines 1-16: As described in Section 3.1, the LSW exhibited increasing DFe concentrations from its source area, the Labrador Sea, toward the other basins with the highest DFe concentrations observed within the Irminger Sea, suggesting that the water mass was enriched in DFe either locally in each basin or during its flow path (Fig. 7). These DFe sources could originate from a combination of high export of PFe and its remineralisation in the mesopelagic area and/or the dissolution of sediment.

Formatted: List Paragraph, Bulleted + Level: 1 +
Aligned at: 0.63 cm + Indent at: 1.27 cm

Deleted: Wuttig et al., 2013

Deleted: Gerringa et al., 2017; Sarthou et al., 2007; Sarthou et al., 2007

Deleted: ¶

Formatted: List Paragraph, Bulleted + Level: 1 +
Aligned at: 0.63 cm + Indent at: 1.27 cm

The Irminger and Labrador Seas exhibited the highest averaged integrated TChl-a concentrations ($98 \pm 32 \text{ mg m}^{-2}$ and $59 \pm 42 \text{ mg m}^{-2}$) compared to the West European and Iceland Basins ($39 \pm 10 \text{ mg m}^{-2}$ and $53 \pm 16 \text{ mg m}^{-2}$), when the influence of margins was discarded. Stations located in the Irminger (stations 40-56) and Labrador (stations 63-77) Seas, were largely dominated by diatoms (>50% of phytoplankton abundances) and displayed the highest chlorophyllid- α concentrations, a tracer of senescent diatom cells, likely reflecting post-bloom condition (Tonnard et al., in prep.). This is in line with the highest POC export data reported by Lemaître et al. (2018) in these two oceanic basins. This likely suggests that biogenic PFe export was also higher in the Labrador and Irminger Seas than in the West European and Iceland Basins. Although, Gourain et al. (2018) highlighted a higher biogenic contribution for particles located in the Irminger and Labrador Seas with relatively high PFe:PAI ratios ($0.44 \pm 0.12 \text{ mol:mol}$ and $0.38 \pm 0.10 \text{ mol:mol}$, respectively) compared to particles from the West European and Iceland Basins (0.22 ± 0.10 and $0.38 \pm 0.14 \text{ mol:mol}$, respectively, see Fig. 6 in Gourain et al., 2018), they reported no difference in PFe concentrations between the four oceanic basins (see Fig. 12A in Gourain et al., 2018) when the influence of margins was discarded, which likely highlighted the remineralisation of PFe within the Irminger and Labrador Seas. Indeed, Lemaître et al. (2017) reported higher remineralisation rates within the Labrador (up to $13 \text{ mmol C m}^{-2} \text{ d}^{-1}$) and Irminger Seas (up to $10 \text{ mmol C m}^{-2} \text{ d}^{-1}$) using the excess barium proxy (Dehairs et al., 1997), compared to the West European and Iceland Basins (ranging from 4 to $6 \text{ mmol C m}^{-2} \text{ d}^{-1}$). Therefore, the intense remineralisation rates measured in the Irminger and Labrador Seas likely resulted in enhanced DFe concentrations within LSW.

Higher DFe concentrations were, however, measured in the Irminger Sea compared to the Labrador Sea and coincided with lower transmissometer values (i.e. 98.0-98.5% vs. >99%), thus suggesting a particle load of the LSW. This could be explained by the reductive dissolution of Newfoundland Margin sediments. Indeed, Lambelet et al. (2016) reported high dissolved neodymium (Nd) concentrations (up to $18.5 \text{ pmol.kg}^{-1}$) within the LSW at the edge of the Newfoundland Margin (45.73°W , 51.82°N) as well as slightly lower Nd isotopic ratio values relative to those observed in the Irminger Sea. They suggested that this water mass had been in contact with sediments approximately within the last 30 years (Charette et al., 2015). Similarly, during GA03, Hatta et al. (2015) attributed the high DFe concentrations in the LSW to continental margin sediments. Consequently, it is also possible that the elevated DFe concentrations from the three LSW branches which entered the West European and Iceland Basins and Irminger Sea was supplied through sediment dissolution (Measures et al., 2013) along the LSW pathway.

The enhanced DFe concentrations measured in the Irminger Sea and within the LSW were thus likely attributed to the combination of higher productivity, POC export and remineralisation as well as a DFe supply from reductive dissolution of Newfoundland sediments to the LSW along its flow path.

Page 12 Line 25: the elevated concentration on station 44, is not this just a single point?

➔ No, the elevated DFe concentrations at station 44 concerned three data points.

Page 12 Line 26ff: Replace “above” by “at”, and what are i) sediment inputs (these are particles), and ii) intrusion of an Fe-rich water mass, please be more specific!

➔ We have changed the sentence as suggested and added precision.

Page 14 Lines 19-20: “... i) vertical diffusion from local sediment, ii) lateral advection of a water mass displaying enhanced DFe concentrations, and iii) local dissolution of Fe from particles.”

Formatted: List Paragraph, Bulleted + Level: 1 +
Aligned at: 0.63 cm + Indent at: 1.27 cm

Formatted: List Paragraph, Bulleted + Level: 1 +
Aligned at: 0.63 cm + Indent at: 1.27 cm

Page 12 Line 33: How often have you analyzed the samples below 2.500 m at site 44. For me this is just one outlier, the two other samples from cast 44 in Fig 8A are not that out of the range.

→ The full station 44 was analysed during two separated analytical sessions on the seaFAST SF-ICP-MS from different sampling bottles with a good agreement between results. Therefore, we do not think that this data point is an outlier.

Page 13 Line 10ff: Your argument is based on four data points, I could also put a straight line through, with a similar R2. However this entire paragraph is highly speculative! In an earlier paragraph you mention that DFe do not fingerprint different water masses, and now they do? You should remove this section!

→ We agree on the fact that the polynomial fitting could also be a linear fitting. However, with either a polynomial or a linear fitting on the 5 data points, the conclusion would be the same with apparently, the dissolution of Fe-rich particles.

→ We reformulated this section as we considered it too speculative.

Page 15 Lines 2-20: However, considering the short residence time of DFe and the circulation of water masses in the Irminger Sea, it is possible that instead of being attributed to one specific water mass, these enhanced DFe concentrations resulted from lateral advection of the deep waters. Figure 8B) shows the concentrations of both DFe and PFe for the mixing line between DSOW/PIW and ISOW at station 44 and considering 100% contribution of ISOW for the shallowest sample (2218 m depth) and of DSOW/PIW for the deepest (2915 m depth), as these were the main water masses. This figure shows increasing DFe concentrations as DSOW/PIW mixed with ISOW. In addition, Le Roy et al. (2018) reported for the GEOVIDE voyage at station 44 a deviation from the conservative behaviour of ^{226}Ra reflecting an input of this tracer centred at 2500 m depth, likely highlighting diffusion from deep-sea sediments and coinciding with the highest DFe concentrations measured at this station. Although the transmissometer values were lower at the sediment interface than at 2500 m depth, Deng et al. (2018) reported a stronger scavenged component of the ^{230}Th at the same depth range, likely suggesting that the mixture of water masses were in contact with highly reactive particles. If there is evidence that the enhanced DFe concentrations observed at station 44 coincided with lateral advection of water masses that were in contact with particles, the difference of behaviour between DFe and ^{230}Th remains unsolved. The only parameter that would explain without any ambiguity such differences of behaviour between DFe and ^{230}Th would be the amounts of Fe-binding organic ligands for these samples. Indeed, although PFe concentrations decreased from the seafloor to the above seawater, this trend would likely be explained by a strong vertical diffusion alone and not necessarily from the dissolution of particles that were laterally advected.

Therefore, the high DFe concentrations observed might be inferred from local processes as ISOW mixes with both PIW and DSOW with a substantial load of Fe-rich particles that might have dissolved in solution due to Fe-binding organic ligands.

Page 13 Line 22: unpublished sources? You need to explain that! Did you look through your Mn and Pb data, when they are also high, we talk about a hydrothermal input of trace metals.

→ We have changed the text for clarification

Page 15 Lines 22-33 and page 16 Lines 1-12: Hydrothermal activity was assessed over the Mid Atlantic Ridge, namely the Reykjanes Ridge, from stations 36 to 42. Indeed, within the interridge database (<http://www.interridge.org>), the Reykjanes Ridge is reported to have active hydrothermal

Deleted: ¶

Formatted: List Paragraph, Bulleted + Level: 1 + Aligned at: 0.63 cm + Indent at: 1.27 cm

Formatted: Normal, No bullets or numbering

Formatted: List Paragraph, Bulleted + Level: 1 + Aligned at: 0.63 cm + Indent at: 1.27 cm

sites that were either confirmed (Baker and German, 2004a; German et al., 1994; Olafsson et al., 1991; Palmer et al., 1995) close to Iceland or inferred (e.g. Chen, 2003; Crane et al., 1997; German et al., 1994; Sinha et al., 1997; Smallwood and White, 1998) closer to the GEOVIDE section as no plume was detected but a high backscatter was reported potentially corresponding to a lava flow. Therefore, hydrothermal activity at the sampling sites remains unclear with no elevated DFe concentrations or temperature anomaly above the ridge (station 38). However, enhanced DFe concentrations (up to $1.5 \pm 0.22 \text{ nmol L}^{-1}$, station 36, 2200 m depth) were measured east of the Reykjanes Ridge (Fig. 4). This could be due to hydrothermal activity and resuspension of sunken particles at sites located North of the section and transported through the ISOW towards the section (Fig. 7). Indeed, Achterberg et al. (2018) highlighted at $\sim 60^\circ\text{N}$ and over the Reykjanes Ridge a southward lateral transport of an Fe plume of up to 250-300 km. In agreement with these observations, previous studies (e.g. Fagel et al., 1996; Fagel et al., 2001; Lackschewitz et al., 1996; Parra et al., 1985) reported marine sediment mineral clays in the Iceland Basin largely dominated by smectite (> 60%), a tracer of hydrothermal alteration of basaltic volcanic materials (Fagel et al., 2001; Tréguer and De La Rocha, 2013). Hence, the high DFe concentrations measured east of the Reykjanes Ridge could be due to a hydrothermal source and/or the resuspension of particles and their subsequent dissolution.

West of the Reykjanes Ridge, a DFe-enrichment was also observed in ISOW within the Irminger Sea (Figs. 4 and 7). The low transmissometer values within ISOW in the Irminger Sea compared to the Iceland Basin suggest a particle load. These particles could come from the Charlie Gibbs Fracture Zone (CGFZ, 52.67°N and 34.61°W) and potentially Bight Fracture Zone (BFZ, 56.91°N and 32.74°W) (Fig. 1) (Lackschewitz et al., 1996; Zou et al., 2017). Indeed, hydrographic sections of the northern valley of the CGFZ showed that below 2000 m depth the passage through the Mid-Atlantic Ridge was mainly filled with the ISOW (Kissel et al., 2009; Shor et al., 1980). Shor et al. (1980) highlighted a total westward transport across the sill, below 2000 m depth of about $2.4 \times 10^6 \text{ m}^3 \text{ s}^{-1}$ with ISOW carrying a significant load of suspended sediment ($25 \mu\text{g L}^{-1}$), including a 100-m-thick benthic nepheloid layer. It thus appears that the increase in DFe within ISOW likely came from sediment resuspension and dissolution as the ISOW flows across CGFZ and BFZ.

→ Note that for Pb, no particular hydrothermal signal was observed during GEOVIDE (Zurbrick et al., 2018). For Mn, data are analysed but not yet processed.

Page 14 Line 3ff: There are no elevated DFe values farther east from the ridge!

→ We have changed the text for clarification (see above). The DFe enrichment east of Reykjanes Ridge corresponded to the section on top of this sentence while further downstream corresponded to west of the Reykjanes Ridge.

Where is the CGFC and BFC. Questions over questions!

→ These two features are now added to Fig. 1

Formatted: List Paragraph, Bulleted + Level: 1 + Aligned at: 0.63 cm + Indent at: 1.27 cm

Deleted: Zurbrick et al. (2018)

Deleted: ¶

Formatted: List Paragraph, Bulleted + Level: 1 + Aligned at: 0.63 cm + Indent at: 1.27 cm

Formatted: List Paragraph, Bulleted + Level: 1 + Aligned at: 0.63 cm + Indent at: 1.27 cm

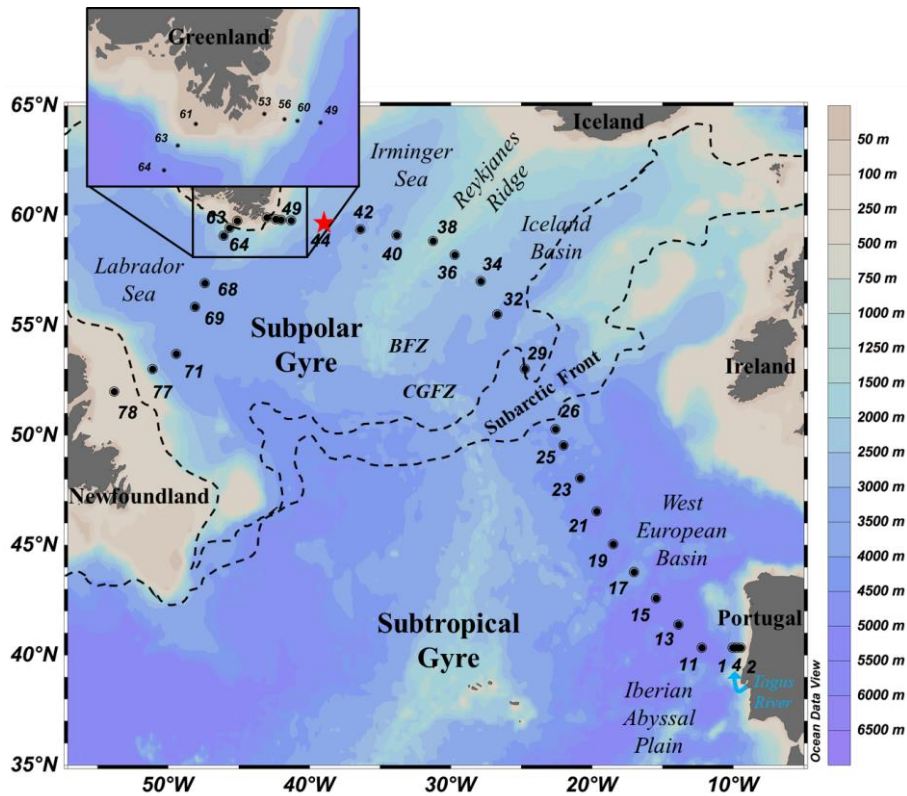


Figure 1: Map of the GEOTRACES GA01 voyage plotted on bathymetry as well as the major topographical features and main basins. Crossover station with GEOTRACES voyage (GA03) is shown as a red star. (Ocean Data View (ODV) software, version 4.7.6, R. Schlitzer, <http://odv.awi.de>, 2016). BFZ: Bight Fracture Zone, CGFZ: Charlie-Gibbs Fracture Zone.

Page 14 Line 13ff: I am confused. Do we talk about station 40 and 1.75nM at 1500 m, this is a single high value for me, and not located in ISOW waters.

→ Yes, we talk about station 40 (one point) and station 42 (three points) that are all located in the ISOW (see Fig. 7).

Formatted: List Paragraph, Bulleted + Level: 1 + Aligned at: 0.63 cm + Indent at: 1.27 cm

Page 14 Line 26ff: The DFe/DAI ratio in seawater can not compared with the Fe/Al ratio of dust particles. Both elements have different fractional solubility's. So the ratio is always different! Remove!

→ We agree with the reviewer and have changed the text as suggested and have added some information

Formatted: List Paragraph, Bulleted + Level: 1 + Aligned at: 0.63 cm + Indent at: 1.27 cm

Page 16 lines 25-28: Our SML DFe inventories were about three times higher at station 1 (~ 1 nmol L⁻¹) than those calculated during the GA03 voyage (~ 0.3 nmol L⁻¹, station 1) during which atmospheric

deposition were about one order of magnitude higher (Shelley et al., 2018; Shelley et al., 2015), the atmospheric source seemed to be minor.

Page 15 Line 1: Remove most of them does not add to the story!

→ We agree and have removed most of them.

Page 16 Line 32 and Page 17 Lines 1-2: Many types of industry (e.g. heavy metallurgy, ore processing, chemical industry) release metals including Fe, which therefore result in high levels recorded in surface sediments, suspended particulate matter, water and organisms in the lower estuary (Santos-Echeandia et al., 2010).

Page 15 Line 5: What do you mean with “..below ground biomass..” In general I do not understand, why you excluded sediments, that could be an additional source.

→ We did not intend to exclude the sediment source and have change the text for clarification.

Page 16 lines 28-30 Consequently, the Tagus River appears to be the most likely source responsible for these enhanced DFe concentrations, either as direct input of DFe or indirectly through Fe-rich sediment carried by the Tagus River and their subsequent dissolution.

Page 15 Line 14ff: Fronts refer to temperature and salinity changes in surface waters, such as the Polar Front, not in the water column. Call it different; just use the term “fresh water lens”. Why multi-year-sea ice?

→ We have changed the text as suggested

Page 17 Lines 9-10: The presence of this freshwater lens suggests that sediment derived enrichment to these surface waters was unlikely.

→ We talked about multiyear sea ice because of drainage processes and the release of brines (see below)

Page 15 Line 18ff: But glacial sources and land ice sheet is the same, just call, it “ . . .freshwater induced by meteoric water and sea-ice melt.” Than all is clear.

→ We have made the correction as suggested (Page17 Lines 10-11)

Page 15 Line 27: Where do get the sea-ice fractions from, and explain how it works, include references! And what have brines to do with it, either ice forms or not! Brines are not part of your story, so far I can tell. Brines always from when sea-ice is formed, or in the desert by evaporation. And in line 31 you switch back to sea-ice formation, please stay with that term.

→ We have included a section in the method on how these fractions were calculated.

Page 5 Lines 23-32, Page 6 Lines 1-9: We separated the mass contributions to samples from stations 53, 61 and 78 in Sea-Ice Melt (SIM) Meteoric Water (MW) and saline seawater inputs using the procedure and mass balance calculations that are fully described in Benetti et al. (2016) (Fig. 5D), E) and F)). Hereafter, we describe briefly the principle. We considered two types of seawater, namely the Atlantic Water (AW) and the Pacific Water (PW). After estimating the relative proportions of AW (f_{AW}) and PW (f_{PW}) and their respective salinity and $\delta^{18}O$ affecting each samples, the contribution of SIM and MW can be determined using measured salinity (S_m) and $\delta^{18}O$ (δO_m^{18}). The mass balance calculations are presented below:

$$f_{AW} + f_{PW} + f_{MW} + f_{SIM} = 1 \text{ (eq.1)}$$

Formatted: English (Australia)

Formatted: English (Australia)

Field Code Changed

Formatted: List Paragraph, Bulleted + Level: 1 +
Aligned at: 0.63 cm + Indent at: 1.27 cm

Formatted: List Paragraph, Bulleted + Level: 1 +
Aligned at: 0.63 cm + Indent at: 1.27 cm

Deleted: ¶

Formatted: List Paragraph, Bulleted + Level: 1 +
Aligned at: 0.63 cm + Indent at: 1.27 cm

Formatted: Normal, No bullets or numbering

Formatted: List Paragraph, Bulleted + Level: 1 +
Aligned at: 0.63 cm + Indent at: 1.27 cm

Formatted: List Paragraph, Bulleted + Level: 1 +
Aligned at: 0.63 cm + Indent at: 1.27 cm

$$f_{AW} \cdot S_{AW} + f_{PW} \cdot S_{PW} + f_{MW} \cdot S_{MW} + f_{SIM} \cdot S_{SIM} = S_m \text{ (eq.2)}$$

$$f_{AW} \cdot \delta O_{AW}^{18} + f_{PW} \cdot \delta O_{PW}^{18} + f_{MW} \cdot \delta O_{MW}^{18} + f_{SIM} \cdot \delta O_{SIM}^{18} = \delta O_m^{18} \text{ (eq.3)}$$

where f_{AW} , f_{PW} , f_{MW} , f_{SIM} are the relative fraction of AW, PW, MW, and SIM. To calculate the relative fractions of AW, PW, MW and SIM we used the following end-members: $S_{AW} = 35$, $\delta O_{AW}^{18} = +0.18\text{‰}$ (Benetti et al., 2016); $S_{PW} = 32.5$, $\delta O_{PW}^{18} = -1\text{‰}$ (Cooper et al., 1997; Woodgate and Aagaard, 2005); $S_{MW} = 0$, $\delta O_{MW}^{18} = -18.4\text{‰}$ (Cooper et al., 2008); $S_{SIM} = 4$, $\delta O_{SIM}^{18} = +0.5\text{‰}$ (Melling and Moore, 1995).

In Figure 5 D), E) and F), negative sea-ice fractions indicated a net brine release while positive sea-ice fractions indicated a net sea-ice melting. Note that for stations over the Greenland Shelf, we assumed that the Pacific Water (PW) contribution was negligible for the calculations, supported by the very low PW fractions found at Cape Farewell in May 2014 (see Figure B1 in Benetti et al., 2017), while for station 78, located on the Newfoundland shelf, we used nutrient measurements to calculate the PW fractions, following the approach from Jones et al. (1998) (the data are published in Benetti et al., 2017).

→ Regarding brines, they can originate from two different processes: either as a result of multiyear sea-ice melting or during sea-ice formation. Indeed, during the early melting season, multiyear sea-ice has a higher porosity and gravitational drainage of brine occur. These two processes of brine release might lead to different TM signatures in brine originating from sea-ice formation and brine originating from early melting of multiyear sea-ice (Petrich and Eicken, 2010; Wadhams, 2000).

Page 15 Line 33: But brines usually sink, because they are heavier than the surrounding water!!! It is really hard to follow your argumentation here.

We agree with the reviewer in the fact that brines sink due to higher density. However, after reaching neutral buoyancy, they will stop sinking.

Page 16 Line 11: You have to explain how you produced these numbers, a citation in an earlier paragraph is not enough!

→ We have included a section in the method on how these fractions were calculated (see above)

Page 16 Line 15: How do you lose a sample! Generally fist you talk about the contribution of MW and then you switch to biological uptake of DFe, that in the same paragraph? You lose the reader here; this entire section needs an overhaul.

→ We have reorganised this section.

Page 18 Lines 3-18; Surface waters (from 0 to ~ 100 m depth) from station 53 and 61 were characterized by high MW fractions (ranging from 8.3 to 7.4% and from 7.7 to 7.3%, respectively, from surface to ~100 m depth, Figs. 5D and E). These high MW fractions were both enriched in PFe and DFe (except station 53 for which no data was available close to the surface) compared to seawater located below 50 m depth, thus suggesting a MW source. These results are in line with previous observations, which highlighted strong inputs of DFe from a meteoric water melting source in Antarctica (Annett et al., 2015). Although the ability of MW from Greenland Ice Sheet and runoffs to deliver DFe and PFe to surrounding waters has previously been demonstrated (Bhatia et al., 2013; Hawkings et al., 2014; Schroth et al., 2014; Statham et al., 2008), both Fe fractions were lower at the sample closest to the surface, then reached a maximum at ~ 50 m depth and decreased at ~ 70 m depth, for station 61 (Fig. 4D). The surface DFe depletion was likely explained by phytoplankton uptake, as indicated by the high TChl- α concentrations (up to 6.6 mg m⁻³) measured from surface to

Formatted: Normal, No bullets or numbering

Deleted: <#>¶

Formatted: Not Highlight

Formatted: Highlight

Formatted: Not Highlight

Formatted: EndNote Bibliography, Bulleted + Level: 1 + Aligned at: 0.25 cm + Indent at: 0.88 cm

Formatted: Not Highlight

Formatted: List Paragraph, Bulleted + Level: 1 + Aligned at: 0.25 cm + Indent at: 0.88 cm

Formatted: Not Highlight

about 40 m depth, drastically decreasing at ~ 50 m depth to 3.9 mg m⁻³ (Fig. 4D). Hence, it seemed that meteoric water inputs from the Greenland Margin likely fertilized surface waters with DFe, enabling the phytoplankton bloom to subsist. The profile of PFe can be explained by two opposite plausible hypotheses: 1) MW inputs did not released PFe, as if it was the case, one should expect higher PFe concentrations at the surface (~25 m depth) than the one measured at 50 m depth due to both the release from MW and the assimilation of DFe by phytoplankton 2) MW inputs can release PFe in a form that is directly accessible to phytoplankton with subsequent export of PFe as phytoplankton died. The latter solution explains the PFe maximum measured at ~ 50 m depth and is thus the most plausible.

Page 16 Line 32: “. decreasing from surface to depth.” Which depth, down to the bottom in 400 m depth? Be precise

→ We have added this precision.

Page 18 Lines 21-22: Newfoundland shelf waters (station 78) were characterized by high MW fractions (up to 7%), decreasing from surface to 200 m depth (~2%).

Page 17 Line 15-25: What has the tropical and subtropical North Atlantic to do with your work! I assume very little, please delete or at least reduce the text.

→ We agree with the reviewer and removed the part on tropical North Atlantic.

Page 18 Lines 32-33 and Page 19 Lines 1-4: On a regional scale, the North Atlantic basin receives the largest amount of atmospheric inputs due to its proximity to the Saharan Desert (Jickells et al., 2005), yet even in this region of high atmospheric deposition, inputs are not evenly distributed. Indeed, aerosol Fe loading measured during GEOVIDE (Shelley et al., 2017) were much lower (up to four orders of magnitude) than those measured during studies from lower latitudes in the North Atlantic (e.g. Baker et al., 2013; Buck et al., 2010; and for GA03, Shelley et al., 2015), but atmospheric inputs could still be an important source of Fe in areas far from land.

Page 17 Line 30: I would rather suggest to say: “Shelley et al. concluded that. . .” because without any trajectories here I can check, and more or less all this work was already published.

→ We have removed this part.

Page 18 Line 13: Do you mean DOM? Or organic material OM. However, you talk about DOM for 7 lines, and then you don't have the data. Once sentence should be enough to point out the importance of DOM.

→ We have removed this part.

Page 18 Line 16: This entire paragraph is very poor! It is interesting to compare elemental ratios of seawater with the soluble fraction of dust. But the reasoning here “. . .whether there was enough atmospheric input to sustain the SML DFe concentrations. . .” without any flux numbers, residence times is unscientific. Even more strange, at the end of the paragraph you don't even say, whether there is enough or not. Similar to the above, this needs serious work to make it worthwhile reading. There is too much hand waving, and too few data, sorry! I suggest you look up the actual flux numbers and then compare them with your data.

→ We agree with the reviewer and removed this section to replace it by Turnover Times relative to Atmospheric Deposition (TTADs) as defined in Guieu et al. (2014).

Formatted: List Paragraph, Bulleted + Level: 1 +
Aligned at: 0.63 cm + Indent at: 1.27 cm

Formatted: Normal, No bullets or numbering

Deleted: 6

Formatted: List Paragraph, Bulleted + Level: 1 +
Aligned at: 0.63 cm + Indent at: 1.27 cm

Formatted: List Paragraph, Bulleted + Level: 1 +
Aligned at: 0.63 cm + Indent at: 1.27 cm

Deleted: ¶

Formatted: List Paragraph, Bulleted + Level: 1 +
Aligned at: 0.63 cm + Indent at: 1.27 cm

Deleted: ¶

Formatted: List Paragraph, Bulleted + Level: 1 +
Aligned at: 0.63 cm + Indent at: 1.27 cm

Page 19 Lines 5-17: In an attempt to estimate whether there was enough atmospheric input to sustain the SML DFe concentrations, we calculated Turnover Times relative to Atmospheric Deposition (TTADs, Guieu et al., 2014). To do so, we made the following assumptions: 1) the aerosol concentrations are a snapshot in time but are representative of the study region, 2) the aerosol solubility estimates based on two sequential leaches are an upper limit of the aerosol Fe in seawater and 3) the water column stratified just before the deposition of atmospheric inputs, so MLD DFe will reflect inputs from above. Thus, the TTADs were defined as the integrated DFe concentrations in the SML for each station divided by the contribution of soluble Fe contained in aerosols averaged per basin to the water volume of the SML. Although, TTADs were lower in the West European and Iceland Basins with an average of $\sim 9 \pm 3$ months compared to other basins (7 ± 2 years and 5 ± 2 years for the Irminger and Labrador Seas, respectively) (Fig. 6) they were about three times higher than those reported for areas impacted by Saharan dust inputs (~ 3 months, Guieu et al., 2014). Therefore, the high TTADs measured in the Irminger and Labrador Seas and ranging from 2 to 15 years provided further evidence that atmospheric deposition were unlikely to supply Fe in sufficient quantity to be the main source of DFe (see Sections 4.2.1 and 4.3.2) while in the West European and Iceland Basins they played an additional source, perhaps the main source of Fe especially at station 36 which displayed TTAD of 3 months.

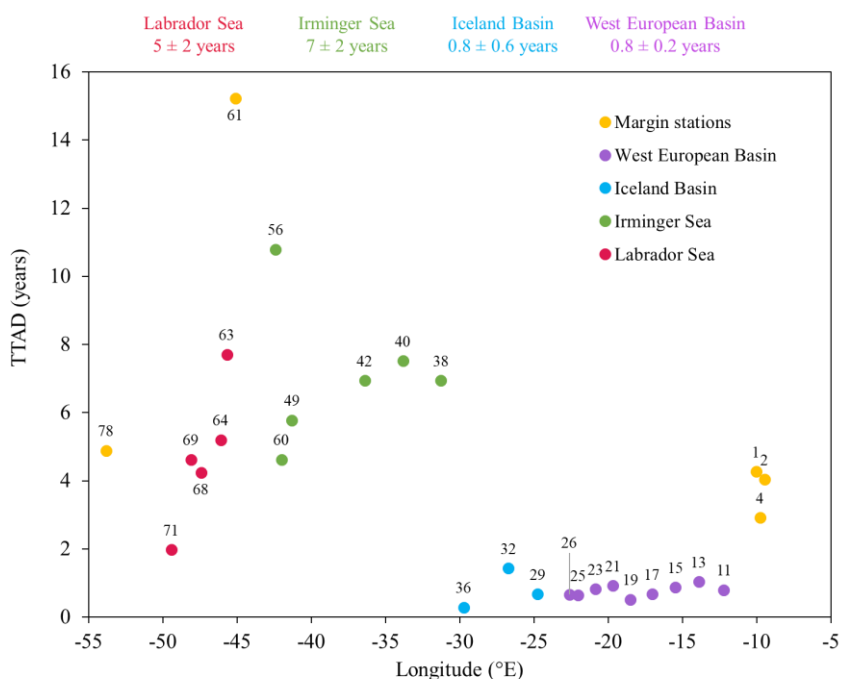


Figure 6: Plot of dissolved Fe (DFe) Turnover Times relative to Atmospheric Deposition (TTADs) calculated from soluble Fe contained in aerosols estimated from a two-stage sequential leach (UHP water, then 25% HAC, Shelley et al., this issue). Note that numbers on top of data points represent station numbers and that the colour coding refers to different region with in yellow, margin stations; in purple, the West European Basin; in blue, the Iceland Basin; in green, the Irminger Sea and in red,

the Labrador Sea. The numbers on top of the plot represent TTADs averaged for each oceanic basin and their standard deviation.

Deleted: ¶

Page 19 Line 5ff: replace “on” by “in”. And which similar pattern followed the station. Be precise! Sentence stating in Line 6 makes no sense, please rewrite!

→ We have corrected the text and rephrased the next sentence as suggested.

Formatted: List Paragraph, Bulleted + Level: 1 +
Aligned at: 0.63 cm + Indent at: 1.27 cm

Page 19 Lines 20-23: DFe concentration profiles from all coastal stations (stations 2, 4, 53, 56, 61 and 78) are reported in Figure 5. To avoid surface processes, only depths below 100 m depth will be considered in the following discussion. DFe and PFe followed a similar pattern at stations 2, 53, 56, and 78 with increasing concentrations towards the sediment, suggesting that either the sources of Fe supplied both Fe fractions (dissolved and particulate) or that PFe dissolution from sediments supplied DFe.

Page 19 Line 11: What has the composition of sediments to do with your PFe value? Nothing. . .

→ We have changed the text for clarification.

Formatted: List Paragraph, Bulleted + Level: 1 +
Aligned at: 0.63 cm + Indent at: 1.27 cm

Page 19 Lines 25-28: DFe:PFe ratios ranged from 0.01 (station 2, bottom sample) to 0.27 (station 4, ~ 400 m depth) mol:mol with an average value of 0.11 ± 0.07 mol:mol (n = 23, Table 4), highlighting a different behaviour of Fe between margins. This could be explained by the different nature of the sediments and/or different sediment conditions (e.g. redox, organic content).

Page 19 Line 15: “Intermediate behavior” of what? And then Chla? This paragraph is very hard to follow, what is the message you want to bring across, I can’t tell!

→ We removed this sentence for clarification.

Formatted: List Paragraph, Bulleted + Level: 1 +
Aligned at: 0.63 cm + Indent at: 1.27 cm

Page 19 Lines 28-33: Based on particulate and dissolved Fe and dissolved Al data (Gourain et al., 2018; Menzel Barraqueta et al., 2018, Table 4), three main different types of margins were reported (Gourain et al., 2018) with the highest lithogenic contribution observed at the Iberian Margin (stations 2 and 4) and the highest biogenic contribution at the Newfoundland Margin (station 78). These observations are consistent with higher TChl- α concentrations measured at the Newfoundland Margin and to a lesser extent at the Greenland Margin and the predominance of diatoms relative to other functional phytoplankton classes at both margins (Tonnard et al., in prep.).

Page 19 Line 26: “respect”? I respect you as a person, but samples usually don’t respect anything?

→ We have changed the word “respected” by “followed”.

Formatted: List Paragraph, Bulleted + Level: 1 +
Aligned at: 0.63 cm + Indent at: 1.27 cm

Page 19 Line 30ff: How do you know its manganese oxide, just use particulate Mn. And why you do not include the transmissometer data. That is what you wanted to show, or not that resuspended sediments control you particulate fraction.

→ We agree with the reviewer in the way that we are not sure these are manganese oxides as they were estimated as the fraction from the PMn that was not originating from a lithogenic fraction using Mn:Ti UCC ratio. Therefore, a biological source or a co-precipitation source without oxidation were not considered. We thus agree with the reviewer and we have changed the MnOx data towards PMn data in the PCA.

Formatted: List Paragraph, Bulleted + Level: 1 +
Aligned at: 0.63 cm + Indent at: 1.27 cm

→ We did not include the transmissometer data as we do not have true values for all samples and used the interpolated data.

Page 20 Line 3ff: You did not do a PCA for dFe, so how can you be sure that the dim1 controls DFe? I cannot follow.

→ Before performing the PCA, a huge number of variables were considered and we only kept the one that were correlated to DFe to build the PCA.

→ We have changed the text for clarification.

Page 20 Lines 6-16; Samples associated with high levels of particles (transmissometer < 99%) and below 500 m depth displayed a huge variability in DFe concentrations. From the entire dataset, 66 samples (~13% of the entire dataset) followed this criterion with 3 samples from the Iberian Margin (station 4), 14 samples from the West European Basin (station 1), 4 samples from the Iceland Basin (stations 29, 32, 36 and 38), 43 samples from the Irminger Sea (stations 40, 42, 44, 49 and 60) and 2 samples from the Labrador Sea (station 69). To determine which parameter was susceptible to explain the variation in DFe concentrations in these nepheloid layers, a Principal Component Analysis (PCA) on these samples. The input variables of the PCA were the particulate Fe, Al, and particulate manganese (PMn) (Gourain et al., 2018), the DAI (Menzel Barraqueta et al., 2018) and the Apparent Oxygen Utilization (AOU) and were all correlated to DFe concentrations explaining all together 93% of the subset variance (Fig. 11). The first dimension of the PCA was represented by the PAI, PFe and PMn concentrations and explained 59.5% of the variance, while the second dimension was represented by the DAI and the AOU parameters, explaining 33.2% of the variance. The two sets of variables were nearly at right angle from each other, indicating no correlation between them.

Page 20 Line 24: You did not show any evident information that would suggest that DFe is controlled by OM (you did not even show any data) and PMn. Like the others this paragraph needs more work!

→ We have reorganised the section and added complementary information.

Page 20 Lines 6-34, Page 21 lines 1-6:

4.4.2 Nepheloid layers:

Samples associated with high levels of particles (transmissometer < 99%) and below 500 m depth displayed a huge variability in DFe concentrations. From the entire dataset, 63 samples (~13% of the entire dataset) followed this criterion with 14 samples from the West European Basin (station 1), 4 samples from the Iceland Basin (stations 29, 32, 36 and 38), 43 samples from the Irminger Sea (stations 40, 42, 44, 49 and 60) and 2 samples from the Labrador Sea (station 69). To determine which parameter was susceptible to explain the variation in DFe concentrations in these nepheloid layers, a Principal Component Analysis (PCA) on these samples. The input variables of the PCA were the particulate Fe, Al, and particulate manganese (PMn) (Gourain et al., 2018), the DAI (Menzel Barraqueta et al., 2018) and the Apparent Oxygen Utilization (AOU) and were all correlated to DFe concentrations explaining all together 93% of the subset variance (see supplementary material Fig. S6). The first dimension of the PCA was represented by the PAI, PFe and PMn concentrations and explained 59.5% of the variance, while the second dimension was represented by the DAI and the AOU parameters, explaining 33.2% of the variance. The two sets of variables were nearly at right angle from each other, indicating no correlation between them.

The variations in DFe concentrations measured in bottom samples from stations 32, 36 (Iceland Basin), 42 and 44 (Irminger Sea) and 69 (Labrador Sea) were mainly explained by the first dimension of the PCA (see supplementary material Fig. S6). Therefore, samples characterized by the lowest DFe concentrations (stations 32 and 69) were driven by particulate Al and Mn concentrations and resulted in an enrichment of Fe within particles. These results are in agreement with previous

Formatted: Not Highlight

Formatted: List Paragraph, Bulleted + Level: 1 + Aligned at: 0.63 cm + Indent at: 1.27 cm

Formatted: Not Highlight

Formatted: Not Highlight

Formatted: Not Highlight

Formatted: List Paragraph, Bulleted + Level: 1 + Aligned at: 0.63 cm + Indent at: 1.27 cm

Formatted: Not Highlight

studies showing that the presence of Mn within particles can induce the formation of Fe-Mn oxides, contributing to the removal of Fe and Mn from the water column (Kan et al., 2012; Teng et al., 2001).

Low DFe concentrations (bottom samples from stations 42 and 1) were linked to DAL inputs and associated with lower AOU values. The release of Al has previously been observed from Fe and Mn oxide coatings on resuspended sediments under mildly reducing conditions (Van Beusekom, 1988). Conversely, higher DFe concentrations were observed for stations 44 and 49 and to a lesser extent station 60 coinciding with low DAL inputs and higher oxygen levels. This observation challenges the traditional view of Fe oxidation with oxygen, either abiotically or microbially induced. Indeed, remineralisation can decrease sediment oxygen concentrations, promoting reductive dissolution of PFe oxyhydroxides to DFe that can then diffuse across the sediment water interface as DFe(II) colloids (Homoky et al., 2011). Such processes will inevitably lead to rapid Fe removal through precipitation of nanoparticulate or colloidal Fe (oxyhydr)oxides, followed by aggregation or scavenging by larger particles (Boyd and Ellwood, 2010; Lohan and Bruland, 2008) unless complexation with Fe-binding organic ligands occurs (Batchelli et al., 2010; Gerringa et al., 2008). There exist, however, another process that is favoured in oxic benthic boundary layers (BBL) with low organic matter degradation and/or low Fe oxides, which implies the dissolution of particles after resuspension, namely the non-reductive dissolution of sediment (Homoky et al., 2013; Radic et al., 2011). In addition, these higher oxygenated samples were located within DSOW, which mainly originate (75% of the overflow) from the Nordic Seas and the Arctic Ocean (Tanhua et al., 2005), in which the ultimate source of Fe was reported by Klunder et al. (2012) to come from Eurasian river waters. The major Arctic rivers were highlighted by Slagter et al. (2017) to be a source of Fe-binding organic ligands that are then further transported via the TPD across the Denmark Strait. Hence, the enhanced DFe concentrations measured within DSOW might result from Fe-binding organic ligand complexation that were transported to the deep ocean as DSOW formed rather than the non-reductive dissolution of sediment.

Deleted: Tanhua et al., 2005

Formatted: Highlight

Page 20 Line 27ff: Include "some" in front of "maxima, Please tell me the difference between "the relationship between DFe and biological uptake" and "Did DFe concentrations potentially limit phytoplankton growth?" This sounds to me very connected with each other! Why not discussing that in the follow up paper?

We have corrected the first sentence as suggested and re-wrote the end of the paragraph for clarification. Note that we wanted to keep this discussion in this paper as it summarises the different processes discussed in this MS.

Deleted: ¶

Page 21 Lines 8-11: Overall, almost all the stations from the GEOVIDE voyage displayed DFe minima in surface water associated with some maxima of TChl-*a* (Fig. 3). In the following section, we specifically address the question of whether DFe concentrations potentially limit phytoplankton growth. Note that macronutrients and DFe limitations relative to phytoplankton functional classes are dealt in Tonnard et al. (in prep.).

Page 20 Line 31: Include mean or average Plus standard deviation

Formatted: Not Highlight

→ We have included the average and SD and corrected few mistakes.

Formatted: List Paragraph, Bulleted + Level: 1 + Aligned at: 0.63 cm + Indent at: 1.27 cm

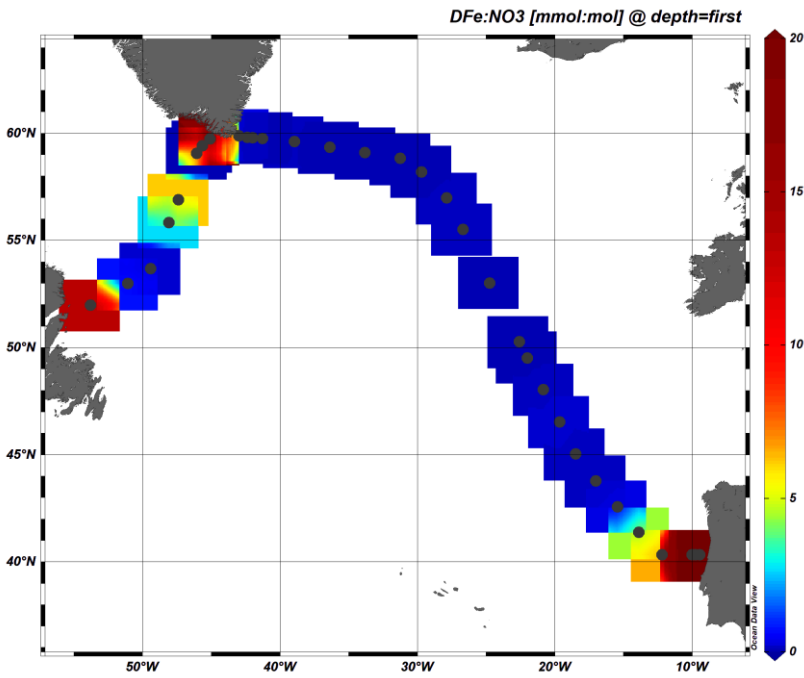
Page 21 Lines 13-14: The DFe:NO₃⁻ ratios in surface waters varied from 0.02 (station 36) to 38.6 (station 61) mmol:mol with an average of 5 ± 10 mmol:mol (see supplementary material Fig. S7).

Formatted: Not Highlight

Formatted: Highlight

Page 21 Line 4: Please include numbers! Following the text in the paragraph, it is very hard to follow, you jump between F:N ratios, water masses and Chl a. Try to keep it short and weed out unnecessary details. Otherwise you will lose the reader!

→ We have changed the text accordingly and added a surface map of DFe:NO₃- ratios.



Formatted: Not Highlight

Formatted: List Paragraph, Bulleted + Level: 1 + Aligned at: 0.63 cm + Indent at: 1.27 cm

Formatted: Not Highlight

Page 21 Lines 12--33 Page 22 Lines 1-34, Page 23 Lines 1-3: A key determinant for assessing the significance of a DFe source is the magnitude of the DFe:macronutrient ratio supplied, since this term determines to which extent DFe will be utilised. The DFe:NO₃⁻ ratios in surface waters varied from 0.02 (station 36) to 38.6 (station 61) mmol:mol with an average of 5 ± 10 mmol:mol (see supplementary material Fig. S7). Values were typically equal or lower than 0.28 mmol mol⁻¹ in all basins except at the margins and at stations 11, 13, 68, 69 and 77. The low nitrate concentrations observed at the eastern and western Greenland and Newfoundland Margins reflected a strong phytoplankton bloom which had reduced the concentrations as highlighted by the elevated integrated TChl-*a* concentrations ranging from 129.6 (station 78) to 398.3 (station 61) mg m⁻². At the Iberian Margin, they likely reflected the influence of the N-limited Tagus River (stations 1, 2 and 4) with its low TChl-*a* integrated concentrations that ranged from 31.2 (station 1) to 46.4 (station 4) mg m⁻². The high DFe:NO₃⁻ ratios determined at those stations, which varied from 13.4 (station 78) to 38.6 (station 61) mmol:mol, suggested that waters from these areas, despite having the lowest NO₃⁻ concentrations, were relatively enriched in DFe compared to waters from Iceland Basin and Irminger Sea.

Formatted: Not Highlight

Formatted: Not Highlight

Formatted: Not Highlight

In our study, DFe:NO₃⁻ ratios displayed a gradient from the West European Basin to Greenland (supplementary material S7 and S8). This trend only reverses when the influence of Greenland was encountered, as also observed by Painter et al. (2014). The remineralisation of organic matter is a

major source of macro and micronutrients in subsurface waters (from 50 to 250 m depth). Remineralisation is associated with the consumption of oxygen and therefore, Apparent Oxygen Utilization (AOU) can provide a quantitative estimate of the amount of material that has been remineralised. While no relationship was observed below 50 m depth for NO_3^- or DFe and AOU considering all the stations, a significant correlation was found in the Subpolar gyre when removing the influence of margins (stations 29-49, 56, 60, 63-77) ($\text{AOU} = 3.88 \text{ NO}_3^- - 39.32$, $R^2=0.79$, $n=69$, p -value < 0.001). This correlation indicates that remineralisation of Particulate Organic Nitrogen (PON) greatly translates into Dissolved Inorganic Nitrogen (DIN) and that NO_3^- can be used as a good tracer for remineralisation in the studied area. Within these Subpolar gyre waters, there was a significant correlation between DFe and AOU ($\text{AOU} = 22.6 \text{ DFe}$, $R^2=0.34$, $n=53$, p -value < 0.001). The open-ocean stations from Subpolar gyre also exhibited a good linear correlation between DFe and NO_3^- ($R^2=0.42$, $n=51$, p -value < 0.05). The slope of the relationship, representing the typical remineralisation ratio, was $R_{\text{Fe:N}} = 0.07 \pm 0.01 \text{ mmol mol}^{-1}$. The intercept of the regression line was $-0.4 \pm 0.2 \text{ nmol L}^{-1}$, reflecting possible excess of preformed NO_3^- compare to DFe in these water masses. These significant correlations allow us to use the Fe^* tracer to assess where DFe concentrations potentially limit phytoplankton growth by subtracting the contribution of organic matter remineralisation from the dissolved Fe pool, as defined by Rijkenberg et al. (2014) and Parekh et al. (2005) for PO_4^{3-} , and modified here for NO_3^- as follow:

$$\text{Fe}^* = [\text{DFe}] - R_{\text{Fe:N}} \times [\text{NO}_3^-] \text{ (eq. 4)}$$

where $R_{\text{Fe:N}}$ refers to the average biological uptake ratio Fe over nitrogen, and $[\text{NO}_3^-]$ refers to nitrate concentrations in seawater. Although, we imposed a fixed biological $R_{\text{Fe:N}}$ of $0.05 \text{ mmol mol}^{-1}$, it is important to note that the biological uptake ratio of $\text{DFe}:\text{NO}_3^-$ is not likely to be constant. Indeed, this ratio has been found to range from 0.05 to 0.9 mmol mol^{-1} depending on species (Ho et al., 2003; Sunda and Huntsman, 1995; Twining et al., 2004). The ratio we choose is thus less drastic to assess potential Fe limitation and more representative of the average biological uptake of DFe over NO_3^- calculated for this study (i.e. $R_{\text{Fe:N}} = 0.07 \pm 0.01 \text{ mmol mol}^{-1}$, for Subpolar waters). Negative values of Fe^* indicate the removal of DFe that is faster than the input through remineralisation or external sources and positive values suggest input of DFe from external sources (Fig. 7). Consequently, figure 7 shows that phytoplankton communities with very high Fe requirements relative to NO_3^- ($R_{\text{Fe:N}} = 0.9$) will only be able to grow above continental shelves where there is a high supply of DFe as previously reported by Nielsdóttir et al. (2009) and Painter et al. (2014). All these results are corroborating the importance of the Tagus River (Iberian Margin, see section 4.2.1), glacial inputs in the Greenland and Newfoundland Margins (see section 4.2.2) and to a lesser extent atmospheric inputs (see section 4.2.3) in supplying Fe with $\text{Fe}:\text{N}$ ratios higher than the average biological uptake/demand ratio. Figure 7 (see also supplementary material S7, S8, S9 and S10) also highlights the Fe limitation for the low-Fe requirement phytoplankton class ($R_{\text{Fe:N}} = 0.05$) within the Iceland Basin, Irminger and Labrador Seas. The Fe deficiency observed in surface waters ($> 50 \text{ m}$ depth) from the Irminger and Labrador Seas might be explained by low atmospheric deposition for the ICPMW and the LSW (Shelley et al., 2017). Low atmospheric Fe supply and sub-optimal $\text{Fe}:\text{N}$ ratios in winter overturned deep water could favour the formation of the High-Nutrient, Low-Chlorophyll (HNLC) conditions. The West European Basin, despite exhibiting some of the highest $\text{DFe}:\text{NO}_3^-$ ratios within surface waters (see supplementary material Fig. S8), displayed the strongest Fe-depletion from 50 m depth down to the bottom, suggesting that the main source of Fe was coming from dust deposition and/or riverine inputs.

Similarly as for the West European Basin, the pattern displayed in the surface map of $\text{DFe}:\text{NO}_3^-$ ratios (supplementary material S8) extended to about 50 m depth, after which the trend reversed (Fig. 7

and supplementary material Fig. S7). Below 50 m depth, the Fe* tracer (Fig. 7) was positive in the Irminger Sea and overall negative in the other basins. In the Irminger Sea positive Fe* values were likely the result of the winter entrainment of Fe-rich LSW (see section 4.2.1) coinciding with high remineralised carbon fluxes in this area (station 44; Lemaître et al., 2017) (see section 4.2.2). The largest drawdown in DFe:NO₃⁻ ratios was observed between stations 34 and 38 and was likely due to the intrusion of the ICSPMW, this water mass exhibiting low DFe and high in NO₃⁻ (from 7 to 8 μmol L⁻¹) concentrations. Similarly, the SAIW exhibited high NO₃⁻ concentrations. Both the ICSPMW and the SAIW sourced from the NAC. The NAC as it flows along the coast of North America receives atmospheric depositions from anthropogenic sources (Shelley et al., 2017; 2015) which deliver high N relative to Fe (Jickells and Moore, 2015) and might be responsible for the observed ranges.

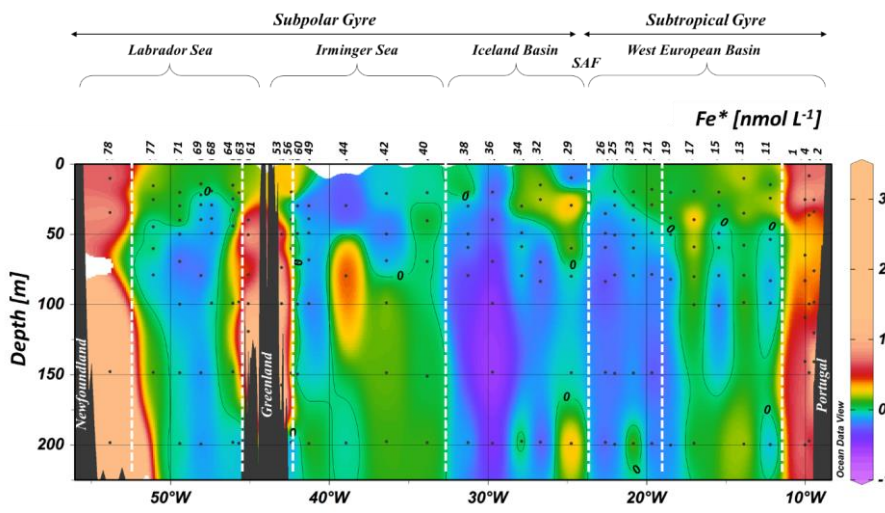
Formatted: Highlight

Page 21 Line 20ff: Can you explain to me why you calculate Fe* for the entire water body (Fig. 13) and explain DFe limitation of the phytoplankton community. They live in the first 100-200 m. Same fro Fig.14.

Formatted: Not Highlight

- ➔ We calculated the Fe* for the entire water body as water mass circulation and/or processes such as deep convection/upwelling, ... can homogenized deep water masses with surface water masses. Thus, looking at DFe:NO₃⁻ ratios in these water masses appeared for us to be as important as just looking at the surface where phytoplankton live.
- ➔ However, we understand the reviewer's opinion and decided to restrict this section to the top 250 meters. Consequently, we did a new plot for Fig. 13 with only the upper water column and removed Fig. 14.

Formatted: List Paragraph, Bulleted + Level: 1 + Aligned at: 0.63 cm + Indent at: 1.27 cm



Formatted: Not Highlight

Reading the last sentence of the section on page 22 "However, atmospheric loading (and especially Fe) was higher within the subtropical gyre than elsewhere in the GEOVIDE section mainly due to the proximity to mineral dust source (i.e. the Sahara Desert)." I feel I am still stuck in the Atmospheric chapter. Please shorten the paragraph and just say what you can prove with data.

Formatted: Not Highlight

- ➔ We have removed the last two sentences to shorten the paragraph.

Formatted: List Paragraph, Bulleted + Level: 1 + Aligned at: 0.63 cm + Indent at: 1.27 cm

Page 22 Line 14ff: The entire conclusion needs an overhaul!

Formatted: Not Highlight

→ We have modified the conclusion to be more specific.

Page 23 Lines 5-31 Page 24 Lines 1-2: The DFe concentrations measured during this study were in good agreement with previous studies that spanned the West European Basin. However, within the Irminger Basin the DFe concentrations measured during this study were up to 3 times higher than the ones measured by Rijkenberg et al. (2014) in deep waters (> 1000 m depth) that was likely explained by the different water masses encountered (i.e. the Polar Intermediate Water, ~ 2800 m depth) and by a stronger signal of the Iceland Scotland Overflow Water (ISOW) from 1200 to 2300 m depth. This corresponded to the most striking feature of the whole section with DFe concentrations reaching up to 2.5 nmol L⁻¹ within the ISOW, Denmark Strait Overflow Water (DSOW) and Labrador Sea Water (LSW), three water masses that are part of the Deep Western Boundary Current and was likely the result of a lateral advection of particles in the Irminger. However, as these water masses reached the Labrador Sea, lower DFe levels were measured. These differences could be explained by different processes occurring within the benthic nepheloid layers, where DFe was sometimes trapped onto particles due to Mn-sediment within the Labrador Sea (Gourain et al., 2018) and sometimes released from the sediment potentially as a result of interactions with dissolved organic matter. Such Fe-binding organic ligands could have also been produced locally due to the intense remineralisation rate reported by Lemaître et al. (2017) of biogenic particles (Boyd et al., 2010; Gourain et al., 2018). The LSW exhibited increasing DFe concentrations along its flow path, likely resulting from sediment inputs at the Newfoundland Margin. Although DFe inputs through hydrothermal activity were expected at the slow spreading Reykjanes Ridge (Baker and German, 2004b; German et al., 1994), our data did not evidence this specific source as previously pointed by Achterberg et al. (2018) further north (~60°N) from our section.

In surface waters several sources of DFe were highlighted especially close to lands, with riverine inputs from the Tagus River at the Iberian margin (Menzel Barraqueta et al., 2018) and meteoric inputs (including coastal runoff and glacial meltwater) at the Newfoundland and Greenland margins (Benetti et al., 2016). Substantial sediment inputs were observed at all margins but with different intensity. The highest DFe sediment input was located at the Newfoundland margin, while the lowest was observed at the eastern Greenland margin. These differences could be explained by the different nature of particles with the most lithogenic located at the Iberian margin and the most biogenic, at the Newfoundland margin (Gourain et al., 2018). Although previous studies (e.g. Jickells et al., 2005; Shelley et al., 2015) reported that atmospheric inputs substantially fertilized surface waters from the West European Basin, in our study only stations located in the West European and Iceland Basins exhibited enhanced SML DFe inventories with lower TTADs. However, these TTADs were about three times higher than those reported for Saharan dust inputs and thus atmospheric deposition appeared to be a minor source of Fe at the sampling period. Finally, there was evidence of convective inputs of the LSW to surface seawater caused by long tip jet event (Piron et al., 2016) that deepened the winter mixed layer down to ~ 1200 m depth (Zunino et al., 2017), in which Fe was in excess of nitrate and where thus Fe was not limiting at the sampling period.

Figures:

Figure 1: great;

Figure 2: increase letter size, it is hard to read;

Figure 3: I am not sure that white contour lines for DFe help to understand Chl a. I would remove DFe and include this figure in the supplementary material.

Formatted: List Paragraph, Bulleted + Level: 1 +
Aligned at: 0.63 cm + Indent at: 1.27 cm

Formatted: English (Australia)

Formatted: English (Australia)

Formatted: English (Australia)

Formatted: English (Australia)

Figure 4, 5 and 6(?): great

Figure 7, 8, 9, 10: can go in the supplementary material, maybe Fig. 9 you can keep

Figure 11 -14: in the sup mat.,

Maybe Figure 13 for the first 200 m can stay!

Table 3 and 4: belongs into the sup. Material

→ As you suggested we only kept Figs 1, 2, 4, 5, 9, 10 (the new one) and 13 (with your suggestions), all other Figures are now in the supplementary material. Tables 3 is also in the supplementary material.

Formatted: List Paragraph, Bulleted + Level: 1 +
Aligned at: 0.63 cm + Indent at: 1.27 cm

Achterberg, E. P., Steigenberger, S., Marsay, C. M., LeMoigne, F. A., Painter, S. C., Baker, A. R., Connelly, D. P., Moore, C. M., Tagliabue, A., and Tanhua, T.: Iron Biogeochemistry in the High Latitude North Atlantic Ocean, *Scientific reports*, 8, 1-15, 10.1038/s41598-018-19472-1, 2018.

Aminot, A., and Kerouel, R.: Dosage automatique des nutriments dans les eaux marines, Quae ed., 2007.

Annett, A. L., Skiba, M., Henley, S. F., Venables, H. J., Meredith, M. P., Statham, P. J., and Ganeshram, R. S.: Comparative roles of upwelling and glacial iron sources in Ryder Bay, coastal western Antarctic Peninsula, *Marine Chemistry*, 176, 21-33, 10.1016/j.marchem.2015.06.017, 2015.

Bacon, S., Gould, W. J., and Jia, Y.: Open-ocean convection in the Irminger Sea, *Geophysical Research Letters*, 30, 1246, doi:10.1029/2002GL016271, 2003.

Baker, A. R., Adams, C., Bell, T. G., Jickells, T. D., and Ganzeveld, L.: Estimation of atmospheric nutrient inputs to the Atlantic Ocean from 50°N to 50°S based on large-scale field sampling: Iron and other dust-associated elements, *Global Biogeochemical Cycles*, 27, 755-767, 10.1002/gbc.20062, 2013.

Baker, A. T., and German, C. R.: On the Global Distribution of Hydrothermal vent Fields, in: *Mid-Ocean Ridges*, edited by: German, C. R., Lin, J., and Parson, L. M., 2004a.

Baker, E. T., and German, C. R.: Hydrothermal Interactions Between the Lithosphere and Oceans, in: *Mid-Ocean Ridges*, edited by: German, C. R., Lin, J., and Parson, L. M., *Geophysical Monograph Series*, AGU, 245-266, 2004b.

Barton, A. D., Greene, C. H., Monger, B. C., and Pershing, A. J.: The Continuous Plankton Recorder survey and the North Atlantic Oscillation: Interannual- to Multidecadal-scale patterns of phytoplankton variability in the North Atlantic Ocean, *Progress in Oceanography*, 58, 337-358, 10.1016/j.pocean.2003.08.012, 2003.

Batchelli, S., Muller, F. L. L., Chang, K. C., and Lee, C. L.: Evidence for Strong but Dynamic Iron-Humic Colloidal Associations in Humic-Rich Coastal Waters., *Environmental Science & Technology*, 44, 8485-8490, 2010.

Benetti, M., Reverdin, G., Pierre, C., Khaliwala, S., Tournadre, B., Olafsdottir, S., and Naamar, A.: Variability of sea ice melt and meteoric water input in the surface Labrador Current off Newfoundland, *Journal of Geophysical Research Oceans*, 121, 2841-2855, doi:10.1002/2015JC011302., 2016.

Benetti, M., Reverdin, G., Lique, C., Yashayaev, I., Holliday, N. P., Tynan, E., Torres-Valdes, S., Lherminier, P., Tréguer, P., and Sarthou, G.: Composition of freshwater in the spring of 2014 on the southern Labrador shelf and slope, *Journal of Geophysical Research: Oceans*, 122, 1102-1121, 10.1002/2016jc012244, 2017.

Bersch, M., Yashayaev, I., and Koltermann, K. P.: Recent changes of the thermohaline circulation in the subpolar North Atlantic, *Ocean Dynamics*, 57, 223-235, 10.1007/s10236-007-0104-7, 2007.

Bhatia, M. P., Kujawinski, E. B., Das, S. B., Breier, C. F., Henderson, P. B., and Charette, M. A.: Greenland meltwater as a significant and potentially bioavailable source of iron to the ocean, *Nature Geoscience*, 2013, 274-278, 10.1038/ngeo1746, 2013.

Bonnet, S., and Guieu, C.: Atmospheric forcing on the annual iron cycle in the western Mediterranean Sea: A 1-year survey, *Journal of Geophysical Research*, 111, 10.1029/2005jc003213, 2006.

Boyd, P. W., Watson, A. J., Law, C. S., Abraham, E. R., Trull, T., Murdoch, R., Bakker, D. C. E., Bowie, A. R., Buesseler, K. O., Chang, H., Charette, M., Croot, P., Downing, K., Frew, R., Gall, M., Hadfield, M., Hall, J., Harvey, M., Jameson, G., LaRoche, J., Liddicoat, M., Ling, R., Maldonado, M. T., McKay, R. M., Nodder, S., Pickmere, S., Pridmore, R., Rintoul, S., Safi, K., Sutton, P., Strzepek, R., Tanneberger, K., Turner, S., Waite, A., and Zeldis, J.: A mesoscale phytoplankton bloom in the polar Southern Ocean stimulated by iron fertilization, *Nature*, 407, 695-702, 2000.

Boyd, P. W., and Ellwood, M. J.: The biogeochemical cycle of iron in the ocean, *Nature Geoscience*, 3, 675-682, 10.1038/ngeo964, 2010.

Formatted: French (France)

Boyd, P. W., Ibsanmi, E., Sander, S. G., Hunter, K. A., and Jackson, G. A.: Remineralization of upper ocean particles: Implications for iron biogeochemistry, *Limnology and Oceanography*, 55, 1271-1288, 10.4319/lo.2010.55.3.1271, 2010.

Buck, C. S., Landing, W. M., Resing, J. A., and Measures, C. I.: The solubility and deposition of aerosol Fe and other trace elements in the North Atlantic Ocean: Observations from the A16N CLIVAR/CO2 repeat hydrography section, *Marine Chemistry*, 120, 57-70, 10.1016/j.marchem.2008.08.003, 2010.

Charette, M. A., Morris, P. J., Henderson, P. B., and Moore, W. S.: Radium isotope distributions during the US GEOTRACES North Atlantic cruises, *Marine Chemistry*, 177, 184-195, 10.1016/j.marchem.2015.01.001, 2015.

Chen, Y. J.: Influence of the Iceland mantle plume on crustal accretion at the inflated Reykjanes Ridge: Magma lens and low hydrothermal activity, *Journal of Geophysical Research*, 108, 2524, 2003.

Conway, T. M., and John, S. G.: Quantification of dissolved iron sources to the North Atlantic Ocean, *Nature*, 511, 212-215, 10.1038/nature13482, 2014.

Cooper, L. W., Whitledge, T. E., Grebmeier, J. M., and Weingartner, T.: The nutrient, salinity, and stable oxygen isotope composition of Bering and Chukchi Seas waters in and near the Bering Strait, *Journal of Geophysical Research*, 102, 12,563-512,573, 1997.

Cooper, L. W., McClelland, J. W., Holmes, R. M., Raymond, P. A., Gibson, J. J., Guay, C. K., and Peterson, B. J.: Flow-weighted values of runoff tracers ($\delta^{18}\text{O}$, DOC, Ba, alkalinity) from the six largest Arctic rivers, *Geophysical Research Letters*, 35, 1-5, 10.1029/2008GL035007, 2008.

Crane, K., Johnson, L., Applegate, B., Nishimura, C., Buck, R., Jones, C., Vogt, P., and Kos'yan, R.: Volcanic and Seismic Swarm Events on the Reykjanes Ridge and Their Similarities to Events on Iceland: Results of a Rapid Response Mission, *Marine Geophysical Researches*, 19, 319-338, 1997.

Dehairs, F., Shopova, D., Ober, S., Veth, C., and Goeyens, L.: Particulate barium stocks and oxygen consumption in the Southern Ocean mesopelagic water column during spring and early summer: Relationship with export production, *Deep Sea Research II*, 44, 497-516, 10.1016/S0967-0645(96)00072-0, 1997.

Deng, F., Henderson, G. M., Castrillejo, M., and Perez, F. F.: Evolution of ^{231}Pa and ^{230}Th in overflow waters of the North Atlantic, *Biogeosciences*, 1-24, 10.5194/bg-2018-191, 2018.

Fagel, N., Robert, C., and Hilaire-Marcel, C.: Clay mineral signature of the NW Atlantic Boundary Undercurrent, *Marine Geology*, 130, 19-28, 1996.

Fagel, N., Robert, C., Preda, M., and Thorez, J.: Smectite composition as a tracer of deep circulation: the case of the Northern North Atlantic, *Marine Geology*, 172, 309-330, 2001.

Follows, M., and Dutkiewicz, S.: Meteorological modulation of the North Atlantic Spring Bloom, *Deep Sea Research Part II: Topical Studies in Oceanography*, 49, 321-344, 2001.

García-Ibáñez, M. I., Pérez, F. F., Lherminier, P., Zunino, P., Mercier, H., and Tréguer, P.: Water mass distributions and transports for the 2014 GEOVIDE cruise in the North Atlantic, *Biogeosciences*, 15, 2075-2090, 10.5194/bg-15-2075-2018, 2018.

German, C. R., Briem, J., Chin, C. S., Danielsen, M., Holland, S., James, R. H., Jonsdottir, A., Ludford, E., Moser, C., Olafsson, J., Palmer, M. R., and Rudnicki, M. D.: Hydrothermal activity on the Reykjanes Ridge: the Steinahóll vent-field at $63^{\circ}06'N$, *Earth and Planetary Science Letters*, 121, 647-654, 1994.

Gerringa, L. J. A., Blain, S., Laan, P., Sarthou, G., Veldhuis, M. J. W., Brussaard, C. P. D., Viollier, E., and Timmermans, K. R.: Fe-binding dissolved organic ligands near the Kerguelen Archipelago in the Southern Ocean (Indian sector), *Deep Sea Research Part II: Topical Studies in Oceanography*, 55, 606-621, 10.1016/j.dsr2.2007.12.007, 2008.

Gerringa, L. J. A., Slagter, H. A., Bown, J., van Haren, H., Laan, P., de Baar, H. J. W., and Rijkenberg, M. J. A.: Dissolved Fe and Fe-binding organic ligands in the Mediterranean Sea – GEOTRACES G04, *Marine Chemistry*, 194, 100-113, 10.1016/j.marchem.2017.05.012, 2017.

Gourain, A., Planquette, H., Cheize, M., Menzel-Barraqueta, J. L., Boutorh, J., Shelley, R. U., Pereira-Contreira, L., Lemaitre, N., Lacan, F., Lherminier, P., and Sarthou, G.: particulate trace metals along the GEOVIDE section, *Biogeosciences*, 2018.

Guieu, C., Aumont, O., Paytan, A., Bopp, L., Law, C. S., Mahowald, N., Achterberg, E. P., Marañón, E., Salihoğlu, B., Crise, A., Wagener, T., Herut, B., Desboeufs, K., Kanakidou, M., Olgun, N., Peters, F., Pulido-Villena, E., Tovar-Sanchez, A., and Völker, C.: The significance of the episodic nature of atmospheric deposition to Low Nutrient Low Chlorophyll regions, *Global Biogeochemical Cycles*, 28, 1179-1198, 10.1002/2014gb004852, 2014.

Harrison, W. G., Yngve Børnsheim, K., Li, W. K. W., Maillet, G. L., Pepin, P., Sakshaug, E., Skogen, M. D., and Yeats, P. A.: Phytoplankton production and growth regulation in the Subarctic North Atlantic: A comparative study of the Labrador Sea-Labrador/Newfoundland shelves and Barents/Norwegian/Greenland seas and shelves, *Progress in Oceanography*, 114, 26-45, 10.1016/j.pocean.2013.05.003, 2013.

Hatta, M., Measures, C. I., Wu, J., Roshan, S., Fitzsimmons, J. N., Sedwick, P., and Morton, P.: An overview of dissolved Fe and Mn distributions during the 2010-2011 US GEOTRACES north Atlantic cruises: GEOTRACES GA03, Deep-Sea Research Part II-Topical Studies in Oceanography, 116, 117-129, 10.1016/j.dsr2.2014.07.005, 2015.

Hawkings, J. R., Wadham, J. L., Tranter, M., Raiswell, R., Benning, L. G., Statham, P. J., Tedstone, A., Nienow, P., Lee, K., and Telling, J.: Ice sheets as a significant source of highly reactive nanoparticulate iron to the oceans, *Nature communications*, 5, 1-8, 10.1038/ncomms4929, 2014.

Henson, S. A., Dunne, J. P., and Sarmiento, J. L.: Decadal variability in North Atlantic phytoplankton blooms, *Journal of Geophysical Research*, 114, 10.1029/2008jc005139, 2009.

Ho, T.-Y., Quigg, A., Finkel, Z. V., Milligan, A. J., Wyman, K., Falkowski, P. G., and Morel, F. M. M.: The elemental composition of some marine phytoplankton, *Journal of Phycology*, 39, 1145-1159, 2003.

Homoky, W. B., Hembury, D. J., Hepburn, L. E., Mills, R. A., Statham, P. J., Fones, G. R., and Palmer, M. R.: Iron and manganese diagenesis in deep sea volcanogenic sediments and the origins of pore water colloids, *Geochimica Et Cosmochimica Acta*, 75, 5032-5048, 10.1016/j.gca.2011.06.019, 2011.

Homoky, W. B., John, S. G., Conway, T. M., and Mills, R. A.: Distinct iron isotopic signatures and supply from marine sediment dissolution, *Nature Communications*, 4, 10.1038/ncomms3143, 2013.

Humphreys, M. P., Griffiths, A. M., Achterberg, E. P., Holliday, N. P., Rérolle, V., Menzel Barraqueta, J. L., Couldrey, M. P., Oliver, K. I., Hartman, S. E., and Esposito, M.: Multidecadal accumulation of anthropogenic and remineralized dissolved inorganic carbon along the Extended Ellett Line in the northeast Atlantic Ocean, *Global Biogeochemical Cycles*, 30, 293-310, doi: 10.1002/2015GB005246, 2016.

Jickells, T., and Moore, C. M.: The importance of atmospheric deposition for ocean productivity, *Annual Review of Ecology, Evolution, and Systematics*, 46, 481-501, 10.1146/annurev-ecolsys-112414-054118, 2015.

Jickells, T. D., An, Z. C., Andersen, K. K., Baker, A. R., Bergametti, G., Brooks, N., Cao, J. J., Boyd, P. W., Duce, R. A., Hunter, K. A., Kawahata, H., Kubilay, N., laRoche, J., Liss, P. S., Mahowald, N., Prospero, J. M., Ridgwell, A. J., Tegen, I., and Torres, R.: Global iron connections between desert dust, ocean biogeochemistry, and climate, *Science*, 308, 67-71, 2005.

Jones, E. P., Anderson, L. G., and Swift, J. H.: Distribution of Atlantic and Pacific waters in the upper Arctic Ocean: Implications for circulation, *Geophysical Research Letters*, 25, 765-768, 1998.

Kan, C. C., Chen, W. H., Wan, M. W., Phatai, P., Wittayakun, J., and Li, K. F.: The preliminary study of iron and manganese removal from groundwater by NaOCl oxidation and MF filtration, *Sustain. Environ. Res.*, 22, 25-30, 2012.

Kissel, C., Laj, C., Mulder, T., Wandres, C., and Cremer, M.: The magnetic fraction: A tracer of deep water circulation in the North Atlantic, *Earth and Planetary Science Letters*, 288, 444-454, 10.1016/j.epsl.2009.10.005, 2009.

Klunder, M. B., Bauch, D., Laan, P., de Baar, H. J. W., van Heuven, S. M. A. C., and Ober, S.: Dissolved iron in the Arctic shelf seas and surface waters of the Central Arctic Ocean: impact of Arctic river water and ice-melt, *Journal of Geophysical Research*, 117, 1-18, 2012.

Kondo, Y., and Moffett, J. W.: Iron redox cycling and subsurface offshore transport in the eastern tropical South Pacific oxygen minimum zone, *Marine Chemistry*, 168, 95-103, 10.1016/j.marchem.2014.11.007, 2015.

Lackschewitz, K. S., Endler, R., Gehrke, B., Wallrabe-Adams, H.-J., and Thiede, J.: Evidence for topography- and current-controlled deposition on the reykjanes Ridge between 59°N and 60°N, *Deep-Sea Research I*, 43, 1683-1711, 1996.

Laes, A., Blain, S., Laan, P., Achterberg, E. P., Sarthou, G., and de Baar, H. J. W.: Deep dissolved iron profiles in the eastern North Atlantic in relation to water masses, *Geophysical Research Letters*, 30, 10.1029/2003gl017902, 2003.

Lagerström, M. E., Field, M. P., Seguret, M., Fischer, L., Hann, S., and Sherrell, R. M.: Automated on-line flow-injection ICP-MS determination of trace metals (Mn, Fe, Co, Ni, Cu and Zn) in open ocean seawater: Application to the GEOTRACES program, *Marine Chemistry*, 155, 71-80, 10.1016/j.marchem.2013.06.001, 2013.

Lambelet, M., van de Flierdt, T., Crocket, K., Rehkemper, M., Katharina, K., Coles, B., Rijkenberg, M. J. A., Gerringa, L. J. A., de Baar, H. J. W., and Steinfeldt, R.: Neodymium isotopic composition and concentration in the western North Atlantic Ocean: Results from the GEOTRACES GA02 section, *Geochimica Et Cosmochimica Acta*, 177, 1-29, 2016.

Le Roy, E., Sanial, V., Charette, M. A., van Beek, P., Lacan, F., Jacquet, S. H. M., Henderson, P. B., Souhaut, M., García-Ibáñez, M. I., Jeandel, C., Pérez, F. F., and Sarthou, G.: The 226Ra–Ba relationship in the North Atlantic during GEOTRACES-GA01, *Biogeosciences*, 15, 3027-3048, 10.5194/bg-15-3027-2018, 2018.

Lemaître, N., Planchon, F., Planquette, H., Dehairs, F., Fonseca-Batista, D., Roukaerts, A., Deman, F., Tang, Y., Mariez, C., and Sarthou, G.: High variability of export fluxes along the North Atlantic GEOTRACES section GA01: Particulate organic carbon export deduced from the 234Th method *Biogeosciences*, 1-38, 10.5194/bg-2018-190, 2018.

Lemaître, N., planquette, H., Planchon, F., Sarthou, G., Jacquet, S., Garcia-Ibanez, M. I., Gourain, A., Cheize, M., Monin, L., Andre, L., Laha, P., Terryn, H., and Dehairs, F.: Particulate barium tracing significant mesopelagic carbon remineralisation in the North Atlantic *Biogeosciences Discussions*, 2017.

Liu, X. W., and Millero, F. J.: The solubility of iron in seawater, *Marine Chemistry*, 77, 43-54, 10.1016/s0304-4203(01)00074-3, 2002.

Lohan, M. C., and Bruland, K. W.: Elevated Fe(II) and Dissolved Fe in Hypoxic Shelf Waters off Oregon and Washington: An Enhanced Source of Iron to Coastal Upwelling Regimes, *Environmental Science & Technology*, 42, 6462-6468, 10.1021/es800144j, 2008.

Longhurst, A. R.: *Ecological geography of the Sea*, Second Edition ed., Elsevier Academic Press publications, Burlington, 542 pp., 2007.

Martin, J. D., and Fitzwater, S. E.: Iron deficiency limits phytoplankton growth in the north-east Pacific subarctic, *Nature*, 331, 341-343, 1988.

Martin, J. H., Fitzwater, S. E., and Gordon, R. M.: Iron deficiencies limits phytoplankton growth in Antarctic waters, *Global Biogeochemical Cycles*, 4, 5-12, 1990.

Martin, J. H., Coale, K. H., Johnson, K. S., Fitzwater, S. E., Gordon, R. M., Tanner, S. J., Hunter, C. N., Elrod, V. A., Nowicki, J. L., Coley, T. L., Barber, R. T., Lindley, S., Watson, A. J., Van Scoy, K., Law, C. S., Liddicoat, M. I., Ling, R., Stanton, T., Stockel, J., Collins, C., Anderson, A., Bidigare, R., Ondrusek, M., Latasa, M., Millero, F. J., Lee, K., Yao, W., Zhang, J. Z., Friederich, G., Sakamoto, C., Chavez, F., Buck, K., Kolber, Z., Greene, R., Falkowski, P., Chisholm, S. W., Hoge, F., Swift, R., Yungel, J., Turner, S., Nightingale, P., Hatton, A., Liss, P., and Tindale, N. W.: Testing the Iron Hypothesis in Ecosystems of the Equatorial Pacific Ocean, *Nature*, 371, 123-129, 10.1038/371123a0, 1994.

Measures, C. I., Brown, M. T., Selph, K. E., Apprill, A., Zhou, M., Hatta, M., and Hiscock, W. T.: The influence of shelf processes in delivering dissolved iron to the HNLC waters of the Drake Passage, Antarctica, *Deep Sea Research Part II: Topical Studies in Oceanography*, 90, 77-88, 10.1016/j.dsr2.2012.11.004, 2013.

Melling, H., and Moore, R. M.: Modification of halocline source waters during freezing on the Beaufort Sea shelf: Evidence from oxygen isotopes and dissolved nutrients, *Continental Shelf Research*, 15, 89-113, 1995.

Menzel Barraqueta, J. L., Schlosser, C., Planquette, H., Gourain, A., Cheize, M., Boutorh, J., Shelley, R. U., Pereira Contreira, L., Gledhill, M., Hopwood, M. J., Lherminier, P., Sarthou, G., and Achterberg, E. P.: Aluminium in the North Atlantic Ocean and the Labrador Sea (GEOTRACES GA01 section): roles of continental inputs and biogenic particle removal, *Biogeosciences Discussions*, 1-28, 10.5194/bg-2018-39, 2018.

Moore, C. M., Mills, M. M., Langlois, R., Milne, A., Achterberg, E. P., La Roche, J., and Geider, R. J.: Relative influence of nitrogen and phosphorus availability on phytoplankton physiology and productivity in the oligotrophic sub-tropical North Atlantic Ocean, *Limnology and Oceanography*, 53, 291-205, 2008.

Moore, C. M., Mills, M. M., Arrigo, K. R., Berman-Frank, I., Bopp, L., Boyd, P. W., Galbraith, E. D., Geider, R. J., Guieu, C., Jaccard, S. L., Jickells, T. D., La Roche, J., Lenton, T. M., Mahowald, N. M., Marañón, E., Marinov, I., Moore, J. K., Nakatsuka, T., Oschlies, A., Saito, M. A., Thingstad, T. F., Tsuda, A., and Ulloa, O.: Processes and patterns of oceanic nutrient limitation, *Nature Geoscience*, 6, 701-710, 10.1038/ngeo1765, 2013.

Moore, G. W. K.: Gale force winds over the Irminger Sea to the east of Cape Farewell, Greenland, *Geophysical Research Letters*, 30, n/a-n/a, 10.1029/2003gl018012, 2003.

Nielsdóttir, M. C., Moore, C. M., Sanders, R., Hinz, D. J., and Achterberg, E. P.: Iron limitation of the postbloom phytoplankton communities in the Iceland Basin, *Global Biogeochemical Cycles*, 23, n/a-n/a, 10.1029/2008gb003410, 2009.

Noble, A. E., Lamborg, C. H., Ohnemus, D. C., Lam, P. J., Goepfert, T. J., Measures, C. I., Frame, C. H., Casciotti, K. L., DiTullio, G. R., Jennings, J., and Saito, M. A.: Basin-scale inputs of cobalt, iron, and manganese from the Benguela-Angola front to the South Atlantic Ocean, *Limnology and Oceanography*, 57, 989-1010, 10.4319/lo.2012.57.4.0989, 2012.

Olafsson, J., Thors, K., and Cann, J. R.: A sudden cruise off Iceland, RIDGE Events, 2, 35-28, 1991.

Oschlies, A.: Nutrient supply to the surface waters of the North Atlantic: A model study, *Journal of Geophysical Research*, 107, 10.1029/2000jc000275, 2002.

Painter, S. C., Henson, S. A., Forryan, A., Steigenberger, S., Klar, J., Stinchcombe, M. C., Rogan, N., Baker, A. R., Achterberg, E. P., and Moore, C. M.: An assessment of the vertical diffusive flux of iron and other nutrients to the surface waters of the subpolar North Atlantic Ocean, *Biogeosciences*, 11, 2113-2130, 10.5194/bg-11-2113-2014, 2014.

Palmer, M. R., Ludford, E. M., German, C. R., and Lilley, M. D.: Dissolved methane and hydrogen in the Steinahóll hydrothermal plume, 63°N, Reykjanes Ridge, in: *Hydrothermal Vents and Processes*, edited by: Parson, L. M., Walker, C. L., and Dixon, D. R., Special Publications, Geological Society, London, 111-120, 1995.

Parekh, P., Follows, M. J., and Boyle, E. A.: Decoupling of iron and phosphate in the global ocean, *Global Biogeochemical Cycle*, 19, 2005.

Parra, M., Delmont, P., Ferragne, A., Latouche, C., Pons, J. C., and Puechmille, C.: Origin and evolution of smectites in recent marine sediments of the NE Atlantic, *Clay Minerals*, 20, 335-346, 1985.

Pérez, F. F., Mercier, H., Vázquez-Rodríguez, M., Lherminier, P., Velo, A., Pardo, P. C., Rosón, G., and Ríos, A. F.: Atlantic Ocean CO₂ uptake reduced by weakening of the meridional overturning circulation, *Nature Geoscience*, 6, 146-152, 10.1038/ngeo1680, 2013.

Pérez, F. F., Treguer, P., Branellec, P., García-Ibáñez, M. I., Lherminier, P., and Sarthou, G.: The 2014 Greenland-Portugal GEOVIDE bottle data (GO-SHIP A25 and GEOTRACES GA01). SEANO (Ed.), 2018.

Petrich, C., and Eicken, H.: Growth, structure and properties of sea ice, in: *Sea Ice*. 2nd ed., edited by: Thomas, D. N., and Dieckmann, G. S., Wiley-Blackwell, Oxford, U.K., 23-77, 2010.

Pickart, R. S., Straneo, F., and Moore, G. W. K.: Is Labrador Sea Water formed in the Irminger basin?, *Deep Sea Research Part I*, 50, 23-52, 2003.

Piron, A., Thierry, V., Mercier, H., and Caniaux, G.: Argo float observations of basin-scale deep convection in the Irminger sea during winter 2011–2012, *Deep Sea Research Part I: Oceanographic Research Papers*, 109, 76-90, 10.1016/j.dsr.2015.12.012, 2016.

Radic, A., Lacan, F., and Murray, J. W.: Iron isotopes in the seawater of the equatorial Pacific Ocean: New constraints for the oceanic iron cycle, *Earth and Planetary Science Letters*, 306, 1-10, 10.1016/j.epsl.2011.03.015, 2011.

Raiswell, R., and Canfield, D. E.: The iron biogeochemical cycle past and present, *Geochemical perspectives*, 1, 2012.

Ras, J., Claustre, H., and Uitz, J.: Spatial variability of phytoplankton pigment distribution in the Subtropical South Pacific Ocean: comparison between *in situ* and predicted data, *Biogeosciences*, 5, 353-369, 2008.

Rijkenberg, M. J., Middag, R., Laan, P., Gerringa, L. J., van Aken, H. M., Schoemann, V., de Jong, J. T., and de Baar, H. J.: The distribution of dissolved iron in the West Atlantic Ocean, *PLoS One*, 9, e101323, 10.1371/journal.pone.0101323, 2014.

Sabine, C. L., Feely, R. A., Gruber, N., Key, R. M., Lee, K., Bullister, J. L., Wanninkhof, R., Wong, C. S., Wallace, D. W. R., Tilbrook, B., Millero, F. J., Peng, T.-H., Kozyr, A., Ono, T., and Rios, A. F.: The Oceanic sink for anthropogenic CO₂, *Science*, 305, 367-371, 2004.

Sanders, R., Brown, L., Henson, S., and Lucas, M.: New production in the Irminger Basin during 2002, *Journal of Marine Systems*, 55, 291-310, <http://dx.doi.org/10.1016/j.jmarsys.2004.09.002>, 2005.

Santos-Echeandia, J., Vale, C., Caetano, M., Pereira, P., and Prego, R.: Effect of tidal flooding on metal distribution in pore waters of marsh sediments and its transport to water column (Tagus estuary, Portugal), *Mar Environ Res*, 70, 358-367, 10.1016/j.marenvres.2010.07.003, 2010.

Sarthou, G., Baker, A. R., Kramer, J., Laan, P., Laës, A., Ussher, S., Achterberg, E. P., de Baar, H. J. W., Timmermans, K. R., and Blain, S.: Influence of atmospheric inputs on the iron distribution in the subtropical North-East Atlantic Ocean, *Marine Chemistry*, 104, 186-202, 10.1016/j.marchem.2006.11.004, 2007.

Sarthou, G., Vincent, D., Christaki, U., Obernosterer, I., Timmermans, K. R., and Brussaard, C. P. D.: The fate of biogenic iron during a phytoplankton bloom induced by natural fertilisation: Impact of copepod grazing, *Deep Sea Research Part II: Topical Studies in Oceanography*, 55, 734-751, 10.1016/j.dsr2.2007.12.033, 2008.

Sarthou, G., Lherminier, P., Achterberg, E. P., Alonso-Pérez, F., Bucciarelli, E., Boutorh, J., Bouvier, V., Boyle, E. A., Branell, P., Carracedo, L. I., Casacuberta, N., Castrillejo, M., Cheize, M., Contreira Pereira, L., Cossa, D., Daniault, N., De Saint-Léger, E., Dehairs, F., Deng, F., Desprez de Gésincourt, F., Devesa, J., Foliot, L., Fonseca-Batista, D., Gallinari, M., García-Ibáñez, M. I., Gourain, A., Grossteffan, E., Hamon, M., Heimbürger, L. E., Henderson, G. M., Jeandel, C., Kermabon, C., Lacan, F., Le Bot, P., Le Goff, M., Le Roy, E., Lefèbvre, A., Leizour, S., Lemaitre, N., Masqué, P., Ménage, O., Menzel Barraqueta, J.-L., Mercier, H., Perault, F., Pérez, F. F., Planquette, H. F., Planchon, F., Roukaerts, A., Sanial, V., Sauzède, R., Shelley, R. U., Stewart, G., Sutton, J. N., Tang, Y., Tisnérat-Laborde, N., Tonnard, M., Tréguer, P., van Beek, P., Zurbrick, C. M., and Zunino, P.: Introduction to the French GEOTRACES North Atlantic Transect (GA01): GEOVIDE cruise, *Biogeosciences Discussions*, 1-24, 10.5194/bg-2018-312, 2018.

Schroth, A. W., Crusius, J., Hoyer, I., and Campbell, R.: Estuarine removal of glacial iron and implications for iron fluxes to the ocean, *Geophysical Research Letters*, 41, 3951-3958, 10.1002/2014GL060199, 2014.

Shelley, R. U., Morton, P. L., and Landing, W. M.: Elemental ratios and enrichment factors in aerosols from the US-GEOTRACES North Atlantic transects, *Deep Sea Research*, 116, 262-272, 2015.

Shelley, R. U., Roca-Martí, M., Castrillejo, M., Sanial, V., Masqué, P., Landing, W. M., van Beek, P., Planquette, H., and Sarthou, G.: Quantification of trace element atmospheric deposition fluxes to the Atlantic Ocean (>40°N; GEOVIDE, GEOTRACES GA01) during spring 2014, *Deep Sea Research Part I: Oceanographic Research Papers*, 119, 34-49, 10.1016/j.dsr.2016.11.010, 2017.

Shelley, R. U., Landing, W. M., Ussher, S. J., Planquette, H., and Sarthou, G.: Characterisation of aerosol provenance from the fractional solubility of Fe (Al, Ti, Mn, Co, Ni, Cu, Zn, Cd and Pb) in North Atlantic aerosols (GEOTRACES cruises GA01 and GA03) using a two stage leach, *Biogeosciences*, 2018.

Shor, A., Lonsdale, P., Hollister, D., and Spencer, D.: Charlie-Gibbs fracture zone: bottom-water transport and its geological effects, *Deep Sea Research*, 27A, 325-345, 1980.

Sinha, M. C., Navin, D. A., MacGregor, L. M., Constable, S., Peirce, C., White, A., Heinson, G., and Inglis, M. A.: Evidence for accumulated melt beneath the slow-spreading Mid-Atlantic Ridge, *Philosophical Transactions of the Royal Society A*, 355, 233-253, 1997.

Slagter, H. A., Reader, H. E., Rijkenberg, M. J. A., Rutgers van der Loeff, M., de Baar, H. J. W., and Gerringa, L. J. A.: Organic Fe speciation in the Eurasian Basins of the Arctic Ocean and its relation to terrestrial DOM, *Marine Chemistry*, 197, 11-25, 10.1016/j.marchem.2017.10.005, 2017.

Smallwood, J. R., and White, R. S.: Crustal accretion at the Reykjanes Ridge, 61°-62°N, *Journal of Geophysical Research: Solid Earth*, 103, 5185-5201, 10.1029/97jb03387, 1998.

Statham, P. J., Skidmore, M., and Tranter, M.: Inputs of glacially derived dissolved and colloidal iron to the coastal ocean and implications for primary productivity, *Global Biogeochemical Cycles*, 22, 1-11, 10.1029/2007GB003106, 2008.

Sunda, W. G., and Huntsman, S. A.: Iron uptake and growth limitation in oceanic and coastal phytoplankton, *Marine Chemistry*, 50, 189-206, 10.1016/0304-4203(95)00035-p, 1995.

Tanhua, T., Olsson, K. A., and Jeansson, E.: Formation of Denmark Strait overflow water and its hydro-chemical composition, *Journal of Marine Systems*, 57, 264-288, 10.1016/j.jmarsys.2005.05.003, 2005.

Teng, Z., Huang, J. Y., Fujito, K., and Takizawa, S.: Manganese removal by hollow fiber micro-filter. Membrane separation for drinking water, *European Conference on Desalination and the Environment*, Amsterdam, 28 May, 2001.

Thuróczy, C. E., Gerringa, L. J. A., Klunder, M. B., Middag, R., Laan, P., Timmermans, K. R., and de Baar, H. J. W.: Speciation of Fe in the Eastern North Atlantic Ocean, *Deep Sea Research Part I: Oceanographic Research Papers*, 57, 1444-1453, 10.1016/j.dsr.2010.08.004, 2010.

Tonnard, M., Donval, A., Lampert, L., Tréguer, P., Bowie, A. R., van der Merwe, P., planquette, H., Claustre, H., Dimier, C., Ras, J., and Sarthou, G.: Phytoplankton assemblages in the North Atlantic Ocean and in the Labrador Sea along the GEOVIDE section (GEOTRACES section GA01) determined by CHEMTAX analysis from HPLC pigment data, *Biogeosciences*, in prep.

Tovar-Sanchez, A., Duarte, C. M., Alonso, J. C., Lacorte, S., Tauler, R., and Galban-Malagon, C.: Impacts of metals and nutrients released from melting multiyear Arctic sea ice, *Journal of Geophysical Research-Oceans*, 115, 10.1029/2009jc005685, 2010.

Tréguer, P. J., and De La Rocha, C. L.: The world ocean silica cycle, *Ann Rev Mar Sci*, 5, 477-501, 10.1146/annurev-marine-121211-172346, 2013.

Twining, B. S., Baines, S. B., Fisher, N. S., and Landry, M. R.: Cellular iron contents of plankton during the Southern Ocean Iron Experiment (SOFeX), *Deep Sea Research Part I: Oceanographic Research Papers*, 51, 1827-1850, 10.1016/j.dsr.2004.08.007, 2004.

Van Beusekom, J. E. E.: Distribution of aluminium in surface waters of the North Sea: influence of suspended matter., in: *Biogeochemistry and Distribution of Suspended Matter in the North Sea and Implications to fisheries Biology*, edited by: Kempe, S., *Mittteilungen aus dem Geologisch-Paläontologischen Institut der Universität Hamburg, SCOPE/UNEP Sonderband*, 117-136, 1988.

Wadhams, P.: *Ice in the Ocean*, Gordon and Breach Science Publishers, London, UK, 2000.

Wagener, T., Guieu, C., and Leblond, N.: Effects of dust deposition on iron cycle in the surface Mediterranean Sea: results from a mesocosm seeding experiment, *Biogeosciences Discussions*, 7, 2799-2830, 2010.

Woodgate, R. A., and Aagaard, K.: Revising the Bering Strait freshwater flux into the Arctic Ocean, *Geophysical Research Letters*, 32, 10.1029/2004GL021747., 2005.

Wuttig, K., Wagener, T., Bressac, M., Dammshäuser, A., Streu, P., Guieu, C., and Croot, P. L.: Impacts of dust deposition on dissolved trace metal concentrations (Mn, Al and Fe) during a mesocosm experiment, *Biogeosciences*, 10, 2583-2600, 10.5194/bg-10-2583-2013, 2013.

Zou, S., Lozier, S., Zenk, W., Bower, A., and Johns, W.: Observed and modeled pathways of the Iceland Scotland Overflow Water in the eastern North Atlantic, *Progress in Oceanography*, 159, 211-222, 10.1016/j.pocean.2017.10.003, 2017.

Zunino, P., Lherminier, P., Mercier, H., Daniault, N., García-Ibáñez, M. I., and Pérez, F. F.: The GEOVIDE cruise in may-June 2014 revealed an intense MOC over a cold and fresh subpolar North Atlantic, *Biogeosciences*, 2017.

Zurbrick, C. M., Boyle, E. A., Kayser, R., Reuer, M. K., Wu, J., Planquette, H., Shelley, R., Boutorh, J., Cheize, M., Contreira, L., Menzel Barraqueta, J.-L., and Sarthou, G.: Dissolved Pb and Pb isotopes in the North Atlantic from the GEOVIDE transect (GEOTRACES GA-01) and their decadal evolution, *Biogeosciences Discussions*, 1-34, 10.5194/bg-2018-29, 2018.

Anonymous Referee#2 reviews

Dear Referee#2 and Editor,

The reviewers are thanked for their insightful comments; these have helped to improve the manuscript considerably. Please see our detailed answers to the referees' comments below. Line numbers refer to the new version.

All the answers are attached as a supplementary file.

Best regards,

Tonnard et al.

Please, note that we added Francois Lacan as a co-author.

Page 1, Line 35: "in the Denmark Straight. . ."

→ We have changed the text accordingly.

Page 1, Line 35: explain what types of particles you are talking about and briefly explain the differences observed (which ones scavenge and which ones release dFe).

→ We have added precision

Page 1 Lines 35-37: Finally, the nepheloid layers located in the different basins and at the Iberian Margin were found to act as either a source or a sink of DFe depending on the nature of particles with organic particles likely releasing DFe and Fe-Mn oxides scavenging DFe.

Page2, Line 4: The reasoning is not flowing properly here. You need to say that (1) high productivity leads to high atmospheric carbon capture and that (2) Deep water formation leads to sequestration of this carbon into deeper waters, where carbon is stored for longer. The last sentence comes a little out of the blue, needs to be better linked – instead close the paragraph highlighting why it is important to study trace metals in this area.

→ We have reorganised the full introduction as suggested.

Page 2 Lines 1-33, Page 3 Lines 1-25:

1 Introduction

The North Atlantic Ocean is known for its pronounced spring phytoplankton blooms (Henson et al., 2009; Longhurst, 2007). Phytoplankton blooms induce the capture of aqueous carbon dioxide through photosynthesis, and conversion into particulate organic carbon (POC). This POC is then exported into deeper waters through the production of sinking biogenic particles and ocean currents. Via these processes, and in conjunction with the physical carbon pump, the North Atlantic Ocean is the largest oceanic sink of anthropogenic CO₂ (Pérez et al., 2013), despite covering only 15% of global ocean area (Humphreys et al., 2016; Sabine et al., 2004) and is therefore crucial for Earth's climate.

Indeed, phytoplankton must obtain, besides light and inorganic carbon, chemical forms of essential elements, termed nutrients to be able of photosynthesis. Indeed, Fe is a key element for a number of metabolic processes (e.g. Morel et al., 2008). The availability of these nutrients in the upper ocean

Formatted: Font: +Headings CS (Times New Roman)

Formatted: French (France)

Formatted: English (Australia)

Formatted: Font: (Default) +Headings CS (Times New Roman), Complex Script Font: +Headings CS (Times New Roman)

Deleted: Abstract¶

Formatted: List Paragraph, Bulleted + Level: 1 + Aligned at: 0.63 cm + Indent at: 1.27 cm

Formatted: Font: (Default) +Headings CS (Times New Roman), Complex Script Font: +Headings CS (Times New Roman)

Moved (insertion) [1]

Deleted: ¶

Formatted: List Paragraph, Bulleted + Level: 1 + Aligned at: 0.25 cm + Indent at: 0.88 cm

Formatted: Font: (Default) +Headings CS (Times New Roman), Complex Script Font: +Headings CS (Times New Roman)

Formatted: Font: (Default) +Headings CS (Times New Roman), Complex Script Font: +Headings CS (Times New Roman)

Moved up [1]: Page 1, Line 35: explain what types of particles you are talking about and briefly explain the differences observed (which ones scavenge and which ones release dFe) ¶

Formatted: Not Highlight

Formatted: Not Highlight

Formatted: EndNote Bibliography

Formatted: Not Highlight

frequently limits the activity and abundance of these organisms together with light conditions (Moore et al., 2013). In particular, winter nutrient reserves in surface waters set an upper limit for biomass accumulation during the annual spring-to-summer bloom and will influence the duration of the bloom (Follows and Dutkiewicz, 2001; Henson et al., 2009; Moore et al., 2013; 2008). Hence, nutrient depletion due to biological consumption is considered as a major factor in the decline of blooms (Harrison et al., 2013).

The extensive studies conducted in the North Atlantic Ocean through the Continuous Plankton Recorder (CPR) have highlighted the relationship between the strength of the westerlies and the displacement of the subarctic front (SAF), (which corresponds to the North Atlantic Oscillation (NAO) index (Bersch et al., 2007)), and the phytoplankton dynamics of the central North Atlantic Ocean (Barton et al., 2003). Therefore, the SAF not only delineates the subtropical gyre from the subpolar gyre but also two distinct systems in which phytoplankton limitations are controlled by different factors. In the North Atlantic Ocean, spring phytoplankton growth is largely light-limited within the subpolar gyre. Light levels are primarily set by freeze-thaw cycles of sea ice and the high-latitude extremes in the solar cycle (Longhurst, 2007). Simultaneously, intense winter mixing supplies surface waters with high concentrations of nutrients. In contrast, within the subtropical gyre, the spring phytoplankton growth is less impacted by the light regime and has been shown to be N and P-co-limited (e.g. Harrison et al., 2013; Moore et al., 2008). This is principally driven by Ekman downwelling with an associated export of nutrients out of the euphotic zone (Oschlies, 2002). Thus, depending on the location of the SAF, phytoplankton communities from the central North Atlantic Ocean will be primarily light or nutrient limited.

However, once the water column stratifies and phytoplankton are released from light limitation, seasonal high-nutrient, low chlorophyll (HNLC) conditions were reported at the transition zone between the gyres, especially in the Irminger Sea and Iceland Basin (Sanders et al., 2005). In these HNLC zones, trace metals are most likely limiting the biological carbon pump. Among all the trace metals, Fe has been recognized as the prime limiting element of North Atlantic primary productivity (e.g. Boyd et al., 2000; Martin et al., 1994; 1988; 1990). However, the phytoplankton community has been shown to become N and/or Fe-(co)-limited in the Iceland Basin and the Irminger Sea (e.g. Nielsdóttir et al., 2009; Painter et al., 2014; Sanders et al., 2005).

In the North Atlantic Ocean, dissolved Fe (DFe) is delivered through multiple pathways such as ice-melting (e.g. Klunder et al., 2012; Tovar-Sanchez et al., 2010), atmospheric inputs (Achterberg et al., 2018; Baker et al., 2013; Shelley et al., 2015; 2017), coastal runoff (Rijkenberg et al., 2014), sediment inputs (Hatta et al., 2015), hydrothermal inputs (Achterberg et al., 2018; Conway and John, 2014) and by water mass circulation (vertical and lateral advections, e.g. Laes et al., 2003). Dissolved Fe can be regenerated through biological recycling (microbial loop, zooplankton grazing, e.g. Boyd et al., 2010; Sarthou et al., 2008). Iron is removed from the dissolved phase by biological uptake, export and scavenging along the water column and precipitation (itself a function of salinity, pH of seawater and ligand concentrations).

Formatted: English (Australia)

Formatted: English (Australia)

Field Code Changed

Field Code Changed

Although many studies investigated the distribution of DFe in the North Atlantic Ocean, much of this work was restricted to the upper layers (< 1000 m depth) or to one basin. Therefore, uncertainties remain on the large-scale distribution of DFe in the North Atlantic Ocean and more specifically within the subpolar gyre where few studies have been undertaken, and even fewer in the Labrador Sea. In this biogeochemically important area, high-resolution studies are still lacking for understanding the processes influencing the cycle of DFe.

The aim of this paper is to elucidate the sources and sinks of DFe, its distribution regarding water masses and assesses the links with biological activity along the GEOVIDE (GEOTRACES-GA01) transect. This transect spanned several biogeochemical provinces including the West European Basin, the Iceland Basin, the Irminger and the Labrador Seas (Fig. 1). In doing so we hope to constrain the potential long-range transport of DFe through the Deep Western Boundary Current (DWBC) via the investigation of the local processes effecting the DFe concentrations within the three main water masses that constitute it: Iceland Scotland Overflow Water (ISOW), Denmark Strait Overflow Water (DSOW) and Labrador Sea Water (LSW).

Page 2, Line10: I can not follow the reasoning in this paragraph. A little bit of a muddle of all the phytoplankton limiting factors (light, nutrients, wind, temp) without a clear insight what factor limits where. Needs to be better explained.

→ We have reorganised the full introduction as suggested (see above).

Page 2, Line 15: the connection between light limitation and nutrient limitation is not clearly explained

→ We have reorganised the full introduction as suggested (see above).

Page 2, Line26: what about soluble Fe? Is this not considered the most bioavailable?

→ Yes, we absolutely agree. Therefore to avoid confusion we have decided to remove the following sentence "...and within its physical speciation, its dissolved form (DFe) is considered to be the most available form for phytoplankton (Morel, 2008; Morel et al., 2008)."

Page 3, Line5: Aims of this paper are a bit poor. Add better understanding of the biogeochemical cycling of dFe in the oceans - inform biogeochemical models – and why this is important, what you expect to achieve. ...

→ We have reorganised the full introduction as suggested (see above).

Page 3, Line 20: remove "national"

→ Removed

Page 3, line 30: do you mean concentrated HCl?

→ We have changed the text for clarification

Page 4 Lines 17-18: Samples were then acidified to ~ pH 1.7 with HCl (Ultrapur® Merck, 2 % v/v) under a class 100 laminar flow hood inside the clean container.

Page 3, Line25: why different filtering methods? Have you compared the Fe concentrations in those fractions? i.e., have you collected the same sample with both filtration cut-offs and checked there is no significant difference?

Formatted: EndNote Bibliography

Formatted: Font: (Default) +Headings CS (Times New Roman), Complex Script Font: +Headings CS (Times New Roman)

Formatted: Not Highlight

Formatted: EndNote Bibliography

Formatted: Font: (Default) +Headings CS (Times New Roman), Complex Script Font: +Headings CS (Times New Roman)

Formatted: EndNote Bibliography

Formatted: Font: (Default) +Headings CS (Times New Roman), Complex Script Font: +Headings CS (Times New Roman)

Formatted: List Paragraph, Bulleted + Level: 1 + Aligned at: 0.25 cm + Indent at: 0.88 cm

Formatted: Font: (Default) +Headings CS (Times New Roman), Complex Script Font: +Headings CS (Times New Roman)

Formatted: Font: (Default) +Headings CS (Times New Roman), Complex Script Font: +Headings CS (Times New Roman)

Deleted: ¶

Formatted: Font: (Default) +Headings CS (Times New Roman), Complex Script Font: +Headings CS (Times New Roman)

Formatted: List Paragraph, Bulleted + Level: 1 + Aligned at: 0.25 cm + Indent at: 0.88 cm

Formatted: List Paragraph, Bulleted + Level: 1 + Aligned at: 0.25 cm + Indent at: 0.88 cm

Formatted: Normal, Indent: Before: 0.25 cm, No bullets or numbering

Deleted: ¶

Formatted: Font: (Default) +Headings CS (Times New Roman), Complex Script Font: +Headings CS (Times New Roman)

→ We added precision for clarification. Note that we did not collect the same samples with the two different techniques.

Page 4, Lines 10-14: Samples were either taken from the filtrate of particulate samples (collected on polyethersulfone filters, 0.45 μm supor[®], see Gourain et al., this issue) or after filtration using 0.2 μm filter cartridges (Sartorius SARTOBRAN[®] 300) due to water budget restriction (Table 1). No significant difference was observed between DFe values filtered through 0.2 μm and 0.45 μm filters (p-value > 0.2, Wilcoxon test) for most stations. Differences were only observed between profiles of stations 11 and 13 and, 13 and 15.

Page 4, Line 4: remove “daily basis”

→ We have changed the text “High-purity grade solutions and water (Milli-Q) were used on a daily basis to prepare the following reagents:” by “High-purity grade solutions and water (Milli-Q) were used to prepare the following reagents each day:” (Page 4 Line 31)

Page 4, Line 14: replace “run” with “analytical session”

→ We have changed the text as suggested (Page 5 Line 10)

Page 4, line 19: replace “in nmol L⁻¹” with “to nmol L⁻¹”

→ We have changed the text as suggested (Page 5 Line 21)

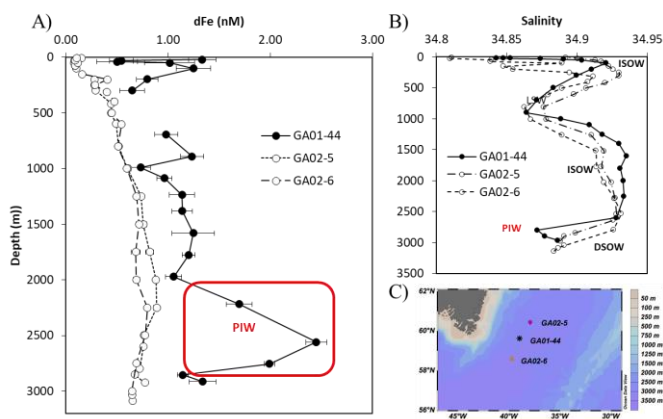
Page 4, Line 19: would it not be more correct to multiply by the specific density of each sample? If you do not have this data (normally this is a standard parameter obtained from temperature and salinity).

→ Yes, we agree with the reviewer. However, the converting factor used for consensus materials has always been 1.025 kg L⁻¹, which is why we used this converting factor.

Page 4, Line 19: Please show a comparison of dFe data at the crossover-station with GA02, as an intercalibration exercise.

→ We did not include an intercalibration exercise with the GA02 voyage as DFe was determined on board by FIA-CL during GA02, which thus means that some refractory DFe was not measured on board with only a short time of acidification (Chever et al., 2010).

→ Just for your information, here after you will find the plot comparing both voyages.



Formatted: List Paragraph, Bulleted + Level: 1 + Aligned at: 0.25 cm + Indent at: 0.88 cm

Formatted: Font: (Default) +Headings CS (Times New Roman), Complex Script Font: +Headings CS (Times New Roman)

Formatted: Font: (Default) +Headings CS (Times New Roman), Complex Script Font: +Headings CS (Times New Roman)

Formatted: Font: (Default) +Headings CS (Times New Roman), Complex Script Font: +Headings CS (Times New Roman)

Formatted: List Paragraph, Bulleted + Level: 1 + Aligned at: 0.25 cm + Indent at: 0.88 cm

Formatted: Font: (Default) +Headings CS (Times New Roman), Complex Script Font: +Headings CS (Times New Roman)

Formatted: Font: (Default) +Headings CS (Times New Roman), Complex Script Font: +Headings CS (Times New Roman)

Formatted: List Paragraph, Bulleted + Level: 1 + Aligned at: 0.25 cm + Indent at: 0.88 cm

Formatted: Font: (Default) +Headings CS (Times New Roman), Complex Script Font: +Headings CS (Times New Roman)

Formatted: List Paragraph, Bulleted + Level: 1 + Aligned at: 0.25 cm + Indent at: 0.88 cm

Formatted: Font: (Default) +Headings CS (Times New Roman), Complex Script Font: +Headings CS (Times New Roman)

Formatted: List Paragraph, Bulleted + Level: 1 + Aligned at: 0.25 cm + Indent at: 0.88 cm

Formatted: Superscript

Formatted: Font: (Default) +Headings CS (Times New Roman), Complex Script Font: +Headings CS (Times New Roman)

Formatted: Font: 11 pt, Complex Script Font: 11 pt

Formatted: Bulleted + Level: 1 + Aligned at: 0.25 cm + Indent at: 0.88 cm

Formatted: Font: (Default) +Headings CS (Times New Roman), 11 pt, Complex Script Font: +Headings CS (Times New Roman), 11 pt

Formatted: Font: (Default) +Headings CS (Times New Roman), 11 pt, Complex Script Font: +Headings CS (Times New Roman), 11 pt

Formatted: Font: (Default) +Headings CS (Times New Roman), 11 pt, Complex Script Font: +Headings CS (Times New Roman), 11 pt

Formatted

Formatted

Page 4, Line 25: Why did you not use the CTD data from the trace metal casts? Please explain

→ We did not use the CTD data from the trace metal casts as the O2 data could not be calibrated. We therefore decided to use all the parameters from the same rosette, i.e. the stainless steel rosette.

Page 5, Line 12: awkward sentence, difficult to follow, please rewrite!

→ We have changed the text for clarification

Page 7, Lines 4-5: Using this water mass determination, DFe concentrations were considered as representative of a specific water mass only when the contribution of this specific water mass was higher than 60% of the total water mass pool.

Page 6, Line 5: which central waters? Names?

→ The central waters are Eastern North Atlantic Central Waters (ENACW). The acronym was added in the text there page 7, line 26.

Page 6, Line 9: to keep consistency, keep "stations 49 and 60" out of the parenthesis. Rephrase the end of the sentence to do so.

→ We have modified the text as suggested

Page 7 Lines 27-30, Page 8 Lines 1: West of the Subarctic Front, Iceland SubPolar Mode Waters (IcSPMW, $7.07 < \theta < 8^{\circ}\text{C}$, $35.16 < S < 35.23$, $280 < O_2 < 289 \mu\text{mol kg}^{-3}$) was encountered from stations 34-40 (accounting for more than 45% of the water mass pool from 0 to ~ 800 m depth) and Irminger SubPolar Mode Waters (IrSPMW, $\theta \approx 5^{\circ}\text{C}$, $S \approx 35.014$) from stations 42-44 (contributing to 40% of the water mass pool from 0 to ~ 250 m depth) and stations 49 and 60 (accounting for 40% of the water mass pool down to 1300 m depth).

Page 6, Line 10: specify which stations

→ We have changed the text as suggested.

Page 8 Lines 1-2: The IcSPMW was also observed within the Subtropical gyre (stations 11-26), subducted below ENACW until ~ 1000 m depth.

Page 6, Line 14: remove "The" from start of sentence

→ We changed the text accordingly.

Page 6, Line 19: what is that contribution? 40 %? Please specify!

→ We have changed the text as suggested.

Page 8 Lines 9-10: The LSW was also observed in surface waters of station 44 with a similar contribution than IrSPMW (~ 40%).

Page 6, Line 28: ... "was" sourced from...

→ We have corrected the text accordingly.

Page 6, Line 30: and "in the" Labrador Sea

→ We have corrected the text accordingly.

Page 6, Line 34: I am getting a little lost with all those branches, not sure when you're talking about the same one and when you change talking about another one. Not clear, please rephrase this section.

Deleted: <#>¶

Formatted: Font: (Default) +Headings CS (Times New Roman), Complex Script Font: +Headings CS (Times New Roman)

Formatted: EndNote Bibliography, Bulleted + Level: 1 + Aligned at: 0.63 cm + Indent at: 1.27 cm

Formatted: Font: (Default) +Headings CS (Times New Roman), Complex Script Font: +Headings CS (Times New Roman)

Formatted: List Paragraph, Bulleted + Level: 1 + Aligned at: 0.25 cm + Indent at: 0.88 cm

Formatted: Font: (Default) +Headings CS (Times New Roman), Complex Script Font: +Headings CS (Times New Roman)

Formatted: Font: (Default) +Headings CS (Times New Roman), Complex Script Font: +Headings CS (Times New Roman)

Formatted: Font: (Default) +Headings CS (Times New Roman), Complex Script Font: +Headings CS (Times New Roman)

Formatted: Font: (Default) +Headings CS (Times New Roman), Complex Script Font: +Headings CS (Times New Roman)

Formatted: Font: (Default) +Headings CS (Times New Roman), Complex Script Font: +Headings CS (Times New Roman)

Formatted: Font: (Default) +Headings CS (Times New Roman), Complex Script Font: +Headings CS (Times New Roman)

Deleted: ¶

Formatted: List Paragraph, Bulleted + Level: 1 + Aligned at: 0.25 cm + Indent at: 0.88 cm

Formatted: Font: (Default) +Headings CS (Times New Roman), Complex Script Font: +Headings CS (Times New Roman)

Formatted

Formatted

Formatted: List Paragraph

Formatted

Formatted

Formatted

Formatted

Formatted

Formatted

Formatted

Formatted

Formatted

Formatted

→ We have changed the text for clarification.

Page 8 Lines 20-22: After convection, LSW splits into three main branches with two main cores separated by the Reykianes Ridge (stations 1-32, West European and Iceland Basins; stations 40-60, Irminger Sea), and the last one entering the West European Basin (Zunino et al., 2017).

Page 7, Line 5: delete "The" from beginning of sentence. In this entire section please remove "the" in front of water masses. The text should be revised by one of the English speaking co-authors before submission.

→ We have changed the text accordingly

Page 7, Line7: "lower" oxygen. . .

→ We have changed the text accordingly.

Page 7, Line 4: what do you mean by dense shelf? Do you mean the water masses have higher density? Please rephrase

→ We have changed the text for clarification

Page 8 Lines 28-32: Polar Intermediate Water (PIW, $\theta \approx 0^\circ\text{C}$, $S \approx 34.65$) is a ventilated, dense, low-salinity water intrusion to the deep overflows within the Irminger and Labrador Seas that is formed at the Greenland shelf. PIW represents only a small contribution to the whole water mass pool (up to 27%) and was observed over the Greenland slope at stations 53 and 61 as well as in surface waters from station 63 (from 0 to ~ 200 m depth), in intermediate waters of stations 49, 60 and 63 (from ~ 500 to ~ 1500 m depth) and in bottom waters of stations 44, 68, 69, 71 and 77 with a contribution higher than 10%.

Page 7, Line 16: "the" Charlie Gibbs. . .

→ We have changed the text as suggested.

Page 7, Line 19: mixing with... remove "of the overflow"

→ These lines have been removed according to Referee #1 comments

Page 7, Line 21: Which stations?

→ The stations numbers were added for the Iceland Basin.

Page 9 Lines 4-6: ISOW was observed from 1500 m depth to the bottom of the entire Iceland Basin (stations 29-38) and from 1800 to 3000 m depth within the Irminger Sea (stations 40-60)

Page 7, Line 30: At least put a nitrate section figure in the supplementary file; otherwise text hard to follow. Data not yet available on the site you referenced

→ Data are now available on the Sarthou et al., 2018 paper. However, we have changed this reference by the accurate one and added the reference of the SEANOE data base and associated paper: García-Ibáñez et al., 2018; Pérez et al., 2018; Sarthou et al., 2018 Please note that in this manuscript, Nitrate data are changed for RFe/N data, therefore we did not added the nitrate data.

Page 8, Line 4: how do you define the "most open ocean station" for the transect? Deepest? Furthest away from land masses? Are you sure this is st 23?

→ We have change the text for clarification and corrected the station number.

Formatted: List Paragraph, Bulleted + Level: 1 + Aligned at: 0.25 cm + Indent at: 0.88 cm

Formatted: Font: (Default) +Headings CS (Times New Roman), Complex Script Font: +Headings CS (Times New Roman)

Formatted: Font: (Default) +Headings CS (Times New Roman), Complex Script Font: +Headings CS (Times New Roman)

Formatted: List Paragraph, Bulleted + Level: 1 + Aligned at: 0.25 cm + Indent at: 0.88 cm

Formatted: List Paragraph, Bulleted + Level: 1 + Aligned at: 0.25 cm + Indent at: 0.88 cm
Formatted: Font: (Default) +Headings CS (Times New Roman), Complex Script Font: +Headings CS (Times New Roman)

Formatted: Font: (Default) +Headings CS (Times New Roman), Complex Script Font: +Headings CS (Times New Roman)

Formatted: Font: (Default) +Headings CS (Times New Roman), Complex Script Font: +Headings CS (Times New Roman)

Formatted: List Paragraph, Bulleted + Level: 1 + Aligned at: 0.25 cm + Indent at: 0.88 cm

Formatted: Font: (Default) +Headings CS (Times New Roman), Complex Script Font: +Headings CS (Times New Roman)

Deleted: ¶

Formatted: Font: (Default) +Headings CS (Times New Roman), Complex Script Font: +Headings CS (Times New Roman)

Formatted: Font: (Default) +Headings CS (Times New Roman), Complex Script Font: +Headings CS (Times New Roman)

Formatted: List Paragraph, Bulleted + Level: 1 + Aligned at: 0.25 cm + Indent at: 0.88 cm

Formatted: Font: (Default) +Headings CS (Times New Roman), Complex Script Font: +Headings CS (Times New Roman)

Formatted: List Paragraph, Bulleted + Level: 1 + Aligned at: 0.25 cm + Indent at: 0.88 cm

Formatted: Font: (Default) +Headings CS (Times New Roman), Complex Script Font: +Headings CS (Times New Roman)

Deleted: <#>¶

Formatted

Formatted: List Paragraph, Bulleted + Level: 1 + Aligned at: 0.25 cm + Indent at: 0.88 cm

Formatted

Page 9, Lines 16-17: The low surface NO₃⁻ concentrations (lower than 6 μmol L⁻¹) in the West European Basin extended from station 2 (closest station to continental land mass) to station 25 (open ocean station) with concentrations ranging from 0.02 (station 11) to 3.9 (station 25) μmol L⁻¹.

Formatted: Font: (Default) +Headings CS (Times New Roman), Complex Script Font: +Headings CS (Times New Roman)

Page 8, Line 4: it is unclear when you switch to talk about non-surface nitrate concentrations. Please rephrase this section to make this clearer.

Formatted: Font: (Default) +Headings CS (Times New Roman), Complex Script Font: +Headings CS (Times New Roman)

→ We have changed the section for clarification as suggested

Formatted: Font: (Default) +Headings CS (Times New Roman), Complex Script Font: +Headings CS (Times New Roman)

Page 9, Lines 12-22: Surface nitrate (NO₃⁻) concentrations (García-Ibáñez et al., 2018; Pérez et al., 2018; Sarthou et al., 2018) ranged from 0.01 to 10.1 μmol L⁻¹ (stations 53 and 63, respectively). There was considerable spatial variability in NO₃⁻ surface distributions with high concentrations found in the Iceland Basin and Irminger Sea (higher than 6 μmol L⁻¹), as well as at stations 63 (10.1 μmol L⁻¹) and 64 (5.1 μmol L⁻¹), and low concentrations observed in the West European Basin, in the Labrador Sea and above continental margins. The low surface concentrations in the West European Basin ranged from 0.02 (station 11) to 3.9 (station 25) μmol L⁻¹. Station 26 delineating the extreme western boundary of the West European Basin exhibited enhanced NO₃⁻ concentrations as a result of mixing between ENACW and ICSPMW, although these surface waters were dominated by ENACW. In the Labrador Sea (stations 68-78) low surface concentrations were observed with values ranging from 0.04 (station 68) to 1.8 (station 71) μmol L⁻¹. At depth, the lowest concentrations (lower than 15.9 μmol L⁻¹) were measured in ENACW (~ 0 - 800 m depth) and DSOW (> 1400 m depth), while the highest concentrations were measured within NEADW (up to 23.5 μmol L⁻¹), and in the mesopelagic zone of the West European and Iceland Basins (higher than 18.4 μmol L⁻¹).

Formatted: List Paragraph, Bulleted + Level: 1 + Aligned at: 0.25 cm + Indent at: 0.88 cm

Formatted: Font: (Default) +Headings CS (Times New Roman), Complex Script Font: +Headings CS (Times New Roman)

Formatted: Font: (Default) +Headings CS (Times New Roman), Complex Script Font: +Headings CS (Times New Roman)

Page 8, Line 6: which depths are you talking about?

Formatted: Font: (Default) +Headings CS (Times New Roman), Complex Script Font: +Headings CS (Times New Roman)

→ We added precision as suggested (see above)

Formatted: List Paragraph, Bulleted + Level: 1 + Aligned at: 0.25 cm + Indent at: 0.88 cm

Page 8, Line 12: isn't the fluorometer calibrated with the Chl-a measurements?

→ We removed this part as suggested by Referee#1. However, the fluorometer was calibrated separately from the Chl-a measurements. To do so, 6 stations (including 6 different water masses) at 6 depths (surface, chlorophyll-max down to the base of the euphotic zone) were sampled. These samples included early morning, late evening and daytime samples to account for non-photochemical quenching, which causes a decrease of fluorescence signal at the surface during day-time. Therefore, all profiles were calibrated using night-time dependency and corrected day-time surface data for non-photochemical quenching.

Formatted: Font: (Default) +Headings CS (Times New Roman), Complex Script Font: +Headings CS (Times New Roman)

Deleted: ¶

Formatted: Bulleted + Level: 1 + Aligned at: 0.25 cm + Indent at: 0.88 cm

Formatted: Font: (Default) +Headings CS (Times New Roman), Complex Script Font: +Headings CS (Times New Roman)

Page 8, Line 13: Specify which depth range you are considering for looking at min/max Chl-a concentrations. Evidently, minimum Chl-a concentrations are found in the deep ocean

Deleted: <#>¶

→ As you said, the minimum Chl-a concentrations are found in the deep ocean and therefore we only reported min and max values for the maximum Chl-a concentrations considering all stations. We have changed the text for clarification

Formatted: List Paragraph, Bulleted + Level: 1 + Aligned at: 0.25 cm + Indent at: 0.88 cm

Page 9 Lines 24-28: Overall, most of the phytoplankton biomass was localised above 100 m depth with lower total chlorophyll-a (TChl-a) concentrations South of the Subarctic Front and higher at higher latitudes (Fig. 3). While comparing TChl-a maxima considering all stations, the lowest value (0.35 mg m⁻³) was measured within the West European Basin (station 19, 50 m depth) while the highest values were measured at the Greenland (up to 4.9 mg m⁻³, 30 m depth, station 53 and up to 6.6 mg m⁻³, 23 m depth, station 61) and Newfoundland (up to 9.6 mg m⁻³, 30 m depth, station 78) margins.

Page 8, Line 19: remind the reader here here that all the dFe data can be found in the supplementary file.

→ We have added this precision as suggested. Note that Referee#1 suggested to gather subsections 3.3.1 and 3.3.2, to remove the first lines from section 3.3 (Page 8 Lines 20-25) and to change section 3.3.3 for section 3.4, which is what we did.

Page 10 Lines 2-3: Dissolved Fe concentrations (see supplementary material) ranged from $0.09 \pm 0.01 \text{ nmol L}^{-1}$ (station 19, 20 m depth) to $7.8 \pm 0.5 \text{ nmol L}^{-1}$ (station 78, 371 m depth) (see Fig. 3).

Page 9, Line 13: when describing the regions, go in same order as in Figure, otherwise confusing (start Labrador Sea and end WEB)

→ We have made the corrections accordingly.

Page 10 Lines 19-32 and Page 11 Lines 1-11: In the Labrador Sea, IrSPMW exhibited an average DFe concentration of $0.61 \pm 0.21 \text{ nmol L}^{-1}$ (n=14). DFe concentrations in the LSW were the lowest in this basin, with an average value of $0.71 \pm 0.27 \text{ nmol L}^{-1}$ (n=53) (Fig. 7). Deeper, ISOW displayed slightly higher average DFe concentrations ($0.82 \pm 0.05 \text{ nmol L}^{-1}$, n=2). Finally, DSOW had the lowest average ($0.68 \pm 0.06 \text{ nmol L}^{-1}$, n=3, Fig. 7) and median (0.65 nmol L^{-1}) DFe values for intermediate and deep waters.

In the Irminger Sea, surface waters were composed of SAIW ($0.56 \pm 0.24 \text{ nmol L}^{-1}$, n=4) and IrSPMW ($0.72 \pm 0.32 \text{ nmol L}^{-1}$, n=34). The highest open-ocean DFe concentrations (up to $2.5 \pm 0.3 \text{ nmol L}^{-1}$, station 44, 2600 m depth) were measured within this basin. In the upper intermediate water LSW was identified only at stations 40 to 44, and had the highest DFe values with an average of $1.2 \pm 0.3 \text{ nmol L}^{-1}$ (n=14). ISOW showed higher DFe concentrations than in the Iceland Basin ($1.3 \pm 0.2 \text{ nmol L}^{-1}$, n=4). At the bottom, DSOW was mainly located at stations 42 and 44 and presented the highest average DFe values ($1.4 \pm 0.4 \text{ nmol L}^{-1}$, n=5) as well as the highest variability from all the water masses presented in this section (Fig. 7).

In the Iceland Basin, SAIW and IcSPMW displayed similar averaged DFe concentrations ($0.67 \pm 0.30 \text{ nmol L}^{-1}$, n=7 and $0.55 \pm 0.34 \text{ nmol L}^{-1}$, n=22, respectively). Averaged DFe concentrations were similar in both LSW and ISOW, and higher than in SAIW and IcSPMW ($0.96 \pm 0.22 \text{ nmol L}^{-1}$, n=21 and $1.0 \pm 0.3 \text{ nmol L}^{-1}$, n=10, respectively, Fig. 7).

Finally, in the West European Basin, DFe concentrations in ENACW were the lowest of the whole section with an average value of $0.30 \pm 0.16 \text{ nmol L}^{-1}$ (n=64). MOW was present deeper in the water column but was not characterized by particularly high or low DFe concentrations relative to the surrounding Atlantic waters (Fig. 7). The median DFe value in MOW was very similar to the median value when considering all water masses (0.77 nmol L^{-1} , Figs. 4 and 7). LSW and IcSPMW displayed slightly elevated DFe concentrations compared to the overall median with mean values of 0.82 ± 0.08 (n=28) and 0.80 ± 0.04 (n=8) nmol L^{-1} , respectively. The DFe concentrations in NEADW were relatively similar to the DFe median value of the GEOVIDE voyage (median DFe = 0.75 nmol L^{-1} , Figs. 4 and 7) with an average value of $0.74 \pm 0.16 \text{ nmol L}^{-1}$ (n=18) and presented relatively low median DFe concentrations (median DFe = 0.71 nmol L^{-1}) compared to other deep water masses.

Page 9, Line 13: remove “the” before MOW and in front of LSW (line 15), SAIW (line 24) and IrSPMW (line 24).

→ We have removed “the” in front of each water masses throughout the section.

Formatted: Font: (Default) +Headings CS (Times New Roman), Complex Script Font: +Headings CS (Times New Roman)

Formatted: List Paragraph, Bulleted + Level: 1 + Aligned at: 0.25 cm + Indent at: 0.88 cm

Formatted: Font: (Default) +Headings CS (Times New Roman), Complex Script Font: +Headings CS (Times New Roman)

Formatted: List Paragraph, Bulleted + Level: 1 + Aligned at: 0.25 cm + Indent at: 0.88 cm

Formatted: Font: (Default) +Headings CS (Times New Roman), Complex Script Font: +Headings CS (Times New Roman)

Formatted: List Paragraph, Bulleted + Level: 1 + Aligned at: 0.25 cm + Indent at: 0.88 cm

Formatted: Font: (Default) +Headings CS (Times New Roman), Complex Script Font: +Headings CS (Times New Roman)

Page 9, Line 20: this is confusing, specify that you mean similar averages and not ranges (the range is larger for IcSPMW)

→ We have added this precision as suggested (see above)

Page 9, Line 22: LSW and ISOW averages are also similar, combine sentences.

→ We have changed the text accordingly (see above).

Page 9, Line 24: “composed of” instead of “characterised by”

→ We have changed the text as suggested (see above).

Page 9, Line 32: Delete “compared to other ones”

→ We have changed as suggested (see above).

Page 10, Line 2: “lowest average dFe value” (DSOW also shows the highest deep water dFe concentrations)

→ We have changed the text as suggested (see above).

Page 10, Line 9: it is a little odd to start explaining what cannot be included in any of your subsections. You start introducing the general structure of your discussion and then you go into much detail explaining dFe trends all the sudden. This is totally out of place here. You should add this paragraph to the end of the discussion or in a new section.

→ We have added a new section for this paragraph but we kept this new section there in the MS, as we think it would be odd to let the reader know at the end of the MS what we did not include.

Page 11 Lines 13-31:

4 Discussion

In the following sections, we will first discuss the high DFe concentrations observed throughout the water column of stations 1 and 17 located in the West European Basin (Section 4.1), then, the relationship between water masses and the DFe concentrations (Section 4.2) in intermediate (Section 4.2.2 and 4.2.3) and deep (Section 4.2.4 and 4.2.5) waters. We will also discuss the role of wind (Section 4.2.1), rivers (Section 4.3.1), meteoric water and sea-ice processes (Section 4.3.2), atmospheric deposition (Section 4.3.3) and sediments (Section 4.4) in delivering DFe. Finally, we will discuss the potential Fe limitation using DFe:NO₃⁻ ratios (Section 4.5).

4.1 High DFe concentrations at station 1 and 17

Considering the entire section, two stations (stations 1 and 17) showed irregularly high DFe concentrations (> 1 nmol L⁻¹) throughout the water column, thus suggesting analytical issues. However, these two stations were analysed twice and provided similar results, therefore discarding any analytical issues. This means that these high values originated either from genuine processes or from contamination issues. If there had been contamination issues, one would expect a more random distribution of DFe concentrations and less consistence throughout the water column. It thus appears that contamination issues were unlikely to happen. Similarly, the influence of water masses to explain these distributions was discarded as the observed high homogenized DFe concentrations were restricted to these two stations. Station 1, located at the continental shelf-break of the Iberian Margin, also showed enhanced PFe concentrations from lithogenic origin suggesting a margin source (Gourain et al., 2018). Conversely, no relationship was observed between DFe and PFe nor transmissometry for station 17. However, Ferron et al. (2016) reported a

Formatted: List Paragraph, Bulleted + Level: 1 + Aligned at: 0.25 cm + Indent at: 0.88 cm

Deleted: ¶

Formatted: Font: (Default) +Headings CS (Times New Roman), Complex Script Font: +Headings CS (Times New Roman)

Formatted: List Paragraph, Bulleted + Level: 1 + Aligned at: 0.25 cm + Indent at: 0.88 cm

Deleted: ¶

Formatted: Font: (Default) +Headings CS (Times New Roman), Complex Script Font: +Headings CS (Times New Roman)

Formatted: Font: (Default) +Headings CS (Times New Roman), Complex Script Font: +Headings CS (Times New Roman)

Formatted: List Paragraph, Bulleted + Level: 1 + Aligned at: 0.25 cm + Indent at: 0.88 cm

Formatted: List Paragraph, Bulleted + Level: 1 + Aligned at: 0.25 cm + Indent at: 0.88 cm

Formatted: Font: (Default) +Headings CS (Times New Roman), Complex Script Font: +Headings CS (Times New Roman)

Formatted: List Paragraph, Bulleted + Level: 1 + Aligned at: 0.25 cm + Indent at: 0.88 cm

Formatted: Font: (Default) +Headings CS (Times New Roman), Complex Script Font: +Headings CS (Times New Roman)

Formatted: List Paragraph, Bulleted + Level: 1 + Aligned at: 0.25 cm + Indent at: 0.88 cm

strong dissipation rate at the Azores-Biscay Rise (station 17) due to internal waves. The associated vertical energy fluxes could explain the homogenized profile of DFe at station 17, although such waves are not clearly evidenced in the velocity profiles. Consequently, the elevated DFe concentrations observed at station 17 remain unsolved.

Page 10, Line 20: I don't understand the aim of discussing dFe with water masses? I'd rather focus on the sources and sinks of dFe along the section. Discuss then the role of water masses in distributing the dFe signals. This means completely changing the focus of this section

→ We decided to discuss DFe with the main water masses, i.e. LSW, ISOW and DSOW as they all constitute the Deep Western Boundary Current (DWBC).

Page 11, Line 2: Flow of thoughts not clear, reasons of deep winter mixing scattered; bits of information thrown in a little randomly. You should start off by saying that deep winter mixing is an important mechanism supplying nutrients to the surface ocean in the North Atlantic Ocean; then say how this deep winter mixing is produced (from what I can understand in your text are you trying to say this is due to the effects of wind + convective mixing+ subduction/upwelling; am I right? This was not clear); then say what the specific conditions were in the year you sampled. I am still giving you corrections on the section, which you can incorporate in your rewritten discussion if fitting. I think you can recycle some parts of your discussion.

→ We have modified the text as suggested for clarification.

Page 12 Lines 12-22: In the North Atlantic Ocean, the warm and salty water masses of the upper limb of the MOC are progressively cooled and become denser, and subduct into the abyssal ocean. In some areas of the SubPolar North Atlantic, deep convective winter mixing provides a rare connection between surface and deep waters of the MOC thus constituting an important mechanism in supplying nutrients to the surface ocean (de Jong et al., 2012; Louanchi and Najjar, 2001). Deep convective winter mixing is triggered by the effect of wind and a pre-conditioning of the ocean in such a way that the inherent stability of the ocean is minimal. Pickart et al. (2003) demonstrated that these conditions are satisfied in the Irminger Sea with the presence of weakly stratified surface water, a close cyclonic circulation, which leads to the shoaling of the thermocline and intense winter air-sea buoyancy fluxes (Marshall and Schott, 1999). Moore (2003) and Piron et al. (2016) described low-level westerly jets centred northeast of Cape Farewell, over the Irminger Sea, known as tip jet events, whose structure depends upon the splitting occurring as the flow encounter the orographic features from Cape Farewell, and that are strong enough to induce deep convective mixing (Bacon et al., 2003; Pickart et al., 2003).

Page 11, Line 7: "events" and "with a positive NAO"

→ We have corrected as suggested.

Page 11, Line 8: "The winter mixed layer depth"

→ We have corrected as suggested.

Page 11, Line 9: instead of " and were" use "which was"

→ We have corrected as suggested.

Page 11, Line 11: "close to those found in LSW"

→ We have corrected as suggested.

Page 11, Line 13: sentence incomprehensible, please rephrase

Deleted: ¶

Formatted: Font: (Default) +Headings CS (Times New Roman), Complex Script Font: +Headings CS (Times New Roman)

Formatted: EndNote Bibliography

Formatted: Font: (Default) +Headings CS (Times New Roman), Complex Script Font: +Headings CS (Times New Roman)

Formatted: EndNote Bibliography

Formatted: Font: (Default) +Headings CS (Times New Roman), Complex Script Font: +Headings CS (Times New Roman)

Formatted: Font: (Default) +Headings CS (Times New Roman), Complex Script Font: +Headings CS (Times New Roman)

Formatted: List Paragraph, Bulleted + Level: 1 + Aligned at: 0.25 cm + Indent at: 0.88 cm

Formatted: List Paragraph, Bulleted + Level: 1 + Aligned at: 0.25 cm + Indent at: 0.88 cm

Formatted: Font: (Default) +Headings CS (Times New Roman), Complex Script Font: +Headings CS (Times New Roman)

Formatted: List Paragraph, Bulleted + Level: 1 + Aligned at: 0.25 cm + Indent at: 0.88 cm

Formatted: Font: (Default) +Headings CS (Times New Roman), Complex Script Font: +Headings CS (Times New Roman)

Formatted: List Paragraph, Bulleted + Level: 1 + Aligned at: 0.25 cm + Indent at: 0.88 cm

Formatted: Font: (Default) +Headings CS (Times New Roman), Complex Script Font: +Headings CS (Times New Roman)

→ This sentence has been removed according to Referee#1 comments and gather with previous sentence.

Formatted: List Paragraph, Bulleted + Level: 1 + Aligned at: 0.25 cm + Indent at: 0.88 cm

Page 12 Lines 26-27: Such winter entrainment was likely the process involved in the vertical supply of DFe within surface waters fuelling the spring phytoplankton bloom with DFe values close to those found in LSW.

Page 11, Line 24: need to improve a little the flow of thoughts in this paragraph. Start by saying why you see no MOW dFe signal, then support/contradict that argument(s) by what has been seen in other studies.

Formatted: Font: (Default) +Headings CS (Times New Roman), Complex Script Font: +Headings CS (Times New Roman)

→ We have modified this section according to your comments and Referee#1 comments.

Formatted: List Paragraph, Bulleted + Level: 1 + Aligned at: 0.25 cm + Indent at: 0.88 cm

Page 12 Lines 29-32 and Page 13 Lines 1-14: On its northern shores, the Mediterranean Sea is bordered by industrialized European countries, which act as a continuous source of anthropogenic derived constituents into the atmosphere, and on the southern shores by the arid and desert regions of north African and Arabian Desert belts, which act as sources of crustal material in the form of dust pulses (Chester et al., 1993; Guerzoni et al., 1999; Martin et al., 1989). During the summer, when thermal stratification occurs, DFe concentrations in the SML can increase over the whole Mediterranean Sea by 1.6-5.3 nmol L⁻¹ in response to the accumulation of atmospheric Fe from both anthropogenic and natural origins (Bonnet and Guieu, 2004; Guieu et al., 2010; Sarthou and Jeandel, 2001). After atmospheric deposition, the fate of Fe will depend on the nature of aerosols, vertical mixing, biological uptake and scavenging processes (Bonnet and Guieu, 2006; Wuttig et al., 2013). During GEOVIDE, MOW was observed from stations 1 to 29 between 1000 and 1200 m depth and associated with high dissolved aluminium (DAI, Menzel Barraqueta et al., 2018) concentrations (up to 38.7 nmol L⁻¹), confirming the high atmospheric deposition in the Mediterranean region. In contrast to Al, no DFe signature was associated with MOW (Figs. 2 and 4). This feature was also reported in some studies (Hatta et al., 2015; Thuróczy et al., 2010), while others measured higher DFe concentrations in MOW (Gerringa et al., 2017; Sarthou et al., 2007). However, MOW coincides with the maximum Apparent Oxygen Utilization (AOU) and it is not possible to distinguish the MOW signal from the remineralisation one (Sarthou et al., 2007). On the other hand, differences between studies are likely originating from the intensity of atmospheric deposition and the nature of aerosols. Indeed, Wagener et al. (2010) highlighted that large dust deposition events can accelerate the export of Fe from the water column through scavenging. As a result, in seawater with high DFe concentrations and where high dust deposition occurs, a strong individual dust deposition event could act as a sink for DFe. It thus becomes less evident to observe a systematic high DFe signature in MOW despite dust inputs.

Page 12, Line 3: “suggesting that the water mass is enriched in dFe during its flow path”

→ We have changed the text as suggested taking into account Referee#1 comments.

Deleted: ¶

Formatted: Font: (Default) +Headings CS (Times New Roman), Complex Script Font: +Headings CS (Times New Roman)

Formatted: List Paragraph, Bulleted + Level: 1 + Aligned at: 0.25 cm + Indent at: 0.88 cm

Page 13 Lines 16-18: As described in Section 3.1, the LSW exhibited increasing DFe concentrations from its source area, the Labrador Sea, toward the other basins with the highest DFe concentrations observed within the Irminger Sea, suggesting that the water mass was enriched in DFe either locally in each basin or during its flow path (see supplementary material Fig. S3).

Page 12, Line 4: start by saying what those sources are and then support with the available literature.

Formatted: Font: (Default) +Headings CS (Times New Roman), Complex Script Font: +Headings CS (Times New Roman)

→ We have reorganised this section based on your comments and Reviewer#1 comments.

Formatted: EndNote Bibliography

Page 13 Lines 16-33, Page 14 Lines 1-16: As described in Section 3.1, the LSW exhibited increasing DFe concentrations from its source area, the Labrador Sea, toward the other basins with the highest

DFe concentrations observed within the Irminger Sea, suggesting that the water mass was enriched in DFe either locally in each basin or during its flow path (Fig. 7). These DFe sources could originate from a combination of high export of PFe and its remineralisation in the mesopelagic area and/or the dissolution of sediment.

The Irminger and Labrador Seas exhibited the highest averaged integrated TChl-a concentrations ($98 \pm 32 \text{ mg m}^{-2}$ and $59 \pm 42 \text{ mg m}^{-2}$) compared to the West European and Iceland Basins ($39 \pm 10 \text{ mg m}^{-2}$ and $53 \pm 16 \text{ mg m}^{-2}$), when the influence of margins was discarded. Stations located in the Irminger (stations 40-56) and Labrador (stations 63-77) Seas, were largely dominated by diatoms (>50% of phytoplankton abundances) and displayed the highest chlorophyllid-a concentrations, a tracer of senescent diatom cells, likely reflecting post-bloom condition (Tonnard et al., in prep.). This is in line with the highest POC export data reported by Lemaître et al. (2018) in these two oceanic basins. This likely suggests that biogenic PFe export was also higher in the Labrador and Irminger Seas than in the West European and Iceland Basins. Although, Gourain et al. (2018) highlighted a higher biogenic contribution for particles located in the Irminger and Labrador Seas with relatively high PFe:PAI ratios ($0.44 \pm 0.12 \text{ mol:mol}$ and $0.38 \pm 0.10 \text{ mol:mol}$, respectively) compared to particles from the West European and Iceland Basins (0.22 ± 0.10 and $0.38 \pm 0.14 \text{ mol:mol}$, respectively, see Fig. 6 in Gourain et al., 2018), they reported no difference in PFe concentrations between the four oceanic basins (see Fig. 12A in Gourain et al., 2018) when the influence of margins was discarded, which likely highlighted the remineralisation of PFe within the Irminger and Labrador Seas. Indeed, Lemaître et al. (2017) reported higher remineralisation rates within the Labrador (up to $13 \text{ mmol C m}^{-2} \text{ d}^{-1}$) and Irminger Seas (up to $10 \text{ mmol C m}^{-2} \text{ d}^{-1}$) using the excess barium proxy (Dehairs et al., 1997), compared to the West European and Iceland Basins (ranging from 4 to $6 \text{ mmol C m}^{-2} \text{ d}^{-1}$). Therefore, the intense remineralisation rates measured in the Irminger and Labrador Seas likely resulted in enhanced DFe concentrations within LSW.

Higher DFe concentrations were, however, measured in the Irminger Sea compared to the Labrador Sea and coincided with lower transmissometry values (i.e. 98.0-98.5% vs. >99%), thus suggesting a particle load of the LSW. This could be explained by the reductive dissolution of Newfoundland Margin sediments. Indeed, Lambelet et al. (2016) reported high dissolved neodymium (Nd) concentrations (up to $18.5 \text{ pmol.kg}^{-1}$) within the LSW at the edge of the Newfoundland Margin (45.73°W , 51.82°N) as well as slightly lower Nd isotopic ratio values relative to those observed in the Irminger Sea. They suggested that this water mass had been in contact with sediments approximately within the last 30 years (Charette et al., 2015). Similarly, during GA03, Hatta et al. (2015) attributed the high DFe concentrations in the LSW to continental margin sediments. Consequently, it is also possible that the elevated DFe concentrations from the three LSW branches which entered the West European and Iceland Basins and Irminger Sea was supplied through sediment dissolution (Measures et al., 2013) along the LSW pathway.

The enhanced DFe concentrations measured in the Irminger Sea and within the LSW were thus likely attributed to the combination of higher productivity, POC export and remineralisation as well as a DFe supply from reductive dissolution of Newfoundland sediments to the LSW along its flow path.

Page 12, Line 6: change “the ones” for “those”

→ We have corrected as suggested (see above).

Page 12, Line 12: Provide a brief description of how the remineralisation rates were measured...

→ We have added this precision (see above).

Deleted: ¶

Formatted: Font: (Default) +Headings CS (Times New Roman), Complex Script Font: +Headings CS (Times New Roman)

Formatted: Font: (Default) +Headings CS (Times New Roman), Complex Script Font: +Headings CS (Times New Roman)

Formatted: List Paragraph, Bulleted + Level: 1 + Aligned at: 0.25 cm + Indent at: 0.88 cm

Formatted: EndNote Bibliography

Page 12, Line 18: You are repeating yourself!

→ We removed this sentence.

Page 12, Line 19: conspicuous? clearly visible? change this word

→ We have changed the text for clarification (see above).

Page 12, Line 21: confusing between remineralisation and bacteria mediated ligand production. Please be clear.

→ We have reformulated this sentence (see above).

Page 12, Line 27: "Hereafter"

→ We have corrected the text.

Page 13, Line 2: you also need to consider vertical/lateral inputs (think in 3D), so sedimentary Fe could be coming from further north, for example, within nepheloid layers. You can't discard sedimentary inputs just by looking at vertical gradients.

→ We have reorganised the idea of this paragraph and we have considered your suggestions (see below).

Page 13, Line 3: remove "the" before "Polar Intermediate Water" and "PIW" (line 6)

→ We have corrected the text accordingly.

Page 13, Line 9: instead of thinking that one water mass carries a certain dFe concentration (think of the short Fe residence times), this water mass might have "picked up" some dFe from, e.g., the sediments, on its pathway or It might have picked up particles in suspension which dissolve over time, etc!

→ We have reorganised the idea of this paragraph and we have considered your suggestions.

Page 15 Lines 2-20: However, considering the short residence time of DFe and the circulation of water masses in the Irminger Sea, it is possible that instead of being attributed to one specific water mass, these enhanced DFe concentrations resulted from lateral advection of the deep waters. Figure 8B) shows the concentrations of both DFe and PFe for the mixing line between DSOW/PIW and ISOW at station 44 and considering 100% contribution of ISOW for the shallowest sample (2218 m depth) and of DSOW/PIW for the deepest (2915 m depth), as these were the main water masses. This figure shows increasing DFe concentrations as DSOW/PIW mixed with ISOW. In addition, Le Roy et al. (2018) reported for the GEOVIDE voyage at station 44 a deviation from the conservative behaviour of ^{226}Ra reflecting an input of this tracer centred at 2500 m depth, likely highlighting diffusion from deep-sea sediments and coinciding with the highest DFe concentrations measured at this station. Although the transmissometer values were lower at the sediment interface than at 2500 m depth, Deng et al. (2018) reported a stronger scavenged component of the ^{230}Th at the same depth range, likely suggesting that the mixture of water masses were in contact with highly reactive particles. If there is evidence that the enhanced DFe concentrations observed at station 44 coincided with lateral advection of water masses that were in contact with particles, the difference of behaviour between DFe and ^{230}Th remains unsolved. The only parameter that would explain without any ambiguity such differences of behaviour between DFe and ^{230}Th would be the amounts of Fe-binding organic ligands for these samples. Indeed, although PFe concentrations decreased from the seafloor to the above seawater, this trend would likely be explained by a strong vertical diffusion alone and not necessarily from the dissolution of particles that were laterally advected.

Deleted: ¶

Formatted: Font: (Default) +Headings CS (Times New Roman), Complex Script Font: +Headings CS (Times New Roman)

Formatted: Font: (Default) +Headings CS (Times New Roman), Complex Script Font: +Headings CS (Times New Roman)

Formatted: List Paragraph, Bulleted + Level: 1 + Aligned at: 0.25 cm + Indent at: 0.88 cm

Formatted: List Paragraph, Bulleted + Level: 1 + Aligned at: 0.25 cm + Indent at: 0.88 cm

Deleted: ¶

Formatted: Font: (Default) +Headings CS (Times New Roman), Complex Script Font: +Headings CS (Times New Roman)

Formatted: EndNote Bibliography

Formatted: Font: (Default) +Headings CS (Times New Roman), Complex Script Font: +Headings CS (Times New Roman)

Formatted: List Paragraph, Bulleted + Level: 1 + Aligned at: 0.25 cm + Indent at: 0.88 cm

Formatted: Font: (Default) +Headings CS (Times New Roman), Complex Script Font: +Headings CS (Times New Roman)

Formatted: EndNote Bibliography

Formatted: Font: (Default) +Headings CS (Times New Roman), Complex Script Font: +Headings CS (Times New Roman)

Formatted: List Paragraph, Bulleted + Level: 1 + Aligned at: 0.25 cm + Indent at: 0.88 cm

Formatted: Font: (Default) +Headings CS (Times New Roman), Complex Script Font: +Headings CS (Times New Roman)

Formatted: EndNote Bibliography

Therefore, the high DFe concentrations observed might be inferred from local processes as ISOW mixes with both PIW and DSOW with a substantial load of Fe-rich particles that might have dissolved in solution due to Fe-binding organic ligands.

Page 13, Line 11: instead of “seawater” use “water masses”

→ We have reformulated this sentence (see above).

Page 13, Line 11: specify what you mean; 100 % contribution of which water mass at which depth

→ We have changed the text as suggested (see above).

Page 13, Line 18: watch out, this leads to miss-understanding as the reader thinks you are saying that particulate Fe is sustained by organic ligands. I don't think that is what you want to say.

→ We have changed the text as suggested (see above).

Page 13, Line 19: restructure this paragraph, say what you think the reasons are behind the high dFe concentrations, then support that by correlations, graphs etc and then compare to literature to confirm or dispute your theory. end the section with a stronger statement of what you think is happening in these deep water masses

→ We have changed the text as suggested (see above).

Page 13, Line 26: your explanation is a little long winded. Say that Mid Ocean Ridges can be a source of dFe but that this has not been found in the Reykjanes Ridge so far

→ We have changed the text according to your comments and referee#1 comments.

Page 15 Lines 22-30: Hydrothermal activity was assessed over the Mid Atlantic Ridge, namely the Reykjanes Ridge, from stations 36 to 42. Indeed, within the interr ridge database (<http://www.interridge.org>), the Reykjanes Ridge is reported to have active hydrothermal sites that were either confirmed (Baker and German, 2004a; German et al., 1994; Olafsson et al., 1991; Palmer et al., 1995) close to Iceland or inferred (e.g. Chen, 2003; Crane et al., 1997; German et al., 1994; Sinha et al., 1997; Smallwood and White, 1998) closer to the GEOVIDE section as no plume was detected but a high backscatter was reported potentially corresponding to a lava flow. Therefore, hydrothermal activity at the sampling sites remains unclear with no elevated DFe concentrations or temperature anomaly above the ridge (station 38).

Page 13, Line 30: you are repeating you pattern again; please first explain the signals you see and then compare to the literature

→ We have changed the text according to your comments and Referee#1 comments.

Page 15 Lines 28-33, Page 16 Lines 1-3: However, enhanced DFe concentrations (up to 1.5 ± 0.22 nmol L⁻¹, station 36, 2200 m depth) were measured east of the Reykjanes Ridge (Fig. 3). This could be due to hydrothermal activity and resuspension of sunken particles at sites located North of the section and transported through the ISOW towards the section (see supplementary material Fig. S3). Indeed, Achterberg et al. (2018) highlighted at ~60°N and over the Reykjanes Ridge a southward lateral transport of an Fe plume of up to 250-300 km. In agreement with these observations, previous studies (e.g. Fagel et al., 1996; Fagel et al., 2001; Lackschewitz et al., 1996; Parra et al., 1985) reported marine sediment mineral clays in the Iceland Basin largely dominated by smectite (> 60%), a tracer of hydrothermal alteration of basaltic volcanic materials (Fagel et al., 2001; Tréguer and De La Rocha, 2013). Hence, the high DFe concentrations measured east of the Reykjanes Ridge

Formatted: Font: (Default) +Headings CS (Times New Roman), Complex Script Font: +Headings CS (Times New Roman)

Formatted: List Paragraph, Bulleted + Level: 1 + Aligned at: 0.25 cm + Indent at: 0.88 cm

Formatted: Font: (Default) +Headings CS (Times New Roman), Complex Script Font: +Headings CS (Times New Roman)

Formatted: Not Highlight

Formatted: EndNote Bibliography

Formatted: Font: (Default) +Headings CS (Times New Roman), Complex Script Font: +Headings CS (Times New Roman)

Formatted: Not Highlight

Formatted: EndNote Bibliography

Formatted: Font: (Default) +Headings CS (Times New Roman), Complex Script Font: +Headings CS (Times New Roman)

Formatted: Not Highlight

Deleted: ¶

Formatted: Font: (Default) +Headings CS (Times New Roman), Complex Script Font: +Headings CS (Times New Roman)

Formatted: List Paragraph, Bulleted + Level: 1 + Aligned at: 0.25 cm + Indent at: 0.88 cm

Formatted: Font: (Default) +Headings CS (Times New Roman), Complex Script Font: +Headings CS (Times New Roman)

Formatted: List Paragraph, Bulleted + Level: 1 + Aligned at: 0.25 cm + Indent at: 0.88 cm

could be due to a hydrothermal source and/or the resuspension of particles and their subsequent dissolution.

Page 14, Line 4-6: are these located on your transect? If not, you need to give their locations (coordinates) and explain where they are relative to your section. Are these GEOVIDE hydrographic sections (I don't think so) or from other cruises? Specify which ones. Cite appropriate Figures, and supporting literature.

Formatted: Font: (Default) +Headings CS (Times New Roman), Complex Script Font: +Headings CS (Times New Roman)

→ We have changed the text as suggested. Note that we also added the location of CGFZ and BFZ on Figure 1.

Formatted: List Paragraph, Bulleted + Level: 1 + Aligned at: 0.25 cm + Indent at: 0.88 cm

Page 16 Lines 4-12: West of the Reykjanes Ridge, a DFe-enrichment was also observed in ISOW within the Irminger Sea (Figs. 4 and 7). The low transmissometer values within ISOW in the Irminger Sea compared to the Iceland Basin suggest a particle load. These particles could come from the Charlie Gibbs Fracture Zone (CGFZ, 52.67°N and 34.61°W) and potentially Bight Fracture Zone (BFZ, 56.91°N and 32.74°W) (Fig. 1) (Lackschewitz et al., 1996; Zou et al., 2017). Indeed, hydrographic sections of the northern valley of the CGFZ showed that below 2000 m depth the passage through the Mid-Atlantic Ridge was mainly filled with the ISOW (Kissel et al., 2009; Shor et al., 1980). Shor et al. (1980) highlighted a total westward transport across the sill, below 2000 m depth of about $2.4 \times 10^6 \text{ m}^3 \text{ s}^{-1}$ with ISOW carrying a significant load of suspended sediment ($25 \mu\text{g L}^{-1}$), including a 100-m-thick benthic nepheloid layer. It thus appears that the increase in DFe within ISOW likely came from sediment resuspension and dissolution as the ISOW flows across CGFZ and BFZ.

Formatted: Font: (Default) +Headings CS (Times New Roman), Complex Script Font: +Headings CS (Times New Roman)

Page 14, Line 11: complete this section with more recent references. There have been previous studies in this area

→ We have removed the following sentence "The seabed of this area has been identified as a depositional environment with patches of ripples and rock fragments surrounded by moat." Based on Referee#1 comments and have changed the text (see above).

Formatted: List Paragraph, Bulleted + Level: 1 + Aligned at: 0.25 cm + Indent at: 0.88 cm

Formatted: Font: (Default) +Headings CS (Times New Roman), Complex Script Font: +Headings CS (Times New Roman)

Page 14, Line 20: restructure, again start by saying what you see, explaining the reason of these signals showing correlations, and then supporting literature

→ We have changed the text as suggested.

Formatted: EndNote Bibliography

Page 16 Lines 19-32, Page 17 Lines 1-2: Enhanced DFe surface concentrations (up to $1.07 \pm 0.12 \text{ nmol L}^{-1}$) were measured over the Iberian Margin (stations 1-4) and coincided with salinity minima ($\sim <35$) and enhanced DA1 concentrations (up to 31.8 nmol L^{-1} , Menzel Barraqueta et al., 2018). DFe and DA1 concentrations were both significantly negatively correlated with salinity ($R^2 = \sim 1$ and 0.94, respectively) from stations 1 to 13 (Fig. 5). Salinity profiles from station 1 to 4 showed evidence of a freshwater source with surface salinity ranging from 34.95 (station 1) to 35.03 (station 4). Within this area, only two freshwater sources were possible: 1) wet atmospheric deposition (4 rain events, Shelley, pers. comm.) and 2) the Tagus River, since the ship SADCP data revealed a northward circulation (P. Lherminier and P. Zunino, Ifremer Brest, pers. comm.). Our SML DFe inventories were about three times higher at station 1 ($\sim 1 \text{ nmol L}^{-1}$) than those calculated during the GA03 voyage ($\sim 0.3 \text{ nmol L}^{-1}$, station 1) during which atmospheric deposition were about one order of magnitude higher (Shelley et al., 2018; Shelley et al., 2015), the atmospheric source seemed to be minor. Consequently, the Tagus River appears as the most likely source responsible for these enhanced DFe concentrations, either as direct input of DFe or indirectly through Fe-rich sediment carried by the Tagus River and their subsequent dissolution. The Tagus estuary is the largest in the western European coast and very industrialized (Canário et al., 2003; de Barros, 1986; Figueres et al., 1985; Gaudencio et al., 1991; Mil-Homens et al., 2009), extends through an area of 320 km^2 and is

Formatted: English (Australia)

Formatted: English (Australia)

Field Code Changed

characterized by a large water flow of $15.5 \cdot 10^9 \text{ m}^3 \text{ y}^{-1}$ (Fiuza, 1984). Many types of industry (e.g. heavy metallurgy, ore processing, chemical industry) release metals including Fe, which therefore result in high levels recorded in surface sediments, suspended particulate matter, water and organisms in the lower estuary (Santos-Echeandia et al., 2010).

Page 14, Line 26: You can't say "et al." in a personal communication. All people should be mentioned. Also State first name and affiliation in a personal communication.

→ We have modified the text to fulfil this comment (P. Lherminier and P. Zunino, Ifremer Brest, pers. comm.).

Page 14, Line 26: Very difficult to follow; why "however"? Start by explaining the typical ratios of different sources before you give the observed ratios in your study. Then discuss the What dFe:dAl ratio is expected from a river source? And from an atmospheric source?

→ We have removed this sentence according to your comment and Referee#1 comment and we have changed the text for clarification (see above).

Page 14, Line 29: Difficult to understand; you need to present each option that could lead to the enhanced dFe signal, discuss and then accept or discard

→ We have changed the text as suggested (see above).

Page 15, Line 18: I don't understand this "extended as close as 200 km from our Greenland stations". Please rephrase. Also avoid parenthesis next to parenthesis, and explain clearly what can be found in the link and what info you got from there.

→ We reword the sentence for clarification.

Page 17 Lines 10-17: The most plausible sources would be freshwater induced by meteoric water and sea-ice melt. Conversely, deeper in the water column, brine signals were calculated at stations 53 (100 m depth, Fig. 5D) 61 (100 m depth, Fig. 5E) and 78 (30 m depth, Fig. 5F). The release of brines could originate from two different processes: the sea-ice formation or the early melting of multiyear sea ice due to gravitational drainage and subsequent brine release (Petrich and Eicken, 2010; Wadhams, 2000). Indeed, during the winter preceding the GEOVIDE voyage, multiyear sea ice extended 200 km far from our Greenland stations (<http://nsidc.org/arcticseaicenews/>).

Page 15, Line 20: how were these calculated? give equations

→ We have included a section in the method on how these fractions were calculated.

Page 5 Lines 23-32, Page 6 Lines 1-9: We separated the mass contributions to samples from stations 53, 61 and 78 in Sea-Ice Melt (SIM) Meteoric Water (MW) and saline seawater inputs using the procedure and mass balance calculations that are fully described in Benetti et al. (2016) (Fig. 5D), E) and F)). Hereafter, we describe briefly the principle. We considered two types of seawater, namely the Atlantic Water (AW) and the Pacific Water (PW). After estimating the relative proportions of AW (f_{AW}) and PW (f_{PW}) and their respective salinity and $\delta^{18}\text{O}$ affecting each samples, the contribution of SIM and MW can be determined using measured salinity (S_m) and $\delta^{18}\text{O}$ ($\delta^{18}\text{O}_m$). The mass balance calculations are presented below:

$$f_{AW} + f_{PW} + f_{MW} + f_{SIM} = 1 \text{ (eq.1)}$$

$$f_{AW} \cdot S_{AW} + f_{PW} \cdot S_{PW} + f_{MW} \cdot S_{MW} + f_{SIM} \cdot S_{SIM} = S_m \text{ (eq.2)}$$

$$f_{AW} \cdot \delta^{18}\text{O}_{AW} + f_{PW} \cdot \delta^{18}\text{O}_{PW} + f_{MW} \cdot \delta^{18}\text{O}_{MW} + f_{SIM} \cdot \delta^{18}\text{O}_{SIM} = \delta^{18}\text{O}_m \text{ (eq.3)}$$

Field Code Changed

Formatted: English (Australia)

Formatted: English (Australia)

Formatted: Font: (Default) +Headings CS (Times New Roman), Complex Script Font: +Headings CS (Times New Roman)

Formatted: List Paragraph, Bulleted + Level: 1 + Aligned at: 0.25 cm + Indent at: 0.88 cm

Formatted: Font: (Default) +Headings CS (Times New Roman), Complex Script Font: +Headings CS (Times New Roman)

Formatted: List Paragraph, Bulleted + Level: 1 + Aligned at: 0.25 cm + Indent at: 0.88 cm

Deleted: ¶

Formatted: Font: (Default) +Headings CS (Times New Roman), Complex Script Font: +Headings CS (Times New Roman)

Formatted: List Paragraph, Bulleted + Level: 1 + Aligned at: 0.25 cm + Indent at: 0.88 cm

Deleted: ¶

Formatted: Font: (Default) +Headings CS (Times New Roman), Complex Script Font: +Headings CS (Times New Roman)

Formatted: Not Highlight

Formatted: EndNote Bibliography

Formatted: Not Highlight

Formatted: Not Highlight

Formatted: Highlight

Formatted: Font: (Default) +Headings CS (Times New Roman), Complex Script Font: +Headings CS (Times New Roman)

Formatted: Not Highlight

Formatted: Not Highlight

where f_{AW} , f_{PW} , f_{MW} , f_{SIM} are the relative fraction of AW, PW, MW, and SIM. To calculate the relative fractions of AW, PW, MW and SIM we used the following end-members: $S_{AW} = 35$, $\delta O_{AW}^{18} = +0.18\%$ (Benetti et al., 2016); $S_{PW} = 32.5$, $\delta O_{PW}^{18} = -1\%$ (Cooper et al., 1997; Woodgate and Aagaard, 2005); $S_{MW} = 0$, $\delta O_{MW}^{18} = -18.4\%$ (Cooper et al., 2008); $S_{SIM} = 4$, $\delta O_{SIM}^{18} = +0.5\%$ (Melling and Moore, 1995).

Negative sea-ice fractions indicated a net brine release while positive sea-ice fractions indicated a net sea-ice melting. Note that for stations over the Greenland Shelf, we assumed that the Pacific Water (PW) contribution was negligible for the calculations, supported by the very low PW fractions found at Cape Farewell in May 2014 (see Figure B1 in Benetti et al., 2017), while for station 78, located on the Newfoundland shelf, we used nutrient measurements to calculate the PW fractions, following the approach from Jones et al. (1998) (the data are published in Benetti et al., 2017).

Page 15, Line 27: I suggest instead of describing the Figures, you should use them to support your discussion. So try to avoid starting sentences and paragraphs describing Figures! You do this very often.

→ We have changed the text as suggested.

Page 17 Lines 20-33, Page 18 Lines 1-2: Considering the sampling period at stations 53 (16 June 2014) and 61 (19 June 2014), sea-ice formation unlikely explained the brine signals calculated as this period coincides with summer melting in both the Central Arctic and East Greenland (Markus et al., 2009). However, it is possible that the brines observed in our study could originate from sea-ice formation, which occurred during the previous winter(s) at 66°N (and/or higher latitudes). The residence time can vary from days (von Appen et al., 2014) to 6-9 months (Sutherland et al., 2009). Due to our observed strong brine signal at station 61 we suggest that the residence time was potentially longer than average. Given that the brine signal was higher at station 61 than at station 53 (which was located upstream in the EGC), we suggest that station 53 was exhibiting a freshening as a result of the transition between the freezing period toward the melting period. This would result in a dilution of the brine signal at the upstream station. Consequently, the salinity of this brine signal may reflect sea ice formation versus melting which may have an effect on the trace metal concentration within this water (Hunke et al., 2011). The associated brine water at station 61 (100 m depth) was slightly depleted in both DFe and PFe, which may be attributed to sea ice formation processes. Indeed, Janssens et al. (2016) highlighted that as soon as sea ice forms, sea salts are efficiently flushed out of the ice while PFe is trapped within the crystal matrix and DFe accumulates, leading to an enrichment factor of these two Fe fractions compared to underlying seawater. Conversely, the brine signal observed at station 53 (100 m depth) showed slight enrichment in DFe, which may be attributed to brine release during early sea ice melting and the associated release of DFe into the underlying water column as the brine sinks until reaching neutral buoyancy due to higher density.

Page 15, Line 27: how is sea-ice fraction calculated? please provide equations (if you calculated it yourself) or references where this data is published. Provide clear info so the reader can understand.

→ We have included a section in the method on how these fractions were calculated (see above).

Page 15, Line 30: explain why you compare to dAl in these profiles.

→ We have removed dAl distribution.

Page 15, Line 33: "originates"

→ We have corrected accordingly.

Formatted: Normal

Deleted: ¶

Formatted: Font: (Default) +Headings CS (Times New Roman), Complex Script Font: +Headings CS (Times New Roman)

Formatted: Not Highlight

Formatted: EndNote Bibliography

Formatted: Not Highlight

Deleted: ¶

Formatted: Highlight

Formatted: Font: (Default) +Headings CS (Times New Roman), Complex Script Font: +Headings CS (Times New Roman)

Formatted: Not Highlight

Formatted: EndNote Bibliography

Formatted: Font: (Default) +Headings CS (Times New Roman), Complex Script Font: +Headings CS (Times New Roman)

Formatted: EndNote Bibliography

Formatted: Font: (Default) +Headings CS (Times New Roman), Complex Script Font: +Headings CS (Times New Roman)

Formatted: Font: (Default) +Headings CS (Times New Roman), Complex Script Font: +Headings CS (Times New Roman)

Formatted: List Paragraph, Bulleted + Level: 1 + Aligned at: 0.25 cm + Indent at: 0.88 cm

Page 16, Line 7: I can't believe that sea-ice can "uptake" Fe! The concentration of Fe in the newly formed ice and in the remaining water should stay the same. You need to find another explanation!

→ We reword the sentence and add a reference for clarification (see above).

Page 16, Line 10: you mean sea-ice formation? Hence release of brine? Also explain that the brine sinks because it is denser (this is why it is observed below the surface)

→ We have changed the text as suggested (see above).

→ Regarding brines, they can originate from two different processes: either as a result of multiyear sea-ice melting or during sea-ice formation. Indeed, during the early melting season, multiyear sea-ice has a higher porosity and gravitational drainage of brine occur. These two processes of brine release might lead to different TM signatures in brine originating from sea-ice formation and brine originating from early melting of multiyear sea-ice (Petrich and Eicken, 2010; Wadhams, 2000).

Page 16, Line 10: "release of dFe"

→ We have corrected accordingly.

Page 16, Line 10: "underlying water column"

→ We have corrected accordingly.

Page 16, Line 11: split this sentence, it is too long

→ We have changed the text as suggested.

Page 16 Lines 29-32: Surface waters (from 0 to ~ 50 m depth) from station 53 and 61 were characterized by high MW fractions (ranging from 8.3 to 7.4% and from 7.7 to 7.4%, respectively, from surface to ~50 m depth). Within these surface waters, station 53 exhibited substantial sea-ice melting contribution (1.5%, 4 m depth) while station 61 exhibited low contribution (0.6%) from brine release that was linearly increasing with depth (1.3% at 50 m depth and 2.2 % at 100 m depth).

Page 16, Line 15: instead of describing the data (this is more appropriate for results section) you should say what correlates with what (e.g., low Fe with low MW). difficult to follow flow of thoughts

→ We have changed the text as suggested.

Page 18 Lines 3-18: Surface waters (from 0 to ~ 100 m depth) from station 53 and 61 were characterized by high MW fractions (ranging from 8.3 to 7.4% and from 7.7 to 7.3%, respectively, from surface to ~100 m depth, Figs. 5D and E). These high MW fractions were both enriched in PFe and DFe (except station 53 for which no data was available close to the surface) compared to seawater located below 50 m depth, thus suggesting a MW source. These results are in line with previous observations, which highlighted strong inputs of DFe from a meteoric water melting source in Antarctica (Annett et al., 2015). Although the ability of MW from Greenland Ice Sheet and runoffs to deliver DFe and PFe to surrounding waters has previously been demonstrated (Bhatia et al., 2013; Hawkings et al., 2014; Schroth et al., 2014; Statham et al., 2008), both Fe fractions were lower at the sample closest to the surface, then reached a maximum at ~ 50 m depth and decreased at ~ 70 m depth, for station 61 (Fig. 4D). The surface DFe depletion was likely explained by phytoplankton uptake, as indicated by the high TChl-*a* concentrations (up to 6.6 mg m⁻³) measured from surface to about 40 m depth, drastically decreasing at ~ 50 m depth to 3.9 mg m⁻³ (Fig. 4D). Hence, it seemed that meteoric water inputs from the Greenland Margin likely fertilized surface waters with DFe, enabling the phytoplankton bloom to subsist. The profile of PFe can be explained by two opposite

Deleted: ¶

Formatted: EndNote Bibliography

Formatted: Font: (Default) +Headings CS (Times New Roman), Complex Script Font: +Headings CS (Times New Roman)

Formatted: List Paragraph, Bulleted + Level: 1 + Aligned at: 0.25 cm + Indent at: 0.88 cm

Formatted: EndNote Bibliography

Deleted: <#>¶

Formatted: Font: (Default) +Headings CS (Times New Roman), Complex Script Font: +Headings CS (Times New Roman)

Formatted: List Paragraph, Bulleted + Level: 1 + Aligned at: 0.25 cm + Indent at: 0.88 cm

Formatted: Font: (Default) +Headings CS (Times New Roman), Complex Script Font: +Headings CS (Times New Roman)

Deleted: ¶

Formatted: Font: (Default) +Headings CS (Times New Roman), Complex Script Font: +Headings CS (Times New Roman)

Formatted: List Paragraph, Bulleted + Level: 1 + Aligned at: 0.25 cm + Indent at: 0.88 cm

Formatted: Font: (Default) +Headings CS (Times New Roman), Complex Script Font: +Headings CS (Times New Roman)

Formatted: EndNote Bibliography

plausible hypotheses: 1) MW inputs did not released PFe, as if it was the case, one should expect higher PFe concentrations at the surface (~25 m depth) than the one measured at 50 m depth due to both the release from MW and the assimilation of DFe by phytoplankton 2) MW inputs can release PFe in a form that is directly accessible to phytoplankton with subsequent export of PFe as phytoplankton died. The latter solution explains the PFe maximum measured at ~ 50 m depth and is thus the most plausible.

Page 16, Line 17: remind the reader in which figure information can be found (Chl-a, ect)

→ We added these precisions throughout this section.

Page 16, Line 24: results in agreement with the capacity of. . .? weird sentence, please change

→ We have changed the text as suggested.

Page 18 Lines 7-11: Although the ability of MW from Greenland Ice Sheet and runoffs to deliver DFe and PFe to surrounding waters have previously been demonstrated (Bhatia et al., 2013; Hawkings et al., 2014; Schroth et al., 2014; Statham et al., 2008), both Fe fractions were lower at the sample closest to the surface, then reached a maximum at ~ 50 m depth and decreased at ~ 70 m depth, for station 61 (Fig. 4D).

Page 16, Line 27: so far you have not talked about dFe:dAl ratio in meteoric water. Explain if this ratio is used to trace MW inputs and what you see in your profiles. should explain at the start.

→ We have added a sentence at the beginning of the section to fulfil this comment and removed the dAl data.

Page 17 Lines 15-17: In the following sections, we discuss the potential for meteoric water supply, sea-ice formation and sea-ice melting to affect DFe distribution.

Page 16, Line 28: change “noting that” for “although”

→ We changed the text as suggested.

Page 17, Line 6: or maybe the brine conditions (pH, salinity etc) make the Fe more bioavailable; or maybe this peak is not Fe related, but related to the release of other TM, or a phytoplankton group that thrives in brine and does not require much Fe? Since this shelf is further south, the environmental conditions may be more favourable for phytoplankton to grow and hence consuming all the dFe more rapidly. You should explore all the possibilities

→ We have changed the text as suggested.

Page 18 Lines 28-30: This either suggests that the brine likely contained important amounts of Fe (dissolved and/or particulate Fe) that were readily available for phytoplankton and consumed at the sampling period by potentially sea-ice algae themselves (Riebesell et al., 1991) or that another nutrient was triggering the phytoplankton bloom.

Page 17, Line 19: You repeat the word “dust” too much

→ We have changed the text according to your comment and Referee#1 comment.

Page 18 Lines 1-2 Page 19 Lines 1-4: On a regional scale, the North Atlantic basin receives the largest amount of atmospheric inputs due to its proximity to the Saharan Desert (Jickells et al., 2005), yet even in this region of high atmospheric deposition, inputs are not evenly distributed. Indeed, aerosol Fe loading measured during GEOVIDE (Shelley et al., 2017) were much lower (up to

Formatted: Font: (Default) +Headings CS (Times New Roman), Complex Script Font: +Headings CS (Times New Roman)

Formatted: List Paragraph, Bulleted + Level: 1 + Aligned at: 0.25 cm + Indent at: 0.88 cm

Formatted: Font: (Default) +Headings CS (Times New Roman), Complex Script Font: +Headings CS (Times New Roman)

Formatted: List Paragraph, Bulleted + Level: 1 + Aligned at: 0.25 cm + Indent at: 0.88 cm

Formatted: Font: (Default) +Headings CS (Times New Roman), Complex Script Font: +Headings CS (Times New Roman)

Formatted: EndNote Bibliography

Formatted: Font: (Default) +Headings CS (Times New Roman), Complex Script Font: +Headings CS (Times New Roman)

Formatted: List Paragraph, Bulleted + Level: 1 + Aligned at: 0.25 cm + Indent at: 0.88 cm

Formatted: Font: (Default) +Headings CS (Times New Roman), Complex Script Font: +Headings CS (Times New Roman)

Formatted: EndNote Bibliography

Formatted: Font: (Default) +Headings CS (Times New Roman), Complex Script Font: +Headings CS (Times New Roman)

Formatted: List Paragraph, Justified, Line spacing: 1.5 lines, Bulleted + Level: 1 + Aligned at: 0.25 cm + Indent at: 0.88 cm

Formatted: Indent: Before: 0.25 cm, No bullets or numbering

four orders of magnitude) than those measured during studies from lower latitudes in the North Atlantic (e.g. Baker et al., 2013; Buck et al., 2010; and for GA03, Shelley et al., 2015), but atmospheric inputs could still be an important source of Fe in areas far from land.

Page 17, Line 20, “proportions”

→ We have changed the text (see above).

Page 18, Line 3: you are going into too much detail here about aerosols, which is part of the Shelley papers

→ We have removed this part.

Page 18, Line 6: Meskhidze et al. (2017) is not in your reference list

→ We added the reference to the reference list.

Page 18, Line 10: information is a little randomly thrown in... what is your point? This is not a review paper

→ We have removed this part.

Page 18, Line 13: What does OM mean? write abbreviations out first time. Do you mean organic matter?

→ Yes, we meant organic matter but we have removed this part.

Page 18, Line 15: So all this background information to lastly say that you don't comment on this? Rephrase, make some assumptions or delete some detail

→ We have removed this part.

Page 18, Line 26: of those stations, station 40 is most similar to total aerosol dFe:dAl ratios. station 26 is closer to the soluble than the total composition, so I don't understand what you are saying

→ We removed all this part and changed it for turnover times relative to atmospheric deposition as defined in Guieu et al., 2014.

Page 19 Lines 5-17: In an attempt to estimate whether there was enough atmospheric input to sustain the SML DFe concentrations, we calculated Turnover Times relative to Atmospheric Deposition (TTADs, Guieu et al., 2014). To do so, we made the following assumptions: 1) the aerosol concentrations are a snapshot in time but are representative of the study region, 2) the aerosol solubility estimates based on two sequential leaches are an upper limit of the aerosol Fe in seawater and 3) the water column stratified just before the deposition of atmospheric inputs, so MLD DFe will reflect inputs from above. Thus, the TTADs were defined as the integrated DFe concentrations in the SML for each station divided by the contribution of soluble Fe contained in aerosols averaged per basin to the water volume of the SML. Although, TTADs were lower in the West European and Iceland Basins with an average of $\sim 9 \pm 3$ months compared to other basins (7 ± 2 years and 5 ± 2 years for the Irminger and Labrador Seas, respectively) (Fig. 6) they were about three times higher than those reported for areas impacted by Saharan dust inputs (~ 3 months, Guieu et al., 2014). Therefore, the high TTADs measured in the Irminger and Labrador Seas and ranging from 2 to 15 years provided further evidence that atmospheric deposition were unlikely to supply Fe in sufficient quantity to be the main source of DFe (see Sections 4.2.1 and 4.3.2) while in the West European and Iceland Basins they played an additional source, perhaps the main source of Fe especially at station 36 which displayed TTAD of 3 months.

Formatted: Font: (Default) +Headings CS (Times New Roman), Complex Script Font: +Headings CS (Times New Roman)

Formatted: Justified, Space After: 0 pt, Line spacing: 1.5 lines

Formatted: Font: (Default) +Headings CS (Times New Roman), Complex Script Font: +Headings CS (Times New Roman)

Formatted: List Paragraph, Bulleted + Level: 1 + Aligned at: 0.25 cm + Indent at: 0.88 cm

Formatted: EndNote Bibliography

Deleted: ¶

Formatted: Font: (Default) +Headings CS (Times New Roman), Complex Script Font: +Headings CS (Times New Roman)

Formatted: List Paragraph, Bulleted + Level: 1 + Aligned at: 0.25 cm + Indent at: 0.88 cm

Formatted: Font: (Default) +Headings CS (Times New Roman), Complex Script Font: +Headings CS (Times New Roman)

Formatted: EndNote Bibliography

Deleted: ¶

Formatted: Font: (Default) +Headings CS (Times New Roman), Complex Script Font: +Headings CS (Times New Roman)

Formatted: List Paragraph, Bulleted + Level: 1 + Aligned at: 0.25 cm + Indent at: 0.88 cm

Formatted: Font: (Default) +Headings CS (Times New Roman), Complex Script Font: +Headings CS (Times New Roman)

Formatted: List Paragraph, Bulleted + Level: 1 + Aligned at: 0.25 cm + Indent at: 0.88 cm

Deleted: ¶

Formatted: Font: (Default) +Headings CS (Times New Roman), Complex Script Font: +Headings CS (Times New Roman)

Formatted: List Paragraph, Bulleted + Level: 1 + Aligned at: 0.25 cm + Indent at: 0.88 cm

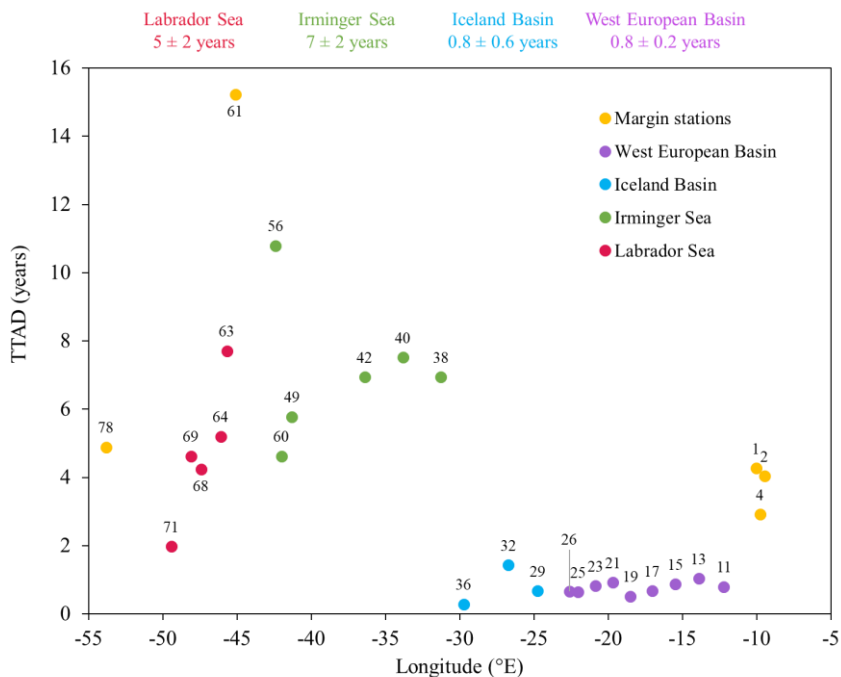


Figure 6: Plot of dissolved Fe (DFe) Turnover Times relative to Atmospheric Deposition (TTADs) calculated from soluble Fe contained in aerosols estimated from a two-stage sequential leach (UHP water, then 25% HAC, Shelley et al., this issue). Note that numbers on top of data points represent station numbers and that the colour coding refers to different region with in yellow, margin stations; in purple, the West European Basin; in blue, the Iceland Basin; in green, the Irminger Sea and in red, the Labrador Sea. The numbers on top of the plot represent TTADs averaged for each oceanic basin and their standard deviation.

Page 18, Line 28: And what about all the other stations where the ratios are different? I would say this is more of a "coincidence" that these data fall onto the black line. The multiple reactions occurring as Fe enters the ocean change this Fe:Al ratio rapidly

→ Same as above, this part has been removed.

Page 18, Line 30: remove "time"

→ This part has been removed (see above).

Page 19, Line 2: I don't understand... these station points on your figure 10 are similar to those of other stations. What makes you think they have a higher atmospheric influence??

→ This part has also been removed (see above).

Page 19, Line 4: in this section you should mention that bottom water dFe concentrations were significantly higher on the Newfoundland margin than on the Greenland margins

Deleted: ¶

Formatted: Font: (Default) +Headings CS (Times New Roman), Complex Script Font: +Headings CS (Times New Roman)

Formatted: Font: (Default) +Headings CS (Times New Roman), Complex Script Font: +Headings CS (Times New Roman)

Formatted: List Paragraph, Bulleted + Level: 1 + Aligned at: 0.25 cm + Indent at: 0.88 cm

Formatted: List Paragraph, Bulleted + Level: 1 + Aligned at: 0.25 cm + Indent at: 0.88 cm

Formatted: Font: (Default) +Headings CS (Times New Roman), Complex Script Font: +Headings CS (Times New Roman)

Formatted: Font: (Default) +Headings CS (Times New Roman), Complex Script Font: +Headings CS (Times New Roman)

Formatted: List Paragraph, Bulleted + Level: 1 + Aligned at: 0.25 cm + Indent at: 0.88 cm

→ We have included this precision.

Page 19 Lines 20-24: DFe concentration profiles from all coastal stations (stations 2, 4, 53, 56, 61 and 78) are reported on Figure 5. To avoid surface processes, only depths below 100 m depth will be considered in the following discussion. Stations where DFe and PFe followed a similar pattern are stations 2, 53, 56, and 78, suggesting that either the sources of Fe supplied both Fe fractions (dissolved and particulate) or that PFe dissolution from sediments supplied DFe. Among the different margins, the Newfoundland Margin exhibited the highest deep-water DFe concentrations.

Page 19, Line 10: “mol:mol” to stay consistent

→ We have changed the text as suggested.

Page 19, Line 10: what is the average useful for? Show a plot with dFe:pFe ratios or a table

→ Because the SD is relatively high thus conferring distinct signature throughout the water column (below 100 m depth) of each station. This allows the comparison station by station instead of comparing each samples. These ratios were added to Table 3.

Page 19, Line 11: as well as different sediment compositions, this could be also due to different supply mechanisms? Different sediment conditions (redox, organic content, temp, etc)

→ We added this precision in the text.

Page 19 Lines 25-28: DFe:PFe ratios ranged from 0.01 (station 2, bottom sample) to 0.27 (station 4, ~ 400 m depth) mol:mol with an average value of 0.11 ± 0.07 mol:mol (n = 23, Table 3), highlighting a different behaviour of Fe between margins. This could be explained by the different nature of the sediments and/or different sediment conditions (e.g. redox, organic content).

Page 19, Line 17: Where is the predominance of diatoms?

→ We changed the sentence for clarification.

Page 19 Lines 31-33: These observations are consistent with the high TChl-a concentrations measured at the Newfoundland Margin and to a lesser extent at the Greenland Margin and the predominance of diatoms relative to other functional phytoplankton classes at both margins (Tonnard et al., in prep.).

Page 19, Line 21: I think this section is great, but you need to organise the ideas clearly. Now difficult to follow. Also name this section “nepheloid layers”

→ We changed the section title as suggested and reorganised the flow of ideas.

Page 19, Line 26: explain the criterion first. Explain briefly the PCA and the results you show in figure 11. Information is thrown in a little randomly. Please organise you paragraphs

→ We reorganised the paragraph as suggested.

Page 20 Lines 6-16: Samples associated with high levels of particles (transmissometer < 99%) and below 500 m depth displayed a huge variability in DFe concentrations. From the entire dataset, 66 samples (~13% of the entire dataset) followed this criterion with 3 samples from the Iberian Margin (station 4), 14 samples from the West European Basin (station 1), 4 samples from the Iceland Basin (stations 29, 32, 36 and 38), 43 samples from the Irminger Sea (stations 40, 42, 44, 49 and 60) and 2 samples from the Labrador Sea (station 69). To determine which parameter was susceptible to explain the variation in DFe concentrations in these nepheloid layers, a Principal Component Analysis (PCA) on these samples. The input variables of the PCA were the particulate Fe, Al, and particulate manganese (PMn) (Gourain et al., 2018), the DAI (Menzel Barraqueta et al., 2018) and

Formatted: List Paragraph, Bulleted + Level: 1 + Aligned at: 0.25 cm + Indent at: 0.88 cm

Formatted: Font: (Default) +Headings CS (Times New Roman), Complex Script Font: +Headings CS (Times New Roman)

Formatted: Font: (Default) +Headings CS (Times New Roman), Complex Script Font: +Headings CS (Times New Roman)

Formatted: List Paragraph, Bulleted + Level: 1 + Aligned at: 0.25 cm + Indent at: 0.88 cm

Formatted: List Paragraph, Bulleted + Level: 1 + Aligned at: 0.25 cm + Indent at: 0.88 cm

Formatted: Font: (Default) +Headings CS (Times New Roman), Complex Script Font: +Headings CS (Times New Roman)

Formatted: List Paragraph, Bulleted + Level: 1 + Aligned at: 0.25 cm + Indent at: 0.88 cm

Formatted: Font: (Default) +Headings CS (Times New Roman), Complex Script Font: +Headings CS (Times New Roman)

Formatted: List Paragraph, Bulleted + Level: 1 + Aligned at: 0.25 cm + Indent at: 0.88 cm

Formatted: Font: (Default) +Headings CS (Times New Roman), Complex Script Font: +Headings CS (Times New Roman)

Formatted: List Paragraph, Bulleted + Level: 1 + Aligned at: 0.25 cm + Indent at: 0.88 cm

Formatted: Font: (Default) +Headings CS (Times New Roman), Complex Script Font: +Headings CS (Times New Roman)

Formatted: EndNote Bibliography

the Apparent Oxygen Utilization (AOU) and were all correlated to DFe concentrations explaining all together 93% of the subset variance (see supplementary material Fig. S6). The first dimension of the PCA was represented by the PAI, PFe and PMn concentrations and explained 59.5% of the variance, while the second dimension was represented by the DAI and the AOU parameters, explaining 33.2% of the variance. The two sets of variables were nearly at right angle from each other, indicating no correlation between them.

Page 20, Line 1: I would not call it AOU “concentrations” find another way to express this

→ We changed “concentrations” for parameters (Page 20 Line 20).

Page 20, Line 13: you should look into non-reducing dissolution of lithogenic material. You are missing out on a big topic! Radic et al., 2011; Labatut et al., 2014; Abadie et al., 2017

→ We included this topic in the text as suggested.

Page 20 Lines 26-34, Page 21 Lines 1-6: This observation challenges the traditional view of Fe oxidation with oxygen, either abiotically or microbially induced. Indeed, remineralisation can decrease sediment oxygen concentrations, promoting reductive dissolution of PFe oxyhydroxides to DFe that can then diffuse across the sediment water interface as DFe(II) colloids (Homoky et al., 2011). Such processes will inevitably lead to rapid Fe removal through precipitation of nanoparticulate or colloidal Fe (oxyhydr)oxides, followed by aggregation or scavenging by larger particles (Boyd and Ellwood, 2010; Lohan and Bruland, 2008) unless complexation with Fe-binding organic ligands occurs (Batchelli et al., 2010; Gerringa et al., 2008). There exist, however, another process that is favoured in oxic benthic boundary layers (BBL) with low organic matter degradation and/or low Fe oxides, which implies the dissolution of particles after resuspension, namely the non-reductive dissolution of sediment (Homoky et al., 2013; Radic et al., 2011). In addition, these higher oxygenated samples were located within DSOW, which mainly originate (75% of the overflow) from the Nordic Seas and the Arctic Ocean (Tanhua et al., 2005), in which the ultimate source of Fe was reported by Klunder et al. (2012) to come from Eurasian river waters. The major Arctic rivers were highlighted by Slagter et al. (2017) to be a source of Fe-binding organic ligands that are then further transported via the TPD across the Denmark Strait. Hence, the enhanced DFe concentrations measured within DSOW might result from Fe-binding organic ligand complexation that were transported to the deep ocean as DSOW formed rather than the non-reductive dissolution of sediment.

Page 20, Line 14: “lead”

→ We changed the text accordingly.

Page 20, Line 16: instead of “these” use “this sediment-derived. . .”

→ We have changed the text accordingly.

Page 20, Line 17: do not state this as facts... these are assumptions

→ We have changed the text as suggested(see above).

Page 20, Line 25: very poor sum-up, please improve

→ We have changed the full section according to your comment (see above).

Formatted: Font: (Default) +Headings CS (Times New Roman), Complex Script Font: +Headings CS (Times New Roman)

Formatted: List Paragraph, Bulleted + Level: 1 + Aligned at: 0.25 cm + Indent at: 0.88 cm

Formatted: Font: (Default) +Headings CS (Times New Roman), Complex Script Font: +Headings CS (Times New Roman)

Formatted: List Paragraph, Bulleted + Level: 1 + Aligned at: 0.25 cm + Indent at: 0.88 cm

Formatted: Font: (Default) +Headings CS (Times New Roman), Complex Script Font: +Headings CS (Times New Roman)

Formatted: List Paragraph, Bulleted + Level: 1 + Aligned at: 0.25 cm + Indent at: 0.88 cm

Formatted: Font: (Default) +Headings CS (Times New Roman), Complex Script Font: +Headings CS (Times New Roman)

Formatted: List Paragraph, Bulleted + Level: 1 + Aligned at: 0.25 cm + Indent at: 0.88 cm

Formatted: Font: (Default) +Headings CS (Times New Roman), Complex Script Font: +Headings CS (Times New Roman)

Formatted: List Paragraph, Bulleted + Level: 1 + Aligned at: 0.25 cm + Indent at: 0.88 cm

Formatted: Font: (Default) +Headings CS (Times New Roman), Complex Script Font: +Headings CS (Times New Roman)

Formatted: EndNote Bibliography

Formatted: Font: (Default) +Headings CS (Times New Roman), Complex Script Font: +Headings CS (Times New Roman)

Page 20, Line 26: You should also compare surface dFe data to AOU to look at dFe released from remineralisation. You have done this for >500 m depth, but it will be worth looking at this more closely below the surface mixed layer, where remineralisation occurs (below 100 m depth).

→ We have included this just before Fe* section.

Formatted: EndNote Bibliography

Page 21 Lines 25-33, Page 22 Lines 1-34, Page 23 Lines 1-3: The remineralisation of organic matter is a major source of macro and micronutrients in subsurface waters (from 50 to 250 m depth). Remineralisation is associated with the consumption of oxygen and therefore, Apparent Oxygen Utilization (AOU) can provide a quantitative estimate of the amount of material that has been remineralised. While no relationship was observed below 50 m depth for NO_3^- or DFe and AOU considering all the stations, a significant correlation was found in the Subpolar gyre when removing the influence of margins (stations 29-49, 56, 60, 63-77) ($\text{AOU} = 3.88 \text{ NO}_3^- - 39.32$, $R^2=0.79$, $n=69$, p -value < 0.001). This correlation indicates that remineralisation of Particulate Organic Nitrogen (PON) greatly translates into Dissolved Inorganic Nitrogen (DIN) and that NO_3^- can be used as a good tracer for remineralisation in the studied area. Within these Subpolar gyre waters, there was a significant correlation between DFe and AOU ($\text{AOU} = 22.6 \text{ DFe}$, $R^2=0.34$, $n=53$, p -value < 0.001). The open-ocean stations from Subpolar gyre also exhibited a good linear correlation between DFe and NO_3^- ($R^2=0.42$, $n=51$, p -value < 0.05). The slope of the relationship, representing the typical remineralisation ratio, was $R_{\text{Fe:N}} = 0.07 \pm 0.01 \text{ mmol mol}^{-1}$. The intercept of the regression line was $-0.4 \pm 0.2 \text{ nmol L}^{-1}$, reflecting possible excess of preformed NO_3^- compare to DFe in these water masses. These significant correlations allow us to use the Fe* tracer to assess where DFe concentrations potentially limit phytoplankton growth by subtracting the contribution of organic matter remineralisation from the dissolved Fe pool, as defined by Rijkenberg et al. (2014) and Parekh et al. (2005) for PO_4^{3-} , and modified here for NO_3^- as follow:

$$\text{Fe}^* = [\text{DFe}] - R_{\text{Fe:N}} \times [\text{NO}_3^-] \text{ (eq. 4)}$$

where $R_{\text{Fe:N}}$ refers to the average biological uptake ratio Fe over nitrogen, and $[\text{NO}_3^-]$ refers to nitrate concentrations in seawater. Although, we imposed a fixed biological $R_{\text{Fe:N}}$ of $0.05 \text{ mmol mol}^{-1}$, it is important to note that the biological uptake ratio of $\text{DFe}:\text{NO}_3^-$ is not likely to be constant. Indeed, this ratio has been found to range from 0.05 to $0.9 \text{ mmol mol}^{-1}$ depending on species (Ho et al., 2003; Sunda and Huntsman, 1995; Twining et al., 2004). The ratio we choose is thus less drastic to assess potential Fe limitation and more representative of the average biological uptake of DFe over NO_3^- calculated for this study (i.e. $R_{\text{Fe:N}} = 0.07 \pm 0.01 \text{ mmol mol}^{-1}$, for Subpolar waters). Negative values of Fe* indicate the removal of DFe that is faster than the input through remineralisation or external sources and positive values suggest input of DFe from external sources (Fig. 7). Consequently, figure 7 shows that phytoplankton communities with very high Fe requirements relative to NO_3^- ($R_{\text{Fe:N}} = 0.9$) will only be able to grow above continental shelves where there is a high supply of DFe as previously reported by Nielsdóttir et al. (2009) and Painter et al. (2014). All these results are corroborating the importance of the Tagus River (Iberian Margin, see section 4.2.1), glacial inputs in the Greenland and Newfoundland Margins (see section 4.2.2) and to a lesser extent atmospheric inputs (see section 4.2.3) in supplying Fe with Fe:N ratios higher than the average biological uptake/demand ratio. Figure 7 (see also supplementary material S7, S8, S9 and S10) also highlights the Fe limitation for the low-Fe requirement phytoplankton class ($R_{\text{Fe:N}} = 0.05$) within the Iceland Basin, Irminger and Labrador Seas. The Fe deficiency observed in surface waters (> 50 m depth) from the Irminger and Labrador Seas might be explained by low atmospheric deposition for the ICSPMW and the LSW (Shelley et al., 2017). Low atmospheric Fe supply and sub-optimal Fe:N ratios in winter overturned deep water could favour the formation of the High-Nutrient, Low-Chlorophyll (HNLC) conditions. The West European Basin, despite exhibiting some of the highest

DFe:NO₃⁻ ratios within surface waters (see supplementary material Fig. S8), displayed the strongest Fe-depletion from 50 m depth down to the bottom, suggesting that the main source of Fe was coming from dust deposition and/or riverine inputs.

Similarly as for the West European Basin, the pattern displayed in the surface map of DFe:NO₃⁻ ratios (supplementary material S8) extended to about 50 m depth, after which the trend reversed (Fig. 7 and supplementary material Fig. S7). Below 50 m depth, the Fe* tracer (Fig. 7) was positive in the Irminger Sea and overall negative in the other basins. In the Irminger Sea positive Fe* values were likely the result of the winter entrainment of Fe-rich LSW (see section 4.2.1) coinciding with high remineralised carbon fluxes in this area (station 44; Lemaître et al., 2017) (see section 4.2.2). The largest drawdown in DFe:NO₃⁻ ratios was observed between stations 34 and 38 and was likely due to the intrusion of the ICSPMW, this water mass exhibiting low DFe and high in NO₃⁻ (from 7 to 8 μmol L⁻¹) concentrations. Similarly, the SAIW exhibited high NO₃⁻ concentrations. Both the ICSPMW and the SAIW sourced from the NAC. The NAC as it flows along the coast of North America receives atmospheric depositions from anthropogenic sources (Shelley et al., 2017; 2015) which deliver high N relative to Fe (Jickells and Moore, 2015) and might be responsible for the observed ranges.

Page 20, Line 30: change the ending of this sentence, not properly expressed

→ We have split and changed the sentence (see above).

Page 20, Line 31: First explain why you talk about Fe:nitrate ratios. THis comes out of the blue! Also cite Fig 12.

→ We have changed the text as suggested (see above).

Page 21, Line 3: what do you mean by influence of the river, and the currents? specify what you mean

→ We have changed the text for clarification (see above).

Page 21, Line 6: Can you provide a different kind of plot to help visualise this gradient you are talking about. In figure 12 this is impossible

→ We have included a surface map of DFe:NO₃⁻ ratios.

Formatted: Font: (Default) +Headings CS (Times New Roman), Complex Script Font: +Headings CS (Times New Roman)

Formatted: Font: (Default) +Body (Calibri), Complex Script Font: +Body CS (Arial)

Formatted: EndNote Bibliography

Deleted: ¶

Formatted: Font: (Default) +Headings CS (Times New Roman), Complex Script Font: +Headings CS (Times New Roman)

Formatted: List Paragraph, Bulleted + Level: 1 + Aligned at: 0.25 cm + Indent at: 0.88 cm

Deleted: ¶

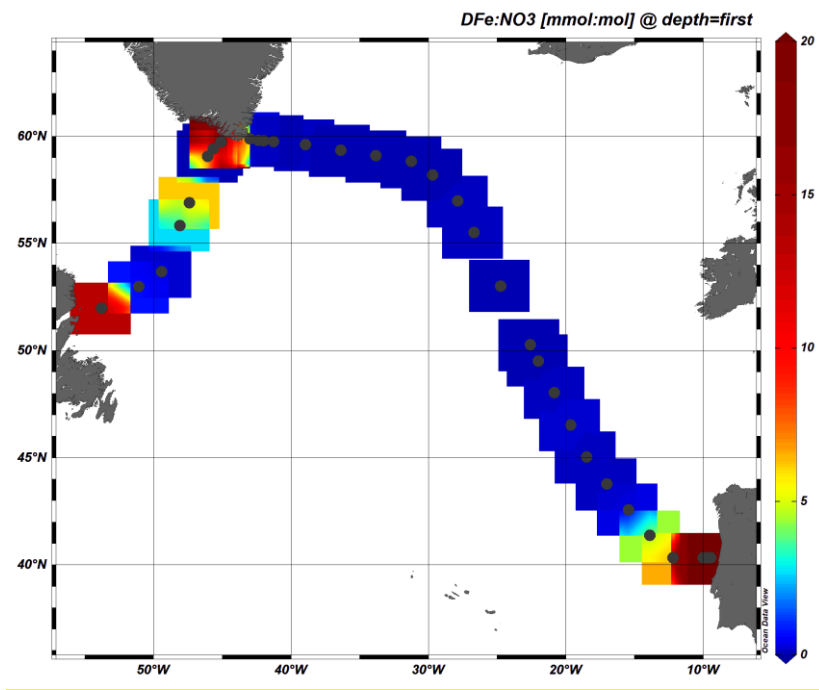
Formatted: Font: (Default) +Headings CS (Times New Roman), Complex Script Font: +Headings CS (Times New Roman)

Formatted: EndNote Bibliography

Deleted: ¶

Formatted: Font: (Default) +Headings CS (Times New Roman), Complex Script Font: +Headings CS (Times New Roman)

Formatted: List Paragraph, Bulleted + Level: 1 + Aligned at: 0.25 cm + Indent at: 0.88 cm



Formatted: Font: (Default) +Headings CS (Times New Roman), Complex Script Font: +Headings CS (Times New Roman)

Formatted: Indent: Before: 0.25 cm

Formatted: Font: (Default) +Headings CS (Times New Roman), Complex Script Font: +Headings CS (Times New Roman)

Formatted: List Paragraph, Bulleted + Level: 1 + Aligned at: 0.25 cm + Indent at: 0.88 cm

Formatted: Not Highlight

Formatted: EndNote Bibliography

Formatted: Font: (Default) +Headings CS (Times New Roman), Complex Script Font: +Headings CS (Times New Roman)

Formatted: EndNote Bibliography

Formatted: Font: (Default) +Headings CS (Times New Roman), Complex Script Font: +Headings CS (Times New Roman)

Formatted: Font: (Default) +Headings CS (Times New Roman), Complex Script Font: +Headings CS (Times New Roman)

Formatted: List Paragraph, Bulleted + Level: 1 + Aligned at: 0.25 cm + Indent at: 0.88 cm

Formatted: Font: (Default) +Headings CS (Times New Roman), Complex Script Font: +Headings CS (Times New Roman)

Formatted: Not Highlight

Formatted: EndNote Bibliography

Formatted: Not Highlight

Formatted: Not Highlight

Formatted: Not Highlight

Formatted: Not Highlight

Formatted: Not Highlight

Page 21, Line 18: “disequilibrium” sounds a bit odd, better use the word “ranges”

→ We have changed the text as suggested (see above).

Page 21, Line 23: do you assume that all the nitrate in seawater comes from remineralisation? Better explain what assumptions this equation relies on.

→ We have modified the text accordingly (see above the response to your comment “Page 20, Line 26”)

Page 21, Line 26: Rather, negative values of Fe^* indicate the removal of dFe that is faster than the input through remineralisation or external sources and positive values suggest input of dFe from external sources

→ We have changed the text as suggested.

Page 21, Line 27: remove “out”

→ We have changed the text as suggested.

Page 21, Line 28: you talk about surface waters here but the calculations are done below 100 m depth. I would keep discussion on the external sources of dFe and then link to inputs of dFe rich water masses to surface waters above.

→ We have reorganised the section according to your comments and Reviewer#1 comments. Therefore we only focus the discussion on the top 200 m depth of the section.

Page 21, Lines 12-33, Page 22, Lines 1-34, Page 23, Lines 1-3: A key determinant for assessing the significance of a DFe source is the magnitude of the DFe:macronutrient ratio supplied, since this

term determines to which extent DFe will be utilised. The DFe:NO₃⁻ ratios in surface waters varied from 0.02 (station 36) to 38.6 (station 61) mmol:mol with an average of 5 ± 10 mmol:mol (see supplementary material Fig. S7). Values were typically equal or lower than 0.28 mmol mol⁻¹ in all basins except at the margins and at stations 11, 13, 68, 69 and 77. The low nitrate concentrations observed at the eastern and western Greenland and Newfoundland Margins reflected a strong phytoplankton bloom which had reduced the concentrations as highlighted by the elevated integrated TChl-*a* concentrations ranging from 129.6 (station 78) to 398.3 (station 61) mg m⁻². At the Iberian Margin, they likely reflected the influence of the N-limited Tagus River (stations 1, 2 and 4) with its low TChl-*a* integrated concentrations that ranged from 31.2 (station 1) to 46.4 (station 4) mg m⁻². The high DFe:NO₃⁻ ratios determined at those stations, which varied from 13.4 (station 78) to 38.6 (station 61) mmol:mol, suggested that waters from these areas, despite having the lowest NO₃⁻ concentrations, were relatively enriched in DFe compared to waters from Iceland Basin and Irminger Sea.

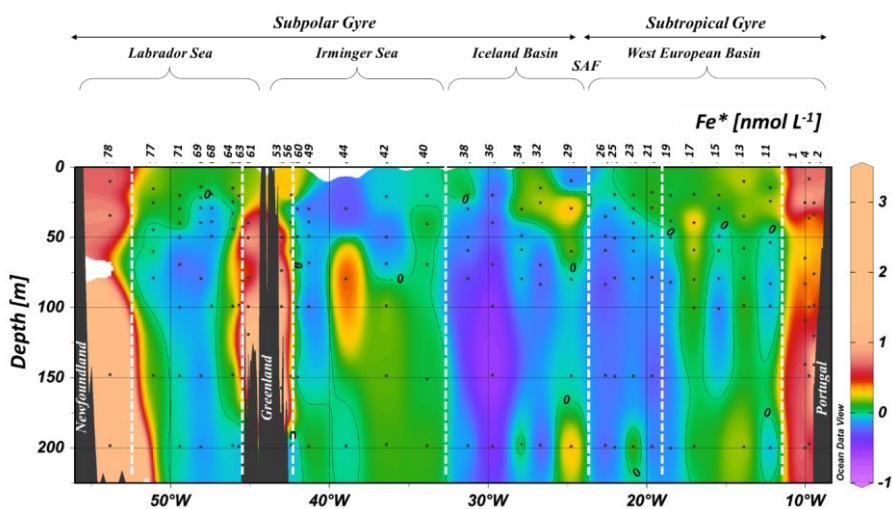
In our study, DFe:NO₃⁻ ratios displayed a gradient from the West European Basin to Greenland (supplementary material S7 and S8). This trend only reverses when the influence of Greenland was encountered, as also observed by Painter et al. (2014). The remineralisation of organic matter is a major source of macro and micronutrients in subsurface waters (from 50 to 250 m depth). Remineralisation is associated with the consumption of oxygen and therefore, Apparent Oxygen Utilization (AOU) can provide a quantitative estimate of the amount of material that has been remineralised. While no relationship was observed below 50 m depth for NO₃⁻ or DFe and AOU considering all the stations, a significant correlation was found in the Subpolar gyre when removing the influence of margins (stations 29-49, 56, 60, 63-77) (AOU = 3.88 NO₃⁻ - 39.32, R²=0.79, n=69, p-value < 0.001). This correlation indicates that remineralisation of Particulate Organic Nitrogen (PON) greatly translates into Dissolved Inorganic Nitrogen (DIN) and that NO₃⁻ can be used as a good tracer for remineralisation in the studied area. Within these Subpolar gyre waters, there was a significant correlation between DFe and AOU (AOU = 22.6 DFe, R²=0.34, n=53, p-value < 0.001). The open-ocean stations from Subpolar gyre also exhibited a good linear correlation between DFe and NO₃⁻ (R²=0.42, n=51, p-value < 0.05). The slope of the relationship, representing the typical remineralisation ratio, was R_{Fe:N} = 0.07 ± 0.01 mmol mol⁻¹. The intercept of the regression line was -0.4 ± 0.2 nmol L⁻¹, reflecting possible excess of preformed NO₃⁻ compare to DFe in these water masses. These significant correlations allow us to use the Fe* tracer to assess where DFe concentrations potentially limit phytoplankton growth by subtracting the contribution of organic matter remineralisation from the dissolved Fe pool, as defined by Rijkenberg et al. (2014) and Parekh et al. (2005) for PO₄³⁻, and modified here for NO₃⁻ as follow:

$$Fe^* = [DFe] - R_{Fe:N} \times [NO_3^-] \text{ (eq. 4)}$$

where R_{Fe:N} refers to the average biological uptake ratio Fe over nitrogen, and [NO₃⁻] refers to nitrate concentrations in seawater. Although, we imposed a fixed biological R_{Fe:N} of 0.05 mmol mol⁻¹, it is important to note that the biological uptake ratio of DFe:NO₃⁻ is not likely to be constant. Indeed, this ratio has been found to range from 0.05 to 0.9 mmol mol⁻¹ depending on species (Ho et al., 2003; Sunda and Huntsman, 1995; Twining et al., 2004). The ratio we choose is thus less drastic to assess potential Fe limitation and more representative of the average biological uptake of DFe over NO₃⁻ calculated for this study (i.e. R_{Fe:N} = 0.07 ± 0.01 mmol mol⁻¹, for Subpolar waters). Negative values of Fe* indicate the removal of DFe that is faster than the input through remineralisation or external sources and positive values suggest input of DFe from external sources (Fig. 7). Consequently, figure 7 shows that phytoplankton communities with very high Fe requirements relative to NO₃⁻ (R_{Fe:N} = 0.9) will only be able to grow above continental shelves where there is a high

supply of DFe as previously reported by Nielsdóttir et al. (2009) and Painter et al. (2014). All these results are corroborating the importance of the Tagus River (Iberian Margin, see section 4.2.1), glacial inputs in the Greenland and Newfoundland Margins (see section 4.2.2) and to a lesser extent atmospheric inputs (see section 4.2.3) in supplying Fe with Fe:N ratios higher than the average biological uptake/demand ratio. Figure 7 (see also supplementary material S7, S8, S9 and S10) also highlights the Fe limitation for the low-Fe requirement phytoplankton class ($R_{Fe:N} = 0.05$) within the Iceland Basin, Irminger and Labrador Seas. The Fe deficiency observed in surface waters (> 50 m depth) from the Irminger and Labrador Seas might be explained by low atmospheric deposition for the ICSPMW and the LSW (Shelley et al., 2017). Low atmospheric Fe supply and sub-optimal Fe:N ratios in winter overturned deep water could favour the formation of the High-Nutrient, Low-Chlorophyll (HNLC) conditions. The West European Basin, despite exhibiting some of the highest DFe:NO₃⁻ ratios within surface waters (see supplementary material Fig. S8), displayed the strongest Fe-depletion from 50 m depth down to the bottom, suggesting that the main source of Fe was coming from dust deposition and/or riverine inputs.

Similarly as for the West European Basin, the pattern displayed in the surface map of DFe:NO₃⁻ ratios (supplementary material S8) extended to about 50 m depth, after which the trend reversed (Fig. 7 and supplementary material Fig. S7). Below 50 m depth, the Fe* tracer (Fig. 7) was positive in the Irminger Sea and overall negative in the other basins. In the Irminger Sea positive Fe* values were likely the result of the winter entrainment of Fe-rich LSW (see section 4.2.1) coinciding with high remineralised carbon fluxes in this area (station 44; Lemaître et al., 2017) (see section 4.2.2). The largest drawdown in DFe:NO₃⁻ ratios was observed between stations 34 and 38 and was likely due to the intrusion of the ICSPMW, this water mass exhibiting low DFe and high in NO₃⁻ (from 7 to 8 μmol L⁻¹) concentrations. Similarly, the SAIW exhibited high NO₃⁻ concentrations. Both the ICSPMW and the SAIW sourced from the NAC. The NAC as it flows along the coast of North America receives atmospheric depositions from anthropogenic sources (Shelley et al., 2017; 2015) which deliver high N relative to Fe (Jickells and Moore, 2015) and might be responsible for the observed ranges.



Page 22, Line 5: what has the low Fe supply to do with the "inefficient" carbon pump? If you want to talk about the carbon pump, and its inefficiency, you need to support with adequate statements/findings. I do not think this is a finding of your study.

Formatted: EndNote Bibliography, Indent: Before: 0.25 cm

Formatted: Highlight

Formatted: Font: (Default) +Headings CS (Times New Roman), Complex Script Font: +Headings CS (Times New Roman)

Formatted: Not Highlight

→ We have removed this part (see above).

Page 22, Line 7: this comes a little out of the blue. Explain a little more the high remineralised carbon fluxes and how they were measured.

→ We replaced in context this sentence and the precision on the measurement of remineralised carbon fluxes is now precised earlier in the MS.

Page 22, Line 12: poor ending. What about other sources? Margins? Rivers?

→ We have changed the text (see above).

Page 22, Line 15: first sentence superfluous

→ We have removed this sentence as suggested.

Page 22, Line 23: depletion of nitrate? That doesn't make sense

→ We have changed the sentence for clarification (see above).

Page 22, Line 27: "entrained it to the deep. . ."

→ We have changed the text as suggested.

Page 22, Line 29: "in the deep ocean"

→ We have changed the text as suggested.

Page 22, Line 30: do you mean particles? Sediments are on the seafloor. Same for line 32

→ Yes you are right, we have changed "sediments" for "particles".

Page 23, Line 3: conclusions need to be rewritten after the discussion is reworked.

→ We have modified the conclusion to be more specific

Page 23 Lines 5-31 Page 24 lines 1-2: The DFe concentrations measured during this study were in good agreement with previous studies that spanned the West European Basin. However, within the Irminger Basin the DFe concentrations measured during this study were up to 3 times higher than the ones measured by Rijkenberg et al. (2014) in deep waters (> 1000 m depth) that was likely explained by the different water masses encountered (i.e. the Polar Intermediate Water, ~ 2800 m depth) and by a stronger signal of the Iceland Scotland Overflow Water (ISOW) from 1200 to 2300 m depth. This corresponded to the most striking feature of the whole section with DFe concentrations reaching up to 2.5 nmol L⁻¹ within the ISOW, Denmark Strait Overflow Water (DSOW) and Labrador Sea Water (LSW), three water masses that are part of the Deep Western Boundary Current and was likely the result of a lateral advection of particles in the Irminger. However, as these water masses reached the Labrador Sea, lower DFe levels were measured. These differences could be explained by different processes occurring within the benthic nepheloid layers, where DFe was sometimes trapped onto particles due to Mn-sediment within the Labrador Sea (Gourain et al., 2018) and sometimes released from the sediment potentially as a result of interactions with dissolved organic matter. Such Fe-binding organic ligands could have also be produced locally due to the intense remineralisation rate reported by Lemaître et al. (2017) of biogenic particles (Boyd et al., 2010; Gourain et al., 2018). The LSW exhibited increasing DFe concentrations along its flow path, likely resulting from sediment inputs at the Newfoundland Margin. Although DFe inputs through hydrothermal activity were expected at the slow spreading Reykjanes Ridge (Baker and German, 2004b; German et al., 1994), our data did not evidence this specific source as previously pointed by Achterberg et al. (2018) further north (~60°N) from our section.

Formatted: EndNote Bibliography

Formatted: Font: (Default) +Headings CS (Times New Roman), Complex Script Font: +Headings CS (Times New Roman)

Formatted: Not Highlight

Formatted: EndNote Bibliography

Formatted: Font: (Default) +Headings CS (Times New Roman), Complex Script Font: +Headings CS (Times New Roman)

Formatted: EndNote Bibliography

Formatted: Font: (Default) +Headings CS (Times New Roman), Complex Script Font: +Headings CS (Times New Roman)

Formatted: List Paragraph, Bulleted + Level: 1 + Aligned at: 0.25 cm + Indent at: 0.88 cm

Formatted: Font: (Default) +Headings CS (Times New Roman), Complex Script Font: +Headings CS (Times New Roman)

Formatted: List Paragraph, Bulleted + Level: 1 + Aligned at: 0.25 cm + Indent at: 0.88 cm

Deleted: ¶

Formatted: Font: (Default) +Headings CS (Times New Roman), Complex Script Font: +Headings CS (Times New Roman)

Formatted: List Paragraph, Bulleted + Level: 1 + Aligned at: 0.25 cm + Indent at: 0.88 cm

Formatted: Font: (Default) +Headings CS (Times New Roman), Complex Script Font: +Headings CS (Times New Roman)

Formatted: Font: (Default) +Headings CS (Times New Roman), Complex Script Font: +Headings CS (Times New Roman)

Formatted: List Paragraph, Bulleted + Level: 1 + Aligned at: 0.25 cm + Indent at: 0.88 cm

Formatted: List Paragraph, Bulleted + Level: 1 + Aligned at: 0.25 cm + Indent at: 0.88 cm

Formatted: Font: (Default) +Headings CS (Times New Roman), Complex Script Font: +Headings CS (Times New Roman)

Formatted: EndNote Bibliography

Formatted: English (Australia)

Formatted: English (Australia)

Formatted: English (Australia)

Formatted: English (Australia)

In surface waters several sources of DFe were highlighted especially close to lands, with riverine inputs from the Tagus River at the Iberian margin (Menzel Barraqueta et al., 2018) and meteoric inputs (including coastal runoff and glacial meltwater) at the Newfoundland and Greenland margins (Benetti et al., 2016). Substantial sediment inputs were observed at all margins but with different intensity. The highest DFe sediment input was located at the Newfoundland margin, while the lowest was observed at the eastern Greenland margin. These differences could be explained by the different nature of particles with the most lithogenic located at the Iberian margin and the most biogenic, at the Newfoundland margin (Gourain et al., 2018). Although previous studies (e.g. Jickells et al., 2005; Shelley et al., 2015) reported that atmospheric inputs substantially fertilized surface waters from the West European Basin, in our study only stations located in the West European and Iceland Basins exhibited enhanced SML DFe inventories with lower TTADs. However, these TTADs were about three times higher than those reported for Saharan dust inputs and thus atmospheric deposition appeared to be a minor source of Fe at the sampling period. Finally, there was evidence of convective inputs of the LSW to surface seawater caused by long tip jet event (Piron et al., 2016) that deepened the winter mixed layer down to ~ 1200 m depth (Zunino et al., 2017), in which Fe was in excess of nitrate and where thus Fe was not limiting at the sampling period.

- ➔ Achterberg, E. P., Steigenberger, S., Marsay, C. M., LeMoigne, F. A., Painter, S. C., Baker, A. R., Connelly, D. P., Moore, C. M., Tagliabue, A., and Tanhua, T.: Iron Biogeochemistry in the High Latitude North Atlantic Ocean, *Scientific reports*, 8, 1-15, 10.1038/s41598-018-19472-1, 2018.
- ➔ Annett, A. L., Skiba, M., Henley, S. F., Venables, H. J., Meredith, M. P., Statham, P. J., and Ganeshram, R. S.: Comparative roles of upwelling and glacial iron sources in Ryder Bay, coastal western Antarctic Peninsula, *Marine Chemistry*, 176, 21-33, 10.1016/j.marchem.2015.06.017, 2015.
- ➔ Bacon, S., Gould, W. J., and Jia, Y.: Open-ocean convection in the Irminger Sea, *Geophysical Research Letters*, 30, 1246, doi:10.1029/2002GL016271, 2003.
- ➔ Baker, A. R., Adams, C., Bell, T. G., Jickells, T. D., and Ganzeveld, L.: Estimation of atmospheric nutrient inputs to the Atlantic Ocean from 50°N to 50°S based on large-scale field sampling: Iron and other dust-associated elements, *Global Biogeochemical Cycles*, 27, 755-767, 10.1002/gbc.20062, 2013.
- ➔ Baker, A. T., and German, C. R.: On the Global Distribution of Hydrothermal vent Fields, in: *Mid-Ocean Ridges*, edited by: German, C. R., Lin, J., and Parson, L. M., 2004a.
- ➔ Baker, E. T., and German, C. R.: Hydrothermal Interactions Between the Lithosphere and Oceans, in: *Mid-Ocean Ridges*, edited by: German, C. R., Lin, J., and Parson, L. M., *Geophysical Monograph Series*, AGU, 245-266, 2004b.
- ➔ Barton, A. D., Greene, C. H., Monger, B. C., and Pershing, A. J.: The Continuous Plankton Recorder survey and the North Atlantic Oscillation: Interannual- to Multidecadal-scale patterns of phytoplankton variability in the North Atlantic Ocean, *Progress in Oceanography*, 58, 337-358, 10.1016/j.pocean.2003.08.012, 2003.
- ➔ Batchelli, S., Muller, F. L. L., Chang, K. C., and Lee, C. L.: Evidence for Strong but Dynamic Iron-Humic Colloidal Associations in Humic-Rich Coastal Waters., *Environmental Science & Technology*, 44, 8485-8490, 2010.
- ➔ Benetti, M., Reverdin, G., Pierre, C., Khatiwala, S., Tournadre, B., Olafsdottir, S., and Naamar, A.: Variability of sea ice melt and meteoric water input in the surface Labrador Current off Newfoundland, *Journal of Geophysical Research Oceans*, 121, 2841-2855, doi:10.1002/2015JC011302, 2016.
- ➔ Benetti, M., Reverdin, G., Lique, C., Yashayaev, I., Holliday, N. P., Tynan, E., Torres-Valdes, S., Lherminier, P., Tréguer, P., and Sarthou, G.: Composition of freshwater in the spring of 2014 on the

Deleted: Achterberg, E. P., Steigenberger, S., Marsay, C. M., LeMoigne, F. A., Painter, S. C., Baker, A. R., Connelly, D. P., Moore, C. M., Tagliabue, A., and Tanhua, T.: Iron Biogeochemistry in the High Latitude North Atlantic Ocean, *Scientific reports*, 8, 1-15, 10.1038/s41598-018-19472-1, 2018.¶

Bacon, S., Gould, W. J., and Jia, Y.: Open-ocean convection in the Irminger Sea, *Geophysical Research Letters*, 30, 1246, doi:10.1029/2002GL016271, 2003.¶

Baker, A. T., and German, C. R.: On the Global Distribution of Hydrothermal vent Fields, in: *Mid-Ocean Ridges*, edited by: German, C. R., Lin, J., and Parson, L. M., 2004.¶

Bhatia, M. P., Kujawinski, E. B., Das, S. B., Breier, C. F., Henderson, P. B., and Charette, M. A.: Greenland meltwater as a significant and potentially bioavailable source of iron to the ocean, *Nature Geoscience*, 2013, 274-278, 10.1038/ngeo1746, 2013.¶

Bonnet, S., and Guieu, C.: Dissolution of atmospheric iron in seawater, *Geophysical Research Letters*, 31, 10.1029/2003gl018423, 2004.¶

Bonnet, S., and Guieu, C.: Atmospheric forcing on the annual iron cycle in the western Mediterranean Sea: A 1-year survey, *Journal of Geophysical Research*, 111, 10.1029/2005jc003213, 2006.¶

Bressac, M., and Guieu, C.: Post-depositional processes: What really happens to new atmospheric iron in the ocean's surface?, *Global Biogeochemical Cycles*, 27, 859-870, 10.1002/gbc.20076, 2013.¶

Bressac, M., Guieu, C., Doxaran, D., Bourrin, F., Desboeufs, K., Leblond, N., and Ridame, C.: Quantification of the lithogenic carbon pump following a simulated dust-deposition event in large mesocosms, *Biogeochemistry*, 11, 1007-1020, 10.5194/bg-11-1007-2014, 2014.¶

Canário, J., Vale, C., Caetano, M., and Madureira, M. J.: Mercury in contaminated sediments and pore waters enriched in sulphate (Tagus Estuary, Portugal), *Environmental Pollution*, 126, 425-433, 10.1016/S0269-7491(03)00234-3, 2003.¶

Chen, Y. J.: Influence of the Iceland mantle plume on crustal accretion at the inflated Reykjanes Ridge: Magma lens and low hydrothermal activity, *Journal of Geophysical Research*, 108, 2524, 2003.¶

Chester, R., Murphy, K. J. T., Lin, F. J., Berry, A. S., Bradshaw, G. A., and Corcoran, P. A.: Factors controlling the solubilities of trace-metals from nonremote aerosols deposited to the sea-surface by the dry deposition mode, *Marine Chemistry*, 42, 107-126, 10.1016/0304-4203(93)90241-f, 1993.¶

Chever, F., Bucciarelli, E., Sarthou, G., Speich, S., Arhan, M., Penven, P., and Tagliabue, A.: Physical speciation of iron in the Atlantic sector of the Southern Ocean, along a transect from the subtropical domain to the Weddell Sea Gyre, *Journal of Geophysical Research*, 115, 1-15, 2010.¶

Crane, K., Johnson, L., Appelgate, B., Nishimura, C., Buck, R., Jones, C., Vogt, P., and Kos'yan, R.: Volcanic and Seismic Swarm Events on the Reykjanes Ridge and Their Similarities to Events on Iceland: Results of a Rapid Response Mission, *Marine Geophysical Researches*, 19, 319-338, 1997.¶

de Barros, M. C.: A case study of waste inputs in the Tagus estuary, in: *The role of the Oceans as a Waste Disposal Option*, edited by: Kullenberg, G., NATO ASI Series; Series C: Mathematical and Physical Sciences, 172, Springer Netherlands, 307-324, 1986.¶

- southern Labrador shelf and slope, *Journal of Geophysical Research: Oceans*, 122, 1102-1121, 10.1002/2016jc012244, 2017.
- ➔ Bersch, M., Yashayaev, I., and Koltermann, K. P.: Recent changes of the thermohaline circulation in the subpolar North Atlantic, *Ocean Dynamics*, 57, 223-235, 10.1007/s10236-007-0104-7, 2007.
 - ➔ Bhatia, M. P., Kujawinski, E. B., Das, S. B., Breier, C. F., Henderson, P. B., and Charette, M. A.: Greenland meltwater as a significant and potentially bioavailable source of iron to the ocean, *Nature Geoscience*, 2013, 274-278, 10.1038/ngeo1746, 2013.
 - ➔ Bonnet, S., and Guieu, C.: Dissolution of atmospheric iron in seawater, *Geophysical Research Letters*, 31, 10.1029/2003gl018423, 2004.
 - ➔ Bonnet, S., and Guieu, C.: Atmospheric forcing on the annual iron cycle in the western Mediterranean Sea: A 1-year survey, *Journal of Geophysical Research*, 111, 10.1029/2005jc003213, 2006.
 - ➔ Boyd, P. W., Watson, A. J., Law, C. S., Abraham, E. R., Trull, T., Murdoch, R., Bakker, D. C. E., Bowie, A. R., Buesseler, K. O., Chang, H., Charette, M., Croot, P., Downing, K., Frew, R., Gall, M., Hadfield, M., Hall, J., Harvey, M., Jameson, G., LaRoche, J., Liddicoat, M., Ling, R., Maldonado, M. T., McKay, R. M., Nodder, S., Pickmere, S., Pridmore, R., Rintoul, S., Safi, K., Sutton, P., Strzepek, R., Tanneberger, K., Turner, S., Waite, A., and Zeldis, J.: A mesoscale phytoplankton bloom in the polar Southern Ocean stimulated by iron fertilization, *Nature*, 407, 695-702, 2000.
 - ➔ Boyd, P. W., and Ellwood, M. J.: The biogeochemical cycle of iron in the ocean, *Nature Geoscience*, 3, 675-682, 10.1038/ngeo964, 2010.
 - ➔ Boyd, P. W., Ibanami, E., Sander, S. G., Hunter, K. A., and Jackson, G. A.: Remineralization of upper ocean particles: Implications for iron biogeochemistry, *Limnology and Oceanography*, 55, 1271-1288, 10.4319/lo.2010.55.3.1271, 2010.
 - ➔ Buck, C. S., Landing, W. M., Resing, J. A., and Measures, C. I.: The solubility and deposition of aerosol Fe and other trace elements in the North Atlantic Ocean: Observations from the A16N CLIVAR/CO2 repeat hydrography section, *Marine Chemistry*, 120, 57-70, 10.1016/j.marchem.2008.08.003, 2010.
 - ➔ Canário, J., Vale, C., Caetano, M., and Madureira, M. J.: Mercury in contaminated sediments and pore waters enriched in sulphate (Tagus Estuary, Portugal), *Environmental Pollution*, 126, 425-433, 10.1016/S0269-7491(03)00234-3, 2003.
 - ➔ Charette, M. A., Morris, P. J., Henderson, P. B., and Moore, W. S.: Radium isotope distributions during the US GEOTRACES North Atlantic cruises, *Marine Chemistry*, 177, 184-195, 10.1016/j.marchem.2015.01.001, 2015.
 - ➔ Chen, Y. J.: Influence of the Iceland mantle plume on crustal accretion at the inflated Reykjanes Ridge: Magma lens and low hydrothermal activity, *Journal of Geophysical Research*, 108, 2524, 2003.
 - ➔ Chester, R., Murphy, K. J. T., Lin, F. J., Berry, A. S., Bradshaw, G. A., and Corcoran, P. A.: Factors controlling the solubilities of trace-metals from nonremote aerosols deposited to the sea-surface by the dry deposition mode, *Marine Chemistry*, 42, 107-126, 10.1016/0304-4203(93)90241-f, 1993.
 - ➔ Chever, F., Bucciarelli, E., Sarthou, G., Speich, S., Arhan, M., Penven, P., and Tagliabue, A.: Physical speciation of iron in the Atlantic sector of the Southern Ocean, along a transect from the subtropical domain to the Weddell Sea Gyre, *Journal of Geophysical Research*, 115, 1-15, 2010.
 - ➔ Conway, T. M., and John, S. G.: Quantification of dissolved iron sources to the North Atlantic Ocean, *Nature*, 511, 212-215, 10.1038/nature13482, 2014.
 - ➔ Cooper, L. W., Whitedge, T. E., Grebmeier, J. M., and Weingartner, T.: The nutrient, salinity, and stable oxygen isotope composition of Bering and Chukchi Seas waters in and near the Bering Strait, *Journal of Geophysical Research*, 102, 12,563-512,573, 1997.

- ➔ Cooper, L. W., McClelland, J. W., Holmes, R. M., Raymond, P. A., Gibson, J. J., Guay, C. K., and Peterson, B. J.: Flow-weighted values of runoff tracers ($\delta^{18}\text{O}$, DOC, Ba, alkalinity) from the six largest Arctic rivers, *Geophysical Research Letters*, 35, 1-5, 10.1029/2008GL035007, 2008.
- ➔ Crane, K., Johnson, L., Appelgate, B., Nishimura, C., Buck, R., Jones, C., Vogt, P., and Kos'yan, R.: Volcanic and Seismic Swarm Events on the Reykjanes Ridge and Their Similarities to Events on Iceland: Results of a Rapid Response Mission, *Marine Geophysical Researches*, 19, 319-338, 1997.
- ➔ de Barros, M. C.: A case study of waste inputs in the Tagus estuary, in: *The role of the Oceans as a Waste Disposal Option*, edited by: Kullenberg, G., NATO ASI Series; Series C: Mathematical and Physical Sciences, 172, Springer Netherlands, 307-324, 1986.
- ➔ de Jong, M. F., van Aken, H. M., Våge, K., and Pickart, R. S.: Convective mixing in the central Irminger Sea: 2002–2010, *Deep Sea Research Part I: Oceanographic Research Papers*, 63, 36-51, 10.1016/j.dsr.2012.01.003, 2012.
- ➔ Dehairs, F., Shopova, D., Ober, S., Veth, C., and Goeyens, L.: Particulate barium stocks and oxygen consumption in the Southern Ocean mesopelagic water column during spring and early summer: Relationship with export production, *Deep Sea Research II*, 44, 497-516, 10.1016/S0967-0645(96)00072-0, 1997.
- ➔ Deng, F., Henderson, G. M., Castrillejo, M., and Perez, F. F.: Evolution of 231Pa and 230Th in overflow waters of the North Atlantic, *Biogeosciences*, 1-24, 10.5194/bg-2018-191, 2018.
- ➔ Fagel, N., Robert, C., and Hilaire-Marcel, C.: Clay mineral signature of the NW Atlantic Boundary Undercurrent, *Marine Geology*, 130, 19-28, 1996.
- ➔ Fagel, N., Robert, C., Preda, M., and Thorez, J.: Smectite composition as a tracer of deep circulation: the case of the Northern North Atlantic, *Marine Geology*, 172, 309-330, 2001.
- ➔ Ferron, B., Kokoszka, F., Mercier, H., Lherminier, P., Huck, T., Rios, A., and Thierry, V.: Variability of the Turbulent Kinetic Energy Dissipation along the A25 Greenland–Portugal Transect Repeated from 2002 to 2012, *Journal of Physical Oceanography*, 46, 1989-2003, 10.1175/jpo-d-15-0186.1, 2016.
- ➔ Figueres, G., Martin, J. M., Meybeck, M., and Seyler, P.: A comparative study of mercury contamination in the Tagus estuary (Portugal) and major French estuaries (Gironde, Loire, Rhone), *Estuarine, Coastal and Shelf Science*, 20, 183-203, 1985.
- ➔ Fiúza, A.: *Hidrologia e dinamica das aguas costeiras de Portugal*, Ph. D., Universidade de Lisboa, Lisboa, Portugal, unpublished, 1984.
- ➔ Follows, M., and Dutkiewicz, S.: Meteorological modulation of the North Atlantic Spring Bloom, *Deep Sea Research Part II: Topical Studies in Oceanography*, 49, 321-344, 2001.
- ➔ García-Ibáñez, M. I., Pérez, F. F., Lherminier, P., Zunino, P., Mercier, H., and Tréguer, P.: Water mass distributions and transports for the 2014 GEOVIDE cruise in the North Atlantic, *Biogeosciences*, 15, 2075-2090, 10.5194/bg-15-2075-2018, 2018.
- ➔ Gaudencio, M. J., Guerra, M. T., and Glemarec, M.: Recherches biosédimentaires sur la zone maritime de l'estuaire du Tage, Portugal: données sédimentaires préliminaires. , in: *Estuaries and Coasts: Spatial and Temporal Intercomparisons*, edited by: Elliot, M., and Ducrotoy, J. C., Olsen and Olsen, Fredensborg, 11-16, 1991.
- ➔ German, C. R., Briem, J., Chin, C. S., Danielsen, M., Holland, S., James, R. H., Jonsdottir, A., Ludford, E., Moser, C., Olafsson, J., Palmer, M. R., and Rudnicki, M. D.: Hydrothermal activity on the Reykjanes Ridge: the Steinahóll vent-field at 63°06'N, *Earth and Planetary Science Letters*, 121, 647-654, 1994.
- ➔ Gerringa, L. J. A., Blain, S., Laan, P., Sarthou, G., Veldhuis, M. J. W., Brussaard, C. P. D., Viollier, E., and Timmermans, K. R.: Fe-binding dissolved organic ligands near the Kerguelen Archipelago in the Southern Ocean (Indian sector), *Deep Sea Research Part II: Topical Studies in Oceanography*, 55, 606-621, 10.1016/j.dsr.2007.12.007, 2008.
- ➔ Gerringa, L. J. A., Slagter, H. A., Bown, J., van Haren, H., Laan, P., de Baar, H. J. W., and Rijkenberg, M. J. A.: Dissolved Fe and Fe-binding organic ligands in the Mediterranean Sea – GEOTRACES G04, *Marine Chemistry*, 194, 100-113, 10.1016/j.marchem.2017.05.012, 2017.

Formatted: French (France)

- ➔ Gourain, A., Planquette, H., Cheize, M., Menzel-Barraqueta, J. L., Boutorh, J., Shelley, R. U., Pereira-Contreira, L., Lemaitre, N., Lacan, F., Lherminier, P., and Sarthou, G.: particulate trace metals along the GEOVIDE section, *Biogeosciences*, 2018.
- ➔ Guerzoni, S., Chester, R., Dulac, F., Herut, B., Loye-Pilot, M.-D., Measures, C., Migon, C., Molinaroli, E., Moulin, C., Rossini, P., Saydam, C., Soudine, A., and Ziveri, P.: The role of atmospheric deposition in the biogeochemistry of the Mediterranean Sea, *Progress in Oceanography*, 44, 147-190, 1999.
- ➔ Guieu, C., Loye-Pilot, M. D., Benyahya, L., and Dufour, A.: Spatial variability of atmospheric fluxes of metals (Al, Fe, Cd, Zn and Pb) and phosphorus over the whole Mediterranean from a one-year monitoring experiment: Biogeochemical implications, *Marine Chemistry*, 120, 164-178, 10.1016/j.marchem.2009.02.004, 2010.
- ➔ Guieu, C., Aumont, O., Paytan, A., Bopp, L., Law, C. S., Mahowald, N., Achterberg, E. P., Marañón, E., Salihoglu, B., Crise, A., Wagener, T., Herut, B., Desboeufs, K., Kanakidou, M., Olgun, N., Peters, F., Pulido-Villena, E., Tovar-Sanchez, A., and Völker, C.: The significance of the episodic nature of atmospheric deposition to Low Nutrient Low Chlorophyll regions, *Global Biogeochemical Cycles*, 28, 1179-1198, 10.1002/2014gb004852, 2014.
- ➔ Harrison, W. G., Yngve Børshheim, K., Li, W. K. W., Maillet, G. L., Pepin, P., Sakshaug, E., Skogen, M. D., and Yeats, P. A.: Phytoplankton production and growth regulation in the Subarctic North Atlantic: A comparative study of the Labrador Sea-Labrador/Newfoundland shelves and Barents/Norwegian/Greenland seas and shelves, *Progress in Oceanography*, 114, 26-45, 10.1016/j.pocean.2013.05.003, 2013.
- ➔ Hatta, M., Measures, C. I., Wu, J., Roshan, S., Fitzsimmons, J. N., Sedwick, P., and Morton, P.: An overview of dissolved Fe and Mn distributions during the 2010-2011 US GEOTRACES north Atlantic cruises: GEOTRACES GA03, Deep-Sea Research Part II-Topical Studies in Oceanography, 116, 117-129, 10.1016/j.dsr2.2014.07.005, 2015.
- ➔ Hawkings, J. R., Wadham, J. L., Tranter, M., Raiswell, R., Benning, L. G., Statham, P. J., Tedstone, A., Nienow, P., Lee, K., and Telling, J.: Ice sheets as a significant source of highly reactive nanoparticulate iron to the oceans, *Nature communications*, 5, 1-8, 10.1038/ncomms4929, 2014.
- ➔ Henson, S. A., Dunne, J. P., and Sarmiento, J. L.: Decadal variability in North Atlantic phytoplankton blooms, *Journal of Geophysical Research*, 114, 10.1029/2008jc005139, 2009.
- ➔ Ho, T.-Y., Quigg, A., Finkel, Z. V., Milligan, A. J., Wyman, K., Falkowski, P. G., and Morel, F. M. M.: The elemental composition of some marine phytoplankton, *Journal of Phycology*, 39, 1145-1159, 2003.
- ➔ Homoky, W. B., Hembury, D. J., Hepburn, L. E., Mills, R. A., Statham, P. J., Fones, G. R., and Palmer, M. R.: Iron and manganese diagenesis in deep sea volcanogenic sediments and the origins of pore water colloids, *Geochimica Et Cosmochimica Acta*, 75, 5032-5048, 10.1016/j.gca.2011.06.019, 2011.
- ➔ Homoky, W. B., John, S. G., Conway, T. M., and Mills, R. A.: Distinct iron isotopic signatures and supply from marine sediment dissolution, *Nature Communications*, 4, 10.1038/ncomms3143, 2013.
- ➔ Humphreys, M. P., Griffiths, A. M., Achterberg, E. P., Holliday, N. P., Rérolle, V., Menzel Barraqueta, J. L., Couldrey, M. P., Oliver, K. I., Hartman, S. E., and Esposito, M.: Multidecadal accumulation of anthropogenic and remineralized dissolved inorganic carbon along the Extended Ellett Line in the northeast Atlantic Ocean, *Global Biogeochemical Cycles*, 30, 293-310, doi: 10.1002/2015GB005246, 2016.
- ➔ Hunke, E. C., Notz, D., Turner, A. K., and Vancoppenolle, M.: The multiphase physics of sea ice: a review for model developers, *The Cryosphere*, 5, 989-1009, 10.5194/tc-5-989-2011, 2011.
- ➔ Janssens, J., Meiners, K. M., Tison, J.-L., Dieckmann, G., Delille, B., and Lannuzel, D.: Incorporation of iron and organic matter into young Antarctic sea ice during its initial growth stages, *Elementa: Science of the Anthropocene*, 4, 000123, 10.12952/journal.elementa.000123, 2016.

- ➔ Jickells, T., and Moore, C. M.: The importance of atmospheric deposition for ocean productivity, *Annual Review of Ecology, Evolution, and Systematics*, 46, 481-501, 10.1146/annurev-ecolsys-112414-054118, 2015.
- ➔ Jickells, T. D., An, Z. C., Andersen, K. K., Baker, A. R., Bergametti, G., Brooks, N., Cao, J. J., Boyd, P. W., Duce, R. A., Hunter, K. A., Kawahata, H., Kubilay, N., laRoche, J., Liss, P. S., Mahowald, N., Prospero, J. M., Ridgwell, A. J., Tegen, I., and Torres, R.: Global iron connections between desert dust, ocean biogeochemistry, and climate, *Science*, 308, 67-71, 2005.
- ➔ Jones, E. P., Anderson, L. G., and Swift, J. H.: Distribution of Atlantic and Pacific waters in the upper Arctic Ocean: Implications for circulation, *Geophysical Research Letters*, 25, 765-768, 1998.
- ➔ Kissel, C., Laj, C., Mulder, T., Wandres, C., and Cremer, M.: The magnetic fraction: A tracer of deep water circulation in the North Atlantic, *Earth and Planetary Science Letters*, 288, 444-454, 10.1016/j.epsl.2009.10.005, 2009.
- ➔ Klunder, M. B., Bauch, D., Laan, P., de Baar, H. J. W., van Heuven, S. M. A. C., and Ober, S.: Dissolved iron in the Arctic shelf seas and surface waters of the Central Arctic Ocean: impact of Arctic river water and ice-melt, *Journal of Geophysical Research*, 117, 1-18, 2012.
- ➔ Lackschewitz, K. S., Endler, R., Gehrke, B., Wallrabe-Adams, H.-J., and Thiede, J.: Evidence for topography- and current-controlled deposition on the reykjanes Ridge between 59°N and 60°N, *Deep-Sea Research I*, 43, 1683-1711, 1996.
- ➔ Laes, A., Blain, S., Laan, P., Achterberg, E. P., Sarthou, G., and de Baar, H. J. W.: Deep dissolved iron profiles in the eastern North Atlantic in relation to water masses, *Geophysical Research Letters*, 30, 10.1029/2003gl017902, 2003.
- ➔ Lambelet, M., van de Flierdt, T., Crocket, K., Rehkamper, M., Katharina, K., Coles, B., Rijkenberg, M. J. A., Gerringa, L. J. A., de Baar, H. J. W., and Steinfeldt, R.: Neodymium isotopic composition and concentration in the western North Atlantic Ocean: Results from the GEOTRACES GA02 section, *Geochimica Et Cosmochimica Acta*, 177, 1-29, 2016.
- ➔ Le Roy, E., Sanial, V., Charette, M. A., van Beek, P., Lacan, F., Jacquet, S. H. M., Henderson, P. B., Souhaut, M., García-Ibáñez, M. I., Jeandel, C., Pérez, F. F., and Sarthou, G.: The 226Ra–Ba relationship in the North Atlantic during GEOTRACES-GA01, *Biogeosciences*, 15, 3027-3048, 10.5194/bg-15-3027-2018, 2018.
- ➔ Lemaitre, N., Planchon, F., Planquette, H., Dehairs, F., Fonseca-Batista, D., Roukaerts, A., Deman, F., Tang, Y., Mariez, C., and Sarthou, G.: High variability of export fluxes along the North Atlantic GEOTRACES section GA01: Particulate organic carbon export deduced from the 234Th method *Biogeosciences*, 1-38, 10.5194/bg-2018-190, 2018.
- ➔ Lemaître, N., planquette, H., Planchon, F., Sarthou, G., Jacquet, S., Garcia-Ibanez, M. I., Gourain, A., Cheize, M., Monin, L., Andre, L., Laha, P., Terryn, H., and Dehairs, F.: Particulate barium tracing significant mesopelagic carbon remineralisation in the North Atlantic *Biogeosciences Discussions*, 2017.
- ➔ Lohan, M. C., and Bruland, K. W.: Elevated Fe(II) and Dissolved Fe in Hypoxic Shelf Waters off Oregon and Washington: An Enhanced Source of Iron to Coastal Upwelling Regimes, *Environmental Science & Technology*, 42, 6462-6468, 10.1021/es800144j, 2008.
- ➔ Longhurst, A. R.: *Ecological geography of the Sea*, Second Edition ed., Elsevier Academic Press publications, Burlington, 542 pp., 2007.
- ➔ Louanchi, F., and Najjar, R. G.: Annual cycles of nutrients and oxygen in the upper layers of the North Atlantic Ocean, *Deep Sea Research Part II: Topical Studies in Oceanography*, 48, 2155-2171, 2001.
- ➔ Markus, T., Stroeve, J. C., and Miller, J.: Recent changes in Arctic sea ice melt onset, freezeup, and melt season length, *Journal of Geophysical Research*, 114, 10.1029/2009jc005436, 2009.
- ➔ Marshall, J., and Schott, F.: Open-ocean convection: observations, theory, and models, *Reviews of Geophysics*, 37, 1-64, doi: 10.1029/98RG02739, 1999.

- ➔ Martin, J.-M., Elbaz-Poulichet, F., Guieu, C., Loÿe-Pilot, M.-D., and Han, G.: River versus atmospheric input of material to the Mediterranean Sea: an overview*, *Marine Chemistry*, 28, 159-182, 1989.
- ➔ Martin, J. D., and Fitzwater, S. E.: Iron deficiency limits phytoplankton growth in the north-east Pacific subarctic, *Nature*, 331, 341-343, 1988.
- ➔ Martin, J. H., Fitzwater, S. E., and Gordon, R. M.: Iron deficiencies limits phytoplankton growth in Antarctic waters, *Global Biogeochemical Cycles*, 4, 5-12, 1990.
- ➔ Martin, J. H., Coale, K. H., Johnson, K. S., Fitzwater, S. E., Gordon, R. M., Tanner, S. J., Hunter, C. N., Elrod, V. A., Nowicki, J. L., Coley, T. L., Barber, R. T., Lindley, S., Watson, A. J., Van Scoy, K., Law, C. S., Liddicoat, M. I., Ling, R., Stanton, T., Stockel, J., Collins, C., Anderson, A., Bidigare, R., Ondrusek, M., Latasa, M., Millero, F. J., Lee, K., Yao, W., Zhang, J. Z., Friederich, G., Sakamoto, C., Chavez, F., Buck, K., Kolber, Z., Greene, R., Falkowski, P., Chisholm, S. W., Hoge, F., Swift, R., Yungel, J., Turner, S., Nightingale, P., Hatton, A., Liss, P., and Tindale, N. W.: Testing the Iron Hypothesis in Ecosystems of the Equatorial Pacific Ocean, *Nature*, 371, 123-129, 10.1038/371123a0, 1994.
- ➔ Measures, C. I., Brown, M. T., Selph, K. E., Apprill, A., Zhou, M., Hatta, M., and Hiscock, W. T.: The influence of shelf processes in delivering dissolved iron to the HNLC waters of the Drake Passage, Antarctica, *Deep Sea Research Part II: Topical Studies in Oceanography*, 90, 77-88, 10.1016/j.dsr2.2012.11.004, 2013.
- ➔ Melling, H., and Moore, R. M.: Modification of halocline source waters during freezing on the Beaufort Sea shelf: Evidence from oxygen isotopes and dissolved nutrients, *Continental Shelf Research*, 15, 89-113, 1995.
- ➔ Menzel Barraqueta, J. L., Schlosser, C., Planquette, H., Gourain, A., Cheize, M., Boutorh, J., Shelley, R. U., Pereira Contreira, L., Gledhill, M., Hopwood, M. J., Lherminier, P., Sarthou, G., and Achterberg, E. P.: Aluminium in the North Atlantic Ocean and the Labrador Sea (GEOTRACES GA01 section): roles of continental inputs and biogenic particle removal, *Biogeosciences Discussions*, 1-28, 10.5194/bg-2018-39, 2018.
- ➔ Mil-Homens, M., Branco, V., Lopes, C., Vale, C., Abrantes, F., Boer, W., and Vicente, M.: Using factor analysis to characterise historical trends of trace metal contamination in a sediment core from the Tagus Prodelt, Portugal, *Water, Air, and Soil Pollution*, 197, 277-287, 2009.
- ➔ Moore, C. M., Mills, M. M., Langlois, R., Milne, A., Achterberg, E. P., La Roche, J., and Geider, R. J.: Relative influence of nitrogen and phosphorus availability on phytoplankton physiology and productivity in the oligotrophic sub-tropical North Atlantic Ocean, *Limnology and Oceanography*, 53, 291-205, 2008.
- ➔ Moore, C. M., Mills, M. M., Arrigo, K. R., Berman-Frank, I., Bopp, L., Boyd, P. W., Galbraith, E. D., Geider, R. J., Guieu, C., Jaccard, S. L., Jickells, T. D., La Roche, J., Lenton, T. M., Mahowald, N. M., Marañoń, E., Marinov, I., Moore, J. K., Nakatsuka, T., Oschlies, A., Saito, M. A., Thingstad, T. F., Tsuda, A., and Ulloa, O.: Processes and patterns of oceanic nutrient limitation, *Nature Geoscience*, 6, 701-710, 10.1038/ngeo1765, 2013.
- ➔ Moore, G. W. K.: Gale force winds over the Irminger Sea to the east of Cape Farewell, Greenland, *Geophysical Research Letters*, 30, n/a-n/a, 10.1029/2003gl018012, 2003.
- ➔ Nielsdóttir, M. C., Moore, C. M., Sanders, R., Hinz, D. J., and Achterberg, E. P.: Iron limitation of the postbloom phytoplankton communities in the Iceland Basin, *Global Biogeochemical Cycles*, 23, n/a-n/a, 10.1029/2008gb003410, 2009.
- ➔ Olafsson, J., Thors, K., and Cann, J. R.: A sudden cruise off Iceland, RIDGE Events, 2, 35-28, 1991.
- ➔ Oschlies, A.: Nutrient supply to the surface waters of the North Atlantic: A model study, *Journal of Geophysical Research*, 107, 10.1029/2000jc000275, 2002.
- ➔ Painter, S. C., Henson, S. A., Forryan, A., Steigenberger, S., Klar, J., Stinchcombe, M. C., Rogan, N., Baker, A. R., Achterberg, E. P., and Moore, C. M.: An assessment of the vertical diffusive flux of iron and other nutrients to the surface waters of the subpolar North Atlantic Ocean, *Biogeosciences*, 11, 2113-2130, 10.5194/bg-11-2113-2014, 2014.

- ➔ Palmer, M. R., Ludford, E. M., German, C. R., and Lilley, M. D.: Dissolved methane and hydrogen in the Steinahóll hydrothermal plume, 63°N, Reykjanes Ridge, in: *Hydrothermal Vents and Processes*, edited by: Parson, L. M., Walker, C. L., and Dixon, D. R., Special Publications, Geological Society, London, 111-120, 1995.
- ➔ Parekh, P., Follows, M. J., and Boyle, E. A.: Decoupling of iron and phosphate in the global ocean, *Global Biogeochemical Cycle*, 19, 2005.
- ➔ Parra, M., Delmont, P., Ferragne, A., Latouche, C., Pons, J. C., and Puechmaile, C.: Origin and evolution of smectites in recent marine sediments of the NE Atlantic, *Clay Minerals*, 20, 335-346, 1985.
- ➔ Pérez, F. F., Mercier, H., Vázquez-Rodríguez, M., Lherminier, P., Velo, A., Pardo, P. C., Rosón, G., and Ríos, A. F.: Atlantic Ocean CO₂ uptake reduced by weakening of the meridional overturning circulation, *Nature Geoscience*, 6, 146-152, 10.1038/ngeo1680, 2013.
- ➔ Pérez, F. F., Treguer, P., Branellec, P., García-Ibáñez, M. I., Lherminier, P., and Sarthou, G.: The 2014 Greenland-Portugal GEOVIDE bottle data (GO-SHIP A25 and GEOTRACES GA01). SEANOE (Ed.), 2018.
- ➔ Petrich, C., and Eicken, H.: Growth, structure and properties of sea ice, in: *Sea Ice*. 2nd ed., edited by: Thomas, D. N., and Dieckmann, G. S., Wiley-Blackwell, Oxford, U.K., 23-77, 2010.
- ➔ Pickart, R. S., Straneo, F., and Moore, G. W. K.: Is Labrador Sea Water formed in the Irminger basin?, *Deep Sea Research Part I*, 50, 23-52, 2003.
- ➔ Piron, A., Thierry, V., Mercier, H., and Caniaux, G.: Argo float observations of basin-scale deep convection in the Irminger sea during winter 2011–2012, *Deep Sea Research Part I: Oceanographic Research Papers*, 109, 76-90, 10.1016/j.dsr.2015.12.012, 2016.
- ➔ Radic, A., Lacan, F., and Murray, J. W.: Iron isotopes in the seawater of the equatorial Pacific Ocean: New constraints for the oceanic iron cycle, *Earth and Planetary Science Letters*, 306, 1-10, 10.1016/j.epsl.2011.03.015, 2011.
- ➔ Riebesell, U., Schloss, I., and Smetacek, V.: Aggregation of algae released from melting sea ice: implications for seeding and sedimentation, *Polar Biology*, 11, 239-248, 1991.
- ➔ Rijkenberg, M. J., Middag, R., Laan, P., Gerringa, L. J., van Aken, H. M., Schoemann, V., de Jong, J. T., and de Baar, H. J.: The distribution of dissolved iron in the West Atlantic Ocean, *PLoS One*, 9, e101323, 10.1371/journal.pone.0101323, 2014.
- ➔ Sabine, C. L., Feely, R. A., Gruber, N., Key, R. M., Lee, K., Bullister, J. L., Wanninkhof, R., Wong, C. S., Wallace, D. W. R., Tilbrook, B., Millero, F. J., Peng, T.-H., Kozyr, A., Ono, T., and Rios, A. F.: The Oceanic sink for anthropogenic CO₂, *Science*, 305, 367-371, 2004.
- ➔ Sanders, R., Brown, L., Henson, S., and Lucas, M.: New production in the Irminger Basin during 2002, *Journal of Marine Systems*, 55, 291-310, <http://dx.doi.org/10.1016/j.jmarsys.2004.09.002>, 2005.
- ➔ Santos-Echeandia, J., Vale, C., Caetano, M., Pereira, P., and Prego, R.: Effect of tidal flooding on metal distribution in pore waters of marsh sediments and its transport to water column (Tagus estuary, Portugal), *Mar Environ Res*, 70, 358-367, 10.1016/j.marenvres.2010.07.003, 2010.
- ➔ Sarthou, G., and Jeandel, C.: Seasonal variations of iron concentrations in the Ligurian Sea and iron budget in the Western Mediterranean Sea, *Marine Chemistry*, 74, 115-129, 10.1016/s0304-4203(00)00119-5, 2001.
- ➔ Sarthou, G., Baker, A. R., Kramer, J., Laan, P., Laës, A., Ussher, S., Achterberg, E. P., de Baar, H. J. W., Timmermans, K. R., and Blain, S.: Influence of atmospheric inputs on the iron distribution in the subtropical North-East Atlantic Ocean, *Marine Chemistry*, 104, 186-202, 10.1016/j.marchem.2006.11.004, 2007.
- ➔ Sarthou, G., Vincent, D., Christaki, U., Obernosterer, I., Timmermans, K. R., and Brussaard, C. P. D.: The fate of biogenic iron during a phytoplankton bloom induced by natural fertilisation: Impact of copepod grazing, *Deep Sea Research Part II: Topical Studies in Oceanography*, 55, 734-751, 10.1016/j.dsr2.2007.12.033, 2008.

- Sarthou, G., Lherminier, P., Achterberg, E. P., Alonso-Pérez, F., Bucciarelli, E., Boutorh, J., Bouvier, V., Boyle, E. A., Branellec, P., Carracedo, L. I., Casacuberta, N., Castrillejo, M., Cheize, M., Contreira Pereira, L., Cossa, D., Daniault, N., De Saint-Léger, E., Dehairs, F., Deng, F., Desprez de Gésincourt, F., Devesa, J., Foliot, L., Fonseca-Batista, D., Gallinari, M., García-Ibáñez, M. I., Gourain, A., Grossteffan, E., Hamon, M., Heimbürger, L. E., Henderson, G. M., Jeandel, C., Kermabon, C., Lacan, F., Le Bot, P., Le Goff, M., Le Roy, E., Lefèbvre, A., Leizour, S., Lemaitre, N., Masqué, P., Ménage, O., Menzel Barraqueta, J.-L., Mercier, H., Perault, F., Pérez, F. F., Planquette, H. F., Planchon, F., Roukaerts, A., Sanial, V., Sauzède, R., Shelley, R. U., Stewart, G., Sutton, J. N., Tang, Y., Tisnérat-Laborde, N., Tonnard, M., Tréguer, P., van Beek, P., Zurbrick, C. M., and Zunino, P.: Introduction to the French GEOTRACES North Atlantic Transect (GA01): GEOVIDE cruise, *Biogeosciences Discussions*, 1-24, 10.5194/bg-2018-312, 2018.
- Schroth, A. W., Crusius, J., Hoyer, I., and Campbell, R.: Estuarine removal of glacial iron and implications for iron fluxes to the ocean, *Geophysical Research Letters*, 41, 3951-3958, 10.1002/2014GL060199, 2014.
- Shelley, R. U., Morton, P. L., and Landing, W. M.: Elemental ratios and enrichment factors in aerosols from the US-GEOTRACES North Atlantic transects, *Deep Sea Research*, 116, 262-272, 2015.
- Shelley, R. U., Roca-Martí, M., Castrillejo, M., Sanial, V., Masqué, P., Landing, W. M., van Beek, P., Planquette, H., and Sarthou, G.: Quantification of trace element atmospheric deposition fluxes to the Atlantic Ocean (>40°N; GEOVIDE, GEOTRACES GA01) during spring 2014, *Deep Sea Research Part I: Oceanographic Research Papers*, 119, 34-49, 10.1016/j.dsr.2016.11.010, 2017.
- Shelley, R. U., Landing, W. M., Ussher, S. J., Planquette, H., and Sarthou, G.: Characterisation of aerosol provenance from the fractional solubility of Fe (Al, Ti, Mn, Co, Ni, Cu, Zn, Cd and Pb) in North Atlantic aerosols (GEOTRACES cruises GA01 and GA03) using a two stage leach, *Biogeosciences*, 2018.
- Shor, A., Lonsdale, P., Hollister, D., and Spencer, D.: Charlie-Gibbs fracture zone: bottom-water transport and its geological effects, *Deep Sea Research*, 27A, 325-345, 1980.
- Sinha, M. C., Navin, D. A., MacGregor, L. M., Constable, S., Peirce, C., White, A., Heinson, G., and Inglis, M. A.: Evidence for accumulated melt beneath the slow-spreading Mid-Atlantic Ridge, *Philosophical Transactions of the Royal Society A*, 355, 233-253, 1997.
- Slagter, H. A., Reader, H. E., Rijkenberg, M. J. A., Rutgers van der Loeff, M., de Baar, H. J. W., and Gerringa, L. J. A.: Organic Fe speciation in the Eurasian Basins of the Arctic Ocean and its relation to terrestrial DOM, *Marine Chemistry*, 197, 11-25, 10.1016/j.marchem.2017.10.005, 2017.
- Smallwood, J. R., and White, R. S.: Crustal accretion at the Reykjanes Ridge, 61°-62°N, *Journal of Geophysical Research: Solid Earth*, 103, 5185-5201, 10.1029/97jb03387, 1998.
- Statham, P. J., Skidmore, M., and Tranter, M.: Inputs of glacially derived dissolved and colloidal iron to the coastal ocean and implications for primary productivity, *Global Biogeochemical Cycles*, 22, 1-11, 10.1029/2007GB003106, 2008.
- Sunda, W. G., and Huntsman, S. A.: Iron uptake and growth limitation in oceanic and coastal phytoplankton, *Marine Chemistry*, 50, 189-206, 10.1016/0304-4203(95)00035-p, 1995.
- Sutherland, D. A., Pickart, R. S., Peter Jones, E., Azetsu-Scott, K., Jane Eert, A., and Ólafsson, J.: Freshwater composition of the waters off southeast Greenland and their link to the Arctic Ocean, *Journal of Geophysical Research*, 114, 10.1029/2008jc004808, 2009.
- Tanhua, T., Olsson, K. A., and Jeansson, E.: Formation of Denmark Strait overflow water and its hydro-chemical composition, *Journal of Marine Systems*, 57, 264-288, 10.1016/j.jmarsys.2005.05.003, 2005.
- Thuróczy, C. E., Gerringa, L. J. A., Klunder, M. B., Middag, R., Laan, P., Timmermans, K. R., and de Baar, H. J. W.: Speciation of Fe in the Eastern North Atlantic Ocean, *Deep Sea Research Part I: Oceanographic Research Papers*, 57, 1444-1453, 10.1016/j.dsr.2010.08.004, 2010.
- Tonnard, M., Donval, A., Lampert, L., Tréguer, P., Bowie, A. R., van der Merwe, P., planquette, H., Claustre, H., Dimier, C., Ras, J., and Sarthou, G.: Phytoplankton assemblages in the

North Atlantic Ocean and in the Labrador Sea along the GEOVIDE section (GEOTRACES section GA01) determined by CHEMTAX analysis from HPLC pigment data, *Biogeosciences*, in prep.

- ➔ Tovar-Sanchez, A., Duarte, C. M., Alonso, J. C., Lacorte, S., Tauler, R., and Galban-Malagon, C.: Impacts of metals and nutrients released from melting multiyear Arctic sea ice, *Journal of Geophysical Research-Oceans*, 115, 10.1029/2009jc005685, 2010.
- ➔ Tréguer, P. J., and De La Rocha, C. L.: The world ocean silica cycle, *Ann Rev Mar Sci*, 5, 477-501, 10.1146/annurev-marine-121211-172346, 2013.
- ➔ Twining, B. S., Baines, S. B., Fisher, N. S., and Landry, M. R.: Cellular iron contents of plankton during the Southern Ocean Iron Experiment (SOFeX), *Deep Sea Research Part I: Oceanographic Research Papers*, 51, 1827-1850, 10.1016/j.dsr.2004.08.007, 2004.
- ➔ von Appen, W.-J., Koszalka, I. M., Pickart, R. S., Haine, T. W. N., Mastropole, D., Magaldi, M. G., Valdimarsson, H., Girtton, J., Jochumsen, K., and Krahnmann, G.: The East Greenland Spill Jet as an important component of the Atlantic Meridional Overturning Circulation, *Deep Sea Research Part I: Oceanographic Research Papers*, 92, 75-84, 10.1016/j.dsr.2014.06.002, 2014.
- ➔ Wadhams, P.: *Ice in the Ocean*, Gordon and Breach Science Publishers, London, UK, 2000.
- ➔ Wagener, T., Guieu, C., and Leblond, N.: Effects of dust deposition on iron cycle in the surface Mediterranean Sea: results from a mesocosm seeding experiment, *Biogeosciences Discussions*, 7, 2799-2830, 2010.
- ➔ Woodgate, R. A., and Aagaard, K.: Revising the Bering Strait freshwater flux into the Arctic Ocean, *Geophysical Research Letters*, 32, 10.1029/2004GL021747., 2005.
- ➔ Wuttig, K., Wagener, T., Bressac, M., Dammshäuser, A., Streu, P., Guieu, C., and Croot, P. L.: Impacts of dust deposition on dissolved trace metal concentrations (Mn, Al and Fe) during a mesocosm experiment, *Biogeosciences*, 10, 2583-2600, 10.5194/bg-10-2583-2013, 2013.
- ➔ Zou, S., Lozier, S., Zenk, W., Bower, A., and Johns, W.: Observed and modeled pathways of the Iceland Scotland Overflow Water in the eastern North Atlantic, *Progress in Oceanography*, 159, 211-222, 10.1016/j.pocean.2017.10.003, 2017.
- ➔ Zunino, P., Lherminier, P., Mercier, H., Daniault, N., García-Ibáñez, M. I., and Pérez, F. F.: The GEOVIDE cruise in may-June 2014 revealed an intense MOC over a cold and fresh subpolar North Atlantic, *Biogeosciences*, 2017.

Formatted: Font: (Default) +Headings CS (Times New Roman), Complex Script Font: +Headings CS (Times New Roman)

1 Dissolved iron in the North Atlantic Ocean and Labrador Sea along 2 the GEOVIDE section (GEOTRACES section GA01)

3 Manon Tonnard^{1,2,3}, H el ene Planquette¹, Andrew R. Bowie^{2,3}, Pier van der Merwe², Morgane Gallinari¹,
4 Floriane Desprez de G esincourt¹, Yoan Germain⁴, Arthur Gourain⁵, Marion Benetti^{6,7}, Gilles Reverdin⁷,
5 Paul Tr eguer¹, Julia Boutorh¹, Marie Cheize¹, [Fran ois Lacan](#)⁸, Jan-Lukas Menzel Barraqueta^{9,10},
6 Leonardo Pereira-Contreira¹¹, Rachel Shelley^{1,12,13}, [Pascale Lherminier](#)⁴, G eraldine Sarthou¹

7 ¹Laboratoire des sciences de l'Environnement MARin – CNRS UMR 6539 – Institut Universitaire Europ een de la Mer,
8 [Universit  de Bretagne Occidentale](#), Plouzan , 29280, France

9 ²Antarctic Climate and Ecosystems – Cooperative Research Centre, [University of Tasmania](#), Hobart, TAS 7001, Australia

10 ³Institute for Marine and Antarctic Studies, University of Tasmania, Hobart, TAS 7001, Australia

11 ⁴Laboratoire Cycles G ochimiques et ressources – Ifremer, Plouzan , 29280, France

12 ⁵Ocean Sciences Department, School of Environmental Sciences, University of Liverpool, L69 3GP, UK

13 ⁶Institute of Earth Sciences, University of Iceland, Reykjavik, Iceland

14 ⁷LOCEAN, Sorbonne Universit s, UPMC/CNRS/IRD/MNHN, Paris, [France](#)

15 ⁸LEGOS, [Universit  de Toulouse - CNRS/IRD/CNES/UPS – Observatoire Midi-Pyr n es](#), Toulouse, France

16 ⁹GEOMAR Helmholtz-Zentrum f ur Ozeanforschung Kiel Wischhofstra e 1-3, Geb. 12 D-24148 Kiel, Germany

17 ¹⁰Department of Earth Sciences, Stellenbosch University, Stellenbosch, 7600, South Africa

18 ¹¹Funda o Universidade Federal do Rio Grande (FURG), R. Luis Lor ea, Rio Grande –RS, 96200-350, Brazil

19 ¹²Dept. Earth, Ocean and Atmospheric Science, Florida State University, 117 N Woodward Ave, Tallahassee, Florida, 32301,
20 USA

21 ¹³School of Geography, Earth and Environmental Sciences, University of Plymouth, Drake Circus, Plymouth, PL4 8AA, UK

22 ¹⁴Ifremer, Universit  de Bretagne Occidentale (UBO), CNRS, IRD, Laboratoire d'Oc anographie Physique et Spatiale
23 (LOPS), IUEM, F-29280, Plouzan , France

24
25 Correspondence to: Manon Tonnard (Manon.Tonnard@utas.edu.au)

26
27 **Abstract.** Dissolved Fe (DFe) samples from the GEOVIDE voyage (GEOTRACES GA01, May-June 2014) in the North
28 Atlantic Ocean were analysed using a SeaFAST-picoTM coupled to an Element XR [SE](#)-ICP-MS and provided interesting
29 insights on the Fe sources in this area. Overall, DFe concentrations ranged from 0.09 ± 0.01 nmol L⁻¹ to 7.8 ± 0.5 nmol L⁻¹.
30 Elevated DFe concentrations were observed above the Iberian, Greenland and Newfoundland Margins likely due to riverine
31 inputs from the Tagus River, meteoric water inputs and sedimentary inputs. [Enhanced air-sea](#) interactions were suspected to
32 be responsible for the increase in DFe concentrations within subsurface waters of the Irminger Sea due to deep convection
33 occurring the previous [winter, which](#) provided iron-to-nitrate ratios sufficient to sustain phytoplankton growth. Increasing DFe
34 concentrations along the flow path of the Labrador Sea Water were attributed to sedimentary inputs from the Newfoundland
35 Margin. Bottom waters from the Irminger Sea displayed high DFe concentrations likely due to the dissolution of Fe-rich
36 particles [in](#) the Denmark Strait Overflow Water and the Polar Intermediate Water. Finally, the nepheloid layers [located in the](#)
37 [different basins and at the Iberian Margin](#) were found to act as either a source or a sink of DFe depending on the nature of
38 particles [with organic particles likely releasing DFe and Mn-particles scavenging DFe](#).

Formatted

Formatted: Superscript

Deleted: ⁸

Deleted: ⁹

Deleted: ⁰

Deleted: ¹

Deleted: ²

Deleted: France

Formatted: Superscript

Deleted: ⁸

Deleted: ¶

Formatted: Font: 10.5 pt, Complex Script Font: 14 pt,
Spanish (Spain, Traditional Sort)

Deleted: ⁹

Deleted: ⁰

Deleted: ¹

Deleted: ²

Deleted: HR

Deleted: A

Deleted: winter, that

Deleted: from

Deleted: .

1 Introduction

The North Atlantic Ocean is known for its pronounced spring phytoplankton blooms (Henson et al., 2009; Longhurst, 2007). Phytoplankton blooms induce the capture of aqueous carbon dioxide through photosynthesis, and conversion into particulate organic carbon (POC). This POC is then exported into deeper waters through the production of sinking biogenic particles and ocean currents. Via these processes, and in conjunction with the physical carbon pump, the North Atlantic Ocean is the largest oceanic sink of anthropogenic CO₂ (Pérez et al., 2013), despite covering only 15% of global ocean area (Humphreys et al., 2016; Sabine et al., 2004) and is therefore crucial for Earth's climate.

Indeed, phytoplankton must obtain, besides light and inorganic carbon, chemical forms of essential elements, termed nutrients to be able of photosynthesis. Indeed, Fe is a key element for a number of metabolic processes (e.g. Morel et al., 2008). The availability of these nutrients in the upper ocean frequently limits the activity and abundance of these organisms together with light conditions (Moore et al., 2013). In particular, winter nutrient reserves in surface waters set an upper limit for biomass accumulation during the annual spring-to-summer bloom and will influence the duration of the bloom (Follows and Dutkiewicz, 2001; Henson et al., 2009; Moore et al., 2013; 2008). Hence, nutrient depletion due to biological consumption is considered as a major factor in the decline of blooms (Harrison et al., 2013).

The extensive studies conducted in the North Atlantic Ocean through the Continuous Plankton Recorder (CPR) have highlighted the relationship between the strength of the westerlies and the displacement of the subarctic front (SAF), (which corresponds to the North Atlantic Oscillation (NAO) index (Bersch et al., 2007)), and the phytoplankton dynamics of the central North Atlantic Ocean (Barton et al., 2003). Therefore, the SAF not only delineates the subtropical gyre from the subpolar gyre but also two distinct systems in which phytoplankton limitations are controlled by different factors. In the North Atlantic Ocean, spring phytoplankton growth is largely light-limited within the subpolar gyre. Light levels are primarily set by freeze-thaw cycles of sea ice and the high-latitude extremes in the solar cycle (Longhurst, 2007). Simultaneously, intense winter mixing supplies surface waters with high concentrations of nutrients. In contrast, within the subtropical gyre, the spring phytoplankton growth is less impacted by the light regime and has been shown to be N and P-co-limited (e.g. Harrison et al., 2013; Moore et al., 2008). This is principally driven by Ekman downwelling with an associated export of nutrients out of the euphotic zone (Oschlies, 2002). Thus, depending on the location of the SAF, phytoplankton communities from the central North Atlantic Ocean will be primarily light or nutrient limited.

However, once the water column stratifies and phytoplankton are released from light limitation, seasonal high-nutrient, low chlorophyll (HNLC) conditions were reported at the transition zone between the gyres, especially in the Irminger Sea and Iceland Basin (Sanders et al., 2005). In these HNLC zones, trace metals are most likely limiting the biological carbon pump. Among all the trace metals, Fe has been recognized as the prime limiting element of North Atlantic primary productivity (e.g.

Moved (insertion) [7]

Deleted: also

Deleted: ,

Deleted: a region of high phytoplankton production

Deleted: that

Deleted: , a key driver of the biological carbon pump through photosynthesis and transfer of energy to higher trophic levels

Deleted: atmospheric

Deleted: which allows its

Deleted: (Henson et al., 2009)

Deleted: ()

Deleted: and through the Atlantic Meridional Overturning Circulation (AMOC), The North Atlantic Ocean is a crucial area for Earth's climate as a result of deep water formation. The formation of the North Atlantic Deep Water (NADW) is essential to the Atlantic Meridional Overturning Circulation (AMOC), which is responsible for transporting large amounts of water, heat, salt, carbon, nutrient(...

Moved up [7]: The North Atlantic Ocean is also a region of high

Deleted: The North Atlantic Ocean is also a region of high

Deleted: shows

Deleted: storagestores huge amounts rate

Deleted: through both the physical and biological carbon pumps

Deleted: the

Moved down [11]: However, the rapid attenuation of light with

Deleted: The extensive studies conducted in the North Atlantic

Moved (insertion) [11]

Deleted: However, the rapid attenuation of light with depth

Deleted: a lower

Deleted: More specifically, i

Deleted: the

Moved (insertion) [8]

Deleted: , which is

Deleted: at its northern boundaries (i.e. the Arctic Ocean, margi(...

Deleted: , as the

Deleted: fuels the

Deleted: as it undergoes an

Deleted: more or less prompt to

Deleted: ations

Deleted: in the subpolar gyre and

Deleted: , thus suggesting that

Deleted: were potentially

Deleted: the

1 [Boyd et al., 2000](#); [Martin et al., 1994](#); [1988](#); [1990](#). However, the phytoplankton community has been shown to become N
2 and/or Fe-(co)-limited in the Iceland Basin and the Irminger Sea (e.g. [Nielsdóttir et al., 2009](#); [Painter et al., 2014](#); [Sanders et
3 al., 2005](#)).

4
5 In the North Atlantic Ocean, dissolved Fe (DFe) is delivered through multiple pathways such as ice-melting (e.g. [Klunder et
6 al., 2012](#); [Tovar-Sanchez et al., 2010](#)), atmospheric inputs ([Achterberg et al., 2018](#); [Baker et al., 2013](#); [Shelley et al., 2015](#);
7 2017), coastal runoff ([Rijkenberg et al., 2014](#)), sediment inputs ([Hatta et al., 2015](#)), hydrothermal inputs ([Achterberg et al.,
8 2018](#); [Conway and John, 2014](#)) and by water mass circulation (vertical and lateral advections, e.g. [Laes et al., 2003](#)). Dissolved
9 Fe can be regenerated through biological recycling (microbial loop, zooplankton grazing, e.g. [Boyd et al., 2010](#); [Sarhou et al.,
10 2008](#)). Iron is removed from the dissolved phase by biological uptake, export and scavenging along the water column and
11 precipitation (itself a function of salinity, pH of seawater and ligand concentrations).

12
13 Although many studies investigated the distribution of DFe in the North Atlantic Ocean, much of this work was restricted to
14 the upper layers (< 1000 m depth) or to one basin. Therefore, uncertainties remain on the large-scale distribution of DFe in the
15 North Atlantic Ocean and more specifically within the subpolar gyre where few studies have been undertaken, and even fewer
16 in the Labrador Sea. In this biogeochemically important area, high-resolution studies are still lacking for understanding the
17 processes influencing the cycle of DFe.

18
19 The aim of this paper is to elucidate the sources and sinks of DFe, its distribution regarding water masses and assesses the
20 links with biological activity along the GEOVIDE (GEOTRACES-GA01) transect. This transect spanned several
21 biogeochemical provinces including the West European Basin, the Iceland Basin, the Irminger and the Labrador Seas (Fig. 1).
22 In doing so we hope to constrain the potential long-range transport of DFe through the Deep Western Boundary Current
23 (DWBC) via the investigation of the local processes effecting the DFe concentrations within the three main water masses that
24 constitute it, Iceland Scotland Overflow Water (ISOW), Denmark Strait Overflow Water (DSOW) and Labrador Sea Water
25 (LSW).

26 2 Material and methods

27 2.1 Study area and sampling activities

28 Samples were collected during the GEOVIDE (GEOTRACES-GA01 section, Fig. 1) oceanographic voyage from 15 May 2014
29 (Lisbon, Portugal) to 30 June 2014 (St. John's, Newfoundland, Canada) aboard *N/O Pourquoi Pas?*. The study was carried
30 out along the OVIDE line (<http://www.umr-lops.fr/Projets/Projets-actifs/OVIDE>, previously referred to as the WOCE A25
31 Greenland to Portugal section), and in the Labrador Sea (corresponding to the WOCE A01 leg 3 Greenland to Newfoundland
32 section). The OVIDE line has been sampled every two years since 2002 in the North Atlantic (e.g. [Mercier et al., 2015](#)), and

Deleted: and t...overherefore... it...he phytoplankton community has been shown to become N or (and...nd/or)

Formatted

Deleted: Recent observations showed a reduction of oceanic heat loss to the atmosphere due to the slowdown of the AMOC resulting to the reduction of carbon uptake ([Pérez et al., 2013](#)). In the North Atlantic Ocean, phytoplankton growth is largely light-limited at its northern boundaries (i.e. the Arctic Ocean, marginal ice zones, polynya areas and the Labrador Shelf) set primarily by freeze-thaw cycles of sea ice and the high-latitude extremes in the solar cycle ([Longhurst, 2007](#)). In contrast, at its more southerly boundaries (i.e. the subpolar and to a lesser extent the subtropical gyres), seasonal wind and thermal cycles that determine mixing patterns, have a greater influence on phytoplankton growth with the consequence that both light and nutrient inventories can limit productivity ([Harrison et al., 2013](#)). If light is thought to be the principal control on the timing of growth, nutrients play a significant role in the phytoplankton community structure. In particular, winter nutrient reserves in surface waters set a lower limit for biomass accumulation during the annual spring-to-summer bloom and will influence the duration of the bloom ([Follows and Dutkiewicz, 2001](#); [Henson et al., 2009](#); [Moore et al., 2013](#); [2008](#)). Hence, nutrient depletion due to biological consumption is considered as a major factor in the decline of blooms ([Harrison et al., 2013](#)). The North Atlantic Ocean is classically considered as a N-limited system ([Moore et al., 2013](#)). However, once the water column stratifies in

Deleted: Indeed, Fe is a key element for a number of metabolic processes (e.g. [Morel et al., 2008](#)) and within its physical speciation

Formatted: French (France)

Formatted: French (France)

Formatted

Formatted

Moved up [8]: phytoplankton growth is largely light-limited at its northern boundaries (i.e. the Arctic Ocean, marginal ice zones,

Formatted

Deleted: D

Field Code Changed

Field Code Changed

Deleted: and t

Deleted: Despite these studies,...uncertainties remain on the large-scale distribution of DFe in the North Atlantic Ocean and more

Deleted: In this context, t...he aim of this paper is to elucidates

Deleted:

Deleted: ,

Deleted:

Deleted:

Deleted: which...spanned several biogeochemical provinces including the West European Basin, the Iceland Basin, the Irminger

Deleted: the...N/O Pourquoi Pas?. The study was carried out along the OVIDE line ([**Deleted:** , which](http://www.umr-lops.fr/Projets/Projets-</p></div><div data-bbox=)

1 in the Labrador Sea (broadly corresponding to the WOCE A01 leg 3 Greenland to Newfoundland section). In total, 32 stations
2 were occupied, and samples were usually collected at 22 depths, except at shallower stations close to the Iberian, Greenland
3 and Canadian shelves (Fig. 1) where fewer samples (between 6 and 11) were collected. To avoid ship contamination of surface
4 waters, the shallowest sampling depth was 15 m at all stations. Therefore, 'surface water samples' refers to 15m depth.

Deleted: These 15 m depth will be herein referred to as

5
6 Samples were collected using a trace metal clean polyurethane powder-coated aluminium frame rosette (hereafter referred to
7 as TMR) equipped with twenty-two 12L, externally closing, Teflon-lined, GO-FLO bottles (General Oceanics) and attached
8 to a Kevlar® line. The cleaning protocols for sampling bottles and equipment followed the guidelines of the GEOTRACES
9 Cookbook (www.geotraces.org, Cutter et al., 2017). After TMR recovery, GO-FLO bottles were transferred into a clean
10 container equipped with a class 100 laminar flow hood. Samples were either taken from the filtrate of particulate samples
11 (collected on polyethersulfone filters, 0.45 µm supor®, see Gourain et al., this issue) or after filtration using 0.2 µm filter
12 cartridges (Sartorius SARTOBRAN® 300) due to water budget restriction (Table 1). No significant difference was observed
13 between DFe values filtered through 0.2 µm and 0.45 µm filters (p-value > 0.2, Wilcoxon test) for most stations. Differences
14 were only observed between profiles of stations 11 and 13 and, 13 and 15. Seawater was collected in acid-cleaned 60 mL

Deleted: the French-national ultra-clean sampling device. This consisted of

15 LDPE bottles, after rinsing 3 times with about 20 mL of seawater. Teflon® tubing used to connect the filter holders or cartridges
16 to the GO-FLO bottles were washed in an acid-bath (10% v/v HCl, Suprapur®, Merck) for at least 12 h and rinsed three times
17 with Ultra High Purity Water (UHPW > 18 MΩ.cm) prior to use. Samples were then acidified to ~ pH 1.7 with HCl (Ultrapur®
18 Merck, 2 %o v/v) under a class 100 laminar flow hood inside the clean container. The sample bottles were then double bagged
19 and stored at ambient temperature in the dark before shore-based analyses.

Deleted: , neither between stations (i.e. stations 17, 19, 21, 25, 26, 29, 32, 34, 42, 44, 49) while swapping between both filtration techniques (p-values > 0.05, Wilcoxon tests paired by depth and against the sign of the alternative hypothesis depending on the filtration technique used), except between station 11 and 13 and 13 and 15.

20 Large volumes of seawater sample (referred hereafter as the in-house standard seawater) were also collected using a towed
21 fish at around 2-3 m deep and filtered in-line inside a clean container through a 0.2 µm pore size filter capsule (Sartorius
22 SARTOBRAN® 300) and was stored unacidified in 20-30 L LDPE carboys (Nalgene™). All the carboys were cleaned
23 following the guidelines of the GEOTRACES Cookbook (Cutter et al., 2017). This in-house standard seawater was used for
24 calibration on the SeaFAST-pico™ - SF-ICP-MS (see Section 2.2) and was acidified to ~ pH 1.7 with HCl (Ultrapur® Merck,
25 2 %o v/v) at least 24h prior to analysis.

Deleted: Samples were either taken from the filtrate of particulate samples (collected on polyethersulfone filters, 0.45 µm supor®, see Gourain et al., this issue) or after filtration on 0.2 µm filter cartridges (Sartorius SARTOBRAN® 300) (Table 1).

Deleted: 1.7 with

Deleted: 2 %o (v/v)

26 2.2 DFe analysis with SeaFAST-pico™

Commented [MT1]: I need information on how long before analysis was the calibration seawater acidified how many samples were run per day and how much samples were between each calibration curve
Also need the way the errors were calculated: standard deviation of the calibration slopes or SD of the Element ?

Deleted: ¶

Deleted: to a

Deleted: via a SeaFAST-pico™ introduction system (Elemental Scientific Incorporated

Deleted: on a daily basis

Formatted: Font: 10 pt, Complex Script Font: 10 pt

Formatted: Font: 10 pt, Complex Script Font: 10 pt, Superscript

Formatted: Font: 10 pt, Complex Script Font: 10 pt

Formatted: Font: 10 pt, Complex Script Font: 10 pt, Superscript

Formatted: Font: 10 pt, Complex Script Font: 10 pt

27 Seawater samples were preconcentrated using a SeaFAST-pico™ (ESI, Elemental Scientific, USA) and the eluent was directly
28 introduced via a PFA-ST nebulizer and a cyclonic spray chamber in an Element XR Sector Field Inductively Coupled Plasma
29 Mass Spectrometry (Element XR SF-ICP-MS, Thermo Fisher Scientific Inc., Omaha, NE), following the protocol of
30 Lagerström et al. (2013).

31 High-purity grade solutions and water (Milli-Q) were used to prepare the following reagents each day: the acetic acid-
32 ammonium acetate buffer (CH₃COO⁻ and NH₄⁺) was made of 140 mL acetic acid (> 99% NORMATOM® - VWR chemicals)
33 and ammonium hydroxide (25%, Merck Suprapur®) in 500 mL PTFE bottles and was adjusted to pH 6.0 ± 0.2 for the on-line

1 pH adjustment of the samples. The eluent was made of 1.4 M nitric acid (HNO₃, Merck Ultrapur®) in Milli-Q water by a 10-
2 fold dilution and spiked with 1 µg L⁻¹ ¹¹⁵In (SCP Science calibration standards) to allow for drift correction. Autosampler and
3 column rinsing solutions were made of HNO₃ 2.5% (v/v) (Merck Suprapur®) in Milli-Q water. The carrier solution driven by
4 the syringe pumps to move the sample and buffer through the flow injection system was made in the same way.

5 All reagents, standards, samples, and blanks were prepared in acid cleaned low density polyethylene (LDPE) or Teflon
6 fluorinated ethylene propylene (FEP) bottles. Bottles were cleaned following the GEOTRACES protocol (Cutter et al., 2017).
7 Mixed element standard solution was prepared gravimetrically using high purity standards (Fe, Mn, Cd, Co, Zn, Cu, Pb; SCP
8 Science calibration standards) in HNO₃ 3% (v/v) (Merck Ultrapur®). A six-point calibration curve was prepared by standard
9 additions of the mixed element standard to our acidified in-house standard and ran at the beginning, the middle and the end of
10 each analytical session. The distribution of the trace metals other than Fe will be reported elsewhere (Planquette et al., in prep.).
11 Final concentrations of samples and procedural blanks were calculated from In-normalized data. Data were blank-corrected
12 by subtracting an average acidified Milli-Q blank that were pre-concentrated on the SeaFAST-pico™ in the same way as the
13 samples and seawater standards. Each analytical session consisted of about fifty samples and two calibrations, one at the
14 beginning and another one at the end of each analytical session. The errors associated to each sample were calculated as the
15 standard deviation for five measurements of low-Fe seawater samples. The mean Milli-Q blank was equal to 0.08 ± 0.09 nmol
16 L⁻¹ (n = 17) all analytical session together. The detection limit, calculated for a given run as three times the standard deviation
17 of the Milli-Q blanks, was on average 0.05 ± 0.05 nmol L⁻¹ (n = 17). Reproducibility was assessed through the standard
18 deviation of replicate samples (every 10th sample was a replicate) and the average of the in-house standard seawater, and was
19 equal to 17% (n = 84). Accuracy was determined from the analysis of consensus (SAFe S, GSP) and certified (NASS-7)
20 seawater matrices (see Table 2) and in-house standard seawater (DFe = 0.42 ± 0.07 nmol L⁻¹, n = 84). Note that all the DFe
21 values were generated in nmol kg⁻¹ using the SeaFAST-pico™ coupled to an Element XR SF₆-ICP-MS and were converted to
22 nmol L⁻¹ (multiplied by a factor of 1.025 kg L⁻¹) to be directly comparable with literature.

23 2.3 Meteoric water and sea ice fraction calculation

24 We separated the mass contributions to samples from stations 53, 61 and 78 in Sea-Ice Melt (SIM) Meteoric Water (MW) and
25 saline seawater inputs using the procedure and mass balance calculations that are fully described in Benetti et al. (2016).
26 Hereafter, we describe briefly the principle. We considered two types of seawater, namely the Atlantic Water (AW) and the
27 Pacific Water (PW). After estimating the relative proportions of AW (f_{AW}) and PW (f_{PW}) and their respective salinity and
28 $\delta^{18}\text{O}$ affecting each samples, the contribution of SIM and MW can be determined using measured salinity (S_m) and $\delta^{18}\text{O}$
29 ($\delta^{18}\text{O}_m^{18}$). The mass balance calculations are presented below:

$$30 f_{AW} + f_{PW} + f_{MW} + f_{SIM} = 1 \text{ (eq.1)}$$

$$31 f_{AW} \cdot S_{AW} + f_{PW} \cdot S_{PW} + f_{MW} \cdot S_{MW} + f_{SIM} \cdot S_{SIM} = S_m \text{ (eq.2)}$$

$$32 f_{AW} \cdot \delta^{18}\text{O}_{AW}^{18} + f_{PW} \cdot \delta^{18}\text{O}_{PW}^{18} + f_{MW} \cdot \delta^{18}\text{O}_{MW}^{18} + f_{SIM} \cdot \delta^{18}\text{O}_{SIM}^{18} = \delta^{18}\text{O}_m^{18} \text{ (eq.3)}$$

Deleted: was made of 0.5 M acetic acid (Merck ultrapur) and 0.6 M ammonium hydroxide (Merck ultrapur) and was adjusted to pH 8.3.

Deleted: tion acid

Deleted: 6

Formatted: Complex Script Font: 10 pt

Deleted: 1 µg mL⁻¹ Indium (In, PlasmaCAL calibration standards) to allow for drift correction.

Formatted: Font: 10 pt, Complex Script Font: 10 pt

Formatted: Font: 10 pt, Complex Script Font: 10 pt, Superscript

Formatted: Font: 10 pt, Complex Script Font: 10 pt

Formatted: Font: 10 pt, Complex Script Font: 10 pt, Superscript

Formatted: Font: 10 pt, Complex Script Font: 10 pt

Deleted: 0.012 M hydrochloric acid

Formatted: Subscript

Deleted: (HCl, Merck ultrapur) in

Deleted: PlasmaCAL

Formatted: Font: 10 pt, Complex Script Font: 10 pt

Formatted: Default, Justified, Line spacing: 1.5 lines

Deleted: calibration

Deleted: 0.8 M

Formatted: Font: 10 pt, Complex Script Font: 10 pt

Deleted: (GEOVIDE filtered seawater, collected at station 69, 40m depth)

Deleted: run

Formatted: Font: 10 pt, Complex Script Font: 10 pt

Formatted: Font: 10 pt, Superscript

Formatted: Font: 10 pt, Complex Script Font: 10 pt

Deleted:

Formatted: Font: 10 pt, Complex Script Font: 10 pt

Formatted: Font: 10 pt, Complex Script Font: 10 pt

Formatted: Font: 10 pt, Complex Script Font: 10 pt

Formatted: Font: 10 pt, Complex Script Font: 10 pt

Formatted: Font: 10 pt, Complex Script Font: 10 pt

Deleted: Precision was assessed through replicate samples (every 10th sample was a replicate) and accuracy was determined from ...

Formatted: Font: 10 pt, Complex Script Font: 10 pt

Deleted: HR

Deleted: in

Formatted: Font: 10 pt, Complex Script Font: 10 pt

1 where f_{AW} , f_{PW} , f_{MW} , f_{SIM} are the relative fraction of AW, PW, MW, and SIM. To calculate the relative fractions of AW, PW,
2 MW and SIM we used the following end-members: $S_{AW} = 35.80_{AW}^{18} = +0.18\%$ (Benetti et al., 2016); $S_{PW} = 32.5.80_{PW}^{18} = -$
3 1% (Cooper et al., 1997; Woodgate and Aagaard, 2005); $S_{MW} = 0.80_{MW}^{18} = -18.4\%$ (Cooper et al., 2008); $S_{SIM} = 4.80_{SIM}^{18} =$
4 $+0.5\%$ (Melling and Moore, 1995).
5 Negative sea-ice fractions indicated a net brine release while positive sea-ice fractions indicated a net sea-ice melting. Note
6 that for stations over the Greenland Shelf, we assumed that the Pacific Water (PW) contribution was negligible for the
7 calculations, supported by the very low PW fractions found at Cape Farewell in May 2014 (see Figure B1 in Benetti et al.,
8 2017), while for station 78, located on the Newfoundland shelf, we used nutrient measurements to calculate the PW fractions,
9 following the approach from Jones et al. (1998) (the data are published in Benetti et al., 2017).

10 2.4 Ancillary measurements and mixed layer depth determination

11 Potential temperature (θ), salinity (S), dissolved oxygen (O_2) and beam attenuation data were retrieved from the CTD sensors
12 (CTD SBE911 equipped with a SBE-43) that were deployed on a stainless steel rosette. Nutrient and pigment samples were
13 obtained from the stainless steel rosette casts and analysed according to Aminot and Kerouel (2007) and Ras et al. (2008),
14 respectively. We used the data from the stainless steel rosette casts that were deployed immediately before or after our TMR
15 casts. All these data are available on the LEFE/CYBER database (<http://www.obs-vlfr.fr/proof/php/geovide/geovide.php>).
16 The mixed layer depth (Z_m) for each station was calculated using the function “calculate.mld” (part of the “realcofi” package,
17 Ed Weber at NOAA SWFSC) created by Sam McClathie (NOAA Federal, 30th December 2013) for R software and where Z_m
18 is defined as an absolute change in the density of seawater at a given temperature ($\Delta\sigma_t \geq 0.125 \text{ kg m}^{-3}$) with respect to an
19 approximately uniform region of density just below the ocean surface (Kara et al., 2000). In addition to the density criterion,
20 the temperature and salinity profiles were inspected at each station for uniformity within this layer. When they were not
21 uniform, the depth of any perturbation in the profile was chosen as the base of the Z_m (Table 1).

22 2.5 Statistical analysis

23 All statistical approaches, namely the comparison between the pore size used for filtration, correlations and Principal
24 Component Analysis (PCA), were performed using the R statistical software (R development Core Team 2012). For all the
25 results, p-values were calculated against the threshold value alpha (α), that we assigned at 0.05, corresponding to a 95% level
26 of confidence. For all data sets, non-normal distributions were observed according to the Shapiro-Wilk test. Therefore, the
27 significance level was determined with a Wilcoxon test.
28 All sections and surface layer plots were prepared using Ocean Data View (Schlitzer, 2016).

Deleted:

Formatted: Font: (Asian) SimSun, Font color: Black, Complex Script Font: 10 pt, English (Australia)

Deleted: 3

Deleted: S

Deleted: CTD

Deleted: CTD casts

Deleted:

Deleted: /will be

Formatted: Subscript

Deleted: ,

Deleted: (

Deleted: 4

Deleted: measured

2.6 Water mass determination and associated DFe concentrations

The water mass structure in the North Atlantic Ocean from the GEOVIDE voyage was quantitatively assessed by means of an extended Optimum Multi-Parameter (eOMP) analysis with 14 water masses (for details see García-Ibáñez et al., 2015; this issue). Using this water mass determination, DFe concentrations were considered as representative of a specific water mass only when the contribution of this specific water mass was higher than 60% of the total water mass pool.

Deleted: 5

2.7 Database

The complete database of dissolved Fe is available in the electronic supplement www.biogeosciences.net. Overall, 540 data points of dissolved Fe are reported, among which 511 values are used in this manuscript. The remaining 29 values (5.7% of the total dataset) are flagged as (suspect) outliers. These 29 outliers were not used in figures and in the interpretation of this manuscript. The criteria for rejection were based on the comparison with other parameters measured from the same GO-FLO sampler, and curve fitting versus samples collected above and below the suspect sample. The complete data set will be available in national and international databases (LEFE-CYBER, <http://www.obs-vlfr.fr/proof/index2.php>, and GEOTRACES <http://www.bodc.ac.uk/geotraces/>).

Deleted: From this water mass determination, we considered only a contribution higher than 60% of a specific water mass to the total water mass pool and calculated the average DFe concentrations within each water mass and considered them as representative of the DFe concentrations within these water masses, as identifying representative end-members was not found to be possible due to the non-conservative behaviour of DFe in seawater.

Deleted: 6

Deleted: relational

Deleted: base

3 Results

3.1 Hydrography

The hydrology and circulation of the main water masses along the OVIDE section in the North Atlantic Subpolar Gyre and their contribution to the Atlantic Meridional Overturning Circulation (AMOC) have been described using an eOMP analysis by García-Ibáñez et al., (2015; this issue) and Zunino et al. (2017). For a schematic of water masses, currents and pathways, see Danialt et al. (2016). Hereafter we summarise the main features (Fig. 1 and 2).

Moved (insertion) [1]

Moved up [1]: For a schematic of water masses, currents and pathways, see Danialt et al. (2016).

Upper waters (~ 0 – 800 m) - The cyclonic circulation of the Eastern North Atlantic Central Water (ENACW) ($12.3 < \theta < 16^{\circ}\text{C}$, $35.66 < S < 36.2$, $241 < O_2 < 251 \mu\text{mol kg}^{-1}$) occupied the water column from 0 to ~ 800 m depth from stations 1 to 25 contributing to 60% of the water mass pool. The sharp Subarctic Front (between stations 26 and 29), caused by the northern branch of the North Atlantic Current (NAC) separated the cyclonic subpolar from the anticyclonic subtropical gyre domains at 50°N and 22.5°W . The ENACW were also encountered to a lesser extent and only in surface waters (from 0 to ~ 100 m depth) between stations 29 and 34 (contributing to less than 40% of the water mass pool). West of the Subarctic Front, Iceland SubPolar Mode Waters (IcSPMW, $7.07 < \theta < 8^{\circ}\text{C}$, $35.16 < S < 35.23$, $280 < O_2 < 289 \mu\text{mol kg}^{-1}$) was encountered from stations 34-40 (accounting for more than 45% of the water mass pool from 0 to ~ 800 m depth) and Irminger SubPolar Mode Waters (IrSPMW, $\theta \approx 5^{\circ}\text{C}$, $S \approx 35.014$) from stations 42-44 (contributing to 40% of the water mass pool from 0 to ~ 250 m

Deleted: se Central Waters

Deleted: were encountered

Deleted: stations 34-40 (accounting for more than 45% of the water mass pool from 0 to ~ 800 m depth) and

Deleted: 60

Deleted: contribution

1 depth) and stations 49 and 60 (accounting for 40% of the water mass pool down to 1300 m depth). The IcSPMW was also
2 observed within the Subtropical gyre (stations 11-26), subducted below ENACW until ~ 1000 m depth. Stations 63 (> ~ 200
3 m depth) and 64 (from surface down to ~ 500 m depth) exhibited a contribution of the IrSPMW higher than 45%. Stations 44,
4 49 and 60, from the Irminger Sea, and 63 from the Labrador Sea were characterised by lower sea-surface salinity ranges ($S =$
5 $[34.636, 34.903]$, stations 63 and 60, respectively). Subarctic Intermediate Water (SAIW, $4.5 < \theta < 6.0^{\circ}\text{C}$, $34.70 < S < 34.80$)
6 contributed to more than 40% of the water mass pool in the Iceland Basin between the surface and ~ 400 m depth at stations
7 29 and 32 and throughout the water column of stations 53, 56 and 61 and from surface down to ~ 200 m depth at station 63.
8 From stations 68 to 78 surface waters were characterized by a minimum of salinity and a maximum of oxygen ($S = 34.91$, O_2
9 $= 285 \mu\text{mol kg}^{-1}$, $\theta \approx 3^{\circ}\text{C}$) and corresponded to the newly formed Labrador Sea Water (LSW). The LSW was also observed in
10 surface waters of station 44 with a similar contribution than IrSPMW (~ 40%).

11
12 *Intermediate waters (~ 800 – 1400 m)* - The Mediterranean Outflow Water (MOW), distinguishable from surrounding Atlantic
13 Water by its high salinity tongue (up to 36.2), a minimum of oxygen ($\text{O}_2 = 210 \mu\text{mol kg}^{-1}$) and relatively high temperatures
14 (up to 11.7°C) was observed from station 1 to 21 between 800 and 1400 m depth at a neutral density ranging from 27.544 to
15 27.751 kg m^{-3} with the maximum contribution to the whole water mass pool seen at station 1 ($64 \pm 6\%$). Its main core was
16 located at ~ 1200 m depth off the Iberian shelf from stations 1 to 11 and then gradually rising westward due to mixing with
17 LSW within the North Atlantic subtropical gyre and a contribution of this water mass decreasing until station 21 down to 10-
18 20%. The LSW ($27.763 < \text{neutral density} < 27.724 \text{ kg m}^{-3}$) was sourced from the SPMW after intense heat loss and led to its
19 deep convection. During GEOVIDE, LSW formed by deep convection the previous winter was found at several stations in the
20 Labrador Sea (68, 69, 71 and 77). After convecting, LSW splits into three main branches with two main cores separated by the
21 Reykjanes Ridge, (stations 1-32, West European and Iceland Basins; stations 40-60, Irminger Sea), and the last one, entering
22 the West European Basin (Zunino et al., 2017).

23
24 *Overflows and Deep waters (~ 1400 - 5500 m)* - North East Atlantic Deep Water (NEADW, $1.98 < \theta < 2.50^{\circ}\text{C}$, $34.895 < S <$
25 34.940) was the dominant water mass in the West European Basin at stations 1-29 from 2000 m depth to the bottom and is
26 characterized by high silicic acid ($42 \pm 4 \mu\text{mol L}^{-1}$), nitrate ($21.9 \pm 1.5 \mu\text{mol L}^{-1}$) concentrations and lower oxygen concentration
27 ($\text{O}_2 \approx 252 \mu\text{mol kg}^{-1}$) (see Sarthou et al., 2018). The core of the NEADW (stations 1-13) was located near the seafloor and
28 gradually decreased westward. Polar Intermediate Water (PIW, $\theta \approx 0^{\circ}\text{C}$, $S \approx 34.65$) is a ventilated, dense, low-salinity water
29 intrusion to the deep overflows within the Irminger and Labrador Seas that is formed at the Greenland shelf. PIW represents
30 only a small contribution to the whole water mass pool (up to 27%) and was observed over the Greenland slope at stations 53
31 and 61 as well as in surface waters from station 63 (from 0 to ~ 200 m depth), in intermediate waters of stations 49, 60 and 63
32 (from ~ 500 to ~ 1500 m depth) and in bottom waters of stations 44, 68, 69, 71 and 77 with a contribution higher than 10%.
33 Iceland Scotland Overflow Water (ISOW, $\theta \approx 2.6^{\circ}\text{C}$, $S \approx 34.98$) is partly formed within the Arctic Ocean by convection of the
34 modified Atlantic water. ISOW comes from the Iceland-Scotland sills and flows southward towards the Charlie-Gibbs Fracture

Deleted: until

Deleted: for stations 49 and 60

Deleted: , respectively

Deleted: the Central Waters

Deleted: The

Deleted: The Mediterranean Water (MW) flows westward from the Mediterranean Sea and is then transported northward by the Azores counter current.

Deleted: GA01

Deleted: new

Deleted: formed by deep convection the previous winter

Deleted: from

Deleted: some the LSW flows north-eastward in the Iceland Basin and Irminger Sea and then back to the Labrador Sea, while some flows along the Canadian coast, more specifically above the Newfoundland Margin as confirmed by hydrographic station 76 (52.5°W , 52.5°N) which exhibited the highest LSW fraction (up to 98% at the closest bottom sample, García-Ibáñez et al., this issue). On its way eastwards, the

Deleted: , that corresponds to its different pathways

Deleted: . One of the branches flows eastward at intermediate depth, following the circulation of the warm surface NAC and

Deleted: s

Deleted: and the Iceland Basin where it splits again into two branches (south-eastward and north-eastward flowing path, respectively).

Deleted: The

Formatted: Superscript

Deleted: Sarthou et al., 2018

Deleted: The

Deleted: shelf

Deleted: in

Deleted: . PIW is in contact with the atmosphere once a year during the time of winter convection (Strass et al., 1993) and hence is ventilated ($\text{O}_2 \approx 310 \mu\text{mol kg}^{-1}$) This water presented

Deleted: low

Deleted: entire

Deleted: . The PIW

Deleted: The

Deleted:

1 Zone (CGFZ) and Bight Fracture Zone (BFZ) (stations 34 and 36) after which it reverses its flowing path northward and enters
2 the Irminger Sea (stations 40 and 42) to finally reach the Labrador Sea close to the Greenland coast (station 49, station 44
3 being located in between this two opposite flow paths). Along the eastern (stations 26-36) and western (stations 40-44) flanks
4 of the Reykjanes Ridge, ISOW had a contribution higher than 50% to the water mass pool. JSOW was observed from 1500 m
5 depth to the bottom of the entire Iceland Basin (stations 29-38) and from 1800 to 3000 m depth within the Irminger Sea
6 (stations 40-60). JSOW, despite having a fraction lower than 45% above the Reykjanes Ridge (station 38), was the main
7 contributor to the water mass pool from 1300 m depth down to the bottom. JSOW was also observed within the Labrador Sea
8 from stations 68 to 77. Finally, the deepest part of the Irminger (stations 42 and 44) and Labrador (stations 68-71) Seas were
9 occupied by Denmark Strait Overflow Water (DSOW, $\theta \approx 1.30^{\circ}\text{C}$, $S \approx 34.905$).

10 3.2 Ancillary data

11 3.2.1 Nitrate

12 Surface nitrate (NO_3^-) concentrations (García-Ibáñez et al., 2018; Pérez et al., 2018; Sarthou et al., 2018) ranged from 0.01 to
13 $10.1 \mu\text{mol L}^{-1}$ (stations 53 and 63, respectively). There was considerable spatial variability in NO_3^- surface distributions with
14 high concentrations found in the Iceland Basin and Irminger Sea (higher than $6 \mu\text{mol L}^{-1}$), as well as at stations 63 ($10.1 \mu\text{mol}$
15 L^{-1}) and 64 ($5.1 \mu\text{mol L}^{-1}$), and low concentrations observed in the West European Basin, in the Labrador Sea and above
16 continental margins. The low surface concentrations in the West European Basin ranged from 0.02 (station 11) to 3.9 (station
17 25) $\mu\text{mol L}^{-1}$. Station 26 delineating the extreme western boundary of the West European Basin exhibited enhanced NO_3^-
18 concentrations as a result of mixing between ENACW and IcSPMW, although these surface waters were dominated by
19 ENACW. In the Labrador Sea (stations 68-78) low surface concentrations were observed with values ranging from 0.04 (station
20 68) to 1.8 (station 71) $\mu\text{mol L}^{-1}$. At depth, the lowest concentrations (lower than $15.9 \mu\text{mol L}^{-1}$) were measured in ENACW (~
21 $0 - 800 \text{ m depth}$) and DSOW ($> 1400 \text{ m depth}$), while the highest concentrations were measured within NEADW (up to 23.5
22 $\mu\text{mol L}^{-1}$), and in the mesopelagic zone of the West European and Iceland Basins (higher than $18.4 \mu\text{mol L}^{-1}$).

23 3.2.2 Chlorophyll-*a*

24 Overall, most of the phytoplankton biomass was localised above 100 m depth with lower total chlorophyll-*a* (TChl-*a*)
25 concentrations south of the Subarctic Front and higher at higher latitudes (see supplementary material Fig. S1). While
26 comparing TChl-*a* maxima considering all stations, the lowest value (0.35 mg m^{-3}) was measured within the West European
27 Basin (station 19, 50 m depth) while the highest values were measured at the Greenland (up to 4.9 mg m^{-3} , 30 m depth, station
28 53 and up to 6.6 mg m^{-3} , 23 m depth, station 61) and Newfoundland (up to 9.6 mg m^{-3} , 30 m depth, station 78) margins.

Deleted: In this study, ISOW properties are defined after the mixing of the overflow with Atlantic Central Water and Labrador Water downstream the sills. ... along the eastern (stations 26-36) and western (stations 40-44) flanks of the Reykjanes Ridge, ISOW had a contribution higher than 50% to the water mass pool. The ...SOW was observed from 1500 m depth to the bottom of the entire Iceland Basin (stations 29-38) and from 1800 to 3000 m depth within the Irminger Sea (stations 40-60). The ...SOW, despite having a fraction lower than 45% above the Reykjanes Ridge (station 38), was the main contributor to the water mass pool from 1300 m depth down to the bottom. The ...SOW was also observed within the Labrador Sea from stations 68 to 77. Finally, the deepest part of the Irminger (stations 42 and 44) and Labrador (stations 68-71) Seas were occupied by the Denmark Strait Overflow Water (DSOW, $\theta \approx 1.30^{\circ}\text{C}$, $S \approx 34.905$), that spills over the Greenland-Scotland ridge system and overflows south-westward into the deep North Atlantic basins. This water mass is formed partly in the Arctic Ocean by convection of the branch of the NAC that flows northward between Greenland, Iceland and Scotland. DSOW is a young water mass with a 3 to 4-year residence time north of the sill after surface contact. ...

Deleted: Sarthou et al., in prep.) ... ranged from 0.01 to $10.1 \mu\text{mol L}^{-1}$ (stations 53 and 63, respectively). There was considerable spatial variability in NO_3^- surface distributions with high est NO_3^- concentrations found in the Iceland Basin and Irminger Sea (higher than $6 \mu\text{mol L}^{-1}$), as well as at stations 63 ($10.1 \mu\text{mol L}^{-1}$) and 64 ($5.1 \mu\text{mol L}^{-1}$), and the lowest concentrations observed in the Western European Basin, in the Labrador Sea and above continental margins. The low surface NO_3^- concentrations in the Western European Basin extended from station 2 (closest station to continental land mass) to station 23 (most open ocean station) with concentrations ranging from 0.02 (station 11) to 3.917 (station 25) $\mu\text{mol L}^{-1}$. Station 26 delineating the extreme western boundary of the West European Basin exhibited enhanced NO_3^- concentrations as a result of mixing between ENACW and IcSPMW, although these surface waters were dominated by ENACW. The low nitrate concentrations in the Labrador Sea (stations 68-78) extended from station 68 to station 78 with low surface concentrations were observed with ranging from 0.04 (station 68) to 1.8 (station 71) $\mu\text{mol L}^{-1}$. At depth, the lowest NO_3^- concentrations (lower than $15.9 \mu\text{mol L}^{-1}$) were measured in surface ENACW (~ $0 - 800 \text{ m depth}$) and deep DSOW ($> 1400 \text{ m depth}$) ... while waters were found in the ...

Deleted: Overall, total chlorophyll-*a* (TChl-*a*) concentrations were significantly correlated with the more extensive dataset from the CTD mounted fluorometer ($R^2 = 0.76$, $n = 162$). TChl-*a* is the universal proxy for phytoplankton organisms. The maximum chlorophyll biomass ranged between 0.35 mg m^{-3} (Station 19, 50 m depth) and 9.4 mg m^{-3} (station 78, 30 m depth) highlighting the intense variability observed throughout this section (Fig. 3). Generally speaking, most of the phytoplankton biomass was above 100 m depth with lower total chlorophyll-*a* (TChl-*a*) concentrations were lower south of the Subarctic Front and higher at higher latitudes (see supplementary material Fig. S1). While comparing TChl-*a* maxima considering all stations, the lowest TChl-*a* value (< 0.75 to 0.35 mg m^{-3}) was measured within the West European Basin (stations 19, 50 m depth) and Iceland (stations 34-38) Basins, while the highest concentrations values were measured at the Greenland (up to 4.9 mg m^{-3} , 30 m depth, stations 53 and up to 6.6 mg m^{-3} , 23 m depth, station 61) and Newfoundland (up to 9.6 mg m^{-3} , 30 m depth, station 78) margins (up to 4.9 , 6.6 and 9.6 mg m^{-3} , respectively) ...

1 3.3 Dissolved Fe concentrations

2 Dissolved Fe concentrations (see supplementary material Table S1) ranged from $0.09 \pm 0.01 \text{ nmol L}^{-1}$ (station 19, 20 m depth)
3 to $7.8 \pm 0.5 \text{ nmol L}^{-1}$ (station 78, 371 m depth) (see Fig. 3). Generally, vertical profiles of DFe for stations above the margins
4 (2, 4, 53, 56, 61, and 78) showed an increase with depth, although sea-surface maxima were observed at stations 2, 4 and 56.
5 For these margin stations, values ranged from 0.7 to 1.0 nmol L^{-1} in the surface waters. Concentrations increased towards the
6 bottom, with more than 7.8 nmol L^{-1} measured at station 78, approximately 1-3 nmol L^{-1} for stations 2, 4, 53, and 61, and just
7 above 0.4 nmol L^{-1} for station 56 (Fig. 4). Considering the four oceanic basins, mean vertical profiles (supplementary material
8 Fig. S2) showed increasing DFe concentrations down to 3000 m depth followed by decreasing DFe concentrations down to
9 the bottom. Among deep-water masses, the lowest DFe concentrations were measured in the West European Basin. The
10 Irminger Sea displayed the highest DFe concentrations from 1000 m depth to the bottom relative to other basins at similar
11 depths (Fig. 4 and supplementary material Fig. S2). In the Labrador Sea, DFe concentrations were low and relatively constant
12 at about $0.87 \pm 0.06 \text{ nmol L}^{-1}$ from 250 m to 3000 m depth (Fig. S2). Overall, surface DFe concentrations were higher ($0.36 \pm$
13 0.18 nmol L^{-1}) in the North Atlantic Subpolar gyre (above 52°N) than in the North Atlantic Subtropical gyre ($0.17 \pm 0.05 \text{ nmol}$
14 L^{-1}). The upper surface DFe concentrations were generally smaller than 0.3 nmol L^{-1} , except for few stations in the Iceland
15 Basin (stations 32 and 38), Irminger (stations 40 and 42) and Labrador (station 63) Seas, where values ranged between 0.4-0.5
16 nmol L^{-1} .

18 3.4 Fingerprinting water masses

19 In the Labrador Sea, IrSPMW exhibited an average DFe concentration of $0.61 \pm 0.21 \text{ nmol L}^{-1}$ (n=14). DFe concentrations in
20 the LSW were the lowest in this basin, with an average value of $0.71 \pm 0.27 \text{ nmol L}^{-1}$ (n=53) (see supplementary material Fig.
21 S3). Deeper, ISOW displayed slightly higher average DFe concentrations ($0.82 \pm 0.05 \text{ nmol L}^{-1}$, n=2). Finally, DSOW had the
22 lowest average ($0.68 \pm 0.06 \text{ nmol L}^{-1}$, n=3, see supplementary material Fig. S3) and median (0.65 nmol L^{-1}) DFe values for
23 intermediate and deep waters.
24 In the Irminger Sea, surface waters were composed of SAIW ($0.56 \pm 0.24 \text{ nmol L}^{-1}$, n=4) and IrSPMW ($0.72 \pm 0.32 \text{ nmol L}^{-1}$,
25 n=34). The highest open-ocean DFe concentrations (up to $2.5 \pm 0.3 \text{ nmol L}^{-1}$, station 44, 2600 m depth) were measured within
26 this basin. In the upper intermediate waters, LSW was identified only at stations 40 to 44, and had the highest DFe values with
27 an average of $1.2 \pm 0.3 \text{ nmol L}^{-1}$ (n=14). ISOW showed higher DFe concentrations than in the Iceland Basin ($1.3 \pm 0.2 \text{ nmol}$
28 L^{-1} , n=4). At the bottom, DSOW was mainly located at stations 42 and 44 and presented the highest average DFe values (1.4
29 $\pm 0.4 \text{ nmol L}^{-1}$, n=5) as well as the highest variability from all the water masses presented in this section (see supplementary
30 material Fig. S3).
31 In the Iceland Basin, SAIW and IcSPMW displayed similar averaged DFe concentrations ($0.67 \pm 0.30 \text{ nmol L}^{-1}$, n=7, and 0.55
32 $\pm 0.34 \text{ nmol L}^{-1}$, n=22, respectively). Averaged DFe concentrations were similar in both LSW and ISOW, and higher than in

Deleted: The dataset is well distributed between upper, intermediate and deep ocean samples with 36% of samples collected at depths shallower than 200 m, 27% of samples between 200 and 1000 m depth and 37% of samples from depths deeper than 1000 m, including 11% of samples below 2500 m depth. Samples are distributed as follows between basins: 38% of samples were collected within the West European Basin (stations 1 and 11-26), 17% with (...)

Deleted: 4

Deleted: ¶

Deleted: were around

Deleted: -

Deleted: 5

Deleted: ¶

Deleted: For all regions

Deleted: Fig. 6

Deleted: from the surface

Deleted: , with the

Deleted: deep values

Deleted: s

Deleted: 6

Deleted: 6

Formatted: Superscript

Deleted: 30

Deleted: Within the low-Fe West European Basin a few stations (...)

Deleted: 3.3.

Moved (insertion) [4]

Deleted: characterized by the

Deleted: the

Deleted: the

Deleted: The

Deleted: the

Deleted: Fig. 7

Deleted: ¶

Deleted: In the West European Basin, the MOW was present bu (...)

Deleted: the

Deleted: the

Deleted: with averaged DFe concentrations of

Deleted: (

Deleted: 7)

Deleted: (

Deleted:)

Deleted: The

1 SAIW and IcSPMW ($0.96 \pm 0.22 \text{ nmol L}^{-1}$, $n=21$ and $1.0 \pm 0.3 \text{ nmol L}^{-1}$, $n=10$, respectively, see supplementary material Fig. S3).
 2
 3 Finally, in the West European Basin, DFe concentrations in ENACW were the lowest of the whole section with an average
 4 value of $0.30 \pm 0.16 \text{ nmol L}^{-1}$ ($n=64$). MOW was present deeper in the water column but was not characterized by particularly
 5 high or low DFe concentrations relative to the surrounding Atlantic waters (see supplementary material Fig. S3). The median
 6 DFe value in MOW was very similar to the median value when considering all water masses (0.77 nmol L^{-1} , Fig. 3 and
 7 supplementary material S3). LSW and IcSPMW displayed slightly elevated DFe concentrations compared to the overall
 8 median with mean values of 0.82 ± 0.08 ($n=28$) and 0.80 ± 0.04 ($n=8$) nmol L^{-1} , respectively. The DFe concentrations in
 9 NEADW were relatively similar to the DFe median value of the GEOVIDE voyage (median DFe = 0.75 nmol L^{-1} , Fig. 3 and
 10 supplementary material Fig. S3) with an average value of $0.74 \pm 0.16 \text{ nmol L}^{-1}$ ($n=18$) and presented relatively low median
 11 DFe concentrations (median DFe = 0.71 nmol L^{-1}) compared to other deep water masses.

12 4 Discussion

13 In the following sections, we will first discuss the high DFe concentrations observed throughout the water column of stations
 14 1 and 17 located in the West European Basin (Section 4.1), then, the relationship between water masses and the DFe
 15 concentrations (Section 4.2) in intermediate (Section 4.2.2 and 4.2.3) and deep (Section 4.2.4 and 4.2.5) waters. We will also
 16 discuss the role of wind (Section 4.2.1), rivers (Section 4.3.1), meteoric water and sea-ice processes (Section 4.3.2),
 17 atmospheric deposition (Section 4.3.3) and sediments (Section 4.4) in delivering DFe. Finally, we will discuss the potential Fe
 18 limitation using DFe:NO₃⁻ ratios (Section 4.5).

19 4.1 High DFe concentrations at station 1 and 17

20 Considering the entire section, two stations (stations 1 and 17) showed irregularly high DFe concentrations ($> 1 \text{ nmol L}^{-1}$)
 21 throughout the water column, thus suggesting analytical issues. However, these two stations were analysed twice and provided
 22 similar results, therefore discarding any analytical issues. This means that these high values originated either from genuine
 23 processes or from contamination issues. If there had been contamination issues, one would expect a more random distribution
 24 of DFe concentrations and less consistence throughout the water column. It thus appears that contamination issues were
 25 unlikely to happen. Similarly, the influence of water masses to explain these distributions was discarded as the observed high
 26 homogenized DFe concentrations were restricted to these two stations. Station 1, located at the continental shelf-break of the
 27 Iberian Margin, also showed enhanced PFe concentrations, from lithogenic origin suggesting a margin source (Gourain et al.,
 28 2018). Conversely, no relationship was observed between DFe and PFe nor transmissometry for station 17. However, Ferron
 29 et al. (2016) reported a strong dissipation rate at the Azores-Biscay Rise (station 17) due to internal waves. The associated
 30 vertical energy fluxes could explain the homogenized profile of DFe at station 17, although such waves are not clearly
 31 evidenced in the velocity profiles. Consequently, the elevated DFe concentrations observed at station 17 remain unsolved.

Deleted: LSW exhibited higher DFe concentrations with an average value of $0.96 \pm 0.22 \text{ nmol L}^{-1}$ ($n=21$). The ISOW had an averaged DFe concentration of $1.0 \pm 0.3 \text{ nmol L}^{-1}$ ($n=10$) (Fig. 7).

Moved up [4]: In the Irminger Sea, surface waters were characterized by the SAIW ($0.56 \pm 0.24 \text{ nmol L}^{-1}$, $n=4$) and the IrSPMW ($0.72 \pm 0.32 \text{ nmol L}^{-1}$, $n=34$). The highest open-ocean DFe concentrations (up to $2.5 \pm 0.3 \text{ nmol L}^{-1}$, station 44, 2600 m depth) were measured within this basin. In the upper intermediate water the LSW was identified only at stations 40 to 44, and had the highest DFe values with an average of $1.2 \pm 0.3 \text{ nmol L}^{-1}$ ($n=14$). The ISOW showed higher DFe concentrations than in the Iceland Basin ($1.3 \pm 0.2 \text{ nmol L}^{-1}$, $n=4$). At the bottom, the DSOW was mainly located at stations 42 and 44 and presented the highest average DFe values ($1.4 \pm 0.4 \text{ nmol L}^{-1}$, $n=5$) as well as the highest variability from all the water masses presented in this section (Fig. 7). ¶

Deleted: in the Labrador Sea, the IrSPMW exhibited an average DFe concentration of $0.61 \pm 0.21 \text{ nmol L}^{-1}$ ($n=14$). DFe concentrations in the LSW were the lowest in this basin compared to the other ones, with an average value of $0.71 \pm 0.27 \text{ nmol L}^{-1}$ ($n=53$) (Fig. 7). Deeper, the ISOW displayed slightly higher DFe concentrations ($0.82 \pm 0.05 \text{ nmol L}^{-1}$, $n=2$). Finally, the DSOW had one of the lowest DFe values for intermediate and deep waters ($0.68 \pm 0.06 \text{ nmol L}^{-1}$, $n=3$, Fig. 7).

Deleted: 1

Deleted: 1

Deleted: 1

Deleted: 1

Deleted: 1

Deleted: 1

Deleted: 2

Deleted: 2

Deleted: 2

Deleted: 3

Deleted: 4

Formatted: Heading 2

Deleted: only

Deleted: . T

Deleted: more likely to be impacted by vertical processes

Deleted: . Another explanation which cannot be discarded would be a contamination issue, especially for station 1 as it was the first station sampled. With this in mind, one would expect a more random distribution of DFe concentrations and less consistence throughout the water column if there had been a problem with contamination.

Moved (insertion) [6]

Deleted: potentially

Moved up [6]: Another explanation which cannot be discarded would be a contamination issue, especially for station 1 as it was the first station sampled. With this in mind, one would expect a more random distribution of DFe concentrations and less consistence

4.2 DFe and hydrology keypoints

4.2.1 How do Air-sea interactions affect DFe concentration in the Irminger Sea?

Among the four distinct basins described in this paper, the Irminger Sea exhibited the highest DFe concentrations within the surface waters (from 0 to 250 m depth) with values ranging from 0.23 to 1.3 nmol L⁻¹ for open-ocean stations. Conversely, low DFe concentrations were previously reported in the central Irminger Sea by Rijkenberg et al. (2014) (April-May, 2010) and Achterberg et al. (2018) (April-May and July-August, 2010) with DFe concentrations ranging from 0.11 to 0.15 and from ~0 to 0.14 nmol L⁻¹, respectively (see supplementary material Fig. S4 and Table S2). Differences might be due to the phytoplankton bloom advancement, the high remineralization rate (Lemaître et al., 2017) observed within the LSW in the Irminger Sea (see Section 4.1.3) and a deeper winter convection in early 2014. Indeed, enhanced surface DFe concentrations measured during GEOVIDE in the Irminger Sea could be due to intense wind forcing events that would deepen the winter Z_{ed} down to the core of the Fe-rich LSW.

In the North Atlantic Ocean, the warm and salty water masses of the upper limb of the MOC are progressively cooled and become denser, and subduct into the abyssal ocean. In some areas of the SubPolar North Atlantic, deep convective winter mixing provides a rare connection between surface and deep waters of the MOC thus constituting an important mechanism in supplying nutrients to the surface ocean (de Jong et al., 2012; Louanchi and Najjar, 2001). Deep convective winter mixing is triggered by the effect of wind and a pre-conditioning of the ocean in such a way that the inherent stability of the ocean is minimal. Pickart et al. (2003) demonstrated that these conditions are satisfied in the Irminger Sea with the presence of weakly stratified surface water, a close cyclonic circulation, which leads to the shoaling of the thermocline and intense winter air-sea buoyancy fluxes (Marshall and Schott, 1999). Moore (2003) and Piron et al. (2016) described low-level westerly jets centred northeast of Cape Farewell, over the Irminger Sea, known as jet events. These events occur when wind is split around the orographic features of Cape Farewell, and are strong enough to induce deep convective mixing (Bacon et al., 2003; Pickart et al., 2003). It has also been shown that during winters with a positive North Atlantic Oscillation (NAO) index, the occurrence of such events is favoured (Moore, 2003; Pickart et al., 2003), which was the case in the winter 2013-2014, preceding the GEOVIDE voyage as opposed to previous studies (Lherminier, pers. comm.). The winter mixed layer depth prior to the cruise reached up to 1200 m depth in the Irminger Sea (Zunino et al., 2017), which was most likely attributed to a final deepening due to wind forcing events (centred at station 44). Such winter entrainment was likely the process involved in the vertical supply of DFe within surface waters fuelling the spring phytoplankton bloom with DFe values close to those found in LSW.

4.2.2 Why don't we see a DFe signature in the Mediterranean Overflow Water (MOW)?

On its northern shores, the Mediterranean Sea is bordered by industrialized European countries, which act as a continuous source of anthropogenic derived constituents into the atmosphere, and on the southern shores by the arid and desert regions of north African and Arabian Desert belts, which act as sources of crustal material in the form of dust pulses (Chester et al., 1993; Guerzoni et al., 1999; Martin et al., 1989). During the summer, when thermal stratification occurs, DFe concentrations in the

Deleted: 1

Deleted: 1

Deleted: ranging from 0.23 to 1.3 nmol L⁻¹ in open-ocean stations and ...rom 0 to 250 m depth) with values ranging from 0.23 to 1.3 nmol L⁻¹ for open-ocean stations. Conversely, low Enhanced surface D...Fe concentrations in the Irminger Sea ...ere previously reported in the central Irminger Sea by Rijkenberg et al. (2014) (April-May, 2010) and Achterberg et al. (2018) (April-May and July- ...ugust, 2010) with DFe concentrations ranging from 0.11 to 0.15 and from ~0 to 0.ranging from

Formatted: Superscript

Deleted: However, DFe concentrations measured during our study (May-June, 2014) in the Irminger Sea were higher than those reported before (Table 3). ...ifferences might be due to the phytoplankton bloom advancement, the high remineralization rate observed

Formatted: Subscript

Deleted: In the ...ubPolar North Atlantic, deep convective winter convective ...ixing provides a rare connection between surface and deep waters of the MOC thus constituting an important mechanism in supplying nutrients to the surface ocean represents the dominant nutrient supply process

Deleted: effect

Deleted: ADDIN EN.CITE <EndNote><Cite AuthorYear="1"><Author>Pickart</Author><Year>2003</Year><RecNum>1951</RecNum><DisplayText>Pickart et al. (2003)</DisplayText><record-><rec-number>1951</rec-number><foreign-keys><key app="EN" db-id="vzp0d0af8wwwepas0vexzytrws2fxffdp" timestamp="1508047470">1951</key><key app="ENWeb" db-id="">0</key></foreign-keys><ref-type name="Journal Article">17</ref-type><contributors><authors><author>Pickart, R. S.</author><author>Straneo, F.</author><author>Moore, G. W. K.</author></authors></contributors><titles><title>Is Labrador Sea Water formed in the Irminger basin?</title><secondary-title>Deep Sea Research Part I:</secondary-title></titles><periodical><full-title>Deep Sea Research Part I:</full-title></periodical><pages>23-52</pages><volume>50</volume><dates><year>2003</year></date><urls></urls></record-></Cite></EndNote>Pickart et al. (2003) demonstrated that these conditions necessary for the development of deep convection ...re satisfied in the Irminger Sea by ...ith the presence of weakly stratified surface water, a close cyclonic

Deleted: ..., whose ...these events occur when wind is split around the structure depends upon the splitting occurring as the flow encounter the ...rographic features from...f Cape Farewell, and th

Deleted: that are characterized by westerly flow over the Irminger Sea, centred northeast of Cape Farewell. ...re strong enough to induce deep convective mixing (Bacon et al., 2003; Pickart et al.,

Deleted: Therefore, the elevated DFe concentrations observed below 100 m depth from the central Irminger Sea were likely due

Deleted: 1

Deleted: Lack of

Deleted: T...he Mediterranean Sea on its northern shores

Deleted: the ...hermal stratification occurs period

1 SML can increase over the whole Mediterranean Sea by 1.6-5.3 nmol L⁻¹ in response to the accumulation of atmospheric Fe
2 from both anthropogenic and natural origins (Bonnet and Guieu, 2004; Guieu et al., 2010; Sarthou and Jeandel, 2001). After
3 atmospheric deposition, the fate of Fe will depend on the nature of aerosols, vertical mixing, biological uptake and scavenging
4 processes (Bonnet and Guieu, 2006; Wuttig et al., 2013). During GEOVIDE, MOW was observed from stations 1 to 29
5 between 1000 and 1200 m depth and associated with high dissolved aluminium (DAL, Menzel Barraqueta et al., 2018)
6 concentrations (up to 38.7 nmol L⁻¹), confirming the high atmospheric deposition in the Mediterranean region. In contrast to
7 Al, no DFe signature was associated with MOW (Figs. 2 and 3). This feature was also reported in some studies (Hatta et al.,
8 2015; Thuróczy et al., 2010), while others measured higher DFe concentrations in MOW (Gerringa et al., 2017; Sarthou et al.,
9 2007). However, MOW coincides with the maximum Apparent Oxygen Utilization (AOU) and it is not possible to distinguish
10 the MOW signal from the remineralisation one (Sarthou et al., 2007). On the other hand, differences between studies are likely
11 originating from the intensity of atmospheric deposition and the nature of aerosols. Indeed, Wagener et al. (2010) highlighted
12 that large dust deposition events can accelerate the export of Fe from the water column through scavenging. As a result, in
13 seawater with high DFe concentrations and where high dust deposition occurs, a strong individual dust deposition event could
14 act as a sink for DFe. It thus becomes less evident to observe a systematic high DFe signature in MOW despite dust inputs. ▽

15 4.2.3 Fe enrichment in Labrador Sea Water (LSW)

16 As described in Section 3.1, the LSW exhibited increasing DFe concentrations from its source area, the Labrador Sea, toward
17 the other basins with the highest DFe concentrations observed within the Irminger Sea, suggesting that the water mass was
18 enriched in DFe either locally in each basin or during its flow path (see supplementary material Fig. S3). These DFe sources
19 could originate from a combination of high export of PFe and its remineralisation in the mesopelagic area and/or the dissolution
20 of sediment.

21 The Irminger and Labrador Seas exhibited the highest averaged integrated TChl-a concentrations (98 ± 32 mg m⁻² and 59 ± 42
22 mg m⁻²) compared to the West European and Iceland Basins (39 ± 10 mg m⁻² and 53 ± 16 mg m⁻²), when the influence of
23 margins was discarded. Stations located in the Irminger (stations 40-56) and Labrador (stations 63-77) Seas, were largely
24 dominated by diatoms (>50% of phytoplankton abundances) and displayed the highest chlorophyllid-a concentrations, a tracer
25 of senescent diatom cells, likely reflecting post-bloom condition (Tonnard et al., in prep.). This is in line with the highest POC
26 export data reported by Lemaitre et al. (2018) in these two oceanic basins. This likely suggests that biogenic PFe export was
27 also higher in the Labrador and Irminger Seas than in the West European and Iceland Basins. In addition, Gourain et al. (2018)
28 highlighted a higher biogenic contribution for particles located in the Irminger and Labrador Seas with relatively high PFe:PAI
29 ratios (0.44 ± 0.12 mol:mol and 0.38 ± 0.10 mol:mol, respectively) compared to particles from the West European and Iceland
30 Basins (0.22 ± 0.10 and 0.38 ± 0.14 mol:mol, respectively, see Fig. 6 in Gourain et al., 2018). However, they reported no
31 difference in PFe concentrations between the four oceanic basins (see Fig. 12A in Gourain et al., 2018) when the influence of
32 margins was discarded, which likely highlighted the remineralisation of PFe within the Irminger and Labrador Seas. Indeed,
33 Lemaitre et al. (2017) reported higher remineralisation rates within the Labrador (up to 13 mmol C m⁻² d⁻¹) and Irminger Seas

Moved (insertion) [2]

Moved up [2]: During our study the MOW signal was clearly observed on dissolved aluminium (DAL, Menzel Barraqueta et al., 2018) with the highest DAL values from the section (up to 38.7 nmol L⁻¹), suggesting intense dust deposition inputs to the Mediterranean Sea.

Deleted: ¶

Despite these high atmospheric depositions into the Mediterranean Sea providing Fe enrichment of Mediterranean waters and the high Apparent Oxygen Utilization (AOU), during the GEOVIDE voyage, no particular DFe signature was associated with the MOW (Figs. 2 and 4), Gourain et al., submitted Gourain et al. (submitted)

Deleted: which was also the case in other studies in the same area (Hatta et al., 2015; Thuróczy et al., 2010). During our study the MOW signal was clearly observed on dissolved aluminium (DAL, Menzel Barraqueta et al., 2018) with the highest DAL values from the section (up to 38.7 nmol L⁻¹), suggesting intense dust deposition inputs to the Mediterranean Sea. Conversely, Gerringa et al. (2017) and Sarthou et al. (2007) observed higher DFe concentrations in the MOW. During our study the MOW signal was clearly observed on dissolved aluminium (DAL, Menzel Barraqueta et al., 2018) with the highest DAL values from the section (up to 38.7 nmol L⁻¹), suggesting intense dust deposition inputs to the Mediterranean Sea. A concurring phenomenon, suggested by Wagener et al. (2010), is likely to explain this absence of MOW DFe signature. They pointed to the fact that large dust deposition events can accelerate the export of Fe from the water column through scavenging. As a result, in seawater with high DFe and where high dust deposition occurs, a strong individual dust deposition event could act as a sink for DFe.

Deleted: the

Deleted: The same explanation was reported by Gerringa et al. (2017) to account for the decrease in DFe concentrations between surface and deep waters from the Western Mediterranean Basin.

Deleted: 1

Deleted: Fe enrichment

Deleted: local sources of DFe

Deleted: may occur along

Deleted: Fig. 7

Formatted: Superscript

Formatted: Superscript

Deleted: Gourain et al. (subm.)

1 (up to 10 mmol C m⁻² d⁻¹) using the excess barium proxy (Dehairs et al., 1997), compared to the West European and Iceland
2 Basins (ranging from 4 to 6 mmol C m⁻² d⁻¹). Therefore, the intense remineralisation rates measured in the Irminger and
3 Labrador Seas likely resulted in enhanced DFe concentrations within LSW.
4 Higher DFe concentrations were, however, measured in the Irminger Sea compared to the Labrador Sea and coincided with
5 lower transmissometry values (i.e. 98.0-98.5% vs. >99%), thus suggesting a particle load of the LSW. This could be explained
6 by the reductive dissolution of Newfoundland Margin sediments. Indeed, Lambelet et al. (2016) reported high dissolved
7 neodymium (Nd) concentrations (up to 18.5 pmol.kg⁻¹) within the LSW at the edge of the Newfoundland Margin (45.73°W,
8 51.82°N) as well as slightly lower Nd isotopic ratio values relative to those observed in the Irminger Sea. They suggested that
9 this water mass had been in contact with sediments approximately within the last 30 years (Charette et al., 2015). Similarly,
10 during GA03, Hatta et al. (2015) attributed the high DFe concentrations in the LSW to continental margin sediments.
11 Consequently, it is also possible that the elevated DFe concentrations from the three LSW branches which entered the West
12 European and Iceland Basins and Irminger Sea was supplied through sediment dissolution (Measures et al., 2013) along the
13 LSW pathway.
14 The enhanced DFe concentrations measured in the Irminger Sea and within the LSW were thus likely attributed to the
15 combination of higher productivity, POC export and remineralisation as well as a DFe supply from reductive dissolution of
16 Newfoundland sediments to the LSW along its flow path.

17 4.2.4 Enhanced DFe concentrations in the Irminger Sea bottom water.

18 Bottom waters from the Irminger Sea exhibited the highest DFe concentrations from the whole section, excluding the stations
19 at the margins. Such a feature could be due to i) vertical diffusion from local sediment, ii) lateral advection of water mass(es)
20 displaying enhanced DFe concentrations, and iii) local dissolution of Fe from particles. Hereafter, we discuss the plausibility
21 of these three hypotheses to occur.

22 The GEOTRACES GA02 voyage (leg 1, 64PE319) which occurred in April-May 2010 from Iceland to Bermuda sampled two
23 stations north and south of our station 44 (~ 38.95°W, 59.62°N); station 5 (~ 37.91°W, 60.43°N) and 6 (~ 39.71°W, 58.60°N),
24 respectively. High DFe concentrations in samples collected close to the bottom were also observed and attributed to sediment
25 inputs highlighting boundary exchange between seawater and surface sediment (Lambelet et al., 2016; Rijkenberg et al., 2014).
26 However, because a decrease in DFe concentrations was observed at our station 44 from 2500 m depth down to the bottom
27 (Fig. 3, see supplementary material Fig. S4 and Table S2), it appeared to be unlikely that these high DFe concentrations will
28 be the result of sediment inputs, as no DFe gradient from the deepest samples to those above was observed.

29 Looking at salinity versus depth for these three stations, one can observe the intrusion of Polar Intermediate Water (PIW) at
30 station 44 from GEOVIDE, which was not observed during the GA02 voyage and which contributed to about 14% of the water
31 mass composition (García-Ibáñez et al., this issue) and might therefore be responsible for the high DFe concentrations (see
32 supplementary material Fig. S5A). On the other hand, the PIW was also observed at station 49 (from 390 to 1240 m depth),
33 60 (from 440 to 1290 m depth), 63 (from 20 to 1540 m depth), 68 (3340 m depth), 69 (from 3200 to 3440 m depth), 71 (from

Deleted: data

Deleted: Boyd and Ellwood (2010)Boyd et al., 2010Boyd and Ellwood, 2010

Deleted: Fonseca-Batista et al., subm.¶
Lambelet et al. (2016) reported high dissolved neodymium (Nd) concentrations (up to 18.5 pmol.kg⁻¹) within the LSW at the edge of the Newfoundland Margin (45.73°W, 51.82°N) as well as slightly lower Nd isotopic ratio values relative to the one observed in the Irminger Sea. They suggested that this water mass had been in contact with sediments approximately within the last 30 years (Charette et al., 2015). Similarly, during GA03, Hatta et al. (2015) attributed the high DFe concentrations in the LSW to continental margin sediments. Consequently, it is also possible that the elevated DFe concentrations from the three LSW branches which entered the West European and Iceland Basins and Irminger Sea was supplied through sediment dissolution (Measures et al., 2013) along the LSW pathway.¶

Lemaître et al. (2017) reported highest remineralization rates within the Labrador and Irminger Seas Dehairs et al., 1997 where high carbon production rates were observed earlier in the season and were attributed to diatoms (>50% of phytoplankton abundances, Tonnard et al., in prep.). In the Labrador Sea, Lemaître et al. (2017) hypothesized that the important convection of the LSW enabled the deepening of the mesopelagic layer allowing these intense remineralization rates coinciding with the LSW in both basins. Gourain et al. (subm.) measured relatively high PFe:PAI ratios (0.39 ± 0.08 mol mol⁻¹) in the LSW from the Irminger and Labrador Seas which could point to a more biogenic PFe contribution. ¶
Remineralization occurred in both the Labrador and Irminger Seas with slightly higher rates in the former (Lemaître et al., 2017). Conspicuous DFe concentrations were, however, observed in the Irminger Sea. This could be explained by the reductive dissolution of Newfoundland Margin sediments. Nevertheless, remineralization of organic matter likely plays an additional role in the observed high DFe concentrations from the Irminger Sea through bacteria-mediated ligand production (Boyd and Ellwood, 2010) helping the DFe supply from reductive dissolution of Newfoundland sediments to the LSW to remain in solution. ¶

Deleted: 1

Deleted: Bottom Water

Deleted: DFe concentrations

Deleted: above

Deleted: inputs

Deleted: intrusion

Deleted: of an Fe-rich

Deleted:

Deleted: above the seafloor

Deleted: 4

Deleted: 3

Deleted: the above ones

Deleted: the

Deleted: GA01

Deleted: 8

1 2950 to 3440 m depth) and 77 (60 and 2500 m depth) with similar or higher contributions of the PIW without such high DFe
2 concentrations (maximum DFe = 1.3 ± 0.1 nmol L⁻¹, 1240 m depth at station 49). However, considering the short residence
3 time of DFe and the circulation of water masses in the Irminger Sea, it is possible that instead of being attributed to one specific
4 water mass, these enhanced DFe concentrations resulted from lateral advection of the deep waters. Figure S5B) shows the
5 concentrations of both DFe and PFe for the mixing line between DSOW/PIW and ISOW at station 44 and considering 100%
6 contribution of ISOW for the shallowest sample (2218 m depth) and of DSOW/PIW for the deepest (2915 m depth), as these
7 were the main water masses. This figure shows increasing DFe concentrations as DSOW/PIW mixed with ISOW. In addition,
8 Le Roy et al. (2018) reported for the GEOVIDE voyage at station 44 a deviation from the conservative behaviour of ²²⁶Ra
9 reflecting an input of this tracer centred at 2500 m depth, likely highlighting diffusion from deep-sea sediments and coinciding
10 with the highest DFe concentrations measured at this station. Although the transmissometry data were lower at the sediment
11 interface than at 2500 m depth. Deng et al. (2018) reported a stronger scavenged component of the ²³⁰Th at the same depth
12 range, likely suggesting that the mixture of water masses were in contact with highly reactive particles. If there is evidence
13 that the enhanced DFe concentrations observed at station 44 coincided with lateral advection of water masses that were in
14 contact with particles, the difference of behaviour between DFe and ²³⁰Th remains unsolved. The only parameter that would
15 explain without any ambiguity such differences of behaviour between DFe and ²³⁰Th would be the amount of Fe-binding
16 organic ligands for these samples. Indeed, although PFe concentrations decreased from the seafloor to the above seawater, this
17 trend would likely be explained by a strong vertical diffusion alone and not necessarily by the dissolution of particles that were
18 laterally advected.

19 Therefore, the high DFe concentrations observed might be inferred from local processes as ISOW mixes with both PIW and
20 DSOW with a substantial load of Fe-rich particles that might have dissolved in solution due to Fe-binding organic ligands.

21 4.2.5 Reykjanes Ridge: Hydrothermal inputs or Fe-rich seawater?

22 Hydrothermal activity was assessed over the Mid Atlantic Ridge, namely the Reykjanes Ridge, from stations 36 to 40. Indeed,
23 within the interridge database (<http://www.interridge.org>), the Reykjanes Ridge is reported to have active hydrothermal sites.
24 The sites were either confirmed (Baker and German, 2004a; German et al., 1994; Olafsson et al., 1991; Palmer et al., 1995)
25 close to Iceland or inferred (e.g. Chen, 2003; Crane et al., 1997; German et al., 1994; Sinha et al., 1997; Smallwood and White,
26 1998) closer to the GEOVIDE section as no plume was detected but a high backscatter was reported potentially corresponding
27 to a lava flow. Therefore, hydrothermal activity at the sampling sites remains unclear with no elevated DFe concentrations nor
28 temperature anomaly above the ridge (station 38). However, enhanced DFe concentrations (up to 1.5 ± 0.22 nmol L⁻¹, station
29 36, 2200 m depth) were measured east of the Reykjanes Ridge (Fig. 3). This could be due to hydrothermal activity and
30 resuspension of sunken particles at sites located North of the section and transported through the ISOW towards the section
31 (see supplementary material Fig. S3). Indeed, Achterberg et al. (2018) highlighted at ~60°N and over the Reykjanes Ridge a
32 southward lateral transport of an Fe plume of up to 250-300 km. In agreement with these observations, previous studies (e.g.
33 Fagel et al., 1996; Fagel et al., 2001; Lackschewitz et al., 1996; Parra et al., 1985) reported marine sediment mineral clays in

Formatted: Superscript

Formatted: Superscript

Deleted: s

Deleted: Le Roy et al., 2018

Deleted: ¶

Figure 8B) also shows the concentrations of both DFe and PFe for the mixing line between DSOW/PIW and ISOW at station 44 and considering 100% of contribution from these seawater at the deepest (2915 m depth) and the shallowest (2218 m depth) samples, respectively, as these were the main water masses. This figure shows an exponential decrease of PFe concentrations as the DSOW/PIW mixed with the ISOW (Gourain et al., subm.). Concomitantly, DFe concentrations followed a polynomial distribution with a theoretical DFe maxima of 2.6 nmol L⁻¹ at 51.5% contribution of the ISOW (48.5% of the DSOW/PIW) and corresponding to a theoretical PFe concentration of ~7.0 nmol L⁻¹. It is possible that as the ISOW mixed with the Fe-rich particles from the DSOW/PIW, DFe concentrations increased until PFe concentrations reached 7.0 nmol L⁻¹ after which the amounts of particles tended to scavenge Fe.

Deleted: dissolvable

Deleted: which

Deleted: might be sustained

Deleted: by

Deleted: 1

Deleted: High DFe concentrations (up to 1.5 ± 0.22 nmol L⁻¹, station 36, 2200 m depth) were measured east of the Reykjanes Ridge (Fig. 4)

Deleted: W

Deleted: , based on a literature review on existing vent-field databases, and on unpublished sources, ~280 sites of active hydrothermal venting on spreading ridges, volcanic arcs and intraplate volcanoes were reported

Deleted: . In this database

Deleted: inferred

Deleted: that

Deleted: Several studies on hydrothermal activity at Reykjanes Ridge have been conducted (e.g. Chen, 2003; German et al., 1994; Sinha et al., 1997; Smallwood and White, 1998) but it

Deleted: ed

Deleted: , as

Deleted: high

Deleted: were observed

Deleted: According to the water mass circulation, if there was an active hydrothermal vent located on the Reykjanes Ridge, the only possibility to observe a signal would occur from a southward transfer of this signal through the ISOW in the Iceland Basin. Interestingly

1 the Iceland Basin largely dominated by smectite (> 60%), a tracer of hydrothermal alteration of basaltic volcanic materials
 2 (Fagel et al., 2001; Tréguer and De La Rocha, 2013). Hence, the high DFe concentrations measured east of the Reykjanes
 3 Ridge could be due to a hydrothermal source and/or the resuspension of particles and their subsequent dissolution,
 4 West of the Reykjanes Ridge, a DFe enrichment was also observed in ISOW within the Irminger Sea (Figs. 4 and 7). The low
 5 transmissometer values within ISOW in the Irminger Sea compared to the Iceland Basin suggest a particle load. These particles
 6 could come from the Charlie Gibbs Fracture Zone (CGFZ, 52.67°N and 34.61°W) and potentially Bight Fracture Zone (BFZ,
 7 56.91°N and 32.74°W) (Fig. 1) (Lackschewitz et al., 1996; Zou et al., 2017). Indeed, hydrographic sections of the northern
 8 valley of the CGFZ showed that below 2000 m depth the passage through the Mid-Atlantic Ridge was mainly filled with the
 9 ISOW (Kissel et al., 2009; Shor et al., 1980). Shor et al. (1980) highlighted a total westward transport across the sill, below
 10 2000 m depth of about $2.4 \times 10^6 \text{ m}^3 \text{ s}^{-1}$ with ISOW carrying a significant load of suspended sediment ($25 \mu\text{g L}^{-1}$), including a
 11 100-m-thick benthic nepheloid layer. It thus appears that the increase in DFe within ISOW likely came from sediment
 12 resuspension and dissolution as the ISOW flows across CGFZ and BFZ.

13 4.3. What are the main sources of DFe in surface waters?

14 During GEOVIDE, enhanced DFe surface concentrations were observed at several stations (stations 1-4, 53, 61, 78)
 15 highlighting an external source of Fe to surface waters. The main sources able to deliver DFe to surface waters are riverine
 16 inputs, glacial inputs and atmospheric deposition. In the following sections, these potential sources of DFe in surface waters
 17 will be discussed.

18 4.3.1 Tagus riverine inputs

19 Enhanced DFe surface concentrations (up to $1.07 \pm 0.12 \text{ nmol L}^{-1}$) were measured over the Iberian Margin (stations 1-4) and
 20 coincided with salinity minima ($\sim <35$) and enhanced DAI concentrations (up to 31.8 nmol L^{-1} , Menzel Barraqueta et al.,
 21 2018). DFe and DAI concentrations were both significantly negatively correlated with salinity ($R^2 = -1$ and 0.94, respectively)
 22 from stations 1 to 13 (Fig. 5). Salinity profiles from station 1 to 4 showed evidence of a freshwater source with surface salinity
 23 ranging from 34.95 (station 1) to 35.03 (station 4). Within this area, only two freshwater sources were possible: 1) wet
 24 atmospheric deposition (4 rain events, Shelley, pers. comm.) and 2) the Tagus River, since the ship SADCP data revealed a
 25 northward circulation (P. Lherminier and P. Zunino, Ifremer Brest, pers. comm.). Our SML DFe inventories were about three
 26 times higher at station 1 ($\sim 1 \text{ nmol L}^{-1}$) than those calculated during the GA03 voyage ($\sim 0.3 \text{ nmol L}^{-1}$, station 1) during which
 27 atmospheric deposition were about one order of magnitude higher (Shelley et al., 2018; Shelley et al., 2015). the atmospheric
 28 source seemed to be minor. Consequently, the Tagus River appears as the most likely source responsible for these enhanced
 29 DFe concentrations, either as direct input of DFe or indirectly through Fe-rich sediment carried by the Tagus River and their
 30 subsequent dissolution. The Tagus estuary is the largest in the western European coast and very industrialized (Canário et al.,
 31 2003; de Barros, 1986; Figueres et al., 1985; Gaudencio et al., 1991; Mil-Homens et al., 2009), extends through an area of 320
 32 km² and is characterized by a large water flow of $15.5 \times 10^9 \text{ m}^3 \text{ y}^{-1}$ (Fiuza, 1984). Many types of industry (e.g. heavy metallurgy,

- Deleted: Lackschewitz et al., 1996.
- Deleted: as previously suggested by Achterberg et al. (2018) w(
- Deleted: While hydrothermalism may explain the enrichment ca
- Deleted:
- Deleted: th
- Deleted: e
- Deleted:
- Moved up [3]: Moreover, higher transmissometer values within
- Moved (insertion) [3]
- Deleted: may come from other sources. An intriguing phenome
- Deleted: 2
- Deleted: M
- Deleted: A01
- Deleted: the
- Deleted: 2
- Deleted: low
- Deleted: ies
- Deleted: .3
- Deleted: 9
- Deleted: ier
- Deleted: et al.,
- Deleted:
- Formatted
- Formatted
- Field Code Changed
- Formatted
- Deleted: However, DFe:DAI ratios were very low (0.036 ± 0.00
- Formatted
- Formatted
- Formatted
- Deleted: which were indicative of a minor
- Formatted
- Formatted
- Formatted
- Formatted
- Deleted: for those stations
- Formatted
- Formatted
- Deleted: T
- Formatted

1 ore processing, chemical industry) release metals including Fe, which therefore result in high levels recorded in surface
2 sediments, suspended particulate matter, water and organisms in the lower estuary (Santos-Echeandia et al., 2010).

3 4.3.2 High latitude, meteoric water and sea-ice processes

4 Potential sources of Fe at stations 53, 61 and 78 include meteoric water (MW, referring to precipitation, runoff and continental
5 glacial melt), sea-ice melt (SIM), seawater interaction with shallow sediments and advection of water transported from the
6 Arctic sourced by the Fe-rich TransPolar Drift (TPD, Klunder et al. (2012); see supplementary material Fig. S4 and Table S2).
7 The vertical profiles of both potential temperature and salinity in the Greenland and Newfoundland Margins (station 53, 61
8 and 78, Fig. 4D, E) and F)) highlighted the influence of fresh waters originating from the Arctic Ocean to separate surface
9 and deeper samples at ~ 60 m (station 53) and ~ 40 m (stations 61 and 78) depth. The presence of this freshwater lens suggests
10 that sediment derived enrichment to these surface waters was unlikely. The most plausible sources would be freshwater induced
11 by meteoric water and sea-ice melt. Deeper in the water column, net brine release were observed at stations 53 (below 40 m
12 depth, Fig. 4D) 61 (in the whole water column, Fig. 4E) and 78 (below 30 m depth, Fig. 4F). The release of brines could
13 originate from two different processes: the sea-ice formation or the early melting of multiyear sea ice due to gravitational
14 drainage and subsequent brine release (Petrich and Eicken, 2010; Wadhams, 2000). Indeed, during the winter preceding the
15 GEOVIDE voyage, multiyear sea ice extended 200 km far from our Greenland stations (<http://nsidc.org/arcticseaicenews/>). In
16 the following sections, we discuss the potential for meteoric water supply, sea-ice formation and sea-ice melting to affect DFe
17 distribution.

18 4.3.2.1 The Greenland shelf

19 Considering the sampling period at stations 53 (16 June 2014) and 61 (19 June 2014), sea-ice formation is unlikely to happen
20 as this period coincides with summer melting in both the Central Arctic and East Greenland (Markus et al., 2009). However,
21 it is possible that the brines observed in our study could originate from sea-ice formation, which occurred during the previous
22 winter(s) at 66°N (and/or higher latitudes). The residence time can vary from days (von Appen et al., 2014) to 6-9 months
23 (Sutherland et al., 2009). Due to our observed strong brine signal at station 61 we suggest that the residence time was potentially
24 longer than average. Given that the brine signal was higher at station 61 than at station 53 (which was located upstream in the
25 EGC), we suggest that station 53 was exhibiting a freshening as a result of the transition between the freezing period toward
26 the melting period. This would result in a dilution of the brine signal at the upstream station. Consequently, the salinity of this
27 brine signal may reflect sea ice formation versus melting which may have an effect on the trace metal concentration within
28 this water (Hunke et al., 2011). The associated brine water at station 61 (100 m depth) was slightly depleted in both DFe and
29 PFe₂, which may be attributed to sea ice formation processes. Indeed, Janssens et al. (2016) highlighted that as soon as sea ice
30 forms, sea salts are efficiently flushed out of the ice while PFe is trapped within the crystal matrix and DFe accumulates,
31 leading to an enrichment factor of these two Fe fractions compared to underlying seawater. Conversely, the brine signal
32 observed at station 53 (100 m depth) showed slight enrichment in DFe, which may be attributed to brine release during early
33

Formatted

Deleted: Many types of industry (e.g. heavy metallurgy, ore processing, chemical industry, petroleum refinery, shipbuilding, chlor-alkali industry, a smelter and a pyrite roasting plant) release heavy metals such as lead (Pb, Carvalho, 1995), mercury (Hg, Canario, 2000; Ferreira, 1997; Figueres et al., 1985), arsenic (As, Andreae et al., 1983), or other trace metals (Cd, Cu, Ni, Zn, Cotté-Krief et al., 2000) into the river which therefore result in high levels of these elements recorded in surface sediments, suspended particulate matter, water and organisms in the lower estuary. Santos-Echeandia et al. (2010) reported that sediments, pore water and belowground biomass colonised by salt marsh plants from the Tagus estuary contained high concentrations of Fe, Mn, Zn, Cu, Pb and Cd which were exported to the water column as a result of tidal inundation. Similar discharge processes releasing large amount of DFe from creeks draining coastal wetland to the ocean have also been reported by Sanders et al. (2015). Consequently, the enhanced DFe concentrations observed above the Iberian Margin likely originated from the Tagus River, wet atmospheric deposition playing a minor additional source

Formatted

Field Code Changed

Deleted: 2

Deleted: s

Deleted: 3...2). The vertical profiles of both potential temperature and salinity in the Greenland and Newfoundland Margins (station 53, 61 and 78, Fig. 45...D, E) and F)) highlighted the influence of fresh and cold waters originating from the Arctic Ocean to separate and deeper samples at ~ 60 m (station 53) and ~ 40 m (stations 61 and 78) depth. The presence of this front freshwater lens suggests that sediment derived enrichment to these surface waters was unlikely. The most plausible sources would be freshwater induced by meteoric water and sea-ice melt. Deeper in the water column, net brine release were observed at stations 53 (below 40 m depth, Fig. 4D) 61 (in the whole water column, Fig. 4E) and 78 (below 30 m depth, Fig. 4F). The release of brines could originate from two different processes: the sea-ice formation or the early melting of multiyear sea ice due to gravitational drainage and subsequent brine release (Petrich and Eicken, 2010; Wadhams, 2000). Indeed, during the winter preceding the GEOVIDE voyage, multiyear sea ice extended glacial sources with multi-year sea-ice (which extended...as close as ...00 km far from our Greenland stations)

Formatted: Not Highlight

Deleted: and land ice sheet.

Formatted: Highlight

Deleted: SIM and MW contributions were determined for stations 53, 61 and 78, with mass balance calculations based on the end-members presented in Benetti et al. (2016). For stations over the

Moved (insertion) [5]

Moved up [5]: In Figure 5 D, E) and F), negative sea-ice fractions indicated a net brine release while positive sea-ice fractions indicated a net sea-ice melting.

Deleted: In Figure 5 D, E) and F), negative sea-ice fractions indicated a net brine release while positive sea-ice fractions indicated a net sea-ice melting. It appears that the highest brine

1 sea ice melting and the associated release of DFe into the underlying water column as the brine sinks until reaching neutral
2 buoyancy due to higher density.

3 Surface waters (from 0 to ~100 m depth) from station 53 and 61 were characterized by high MW fractions (ranging from 8.3
4 to 7.4% and from 7.7 to 7.3%, respectively, from surface to ~100 m depth, Figs. 5D and E). These high MW fractions were
5 both enriched in PFe and DFe (except station 53 for which no data was available close to the surface) compared to seawater
6 located below 50 m depth, thus suggesting a MW source. These results are in line with previous observations, which
7 highlighted strong inputs of DFe from a meteoric water melting source in Antarctica (Annett et al., 2015). Although the ability
8 of MW from Greenland Ice Sheet and runoffs to deliver DFe and PFe to surrounding waters has previously been demonstrated
9 (Bhatia et al., 2013; Hawkings et al., 2014; Schroth et al., 2014; Statham et al., 2008), both Fe fractions were lower at the
10 sample closest to the surface, then reached a maximum at ~50 m depth and decreased at ~70 m depth, for station 61 (Fig.
11 4D). The surface DFe depletion was likely explained by phytoplankton uptake, as indicated by the high TChl-*a* concentrations
12 (up to 6.6 mg m⁻³) measured from surface to about 40 m depth, drastically decreasing at ~50 m depth to 3.9 mg m⁻³ (Fig. 4D).
13 Hence, it seemed that meteoric water inputs from the Greenland Margin likely fertilized surface waters with DFe, enabling the
14 phytoplankton bloom to subsist. The profile of PFe can be explained by two opposite plausible hypotheses: 1) MW inputs did
15 not release PFe, as if it was the case, one should expect higher PFe concentrations at the surface (~25 m depth) than the one
16 measured at 50 m depth due to both the release from MW and the assimilation of DFe by phytoplankton 2) MW inputs can
17 release PFe in a form that is directly accessible to phytoplankton with subsequent export of PFe as phytoplankton died. The
18 latter solution explains the PFe maximum measured at ~50 m depth and is thus the most plausible.

19 4.3.2.2 The Newfoundland shelf

20 Newfoundland shelf waters (station 78) were characterized by high MW fractions (up to 7%), decreasing from surface to 200
21 m depth (~2%). These waters were associated with a net sea-ice melting signal from the near surface to ~10 m depth followed
22 by a brine release signal down to 200 m depth with the maximum contribution measured at ~30 m depth. Within the surface
23 waters (above 20 m depth), no elevation in DFe, DA1 nor PFe was noticed despite the low measured TChl-*a* concentrations
24 (TChl-*a* ~ 0.20 mg m⁻³). This suggests that none of these inputs (sea-ice melting and meteoric water) were able to deliver DFe
25 or that these inputs were minor compared to sediment inputs from the Newfoundland Margin. Surprisingly, the highest TChl-*a*
26 biomass (TChl-*a* > 9 mg m⁻³) from the whole section was measured at 30 m depth corresponding to the strongest brine release
27 signal. This either suggests that the brine likely contained important amounts of Fe (dissolved and/or particulate Fe) that were
28 readily available for phytoplankton and consumed at the sampling period by potentially sea-ice algae themselves (Riebesell et
29 al., 1991) or that another nutrient was triggering the phytoplankton bloom.

30 4.3.3 Atmospheric deposition

31 On a regional scale, the North Atlantic basin receives the largest amount of atmospheric inputs due to its proximity to the
32 Saharan Desert (Jickells et al., 2005), yet even in this region of high atmospheric deposition, inputs are not evenly distributed.

Deleted: sea

Deleted: .

Deleted: 5

Deleted: 4

Deleted: 5

Deleted: with sea-ice melting contribution (1.5% at 4 m depth) for station 53 and low contribution (0.6%) from brine release at the surface, linearly increasing with depth (1.3% at 50 m depth and 2.2% at 100 m depth).

Deleted: Station 53, exhibited enhanced PFe concentrations (19 nmol L⁻¹, 25 m depth) at the surface. The corresponding DFe sample was lost and therefore no information was available. Conversely,

Deleted: .

Deleted: t

Deleted: These results are in agreement with the capacity of MW from Greenland Ice Sheet and runoffs to deliver DFe and PFe to surrounding waters (Bhatia et al., 2013; Hawkings et al., 2014; Schroth et al., 2014; Statham et al., 2008).

Deleted: These results are also in line with previous observations which highlighted strong inputs of DFe from a meteoric water melting source in Antarctica (Annett et al., 2015), with DFe:DA1 ratios up to 1.6 mol mol⁻¹; Hawkings et al., 2014), noting that our DFe:DA1 ratios from a MW source were 3 to 5 times lower than the one observed by Annett et al. (2015). These differences were likely explained by the sampling period and the stage of phytoplankton bloom development in our study. ¶

Deleted:

Deleted: Tonnard et al., in prep. Sarthou et al., 2018; Tonnard et al., in prep.. If such was the case, then a PFe maximum should be noticed at the same depth. However, it should be noted that TChl-*a* and δ¹⁸O samples were collected about four hours prior to sampling for DFe and PFe. Therefore, it is more likely that by the time DFe and PFe samples were collected, the PFe was exported deeper in the water column. Indeed, Krembs et al. (2002) highlighted the presence of exopolymeric substances (EPS) in sea ice. Such compounds were reported to undergo fast aggregation (minutes to hours) from the colloidal to the particulate phase (i.e. Transparent Exopolymer Particles, TEP) (e.g. Baalousha et al., 2006; Verdugo et al., 2004) taking in-depth other particulate material as they sank.

Deleted: 2

1 Indeed, aerosol Fe loading measured during GEOVIDE (Shelley et al., 2017) were much lower (up to four orders of magnitude)
2 than those measured during studies from lower latitudes in the North Atlantic (e.g. Baker et al., 2013; Buck et al., 2010; and
3 for GA03, Shelley et al., 2015), but atmospheric inputs could still be an important source of Fe to surface waters in areas far
4 from land.

5 In an attempt to estimate whether there was enough atmospheric input to sustain the SML DFe concentrations, we calculated
6 Turnover Times relative to Atmospheric Deposition (TTADs, Guieu et al., 2014). To do so, we made the following
7 assumptions: 1) the aerosol concentrations are a snapshot in time but are representative of the study region, 2) the aerosol
8 solubility estimates based on two sequential leaches are an upper limit of the aerosol Fe in seawater and 3) the water column
9 stratified just before the deposition of atmospheric inputs, so MLD DFe will reflect inputs from above. Thus, the TTADs were
10 defined as the integrated DFe concentrations in the SML for each station divided by the contribution of soluble Fe contained
11 in aerosols averaged per basin to the water volume of the SML. Although, TTADs were lower in the West European and
12 Iceland Basins with an average of $\sim 9 \pm 3$ months compared to other basins (7 ± 2 years and 5 ± 2 years for the Irminger and
13 Labrador Seas, respectively) (Fig. 6) they were about three times higher than those reported for areas impacted by Saharan
14 dust inputs (~ 3 months, Guieu et al., 2014). Therefore, the high TTADs measured in the Irminger and Labrador Seas and
15 ranging from 2 to 15 years provided further evidence that atmospheric deposition were unlikely to supply Fe in sufficient
16 quantity to be the main source of DFe (see Sections 4.2.1 and 4.3.2) while in the West European and Iceland Basins they
17 played an additional source, perhaps the main source of Fe especially at station 36 which displayed TTAD of 3 months.

18 4.4 Sediment input

19 4.4.1 Margins:

20 DFe concentration profiles from all coastal stations (stations 2, 4, 53, 56, 61 and 78) are reported in Figure 4. To avoid surface
21 processes, only depths below 100 m depth will be considered in the following discussion. DFe and PFe followed a similar
22 pattern at stations 2, 53, 56, and 78 with increasing concentrations towards the sediment, suggesting that either the sources of
23 Fe supplied both Fe fractions (dissolved and particulate) or that PFe dissolution from sediments supplied DFe. Among the
24 different margins, the Newfoundland Margin exhibited the highest deep-water DFe concentrations. Conversely, stations 4 and
25 61 exhibited a decrease in DFe concentrations at the closest samples to the seafloor whereas PFe increased. DFe:PFe ratios
26 ranged from 0.01 (station 2, bottom sample) to 0.27 (station 4, ~ 400 m depth) $\text{mol} \cdot \text{mol}^{-1}$ with an average value of 0.11 ± 0.07
27 $\text{mol} \cdot \text{mol}^{-1}$ ($n = 23$, Table 3), highlighting a different behaviour of Fe among margins. This could be explained by the different
28 nature of the sediments and/or different sediment conditions (e.g. redox, organic content). Based on particulate and dissolved
29 Fe and dissolved Al data (Gourain et al., 2018; Menzel Barraqueta et al., 2018, Table 3), three main different types of margins
30 were reported (Gourain et al., 2018) with the highest lithogenic contribution observed at the Iberian Margin (stations 2 and 4)
31 and the highest biogenic contribution at the Newfoundland Margin (station 78). These observations are consistent with higher
32 TChl-*a* concentrations measured at the Newfoundland Margin and to a lesser extent at the Greenland Margin and the
33 predominance of diatoms relative to other functional phytoplankton classes at both margins (Tonnard et al., in prep.). To sum

Deleted: in the North Atlantic, two areas can be separated: from ~ 5 to 30°N which receives the vast majority of mineral dust from the Saharan outflow, and north of $\sim 30^\circ\text{N}$, which is frequently (but not always) outside of the influence of the atmospheric transport of dust from North African dust source regions and where atmospheric inputs are more likely to contain a higher proportion of anthropogenic aerosols (from Europe and North America) and high latitude sources in Iceland and Greenland, and occasionally volcanic sources (Achterberg et al., 2013; Bullard et al., 2016; Jickells and Moore, 2015). This division in atmospheric inputs was reflected in the aerosol Fe loading observed during GA01 (Shelley et al., 2017b) which were much lower (up to four orders of magnitude) than those measured during studies from lower latitudes in the North Atlantic (e.g. Baker et al., 2013; Buck et al., 2010; and for GA03, Shelley et al., 2015), but atmospheric inputs could still be an important source of Fe in areas far from land. During GA01, 18 aerosol samples were collected roughly every 48 h (Shelley et al., 2017a; 2017b). Shelley et al. (2017a; 2017b) used a combination of air mass back trajectories (five-day simulation period), aerosol trace element concentrations, elemental ratios and multivariate statistics to broadly group the aerosol samples by their dominant, but not mutually-exclusive, source(s). Using this approach, the GA01 transect can be split into four sections. Shelley et al. (2017b) These are those predominantly influenced by: (1) atmospheric inputs from sources in Iceland and Greenland which likely include proglacial till (stations 11-29), (2) (...)

Formatted: Font: 12 pt

Deleted: compare the integrated SML DFe concentrations for ea (...)

Deleted: To do so, we made the following assumptions: 1) the (...)

Deleted: s

Deleted: might be

Deleted: 2

Deleted: . However, atmospheric deposition could potentially ha (...)

Deleted: 3

Deleted: o

Deleted: 5

Deleted: Stations where

Deleted: followed a similar pattern are s

Deleted:

Deleted: -1

Deleted:

Deleted: -1

Deleted: between DFe

Deleted: and

Deleted: PFe and suggesting

Deleted: different composition of sediments between different (...)

Deleted: 4

Deleted: .

Deleted: The East (stations 53 and 56) and West (station 61) (...)

Deleted: the

1 up, the most biogenic sediments (Newfoundland Margin) were able to mobilise more Fe in the dissolved phase than the most
2 lithogenic sediments (Iberian Margin), in agreement with Boyd et al. (2010) who reported greater remineralization of PFe from
3 biogenic PFe than from lithogenic PFe based on field experiment and modelling simulations.

5 4.4.2 Nepheloid layers:

6 Samples associated with high levels of particles (transmissometer < 99%) and below 500 m depth displayed a huge variability
7 in DFe concentrations. From the entire dataset, 63 samples (~13% of the entire dataset) followed this criterion with 14 samples
8 from the West European Basin (station 1), 4 samples from the Iceland Basin (stations 29, 32, 36 and 38), 43 samples from the
9 Irminger Sea (stations 40, 42, 44, 49 and 60) and 2 samples from the Labrador Sea (station 69). To determine which parameter
10 was susceptible to explain the variation in DFe concentrations in these nepheloid layers, a Principal Component Analysis
11 (PCA) on these samples. The input variables of the PCA were the particulate Fe, Al, and particulate manganese (PMn) (Gourain
12 et al., 2018), the DAI (Menzel Barraqueta et al., 2018) and the Apparent Oxygen Utilization (AOU) and were all correlated to
13 DFe concentrations explaining all together 93% of the subset variance (see supplementary material Fig. S6). The first
14 dimension of the PCA was represented by the PAI, PFe and PMn concentrations and explained 59.5% of the variance, while
15 the second dimension was represented by the DAI and the AOU parameters, explaining 33.2% of the variance. The two sets
16 of variables were nearly at right angle from each other, indicating no correlation between them.

17 The variations in DFe concentrations measured in bottom samples from stations 32, 36 (Iceland Basin), 42 and 44 (Irminger
18 Sea) and 69 (Labrador Sea) were mainly explained by the first dimension of the PCA (see supplementary material Fig. S6).
19 Therefore, samples characterized by the lowest DFe concentrations (stations 32 and 69) were driven by particulate Al and Mn
20 concentrations and resulted in an enrichment of Fe within particles. These results are in agreement with previous studies
21 showing that the presence of Mn within particles can induce the formation of Fe-Mn oxides, contributing to the removal of Fe
22 and Mn from the water column (Kan et al., 2012; Teng et al., 2001).

23 Low DFe concentrations (bottom samples from stations 42 and 1) were linked to DAI inputs and associated with lower AOU
24 values. The release of Al has previously been observed from Fe and Mn oxide coatings on resuspended sediments under mildly
25 reducing conditions (Van Beusekom, 1988). Conversely, higher DFe concentrations were observed for stations 44 and 49 and
26 to a lesser extent station 60 coinciding with low DAI inputs and higher oxygen levels. This observation challenges the
27 traditional view of Fe oxidation with oxygen, either abiotically or microbially induced. Indeed, remineralisation can decrease
28 sediment oxygen concentrations, promoting reductive dissolution of PFe oxyhydroxides to DFe that can then diffuse across
29 the sediment water interface as DFe(II) colloids (Homoky et al., 2011). Such processes will inevitably lead to rapid Fe removal
30 through precipitation of nanoparticulate or colloidal Fe (oxyhydr)oxides, followed by aggregation or scavenging by larger
31 particles (Boyd and Ellwood, 2010; Lohan and Bruland, 2008) unless complexation with Fe-binding organic ligands occurs
32 (Batchelli et al., 2010; Gerringa et al., 2008). There exist, however, another process that is favoured in oxic benthic boundary
33 layers (BBL) with low organic matter degradation and/or low Fe oxides, which implies the dissolution of particles after
34 resuspension, namely the non-reductive dissolution of sediment (Homoky et al., 2013; Radic et al., 2011). In addition, these

Deleted: was performed on samples which exhibited a transmissometry lower than 99% and below 500 m depth to avoid surface processes.

Deleted: From the entire dataset, 66 samples (~13% of the entire dataset) respected this criterion with 3 samples from the Iberian Margin (station 4), 14 samples from the West European Basin (station 1), 4 samples from the Iceland Basin (stations 29, 32, 36 and 38), 43 samples from the Irminger Sea (stations 40, 42, 44, 49 and 60) and 2 samples from the Labrador Sea (station 69). T

Deleted: oxides

Deleted: O₂

Deleted: were the input variables of the PCA and explained ~93% of the subset

Deleted: Fig. 11

Deleted: O₂

Deleted: concentrations

Deleted: Fig. 11

Deleted: O₂

Deleted: oxide

Deleted: accelerates

Deleted: O₂

Deleted: concentrations

Deleted:

Deleted: which will inevitably leads to rapid Fe removal through precipitation of nanoparticulate or colloidal Fe (oxyhydr)oxides, followed by aggregation or scavenging by larger particles (Boyd and Ellwood, 2010; Lohan and Bruland, 2008). Liu and Millero, 2002 It is only when sufficient organic matter and more specifically organic ligands are present in solution, that these sediment-derived DFe can remain in solution in excess of its solubility through complexation (Kondo and Moffett, 2015; Noble et al., 2012) or in suspension as colloids or nanoparticles (Raiswell and Canfield, 2012). T

1 higher oxygenated samples were located within DSO_W, which mainly originate (75% of the overflow) from the Nordic Seas
2 and the Arctic Ocean (Tanhua et al., 2005), in which the ultimate source of Fe was reported by Klunder et al. (2012) to come
3 from Eurasian river waters. The major Arctic rivers were highlighted by Slagter et al. (2017) to be a source of Fe-binding
4 organic ligands that are then further transported via the TPD across the Denmark Strait. Hence, the enhanced DFe
5 concentrations measured within DSO_W might result from Fe-binding organic ligand complexation that were transported to the
6 deep ocean as DSO_W formed rather than the non-reductive dissolution of sediment.

7 4.5. How does biological activity modify DFe distribution?

8 Overall, almost all the stations from the GEOVIDE voyage displayed DFe minima in surface water associated with some
9 maxima of TChl-*a* (see supplementary material Fig. S1). In the following section, we specifically address the question of
10 whether DFe concentrations potentially limit phytoplankton growth. Note that macronutrients and DFe limitations relative to
11 phytoplankton functional classes are dealt in Tonnard et al. (in prep.).

12 A key determinant for assessing the significance of a DFe source is the magnitude of the DFe:macronutrient ratio supplied,
13 since this term determines to which extent DFe will be utilised. The DFe:NO₃⁻ ratios in surface waters varied from 0.02 (station
14 36) to 38.6 (station 61) mmol:mol⁻¹ with an average of 5 ± 10 mmol:mol⁻¹ (see supplementary material Fig. S7). Values were
15 typically equal or lower than 0.28 mmol mol⁻¹ in all basins except at the margins and at stations 11, 13, 68, 69 and 77. The low
16 nitrate concentrations observed at the eastern and western Greenland and Newfoundland Margins reflected a strong
17 phytoplankton bloom which had reduced the concentrations as highlighted by the elevated integrated TChl-*a* concentrations
18 ranging from 129.6 (station 78) to 398.3 (station 61) mg m⁻². At the Iberian Margin, they likely reflected the influence of the
19 N-limited Tagus River (stations 1, 2 and 4) with its low TChl-*a* integrated concentrations that ranged from 31.2 (station 1) to
20 46.4 (station 4) mg m⁻². The high DFe:NO₃⁻ ratios determined at those stations, which varied from 13.4 (station 78) to 38.6
21 (station 61) mmol:mol⁻¹, suggested that waters from these areas, despite having the lowest NO₃⁻ concentrations, were relatively
22 enriched in DFe compared to waters from Iceland Basin and Irminger Sea.

23 In our study, DFe:NO₃⁻ ratios displayed a gradient from the West European Basin to Greenland (supplementary material S7
24 and S8). This trend only reverses when the influence of Greenland was encountered, as also observed by Painter et al. (2014).
25 The remineralisation of organic matter is a major source of macro and micronutrients in subsurface waters (from 50 to 250 m
26 depth). Remineralisation is associated with the consumption of oxygen and therefore, Apparent Oxygen Utilization (AOU)
27 can provide a quantitative estimate of the amount of material that has been remineralised. While no relationship was observed
28 below 50 m depth for NO₃⁻ or DFe and AOU considering all the stations, a significant correlation was found in the Subpolar
29 gyre when removing the influence of margins (stations 29-49, 56, 60, 63-77) (AOU = 3.88 NO₃⁻ - 39.32, R²=0.79, n=69, p-
30 value < 0.001). This correlation indicates that remineralisation of Particulate Organic Nitrogen (PON) greatly translates into
31 Dissolved Inorganic Nitrogen (DIN) and that NO₃⁻ can be used as a good tracer for remineralisation in the studied area. Within
32 these Subpolar gyre waters, there was a significant correlation between DFe and AOU (AOU = 22.6 DFe, R²=0.34, n=53, p-
33 value < 0.001). The open-ocean stations from Subpolar gyre also exhibited a good linear correlation between DFe and NO₃⁻

Deleted: the

Deleted: has been reported by Tanhua et al. (2005) to mainly originate (75% of the overflow) from the Nordic Seas and the Arctic Ocean. Klunder et al. (2012) noticed that the ultimate source of Fe to the Arctic Ocean is coming from Eurasian river waters and

Deleted: reported that the

Deleted: and therefore the Arctic major rivers are a source of Fe-binding organic ligands. Consequently, these

Deleted: s

Deleted: are likely

Deleted: the

Deleted: enabling higher DFe concentrations in seawater.

Deleted: In summary, the occurrence of particulate MnO₂ and the amount of organic matter are the main drivers explaining the DFe distributions within the benthic nepheloid layers. ¶

Deleted: 4

Deleted:

Deleted: and biological activity

Deleted: GA01

Deleted: Fig. 3

Deleted: Consideration of the relationship between DFe and biological uptake are

Deleted: discussed in Tonnard et al. (in prep.), while following discussion specifically

Deleted: es

Deleted: "Did

Deleted: ?"

Deleted: ¶

Deleted: ¶

Deleted: 7

Deleted: 68

Deleted:

Deleted: I¹

Deleted: 7

Deleted: The

Formatted: Superscript

Deleted: at

Formatted: Superscript

Deleted: East Greenland, West Greenland and Newfoundland Margins reflected both a strong phytoplankton bloom which had ...

Formatted: Highlight

Formatted: Normal, Indent: Before: 0 cm

Deleted: Phytoplankton cellular Fe:N ratios have been found to ...

1 ($R^2=0.42$, $n=51$, p -value < 0.05). The slope of the relationship, representing the typical remineralisation ratio, was $R_{Fe:N} = 0.07$
2 ± 0.01 mmol mol⁻¹. The intercept of the regression line was -0.4 ± 0.2 nmol L⁻¹, reflecting possible excess of preformed NO_3^-
3 compare to DFe in these water masses. These significant correlations allow us to use the Fe* tracer to assess where DFe
4 concentrations potentially limit phytoplankton growth by subtracting the contribution of organic matter remineralisation from
5 the dissolved Fe pool, as defined by Rijkenberg et al. (2014) and Parekh et al. (2005) for PO_4^{3-} , and modified here for NO_3^- as
6 follow:

$$Fe^* = [DFe] - R_{Fe:N} \times [NO_3^-] \quad (\text{eq. 4})$$

7
8 where $R_{Fe:N}$ refers to the average biological uptake ratio Fe over nitrogen, and $[NO_3^-]$ refers to nitrate concentrations in
9 seawater. Although, we imposed a fixed biological $R_{Fe:N}$ of 0.05 mmol mol⁻¹, it is important to note that the biological uptake
10 ratio of DFe: NO_3^- is not likely to be constant. Indeed, this ratio has been found to range from 0.05 to 0.9 mmol mol⁻¹ depending
11 on species (Ho et al., 2003; Sunda and Huntsman, 1995; Twining et al., 2004). The ratio we choose is thus less drastic to assess
12 potential Fe limitation and more representative of the average biological uptake of DFe over NO_3^- calculated for this study (i.e.
13 $R_{Fe:N} = 0.07 \pm 0.01$ mmol mol⁻¹, for Subpolar waters). Negative values of Fe* indicate the removal of DFe that is faster than
14 the input through remineralisation or external sources and positive values suggest input of DFe from external sources (Fig. 7).

15 Consequently, figure 7 shows that phytoplankton communities with very high Fe requirements relative to NO_3^- ($R_{Fe:N} = 0.9$)
16 will only be able to grow above continental shelves where there is a high supply of DFe as previously reported by Nielsdóttir
17 et al. (2009) and Painter et al. (2014). All these results are corroborating the importance of the Tagus River (Iberian Margin,
18 see section 4.2.1), glacial inputs in the Greenland and Newfoundland Margins (see section 4.2.2) and to a lesser extent
19 atmospheric inputs (see section 4.2.3) in supplying Fe with Fe:N ratios higher than the average biological uptake/demand ratio.
20 Figure 7 (see also supplementary material S7, S8, S9 and S10) also highlights the Fe limitation for the low-Fe requirement
21 phytoplankton class ($R_{Fe:N} = 0.05$) within the Iceland Basin, Irminger and Labrador Seas. The Fe deficiency observed in surface
22 waters (> 50 m depth) from the Irminger and Labrador Seas might be explained by low atmospheric deposition for the ICSPMW
23 and the LSW (Shelley et al., 2017). Low atmospheric Fe supply and sub-optimal Fe:N ratios in winter overturned deep water
24 could favour the formation of the High-Nutrient, Low-Chlorophyll (HNLC) conditions. The West European Basin, despite
25 exhibiting some of the highest DFe: NO_3^- ratios within surface waters (see supplementary material Fig. S8), displayed the
26 strongest Fe-depletion from 50 m depth down to the bottom, suggesting that the main source of Fe was coming from dust
27 deposition and/or riverine inputs.

28 Similarly as for the West European Basin, the pattern displayed in the surface map of DFe: NO_3^- ratios (supplementary material
29 S8) extended to about 50 m depth, after which the trend reversed (Fig. 7 and supplementary material Fig. S7). Below 50 m
30 depth, the Fe* tracer (Fig. 7) was positive in the Irminger Sea and overall negative in the other basins. In the Irminger Sea
31 positive Fe* values were likely the result of the winter entrainment of Fe-rich LSW (see section 4.2.1) coinciding with high
32 remineralised carbon fluxes in this area (station 44; Lemaître et al., 2017) (see section 4.2.2). The largest drawdown in
33 DFe: NO_3^- ratios was observed between stations 34 and 38 and was likely due to the intrusion of the ICSPMW, this water mass
34 exhibiting low DFe and high in NO_3^- (from 7 to 8 $\mu\text{mol L}^{-1}$) concentrations. Similarly, the SAIW exhibited high NO_3^-

Formatted: Normal, Centered, Indent: Before: 0 cm

Deleted: To assess where DFe concentrations potentially limit phytoplankton growth we subtracted the contribution of organic matter remineralization to the dissolved Fe pool using the tracer Fe*, as defined by Rijkenberg et al. (2014) and Parekh et al. (2005) for PO_4^{3-} , and modified here for NO_3^- as follow:
 $Fe^* = [DFe] - R_{Fe:N} \times [NO_3^-]$ (eq. 1)

Deleted: In the following, we use the two end-member ratios $R_{Fe:N}$ ratios which represented the lowest and highest Fe:N uptake found in literature ($R_{Fe:N} = 0.05$ and 0.9 mmol mol⁻¹, respectively).

Deleted: a deficit in DFe concentrations whereas positive values are pointing out to a source of DFe relative to the uptake of NO_3^-

Deleted: 13

Moved (insertion) [9]

Deleted: 13

Deleted: Fonseca-Batista et al., subm.

Formatted: Font: Not Bold, Font color: Auto, Complex Script
Font: Times New Roman, Not Bold

Deleted: ¶

Moved (insertion) [10]

Deleted: z

Deleted: .

1 concentrations. Both the IcSPMW and the SAIW sourced from the NAC. The NAC as it flows along the coast of North
2 America receives atmospheric depositions from anthropogenic sources (Shelley et al., 2017; 2015) which deliver high N
3 relative to Fe (Jickells and Moore, 2015) and might be responsible for the observed ranges.

4 **5 Conclusion**

5 The DFe concentrations measured during this study were in good agreement with previous studies that spanned the West
6 European Basin. However, within the Irminger Basin the DFe concentrations measured during this study were up to 3 times
7 higher than those measured by Rijkenberg et al. (2014) in deep waters (> 1000 m depth). This is likely explained by the
8 different water masses encountered (i.e. the Polar Intermediate Water, ~ 2800 m depth) and by a stronger signal of the Iceland
9 Scotland Overflow Water (ISOW) from 1200 to 2300 m depth. This corresponded to the most striking feature of the whole
10 section with DFe concentrations reaching up to 2.5 nmol L⁻¹ within the ISOW, Denmark Strait Overflow Water (DSOW) and
11 Labrador Sea Water (LSW), three water masses that are part of the Deep Western Boundary Current and was likely the result
12 of a lateral advection of particles in the Irminger. However, as these water masses reached the Labrador Sea, lower DFe levels
13 were measured. These differences could be explained by different processes occurring within the benthic nepheloid layers,
14 where DFe was sometimes trapped onto particles due to Mn-sediment within the Labrador Sea (Gourain et al., 2018) and
15 sometimes released from the sediment potentially as a result of interactions with dissolved organic matter. Such Fe-binding
16 organic ligands could have also been produced locally due to the intense remineralisation rate reported by Lemaître et al.
17 (2017) of biogenic particles (Boyd et al., 2010; Gourain et al., 2018). The LSW exhibited increasing DFe concentrations along
18 its flow path, likely resulting from sediment inputs at the Newfoundland Margin. Although DFe inputs through hydrothermal
19 activity were expected at the slow spreading Reykjanes Ridge (Baker and German, 2004b; German et al., 1994), our data did
20 not provide evidence of this specific source as previously suggested by Achterberg et al. (2018) at ~60°N.

21 In surface waters several sources of DFe were highlighted especially close to land, with riverine inputs from the Tagus River
22 at the Iberian margin (Menzel Barraqueta et al., 2018) and meteoric inputs (including coastal runoff and glacial meltwater) at
23 the Newfoundland and Greenland margins (Benetti et al., 2016). Substantial sediment input was observed at all margins but
24 with varying intensity. The highest DFe sediment input was located at the Newfoundland margin, while the lowest was
25 observed at the eastern Greenland margin. These differences could be explained by the different nature of particles with the
26 most lithogenic located at the Iberian margin and the most biogenic, at the Newfoundland margin (Gourain et al., 2018).
27 Although previous studies (e.g. Jickells et al., 2005; Shelley et al., 2015) reported that atmospheric inputs substantially
28 fertilized surface waters from the West European Basin, in our study, only stations located in the West European and Iceland
29 Basins exhibited enhanced SML DFe inventories with lower TTADs. However, these TTADs were about three times higher
30 than those reported for Saharan dust inputs and thus atmospheric deposition appeared to be a minor source of Fe during the
31 sampling period. Finally, there was evidence of convective inputs of the LSW to surface seawater caused by long tip jet event

Moved up [9]: Consequently, figure 13 shows that phytoplankton communities with very high Fe requirements relative to NO₃ (R_{Fe:N} = 0.9) will only be able to grow above continental shelves where there is a high supply of DFe. All these results are corroborating the importance of the Tagus River (Iberian Margin, see section 4.2.1), glacial inputs in the Greenland and Newfoundland Margins (see section 4.2.2) and to a lesser extent atmospheric inputs (see section 4.2.3) in supplying Fe with Fe:N ratios higher than the average biological uptake/demand ratio. ¶

Moved up [10]: coinciding with high remineralized carbon fluxes in this area (station 44; Lemaître et al., 2017).

Deleted: ¶
Figures 12 and 14 also highlight the Fe limitation for the low-Fe requirement phytoplankton class (R_{Fe:N} = 0.05, Fig. 13) within the Iceland Basin, Irminger and Labrador Seas. The Fe deficiency from the Iceland Basin and Labrador Sea might be explained by low atmospheric Fe supply and sub-optimal Fe:N ratios in winter overturned deep water could facilitate the formation of the High-Nutrient, Low-Chlorophyll (HNLC) conditions, representing the inefficiency of the biological carbon pump as little or no carbon is transferred below 1000 m depth (Lemaître et al., 2017; Nielsdóttir et al., 2009). Consequently, the low DFe:NO₃ ratios observed above 100 m depth were probably due to the phytoplankton bloom advancement, coinciding with high remineralized carbon fluxes in this area (station 44; Lemaître et al., 2017). The West European Basin, despite exhibiting some of the highest DFe:NO₃ ratios within surface waters (Fig. 12), displayed the strongest Fe-depletion from 50 m depth down to the bottom, suggesting that the main source of Fe was coming from dust deposition. In our study, Shelley et al. (2017b) reported low aerosol Fe loading compared to other studies in the ...

Formatted: Indent: First line: 0 cm

Deleted: the ones

Deleted: that was

Deleted:

Formatted: English (Australia)

Formatted: English (Australia)

Formatted: English (Australia)

Formatted: English (Australia)

Deleted: pointed

Deleted: further north

Deleted: (-

Deleted:) from our section

Formatted: Normal

Deleted: s

Deleted: s

Deleted: ere

Deleted: different

Deleted: t

Deleted: at

1 (Piron et al., 2016) that deepened the winter mixed layer down to ~ 1200 m depth (Zunino et al., 2017), in which Fe was in
2 excess of nitrate and therefore, Fe was not limiting.

3 Acknowledgements

4 We are greatly indebted to the master, Gilles Ferrand, the officers and crew from the N/O *Pourquoi Pas?* for their logistic
5 support during the GEOVIDE voyage. We would like to give a special thanks to Pierre Branellec, Michel Hamon, Catherine
6 Kermabon, Philippe Le Bot, Stéphane Leizour, Olivier Ménage (Laboratoire d'Océanographie Physique et Spatiale), Fabien
7 Pérault and Emmanuel de Saint Léger (Division Technique de l'INSU, Plouzané, France) for their technical expertise during
8 clean CTD deployments as well as Emilie Grosseffan and Manon Le Goff for the analysis of nutrients. We also wanted to
9 thank the Pôle Spectrométrie Océan (PSO, Plouzané, France) for letting us use the Element XR HR-ICP-MS. Greg Cutter is
10 also strongly acknowledged for his help in setting up the new French clean sampling system. Catherine Schmechtig is thanked
11 for the LEFE-CYBER database management. This work was funded by the French National Research Agency ANR
12 GEOVIDE (ANR-13-BS06-0014) and RPOC BITMAP (ANR-12-PDOC-0025-01), the French National Center for
13 Scientific Research (CNRS-LEFE-CYBER), the LabexMER (ANR-10-LABX-19) and Ifremer and was supported for the
14 logistic by DT-INSU and GENAVIR. Manon Tonnard was supported by a cotutelle joint PhD scholarship from the Université
15 de Bretagne Occidentale (UBO-IUEM) and the University of Tasmania (UTAS-IMAS).

16
17 All dissolved iron (DFe) data are available in the supplementary material S1.

19 References

20 Achterberg, E. P., Steigenberger, S., Marsay, C. M., LeMoigne, F. A., Painter, S. C., Baker, A. R., Connelly, D. P.,
21 Moore, C. M., Tagliabue, A., and Tanhua, T.: Iron Biogeochemistry in the High Latitude North Atlantic Ocean, Scientific
22 reports, 8, 1-15, 10.1038/s41598-018-19472-1, 2018.

23 Aminot, A., and Kerouel, R.: Dosage automatique des nutriments dans les eaux marines, Quae ed., 2007.

24 Annett, A. L., Skiba, M., Henley, S. F., Venables, H. J., Meredith, M. P., Statham, P. J., and Ganeshram, R. S.:
25 Comparative roles of upwelling and glacial iron sources in Ryder Bay, coastal western Antarctic Peninsula, Marine
26 Chemistry, 176, 21-33, 10.1016/j.marchem.2015.06.017, 2015.

27 Bacon, S., Gould, W. J., and Jia, Y.: Open-ocean convection in the Irminger Sea, Geophysical Research Letters, 30,
28 1246, doi:10.1029/2002GL016271, 2003.

29 Baker, A. R., Adams, C., Bell, T. G., Jickells, T. D., and Ganzeveld, L.: Estimation of atmospheric nutrient inputs
30 to the Atlantic Ocean from 50°N to 50°S based on large-scale field sampling: Iron and other dust-associated elements,
31 Global Biogeochemical Cycles, 27, 755-767, 10.1002/gbc.20062, 2013.

Deleted: where thus

Deleted: at the sampling period.

Formatted: Font: (Default) +Headings CS (Times New Roman), Complex Script Font: +Headings CS (Times New Roman)

Deleted: The objectives of the present paper were to describe and discuss the DFe distributions over the whole water column along the 5000 km long transect in the North Atlantic Ocean and the Labrador Sea. ¶

The most striking feature observed during the GEOVIDE voyage was the increasing DFe concentrations inherent to the LSW along its flow path which were likely explained by two processes: i) dissolution of Newfoundland sediments, and ii) potential bacteria-mediated Fe-binding organic ligand production as indicated by intense remineralization rates in the Irminger Sea. This observation has a broader implication in terms of primary production. Indeed, the intense wind-forcing of deep convection occurring in the Irminger Sea enables the LSW with its enhanced DFe concentrations to reach surface waters, thus initially sustaining intense phytoplankton growth during spring, but which will potentially limit the biological activity later on in the season due to its relative depletion in NO₃ as indicated by Fe*. ¶

The distribution of DFe along the section also revealed the influence of external sources such as meteoric water melting in the subpolar gyre close to margins and the input of DFe from the Tagus river above the Iberian Margin. The latter source appears to have less impact as DFe is scavenged onto particles which will inevitably remove it from the mixed layer and entrained it to deep ocean. Dust deposition appears to have been only a minor source of DFe into surface waters, except in the subtropical gyre closer to the African continent. ¶

If the partition between dissolved and particulate forms of Fe is still not well understood in deep ocean, it is clear that it is mainly dependant of the nature of the sediments and not a direct function of the hydrographic characteristics. Indeed, different processes occurring within the DSOW in the Irminger and Labrador Seas result in DFe sometimes being scavenged onto particles due to Mn-oxide-sediment composition, yet at other times being released from the sediment. We have no clear explanation regarding the unusually high DFe concentrations (for a non-hydrothermal source) measured between 2000 and 3000 m depth in the Irminger Sea, except from dissolution of Fe-rich particles within DSOW and PIW as they mixed with ISOW. ¶

Formatted: French (France)

1 Baker, A. T., and German, C. R.: On the Global Distribution of Hydrothermal vent Fields, in: Mid-Ocean Ridges,
2 edited by: German, C. R., Lin, J., and Parson, L. M., 2004a.

3 Baker, E. T., and German, C. R.: Hydrothermal Interactions Between the Lithosphere and Oceans, in: Mid-Ocean
4 Ridges, edited by: German, C. R., Lin, J., and Parson, L. M., Geophysical Monograph Series, AGU, 245-266, 2004b.

5 Barton, A. D., Greene, C. H., Monger, B. C., and Pershing, A. J.: The Continuous Plankton Recorder survey and the
6 North Atlantic Oscillation: Interannual- to Multidecadal-scale patterns of phytoplankton variability in the North Atlantic
7 Ocean, *Progress in Oceanography*, 58, 337-358, 10.1016/j.pocean.2003.08.012, 2003.

8 Batchelli, S., Muller, F. L. L., Chang, K. C., and Lee, C. L.: Evidence for Strong but Dynamic Iron-Humic
9 Colloidal Associations in Humic-Rich Coastal Waters., *Environmental Science & Technology*, 44, 8485-8490, 2010.

10 Benetti, M., Reverdin, G., Pierre, C., Khatiwala, S., Tournadre, B., Olafsdottir, S., and Naamar, A.: Variability of
11 sea ice melt and meteoric water input in the surface Labrador Current off Newfoundland, *Journal of Geophysical Research*
12 *Oceans*, 121, 2841-2855, doi:10.1002/2015JC011302., 2016.

13 Benetti, M., Reverdin, G., Lique, C., Yashayaev, I., Holliday, N. P., Tynan, E., Torres-Valdes, S., Lherminier, P.,
14 Tréguer, P., and Sarthou, G.: Composition of freshwater in the spring of 2014 on the southern Labrador shelf and slope,
15 *Journal of Geophysical Research: Oceans*, 122, 1102-1121, 10.1002/2016jc012244, 2017.

16 Bersch, M., Yashayaev, I., and Koltermann, K. P.: Recent changes of the thermohaline circulation in the subpolar
17 North Atlantic, *Ocean Dynamics*, 57, 223-235, 10.1007/s10236-007-0104-7, 2007.

18 Bhatia, M. P., Kujawinski, E. B., Das, S. B., Breier, C. F., Henderson, P. B., and Charette, M. A.: Greenland
19 meltwater as a significant and potentially bioavailable source of iron to the ocean, *Nature Geoscience*, 2013, 274-278,
20 10.1038/ngeo1746, 2013.

21 Bonnet, S., and Guieu, C.: Dissolution of atmospheric iron in seawater, *Geophysical Research Letters*, 31,
22 10.1029/2003gl018423, 2004.

23 Bonnet, S., and Guieu, C.: Atmospheric forcing on the annual iron cycle in the western Mediterranean Sea: A 1-
24 year survey, *Journal of Geophysical Research*, 111, 10.1029/2005jc003213, 2006.

25 Boyd, P. W., Watson, A. J., Law, C. S., Abraham, E. R., Trull, T., Murdoch, R., Bakker, D. C. E., Bowie, A. R.,
26 Buesseler, K. O., Chang, H., Charette, M., Croot, P., Downing, K., Frew, R., Gall, M., Hadfield, M., Hall, J., Harvey, M.,
27 Jameson, G., LaRoche, J., Liddicoat, M., Ling, R., Maldonado, M. T., McKay, R. M., Nodder, S., Pickmere, S., Pridmore,
28 R., Rintoul, S., Safi, K., Sutton, P., Strzepek, R., Tanneberger, K., Turner, S., Waite, A., and Zeldis, J.: A mesoscale
29 phytoplankton bloom in the polar Southern Ocean stimulated by iron fertilization, *Nature*, 407, 695-702, 2000.

30 Boyd, P. W., and Ellwood, M. J.: The biogeochemical cycle of iron in the ocean, *Nature Geoscience*, 3, 675-682,
31 10.1038/ngeo964, 2010.

32 Boyd, P. W., Ibsanmi, E., Sander, S. G., Hunter, K. A., and Jackson, G. A.: Remineralization of upper ocean
33 particles: Implications for iron biogeochemistry, *Limnology and Oceanography*, 55, 1271-1288, 10.4319/lo.2010.55.3.1271,
34 2010.

35 Buck, C. S., Landing, W. M., Resing, J. A., and Measures, C. I.: The solubility and deposition of aerosol Fe and
36 other trace elements in the North Atlantic Ocean: Observations from the A16N CLIVAR/CO2 repeat hydrography section,
37 *Marine Chemistry*, 120, 57-70, 10.1016/j.marchem.2008.08.003, 2010.

1 Canário, J., Vale, C., Caetano, M., and Madureira, M. J.: Mercury in contaminated sediments and pore waters
2 enriched in sulphate (Tagus Estuary, Portugal), *Environmental Pollution*, 126, 425-433, 10.1016/S0269-7491(03)00234-3,
3 2003.

4 Charette, M. A., Morris, P. J., Henderson, P. B., and Moore, W. S.: Radium isotope distributions during the US
5 GEOTRACES North Atlantic cruises, *Marine Chemistry*, 177, 184-195, 10.1016/j.marchem.2015.01.001, 2015.

6 Chen, Y. J.: Influence of the Iceland mantle plume on crustal accretion at the inflated Reykjanes Ridge: Magma lens
7 and low hydrothermal activity, *Journal of Geophysical Research*, 108, 2524, 2003.

8 Chester, R., Murphy, K. J. T., Lin, F. J., Berry, A. S., Bradshaw, G. A., and Corcoran, P. A.: Factors controlling the
9 solubilities of trace-metals from nonremote aerosols deposited to the sea-surface by the dry deposition mode, *Marine*
10 *Chemistry*, 42, 107-126, 10.1016/0304-4203(93)90241-f, 1993.

11 Conway, T. M., and John, S. G.: Quantification of dissolved iron sources to the North Atlantic Ocean, *Nature*, 511,
12 212-215, 10.1038/nature13482, 2014.

13 Cooper, L. W., Whitley, T. E., Grebmeier, J. M., and Weingartner, T.: The nutrient, salinity, and stable oxygen
14 isotope composition of Bering and Chukchi Seas waters in and near the Bering Strait, *Journal of Geophysical Research*, 102,
15 12,563-512,573, 1997.

16 Cooper, L. W., McClelland, J. W., Holmes, R. M., Raymond, P. A., Gibson, J. J., Guay, C. K., and Peterson, B. J.:
17 Flow-weighted values of runoff tracers ($\delta^{18}\text{O}$, DOC, Ba, alkalinity) from the six largest Arctic rivers, *Geophysical Research*
18 *Letters*, 35, 1-5, 10.1029/2008GL035007, 2008.

19 Crane, K., Johnson, L., Appelgate, B., Nishimura, C., Buck, R., Jones, C., Vogt, P., and Kos'yan, R.: Volcanic and
20 Seismic Swarm Events on the Reykjanes Ridge and Their Similarities to Events on Iceland: Results of a Rapid Response
21 Mission, *Marine Geophysical Researches*, 19, 319-338, 1997.

22 Cutter, G., Casciotti, K., Croot, P., Geibert, W., Heimbürger, L. E., Lohan, M., Planquette, H., and van de Fliedert,
23 T.: Sampling and the Sample-handling Protocols for GEOTRACES Cruises, 2017.

24 Daniault, N., Mercier, H., Lherminier, P., Sarafanov, A., Falina, A., Zunino, P., Pérez, F. F., Ríos, A. F., Ferron, B.,
25 Huck, T., Thierry, V., and Gladyshev, S.: The northern North Atlantic Ocean mean circulation in the early 21st century,
26 *Progress in Oceanography*, 146, 142-158, 10.1016/j.pocean.2016.06.007, 2016.

27 de Barros, M. C.: A case study of waste inputs in the Tagus estuary, in: *The role of the Oceans as a Waste Disposal*
28 *Option*, edited by: Kullenberg, G., NATO ASI Series; Series C: Mathematical and Physical Sciences, 172, Springer
29 Netherlands, 307-324, 1986.

30 de Jong, M. F., van Aken, H. M., Våge, K., and Pickart, R. S.: Convective mixing in the central Irminger Sea:
31 2002–2010, *Deep Sea Research Part I: Oceanographic Research Papers*, 63, 36-51, 10.1016/j.dsr.2012.01.003, 2012.

32 Dehairs, F., Shopova, D., Ober, S., Veth, C., and Goeyens, L.: Particulate barium stocks and oxygen consumption
33 in the Southern Ocean mesopelagic water column during spring and early summer: Relationship with export production,
34 *Deep Sea Research II*, 44, 497-516, 10.1016/S0967-0645(96)00072-0, 1997.

35 Deng, F., Henderson, G. M., Castrillejo, M., and Perez, F. F.: Evolution of ^{231}Pa and ^{230}Th in overflow waters of
36 the North Atlantic, *Biogeosciences*, 1-24, 10.5194/bg-2018-191, 2018.

1 Fagel, N., Robert, C., and Hilaire-Marcel, C.: Clay mineral signature of the NW Atlantic Boundary Undercurrent,
2 *Marine Geology*, 130, 19-28, 1996.

3 Fagel, N., Robert, C., Preda, M., and Thorez, J.: Smectite composition as a tracer of deep circulation: the case of the
4 Northern North Atlantic, *Marine Geology*, 172, 309-330, 2001.

5 Ferron, B., Kokoszka, F., Mercier, H., Lherminier, P., Huck, T., Ríos, A., and Thierry, V.: Variability of the
6 Turbulent Kinetic Energy Dissipation along the A25 Greenland–Portugal Transect Repeated from 2002 to 2012, *Journal of*
7 *Physical Oceanography*, 46, 1989-2003, 10.1175/jpo-d-15-0186.1, 2016.

8 Figueres, G., Martin, J. M., Meybeck, M., and Seyler, P.: A comparative study of mercury contamination in the
9 Tagus estuary (Portugal) and major French estuaries (Gironde, Loire, Rhone), *Estuarine, Coastal and Shelf Science*, 20, 183-
10 203, 1985.

11 Fiúza, A.: *Hidrologia e dinamica das aguas costeiras de Portugal*, Ph. D., Universidade de Lisboa, Lisboa, Portugal,
12 unpublished, 1984.

13 Follows, M., and Dutkiewicz, S.: Meteorological modulation of the North Atlantic Spring Bloom, *Deep Sea*
14 *Research Part II: Topical Studies in Oceanography*, 49, 321-344, 2001.

15 García-Ibáñez, M. I., Pardo, P. C., Carracedo, L. I., Mercier, H., Lherminier, P., Ríos, A. F., and Pérez, F. F.:
16 Structure, transports and transformations of the water masses in the Atlantic Subpolar Gyre, *Progress in Oceanography*, 135,
17 18-36, 10.1016/j.pocean.2015.03.009, 2015.

18 García-Ibáñez, M. I., Pérez, F. F., Lherminier, P., Zunino, P., Mercier, H., and Tréguer, P.: Water mass distributions
19 and transports for the 2014 GEOVIDE cruise in the North Atlantic, *Biogeosciences*, 15, 2075-2090, 10.5194/bg-15-2075-
20 2018, 2018.

21 García-Ibáñez, M. I., Pérez, F. F., Lherminier, P., Zunino, P., and Tréguer, P.: Water mass distributions and
22 transports for the 2014 GEOVIDE cruise in the North Atlantic, *Biogeosciences*, this issue.

23 Gaudencio, M. J., Guerra, M. T., and Glemarec, M.: Recherches biosédimentaires sur la zone maritime de l'estuaire
24 du Tage, Portugal: données sédimentaires préliminaires. , in: *Estuaries and Coasts: Spatial and Temporal Intercomparisons*,
25 edited by: Elliot, M., and Ducrottoy, J. C., Olsen and Olsen, Fredensborg, 11-16, 1991.

26 German, C. R., Briem, J., Chin, C. S., Danielsen, M., Holland, S., James, R. H., Jonsdottir, A., Ludford, E., Moser,
27 C., Olafsson, J., Palmer, M. R., and Rudnicki, M. D.: Hydrothermal activity on the Reykjanes Ridge: the Steinahóll vent-
28 field at 63°06'N, *Earth and Planetary Science Letters*, 121, 647-654, 1994.

29 Gerringa, L. J. A., Blain, S., Laan, P., Sarthou, G., Veldhuis, M. J. W., Brussaard, C. P. D., Viollier, E., and
30 Timmermans, K. R.: Fe-binding dissolved organic ligands near the Kerguelen Archipelago in the Southern Ocean (Indian
31 sector), *Deep Sea Research Part II: Topical Studies in Oceanography*, 55, 606-621, 10.1016/j.dsr2.2007.12.007, 2008.

32 Gerringa, L. J. A., Slagter, H. A., Bown, J., van Haren, H., Laan, P., de Baar, H. J. W., and Rijkenberg, M. J. A.:
33 Dissolved Fe and Fe-binding organic ligands in the Mediterranean Sea – GEOTRACES G04, *Marine Chemistry*, 194, 100-
34 113, 10.1016/j.marchem.2017.05.012, 2017.

35 Gourain, A., Planquette, H., Cheize, M., Menzel-Barraqueta, J. L., Boutorh, J., Shelley, R. U., Pereira-Contreira, L.,
36 Lemaitre, N., Lacan, F., Lherminier, P., and Sarthou, G.: particulate trace metals along the GEOVIDE section,
37 *Biogeosciences*, 2018.

Formatted: French (France)

1 Guerzoni, S., Chester, R., Dulac, F., Herut, B., Loye-Pilot, M.-D., Measures, C., Migon, C., Molinaroli, E., Moulin,
2 C., Rossini, P., Saydam, C., Soudine, A., and Ziveri, P.: The role of atmospheric deposition in the biogeochemistry of the
3 Mediterranean Sea, *Progress in Oceanography*, 44, 147-190, 1999.

4 Guieu, C., Loye-Pilot, M. D., Benyahya, L., and Dufour, A.: Spatial variability of atmospheric fluxes of metals (Al,
5 Fe, Cd, Zn and Pb) and phosphorus over the whole Mediterranean from a one-year monitoring experiment: Biogeochemical
6 implications, *Marine Chemistry*, 120, 164-178, 10.1016/j.marchem.2009.02.004, 2010.

7 Guieu, C., Aumont, O., Paytan, A., Bopp, L., Law, C. S., Mahowald, N., Achterberg, E. P., Marañón, E., Salihoglu,
8 B., Crise, A., Wagener, T., Herut, B., Desboeufs, K., Kanakidou, M., Olgun, N., Peters, F., Pulido-Villena, E., Tovar-
9 Sanchez, A., and Völker, C.: The significance of the episodic nature of atmospheric deposition to Low Nutrient Low
10 Chlorophyll regions, *Global Biogeochemical Cycles*, 28, 1179-1198, 10.1002/2014gb004852, 2014.

11 Harrison, W. G., Yngve Børshiem, K., Li, W. K. W., Maillet, G. L., Pepin, P., Sakshaug, E., Skogen, M. D., and
12 Yeats, P. A.: Phytoplankton production and growth regulation in the Subarctic North Atlantic: A comparative study of the
13 Labrador Sea-Labrador/Newfoundland shelves and Barents/Norwegian/Greenland seas and shelves, *Progress in*
14 *Oceanography*, 114, 26-45, 10.1016/j.pcean.2013.05.003, 2013.

15 Hatta, M., Measures, C. I., Wu, J., Roshan, S., Fitzsimmons, J. N., Sedwick, P., and Morton, P.: An overview of
16 dissolved Fe and Mn distributions during the 2010-2011 US GEOTRACES north Atlantic cruises: GEOTRACES GA03,
17 *Deep-Sea Research Part II-Topical Studies in Oceanography*, 116, 117-129, 10.1016/j.dsr2.2014.07.005, 2015.

18 Hawkings, J. R., Wadham, J. L., Tranter, M., Raiswell, R., Benning, L. G., Statham, P. J., Tedstone, A., Nienow, P.,
19 Lee, K., and Telling, J.: Ice sheets as a significant source of highly reactive nanoparticulate iron to the oceans, *Nature*
20 *communications*, 5, 1-8, 10.1038/ncomms4929, 2014.

21 Henson, S. A., Dunne, J. P., and Sarmiento, J. L.: Decadal variability in North Atlantic phytoplankton blooms,
22 *Journal of Geophysical Research*, 114, 10.1029/2008jc005139, 2009.

23 Ho, T.-Y., Quigg, A., Finkel, Z. V., Milligan, A. J., Wyman, K., Falkowski, P. G., and Morel, F. M. M.: The
24 elemental composition of some marine phytoplankton, *Journal of Phycology*, 39, 1145-1159, 2003.

25 Homoky, W. B., Hembury, D. J., Hepburn, L. E., Mills, R. A., Statham, P. J., Fones, G. R., and Palmer, M. R.: Iron
26 and manganese diagenesis in deep sea volcanogenic sediments and the origins of pore water colloids, *Geochimica Et*
27 *Cosmochimica Acta*, 75, 5032-5048, 10.1016/j.gca.2011.06.019, 2011.

28 Homoky, W. B., John, S. G., Conway, T. M., and Mills, R. A.: Distinct iron isotopic signatures and supply from
29 marine sediment dissolution, *Nature Communications*, 4, 10.1038/ncomms3143, 2013.

30 Humphreys, M. P., Griffiths, A. M., Achterberg, E. P., Holliday, N. P., Rérolle, V., Menzel Barraqueta, J. L.,
31 Couldrey, M. P., Oliver, K. I., Hartman, S. E., and Esposito, M.: Multidecadal accumulation of anthropogenic and
32 remineralized dissolved inorganic carbon along the Extended Ellett Line in the northeast Atlantic Ocean, *Global*
33 *Biogeochemical Cycles*, 30, 293-310, doi: 10.1002/2015GB005246, 2016.

34 Hunke, E. C., Notz, D., Turner, A. K., and Vancoppenolle, M.: The multiphase physics of sea ice: a review for
35 model developers, *The Cryosphere*, 5, 989-1009, 10.5194/tc-5-989-2011, 2011.

36 Janssens, J., Meiners, K. M., Tison, J.-L., Dieckmann, G., Delille, B., and Lannuzel, D.: Incorporation of iron and
37 organic matter into young Antarctic sea ice during its initial growth stages, *Elementa: Science of the Anthropocene*, 4,
38 000123, 10.12952/journal.elementa.000123, 2016.

1 Jickells, T., and Moore, C. M.: The importance of atmospheric deposition for ocean productivity, *Annual Review of*
2 *Ecology, Evolution, and Systematics*, 46, 481-501, 10.1146/annurev-ecolsys-112414-054118, 2015.

3 Jickells, T. D., An, Z. C., Andersen, K. K., Baker, A. R., Bergametti, G., Brooks, N., Cao, J. J., Boyd, P. W., Duce,
4 R. A., Hunter, K. A., Kawahata, H., Kubilay, N., laRoche, J., Liss, P. S., Mahowald, N., Prospero, J. M., Ridgwell, A. J.,
5 Tegen, I., and Torres, R.: Global iron connections between desert dust, ocean biogeochemistry, and climate, *Science*, 308,
6 67-71, 2005.

7 Jones, E. P., Anderson, L. G., and Swift, J. H.: Distribution of Atlantic and Pacific waters in the upper Arctic
8 Ocean: Implications for circulation, *Geophysical Research Letters*, 25, 765-768, 1998.

9 Kan, C. C., Chen, W. H., Wan, M. W., Phatai, P., Wittayakun, J., and Li, K. F.: The preliminary study of iron and
10 manganese removal from groundwater by NaOCl oxidation and MF filtration, *Sustain. Environ. Res.*, 22, 25-30, 2012.

11 Kara, A. B., Rochford, P. A., and Hurlburt, H. E.: An optimal definition for ocean mixed layer depth, *Journal of*
12 *Geophysical Research*, 105, 16,803-816,821, 10.1029/2000JC900072, 2000.

13 Kissel, C., Laj, C., Mulder, T., Wandres, C., and Cremer, M.: The magnetic fraction: A tracer of deep water
14 circulation in the North Atlantic, *Earth and Planetary Science Letters*, 288, 444-454, 10.1016/j.epsl.2009.10.005, 2009.

15 Klunder, M. B., Bauch, D., Laan, P., de Baar, H. J. W., van Heuven, S. M. A. C., and Ober, S.: Dissolved iron in
16 the Arctic shelf seas and surface waters of the Central Arctic Ocean: impact of Arctic river water and ice-melt, *Journal of*
17 *Geophysical Research*, 117, 1-18, 2012.

18 Lackschewitz, K. S., Endler, R., Gehrke, B., Wallrabe-Adams, H.-J., and Thiede, J.: Evidence for topography- and
19 current-controlled deposition on the Reykjanes Ridge between 59°N and 60°N, *Deep-Sea Research I*, 43, 1683-1711, 1996.

20 Laes, A., Blain, S., Laan, P., Achterberg, E. P., Sarthou, G., and de Baar, H. J. W.: Deep dissolved iron profiles in
21 the eastern North Atlantic in relation to water masses, *Geophysical Research Letters*, 30, 10.1029/2003gl017902, 2003.

22 Lagerström, M. E., Field, M. P., Seguret, M., Fischer, L., Hann, S., and Sherrell, R. M.: Automated on-line flow-
23 injection ICP-MS determination of trace metals (Mn, Fe, Co, Ni, Cu and Zn) in open ocean seawater: Application to the
24 GEOTRACES program, *Marine Chemistry*, 155, 71-80, 10.1016/j.marchem.2013.06.001, 2013.

25 Lambelet, M., van de Fliedert, T., Crocket, K., Rehkamper, M., Katharina, K., Coles, B., Rijkenberg, M. J. A.,
26 Gerringa, L. J. A., de Baar, H. J. W., and Steinfeldt, R.: Neodymium isotopic composition and concentration in the western
27 North Atlantic Ocean: Results from the GEOTRACES GA02 section, *Geochimica Et Cosmochimica Acta*, 177, 1-29, 2016.

28 Le Roy, E., Sanial, V., Charette, M. A., van Beek, P., Lacan, F., Jacquet, S. H. M., Henderson, P. B., Souhaut, M.,
29 García-Ibáñez, M. I., Jeandel, C., Pérez, F. F., and Sarthou, G.: The 226Ra–Ba relationship in the North Atlantic during
30 GEOTRACES-GA01, *Biogeosciences*, 15, 3027-3048, 10.5194/bg-15-3027-2018, 2018.

31 Lemaître, N., Planchon, F., Planquette, H., Dehairs, F., Fonseca-Batista, D., Roukaerts, A., Deman, F., Tang, Y.,
32 Mariez, C., and Sarthou, G.: High variability of export fluxes along the North Atlantic GEOTRACES section GA01:
33 Particulate organic carbon export deduced from the 234Th method *Biogeosciences*, 1-38, 10.5194/bg-2018-190, 2018.

34 Lemaître, N., planquette, H., Planchon, F., Sarthou, G., Jacquet, S., Garcia-Ibanez, M. I., Gourain, A., Cheize, M.,
35 Monin, L., Andre, L., Laha, P., Terryn, H., and Dehairs, F.: Particulate barium tracing significant mesopelagic carbon
36 remineralisation in the North Atlantic *Biogeosciences Discussions*, 2017.

1 Lohan, M. C., and Bruland, K. W.: Elevated Fe(II) and Dissolved Fe in Hypoxic Shelf Waters off Oregon and
2 Washington: An Enhanced Source of Iron to Coastal Upwelling Regimes, *Environmental Science & Technology*, 42, 6462-
3 6468, 10.1021/es800144j, 2008.

4 Longhurst, A. R.: *Ecological geography of the Sea*, Second Edition ed., Elsevier Academic Press publications,
5 Burlington, 542 pp., 2007.

6 Louanchi, F., and Najjar, R. G.: Annual cycles of nutrients and oxygen in the upper layers of the North Atlantic
7 Ocean, *Deep Sea Research Part II: Topical Studies in Oceanography*, 48, 2155-2171, 2001.

8 Markus, T., Stroeve, J. C., and Miller, J.: Recent changes in Arctic sea ice melt onset, freezeup, and melt season
9 length, *Journal of Geophysical Research*, 114, 10.1029/2009jc005436, 2009.

10 Marshall, J., and Schott, F.: Open-ocean convection: observations, theory, and models, *Reviews of Geophysics*, 37,
11 1-64, doi: 10.1029/98RG02739, 1999.

12 Martin, J.-M., Elbaz-Poulichet, F., Guieu, C., Loÿe-Pilot, M.-D., and Han, G.: River versus atmospheric input of
13 material to the Mediterranean Sea: an overview*, *Marine Chemistry*, 28, 159-182, 1989.

14 Martin, J. D., and Fitzwater, S. E.: Iron deficiency limits phytoplankton growth in the north-east Pacific subarctic,
15 *Nature*, 331, 341-343, 1988.

16 Martin, J. H., Fitzwater, S. E., and Gordon, R. M.: Iron deficiencies limits phytoplankton growth in Antarctic
17 waters, *Global Biogeochemical Cycles*, 4, 5-12, 1990.

18 Martin, J. H., Coale, K. H., Johnson, K. S., Fitzwater, S. E., Gordon, R. M., Tanner, S. J., Hunter, C. N., Elrod, V.
19 A., Nowicki, J. L., Coley, T. L., Barber, R. T., Lindley, S., Watson, A. J., Van Scoy, K., Law, C. S., Liddicoat, M. I., Ling,
20 R., Stanton, T., Stockel, J., Collins, C., Anderson, A., Bidigare, R., Ondrusek, M., Latasa, M., Millero, F. J., Lee, K., Yao,
21 W., Zhang, J. Z., Friederich, G., Sakamoto, C., Chavez, F., Buck, K., Kolber, Z., Greene, R., Falkowski, P., Chisholm, S.
22 W., Hoge, F., Swift, R., Yungel, J., Turner, S., Nightingale, P., Hatton, A., Liss, P., and Tindale, N. W.: Testing the Iron
23 Hypothesis in Ecosystems of the Equatorial Pacific Ocean, *Nature*, 371, 123-129, 10.1038/371123a0, 1994.

24 Measures, C. I., Brown, M. T., Selph, K. E., Apprill, A., Zhou, M., Hatta, M., and Hiscock, W. T.: The influence of
25 shelf processes in delivering dissolved iron to the HNLC waters of the Drake Passage, Antarctica, *Deep Sea Research Part*
26 *II: Topical Studies in Oceanography*, 90, 77-88, 10.1016/j.dsr2.2012.11.004, 2013.

27 Melling, H., and Moore, R. M.: Modification of halocline source waters during freezing on the Beaufort Sea shelf:
28 Evidence from oxygen isotopes and dissolved nutrients, *Continental Shelf Research*, 15, 89-113, 1995.

29 Menzel Barraqueta, J. L., Schlosser, C., Planquette, H., Gourain, A., Cheize, M., Boutorh, J., Shelley, R. U., Pereira
30 Contreira, L., Gledhill, M., Hopwood, M. J., Lherminier, P., Sarthou, G., and Achterberg, E. P.: Aluminium in the North
31 Atlantic Ocean and the Labrador Sea (GEOTRACES GA01 section): roles of continental inputs and biogenic particle
32 removal, *Biogeosciences Discussions*, 1-28, 10.5194/bg-2018-39, 2018.

33 Mercier, H., Lherminier, P., Sarafanov, A., Gaillard, F., Daniault, N., Desbruyères, D., Falina, A., Ferron, B.,
34 Gourcuff, C., Huck, T., and Thierry, V.: Variability of the meridional overturning circulation at the Greenland–Portugal
35 OVIDE section from 1993 to 2010, *Progress in Oceanography*, 132, 250-261, 10.1016/j.pocean.2013.11.001, 2015.

1 Mil-Homens, M., Branco, V., Lopes, C., Vale, C., Abrantes, F., Boer, W., and Vicente, M.: Using factor analysis to
2 characterise historical trends of trace metal contamination in a sediment core from the Tagus Prodelta, Portugal, *Water, Air,
3 and Soil Pollution*, 197, 277-287, 2009.

4 Moore, C. M., Mills, M. M., Langlois, R., Milne, A., Achterberg, E. P., La Roche, J., and Geider, R. J.: Relative
5 influence of nitrogen and phosphorus availability on phytoplankton physiology and productivity in the oligotrophic sub-
6 tropical North Atlantic Ocean, *Limnology and Oceanography*, 53, 291-205, 2008.

7 Moore, C. M., Mills, M. M., Arrigo, K. R., Berman-Frank, I., Bopp, L., Boyd, P. W., Galbraith, E. D., Geider, R. J.,
8 Guieu, C., Jaccard, S. L., Jickells, T. D., La Roche, J., Lenton, T. M., Mahowald, N. M., Marañón, E., Marinov, I., Moore, J.
9 K., Nakatsuka, T., Oschlies, A., Saito, M. A., Thingstad, T. F., Tsuda, A., and Ulloa, O.: Processes and patterns of oceanic
10 nutrient limitation, *Nature Geoscience*, 6, 701-710, 10.1038/ngeo1765, 2013.

11 Moore, G. W. K.: Gale force winds over the Irminger Sea to the east of Cape Farewell, Greenland, *Geophysical
12 Research Letters*, 30, n/a-n/a, 10.1029/2003gl018012, 2003.

13 Nielsdóttir, M. C., Moore, C. M., Sanders, R., Hinz, D. J., and Achterberg, E. P.: Iron limitation of the postbloom
14 phytoplankton communities in the Iceland Basin, *Global Biogeochemical Cycles*, 23, n/a-n/a, 10.1029/2008gb003410, 2009.

15 Olafsson, J., Thors, K., and Cann, J. R.: A sudden cruise off Iceland, *RIDGE Events*, 2, 35-28, 1991.

16 Oschlies, A.: Nutrient supply to the surface waters of the North Atlantic: A model study, *Journal of Geophysical
17 Research*, 107, 10.1029/2000jc000275, 2002.

18 Painter, S. C., Henson, S. A., Forryan, A., Steigenberger, S., Klar, J., Stinchcombe, M. C., Rogan, N., Baker, A. R.,
19 Achterberg, E. P., and Moore, C. M.: An assessment of the vertical diffusive flux of iron and other nutrients to the surface
20 waters of the subpolar North Atlantic Ocean, *Biogeosciences*, 11, 2113-2130, 10.5194/bg-11-2113-2014, 2014.

21 Palmer, M. R., Ludford, E. M., German, C. R., and Lilley, M. D.: Dissolved methane and hydrogen in the
22 Steinahóll hydrothermal plume, 63°N, Reykjanes Ridge, in: *Hydrothermal Vents and Processes*, edited by: Parson, L. M.,
23 Walker, C. L., and Dixon, D. R., Special Publications, Geological Society, London, 111-120, 1995.

24 Parekh, P., Follows, M. J., and Boyle, E. A.: Decoupling of iron and phosphate in the global ocean, *Global
25 Biogeochemical Cycle*, 19, 2005.

26 Parra, M., Delmont, P., Ferragne, A., Latouche, C., Pons, J. C., and Puechmaille, C.: Origin and evolution of
27 smectites in recent marine sediments of the NE Atlantic, *Clay Minerals*, 20, 335-346, 1985.

28 Pérez, F. F., Mercier, H., Vázquez-Rodríguez, M., Lherminier, P., Velo, A., Pardo, P. C., Rosón, G., and Ríos, A.
29 F.: Atlantic Ocean CO₂ uptake reduced by weakening of the meridional overturning circulation, *Nature Geoscience*, 6, 146-
30 152, 10.1038/ngeo1680, 2013.

31 Pérez, F. F., Treguer, P., Branellec, P., García-Ibáñez, M. I., Lherminier, P., and Sarthou, G.: The 2014 Greenland-
32 Portugal GEOVIDE bottle data (GO-SHIP A25 and GEOTRACES GA01). SEANOE (Ed.), 2018.

33 Petrich, C., and Eicken, H.: Growth, structure and properties of sea ice, in: *Sea Ice*. 2nd ed., edited by: Thomas, D.
34 N., and Dieckmann, G. S., Wiley-Blackwell, Oxford, U.K., 23-77, 2010.

35 Pickart, R. S., Straneo, F., and Moore, G. W. K.: Is Labrador Sea Water formed in the Irminger basin?, *Deep Sea
36 Research Part I*, 50, 23-52, 2003.

1 Piron, A., Thierry, V., Mercier, H., and Caniaux, G.: Argo float observations of basin-scale deep convection in the
2 Irminger sea during winter 2011–2012, *Deep Sea Research Part I: Oceanographic Research Papers*, 109, 76-90,
3 10.1016/j.dsr.2015.12.012, 2016.

4 Radic, A., Lacan, F., and Murray, J. W.: Iron isotopes in the seawater of the equatorial Pacific Ocean: New
5 constraints for the oceanic iron cycle, *Earth and Planetary Science Letters*, 306, 1-10, 10.1016/j.epsl.2011.03.015, 2011.

6 Ras, J., Claustre, H., and Uitz, J.: Spatial variability of phytoplankton pigment distribution in the Subtropical South
7 Pacific Ocean: comparison between *in situ* and predicted data, *Biogeosciences*, 5, 353-369, 2008.

8 Riebesell, U., Schloss, I., and Smetacek, V.: Aggregation of algae released from melting sea ice: implications for
9 seeding and sedimentation, *Polar Biology*, 11, 239-248, 1991.

10 Rijkenberg, M. J., Middag, R., Laan, P., Gerringa, L. J., van Aken, H. M., Schoemann, V., de Jong, J. T., and de
11 Baar, H. J.: The distribution of dissolved iron in the West Atlantic Ocean, *PLoS One*, 9, e101323,
12 10.1371/journal.pone.0101323, 2014.

13 Sabine, C. L., Feely, R. A., Gruber, N., Key, R. M., Lee, K., Bullister, J. L., Wanninkhof, R., Wong, C. S., Wallace,
14 D. W. R., Tilbrook, B., Millero, F. J., Peng, T.-H., Kozyr, A., Ono, T., and Rios, A. F.: The Oceanic sink for anthropogenic
15 CO₂, *Science*, 305, 367-371, 2004.

16 Sanders, R., Brown, L., Henson, S., and Lucas, M.: New production in the Irminger Basin during 2002, *Journal of*
17 *Marine Systems*, 55, 291-310, [http:// dx.doi.org/10.1016/j.jmarsys.2004.09.002](http://dx.doi.org/10.1016/j.jmarsys.2004.09.002), 2005.

18 Santos-Echeandia, J., Vale, C., Caetano, M., Pereira, P., and Prego, R.: Effect of tidal flooding on metal distribution
19 in pore waters of marsh sediments and its transport to water column (Tagus estuary, Portugal), *Mar Environ Res*, 70, 358-
20 367, 10.1016/j.marenvres.2010.07.003, 2010.

21 Sarthou, G., and Jeandel, C.: Seasonal variations of iron concentrations in the Ligurian Sea and iron budget in the
22 Western Mediterranean Sea, *Marine Chemistry*, 74, 115-129, 10.1016/s0304-4203(00)00119-5, 2001.

23 Sarthou, G., Baker, A. R., Kramer, J., Laan, P., Laës, A., Ussher, S., Achterberg, E. P., de Baar, H. J. W.,
24 Timmermans, K. R., and Blain, S.: Influence of atmospheric inputs on the iron distribution in the subtropical North-East
25 Atlantic Ocean, *Marine Chemistry*, 104, 186-202, 10.1016/j.marchem.2006.11.004, 2007.

26 Sarthou, G., Vincent, D., Christaki, U., Obermosterer, I., Timmermans, K. R., and Brussaard, C. P. D.: The fate of
27 biogenic iron during a phytoplankton bloom induced by natural fertilisation: Impact of copepod grazing, *Deep Sea Research*
28 *Part II: Topical Studies in Oceanography*, 55, 734-751, 10.1016/j.dsr2.2007.12.033, 2008.

29 Sarthou, G., Lherminier, P., Achterberg, E. P., Alonso-Pérez, F., Bucciarelli, E., Boutorh, J., Bouvier, V., Boyle, E.
30 A., Branellec, P., Carracedo, L. I., Casacuberta, N., Castrillejo, M., Cheize, M., Contreira Pereira, L., Cossa, D., Danialt,
31 N., De Saint-Léger, E., Dehairs, F., Deng, F., Desprez de Gésincourt, F., Devesa, J., Foliot, L., Fonseca-Batista, D.,
32 Gallinari, M., García-Ibáñez, M. I., Gourain, A., Grossteffan, E., Hamon, M., Heimbürger, L. E., Henderson, G. M., Jeandel,
33 C., Kermabon, C., Lacan, F., Le Bot, P., Le Goff, M., Le Roy, E., Lefèbvre, A., Leizour, S., Lemaitre, N., Masqué, P.,
34 Ménage, O., Menzel Barraqueta, J.-L., Mercier, H., Perault, F., Pérez, F. F., Planquette, H. F., Planchon, F., Roukaerts, A.,
35 Sanial, V., Sauzède, R., Shelley, R. U., Stewart, G., Sutton, J. N., Tang, Y., Tisnérat-Laborde, N., Tonnard, M., Tréguer, P.,
36 van Beek, P., Zurbrick, C. M., and Zunino, P.: Introduction to the French GEOTRACES North Atlantic Transect (GA01):
37 GEOVIDE cruise, *Biogeosciences Discussions*, 1-24, 10.5194/bg-2018-312, 2018.

38 Ocean Data View, <https://odv.awi.de> ODV4, version 4.7.6 (23 March 2016), access: 6 April, 2016.

1 Schroth, A. W., Crusius, J., Hoyer, I., and Campbell, R.: Estuarine removal of glacial iron and implications for iron
2 fluxes to the ocean, *Geophysical Research Letters*, 41, 3951-3958, 10.1002/2014GL060199, 2014.

3 Shelley, R. U., Morton, P. L., and Landing, W. M.: Elemental ratios and enrichment factors in aerosols from the
4 US-GEOTRACES North Atlantic transects, *Deep Sea Research*, 116, 262-272, 2015.

5 Shelley, R. U., Roca-Martí, M., Castrillejo, M., Sanial, V., Masqué, P., Landing, W. M., van Beek, P., Planquette,
6 H., and Sarthou, G.: Quantification of trace element atmospheric deposition fluxes to the Atlantic Ocean (>40°N;
7 GEOVIDE, GEOTRACES GA01) during spring 2014, *Deep Sea Research Part I: Oceanographic Research Papers*, 119, 34-
8 49, 10.1016/j.dsr.2016.11.010, 2017.

9 Shelley, R. U., Landing, W. M., Ussher, S. J., Planquette, H., and Sarthou, G.: Characterisation of aerosol
10 provenance from the fractional solubility of Fe (Al, Ti, Mn, Co, Ni, Cu, Zn, Cd and Pb) in North Atlantic aerosols
11 (GEOTRACES cruises GA01 and GA03) using a two stage leach, *Biogeosciences*, 2018.

12 Shor, A., Lonsdale, P., Hollister, D., and Spencer, D.: Charlie-Gibbs fracture zone: bottom-water transport and its
13 geological effects, *Deep Sea Research*, 27A, 325-345, 1980.

14 Sinha, M. C., Navin, D. A., MacGregor, L. M., Constable, S., Peirce, C., White, A., Heinson, G., and Inglis, M. A.:
15 Evidence for accumulated melt beneath the slow-spreading Mid-Atlantic Ridge, *Philosophical Transactions of the Royal
16 Society A*, 355, 233-253, 1997.

17 Slagter, H. A., Reader, H. E., Rijkenberg, M. J. A., Rutgers van der Loeff, M., de Baar, H. J. W., and Gerringa, L. J.
18 A.: Organic Fe speciation in the Eurasian Basins of the Arctic Ocean and its relation to terrestrial DOM, *Marine Chemistry*,
19 197, 11-25, 10.1016/j.marchem.2017.10.005, 2017.

20 Smallwood, J. R., and White, R. S.: Crustal accretion at the Reykjanes Ridge, 61°-62°N, *Journal of Geophysical
21 Research: Solid Earth*, 103, 5185-5201, 10.1029/97jb03387, 1998.

22 Statham, P. J., Skidmore, M., and Tranter, M.: Inputs of glacially derived dissolved and colloidal iron to the coastal
23 ocean and implications for primary productivity, *Global Biogeochemical Cycles*, 22, 1-11, 10.1029/2007GB003106, 2008.

24 Sunda, W. G., and Huntsman, S. A.: Iron uptake and growth limitation in oceanic and coastal phytoplankton,
25 *Marine Chemistry*, 50, 189-206, 10.1016/0304-4203(95)00035-p, 1995.

26 Sutherland, D. A., Pickart, R. S., Peter Jones, E., Azetsu-Scott, K., Jane Eert, A., and Ólafsson, J.: Freshwater
27 composition of the waters off southeast Greenland and their link to the Arctic Ocean, *Journal of Geophysical Research*, 114,
28 10.1029/2008jc004808, 2009.

29 Tanhua, T., Olsson, K. A., and Jeansson, E.: Formation of Denmark Strait overflow water and its hydro-chemical
30 composition, *Journal of Marine Systems*, 57, 264-288, 10.1016/j.jmarsys.2005.05.003, 2005.

31 Teng, Z., Huang, J. Y., Fujito, K., and Takizawa, S.: Manganese removal by hollow fiber micro-filter.Membrane
32 separation for drinking water, *European Conference on Desalination and the Environment*, Amsterdam, 28 May, 2001.

33 Thuróczy, C. E., Gerringa, L. J. A., Klunder, M. B., Middag, R., Laan, P., Timmermans, K. R., and de Baar, H. J.
34 W.: Speciation of Fe in the Eastern North Atlantic Ocean, *Deep Sea Research Part I: Oceanographic Research Papers*, 57,
35 1444-1453, 10.1016/j.dsr.2010.08.004, 2010.

1 Tonnard, M., Donval, A., Lampert, L., Tréguer, P., Bowie, A. R., van der Merwe, P., planquette, H., Claustre, H.,
2 Dimier, C., Ras, J., and Sarthou, G.: Phytoplankton assemblages in the North Atlantic Ocean and in the Labrador Sea along
3 the GEOVIDE section (GEOTRACES section GA01) determined by CHEMTAX analysis from HPLC pigment data,
4 *Biogeosciences*, in prep.

5 Tovar-Sanchez, A., Duarte, C. M., Alonso, J. C., Lacorte, S., Tauler, R., and Galban-Malagon, C.: Impacts of
6 metals and nutrients released from melting multiyear Arctic sea ice, *Journal of Geophysical Research-Oceans*, 115,
7 10.1029/2009jc005685, 2010.

8 Tréguer, P. J., and De La Rocha, C. L.: The world ocean silica cycle, *Ann Rev Mar Sci*, 5, 477-501,
9 10.1146/annurev-marine-121211-172346, 2013.

10 Twining, B. S., Baines, S. B., Fisher, N. S., and Landry, M. R.: Cellular iron contents of plankton during the
11 Southern Ocean Iron Experiment (SOFeX), *Deep Sea Research Part I: Oceanographic Research Papers*, 51, 1827-1850,
12 10.1016/j.dsr.2004.08.007, 2004.

13 Van Beusekom, J. E. E.: Distribution of aluminium in surface waters of the North Sea: influence of suspended
14 matter., in: *Biogeochemistry and Distribution of Suspended Matter in the North Sea and Implications to fisheries Biology*,
15 edited by: Kempe, S., *Mitteilungen aus dem Geologisch-Paläontologischen Institut der Universität Hamburg*,
16 SCOPE/UNEP Sonderband, 117-136, 1988.

17 von Appen, W.-J., Koszalka, I. M., Pickart, R. S., Haine, T. W. N., Mastropole, D., Magaldi, M. G., Valdimarsson,
18 H., Giron, J., Jochumsen, K., and Krahnmann, G.: The East Greenland Spill Jet as an important component of the Atlantic
19 Meridional Overturning Circulation, *Deep Sea Research Part I: Oceanographic Research Papers*, 92, 75-84,
20 10.1016/j.dsr.2014.06.002, 2014.

21 Wadhams, P.: *Ice in the Ocean*, Gordon and Breach Science Publishers, London, UK, 2000.

22 Wagener, T., Guieu, C., and Leblond, N.: Effects of dust deposition on iron cycle in the surface Mediterranean Sea:
23 results from a mesocosm seeding experiment, *Biogeosciences Discussions*, 7, 2799-2830, 2010.

24 Woodgate, R. A., and Aagaard, K.: Revising the Bering Strait freshwater flux into the Arctic Ocean, *Geophysical*
25 *Research Letters*, 32, 10.1029/2004GL021747., 2005.

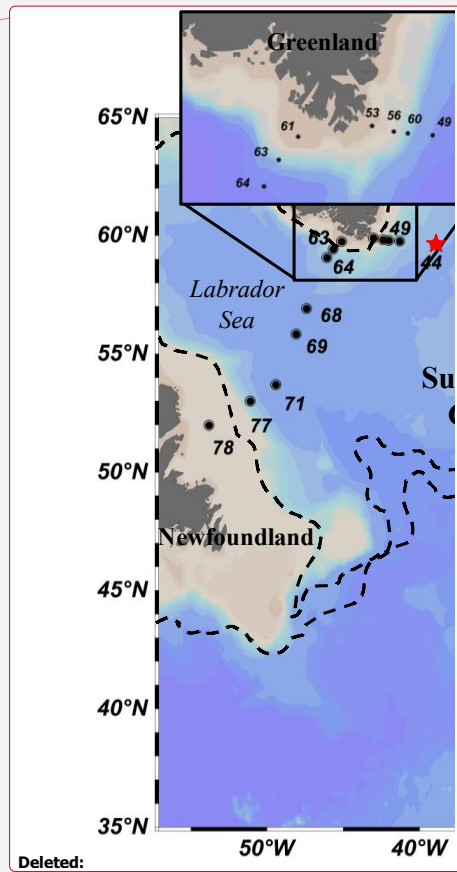
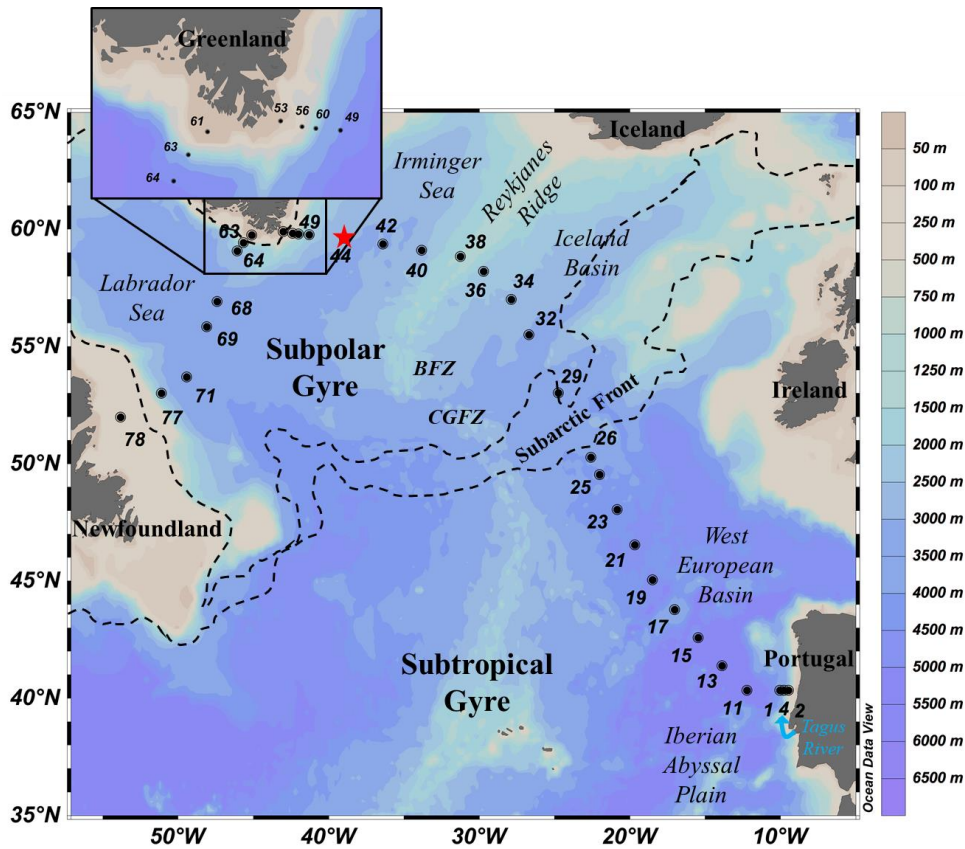
26 Wuttig, K., Wagener, T., Bressac, M., Dammshäuser, A., Streu, P., Guieu, C., and Croot, P. L.: Impacts of dust
27 deposition on dissolved trace metal concentrations (Mn, Al and Fe) during a mesocosm experiment, *Biogeosciences*, 10,
28 2583-2600, 10.5194/bg-10-2583-2013, 2013.

29 Zou, S., Lozier, S., Zenk, W., Bower, A., and Johns, W.: Observed and modeled pathways of the Iceland Scotland
30 Overflow Water in the eastern North Atlantic, *Progress in Oceanography*, 159, 211-222, 10.1016/j.pocean.2017.10.003,
31 2017.

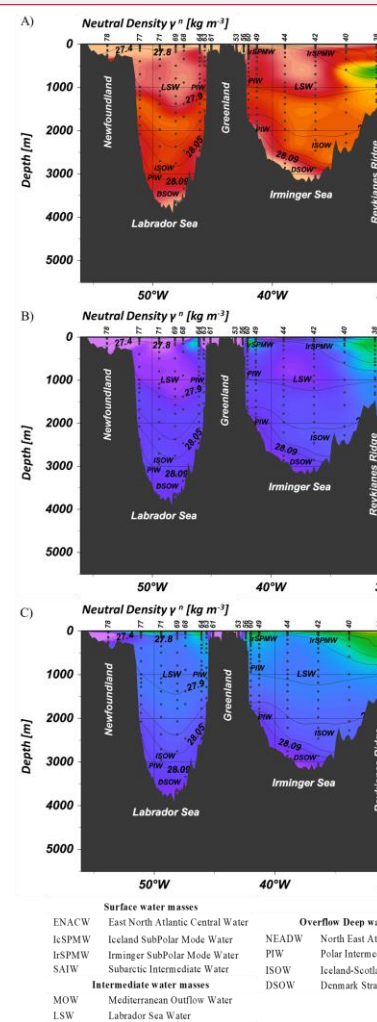
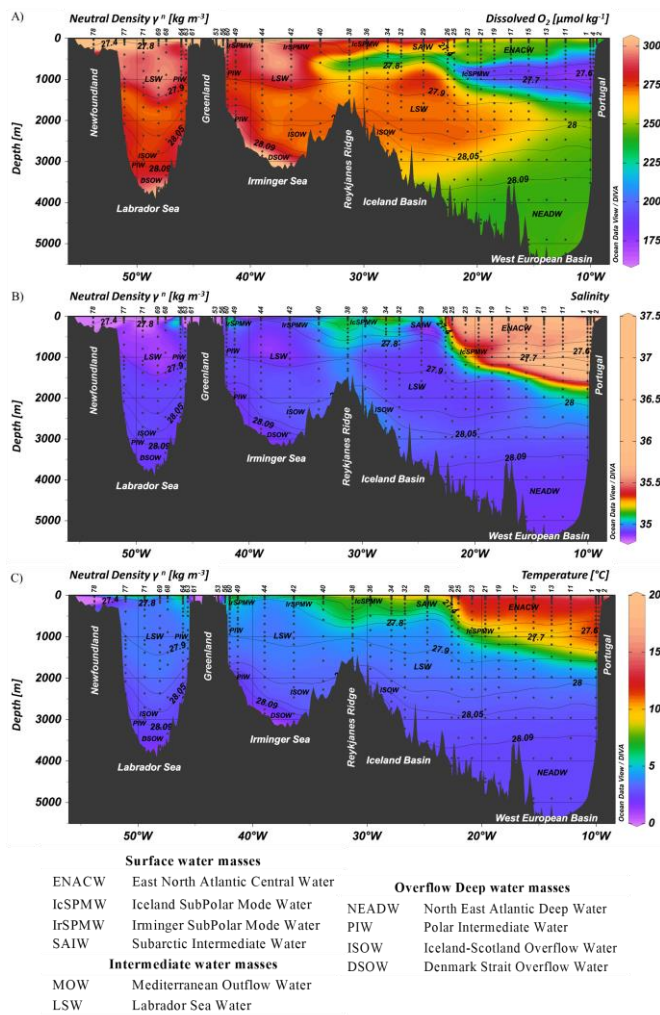
32 Zunino, P., Lherminier, P., Mercier, H., Danialt, N., García-Ibáñez, M. I., and Pérez, F. F.: The GEOVIDE cruise
33 in may-June 2014 revealed an intense MOC over a cold and fresh subpolar North Atlantic, *Biogeosciences*, 2017.

34
35

1 Figure 1: Map of the GEOTRACES GA01 voyage plotted on bathymetry as well as the major topographical features and main
 2 basins. Crossover station with GEOTRACES voyage (GA03) is shown as a red star. (Ocean Data View (ODV) software, version
 3 4.7.6, R. Schlitzer, <http://odv.awi.de>, 2016). **BFZ: Bight Fracture Zone**, **CGFZ: Charlie-Gibbs Fracture Zone**.

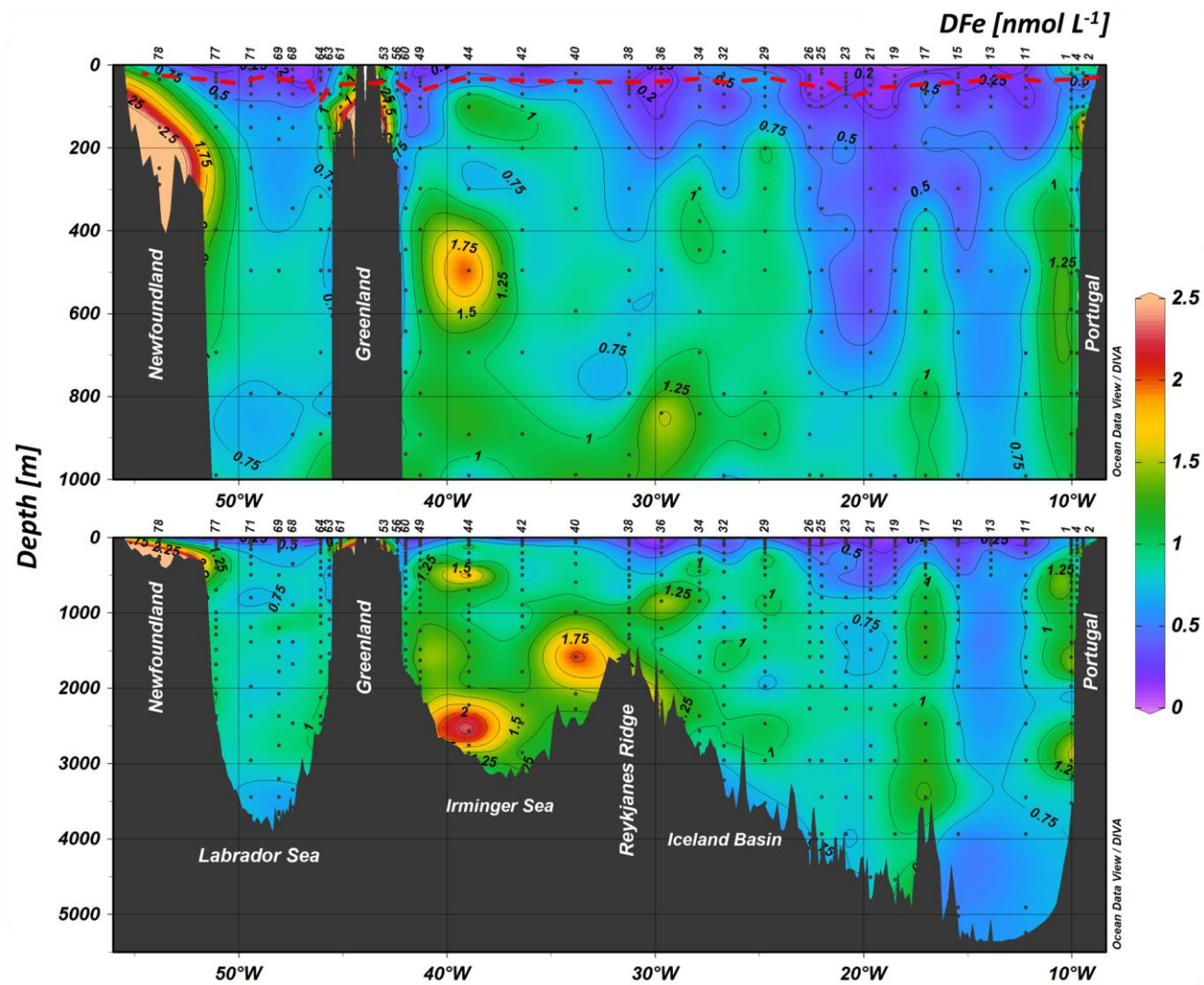


1 Figure 2: Parameters measured from the regular CTD cast represented as a function of depth for GA01 section for (A) Dissolved
 2 Oxygen (O_2 , $\mu\text{mol kg}^{-3}$), (B) Salinity and (C) Temperature ($^{\circ}\text{C}$). The contour lines represent isopycnals (neutral density, γ^n , in units
 3 of kg m^{-3}).



Deleted:

Figure 3: Contour plot of the distribution of dissolved iron (DFe) concentrations in nmol L^{-1} along the GA01 voyage transect: upper 1000 m (top) and full depth range (bottom). The red dashed line indicates the depth of the Surface Mixed Layer (SML). Small black dots represent collected water samples at each sampling station. (Ocean Data View (ODV) software, version 4.7.6, R. Schlitzer, <http://odv.awi.de>, 2016).



Deleted: Figure 3: Contour plot of the distribution of dissolved iron (DFe) concentrations in nmol L^{-1} along the GA01 voyage transect: upper 1000 m (top) and full depth range (bottom). The red dashed line indicates the depth of the Surface Mixed Layer (SML). Small black dots represent collected water samples at each sampling station. (Ocean Data View (ODV) software, version 4.7.6, R. Schlitzer, <http://odv.awi.de>, 2016).

Depth [m]

0

50

100

150

200

250

Deleted: 4

Figure 4: Vertical profiles of dissolved iron (DFe, black dots, solid line), particulate iron (PFe, black open dots, dashed line, Gourain et al., in prep.) and dissolved aluminium (DAI, grey dots, Menzel Barraqueta et al., 2018) at Stations 2 (A), and 4 (B) located above the Iberian shelf, Station 56 (C), Stations 53 (D) 53 and Station 61 (E) located above the Greenland shelf and Station 78 (F) located above the Newfoundland shelf. Note that for stations 53, 61 and 78, plots of the percentage of meteoric water (open dots and dashed line) (Benetti et al., see text for details), Total Chlorophyll-*a* (TChl-*a*, green), temperature (blue) and salinity (black) are also displayed as a function of depth.

Deleted: 5

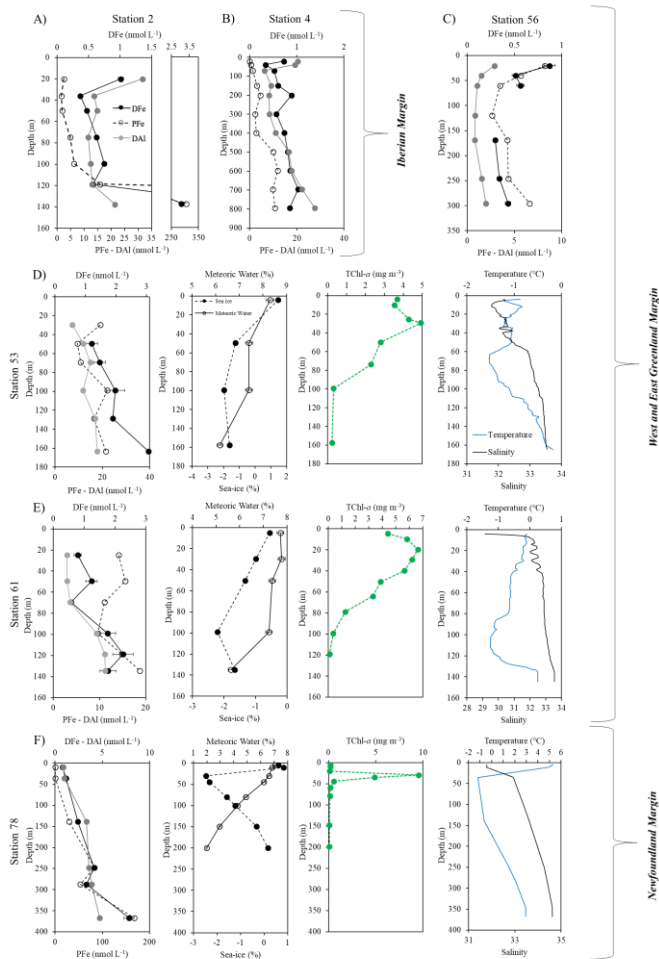
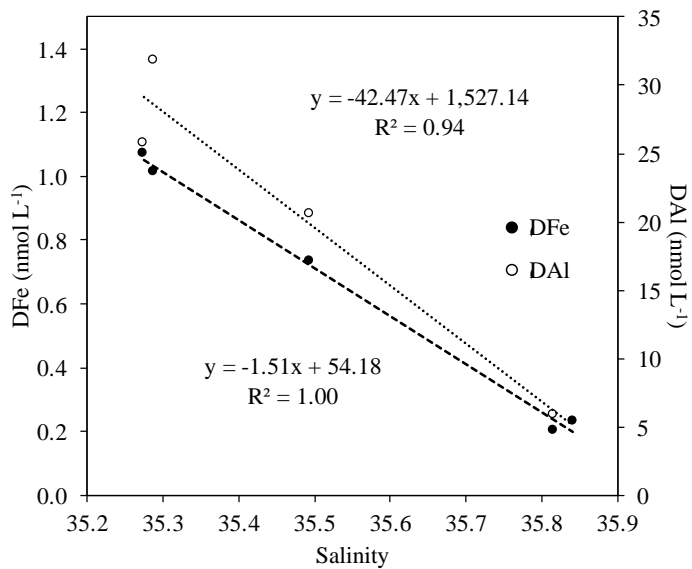
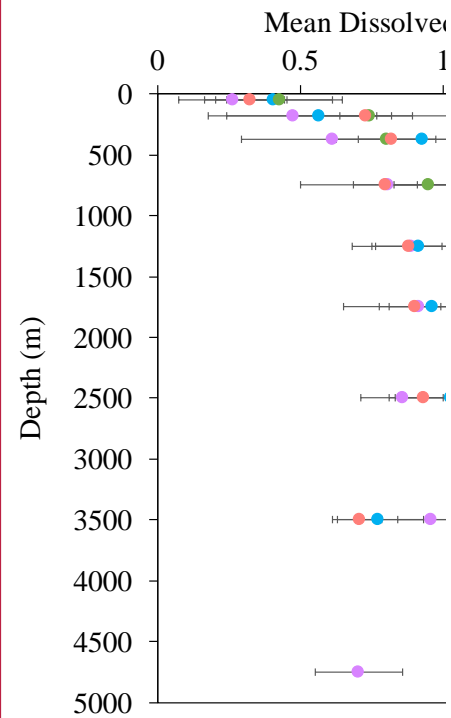


Figure 5: Plot of dissolved iron (DFe, black circles) and dissolved aluminium (DAL, white circles, Menzel Barraqueta et al., 2018) along the salinity gradient between stations 1, 2, 4, 11 and 13 with linear regression equations. Numbers close to sample points representing station numbers.



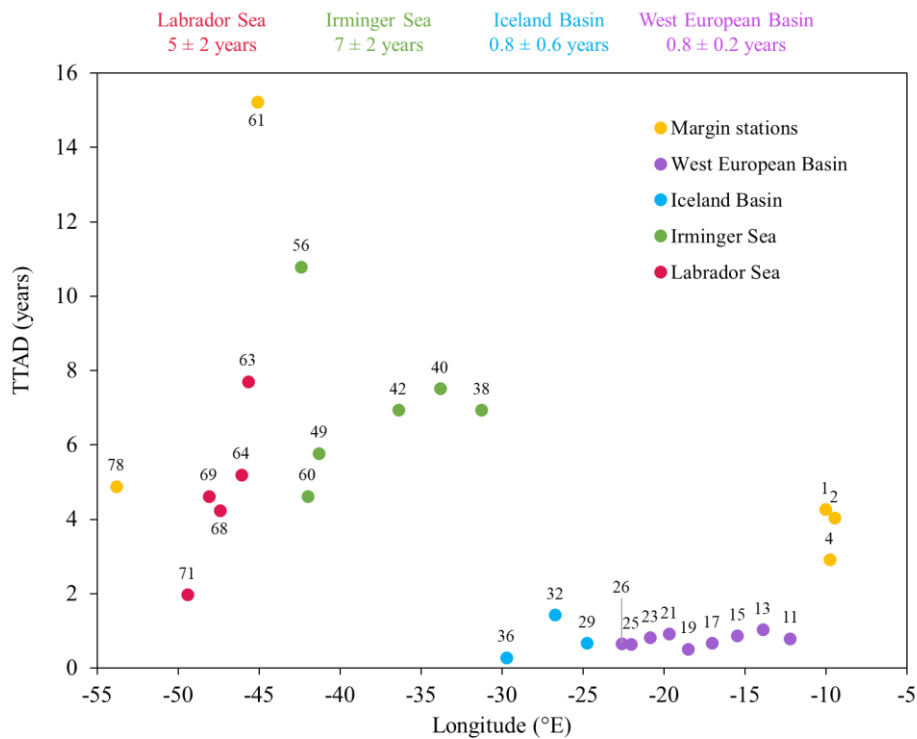
5

Deleted: Figure 6: Mean profiles of dissolved iron (Fe) along the North Atlantic section in the West European Basin (purple), Iceland Basin (blue), Irminger Sea (green) and Labrador Sea (red) over the depth intervals: 0-100 m, 100-250 m, 250-500 m, 500-1000 m, 1000-1500 m, 1500-2000 m, 2000-3000 m, 3000-4000 m, 4000-5500 m without considering stations located above the continental plateau.¶



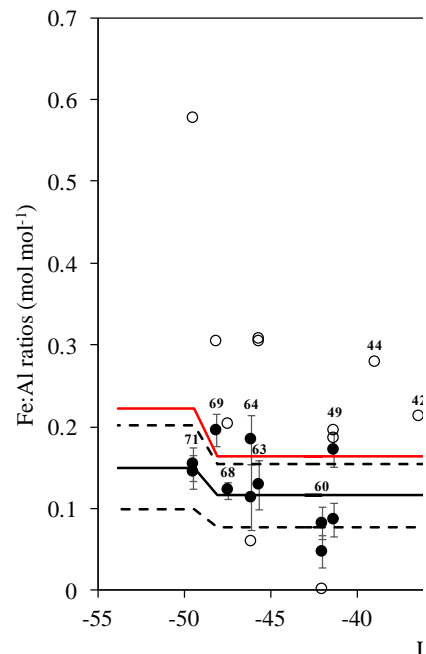
Deleted: 9

Figure 6: Plot of dissolved Fe (DFe) Turnover Times relative to Atmospheric Deposition (TTADs) calculated from soluble Fe contained in aerosols estimated from a two-stage sequential leach (UHP water, then 25% HAc, Shelley et al., this issue). Note that numbers on top of points represent station numbers and that the colour coding refers to different region with in yellow, margin stations; in purple, the West European Basin; in blue, the Iceland Basin; in green, the Irminger Sea and in red, the Labrador Sea. The numbers on top of the plot represent TTADs averaged for each oceanic basin and their standard deviation.



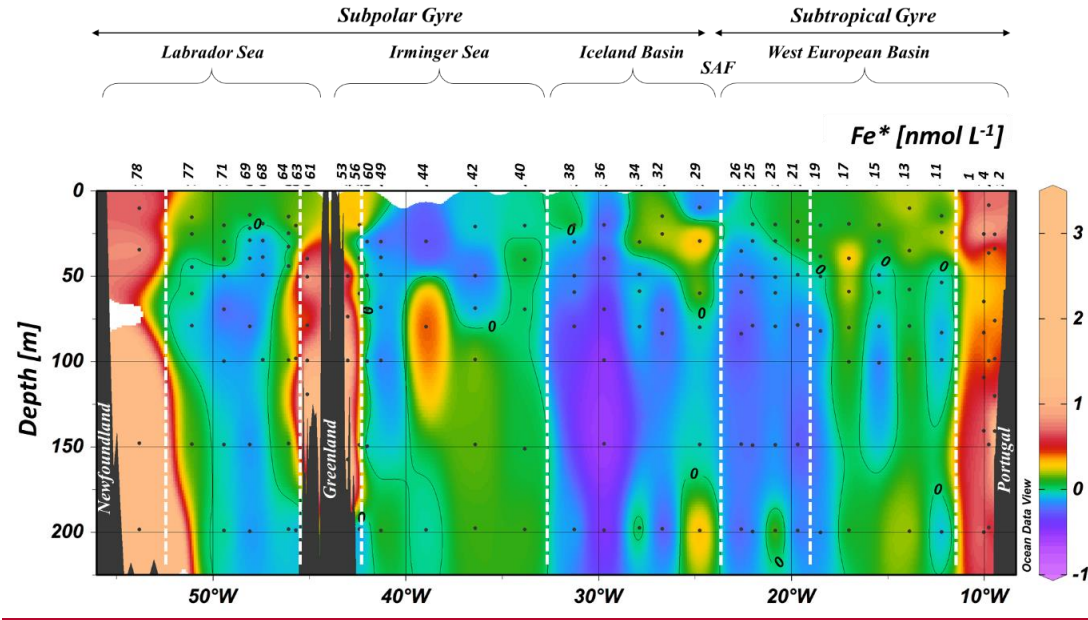
Deleted: 10

Deleted: Graph of iron:aluminium (Fe:Al) ratios for: dissolved (DFe:DAI, black dots, Menzel Barraqueta et al., 2018), particulate (PFe:PAI, open dots, Gourain et al., in prep.), total aerosol (Fe:Al aerosols total, red continuous line) and soluble aerosol (Fe:Al aerosols soluble, black continuous line and dashed lines as standard deviation (SD) estimated from a two-stage sequential leach (UHP water, then 25% HAc, Shelley et al., this issue). Note that for total and soluble aerosols the Fe:Al ratios are averages per section of transect grouped by aerosol source region (Europe, N. America, High latitude, Marine; Shelley et al., this issue). Note that numbers on top of points represent station numbers. ¶



Page Break

Figure 7: Section plot of the Fe* tracer in the North Atlantic Ocean with a remineralization rate ($R_{Fe:N}$) of $0.05 \text{ mmol mol}^{-1}$ from surface to 225 m depth. A contour line of 0 separates areas of negative Fe* from areas with positive Fe*. Positive values of Fe* imply there is enough iron to support complete consumption of NO_3^- when this water is brought to surface, and negative Fe* values imply a deficit. See text for details.



Formatted: Ca

Deleted: Figure 7: Section plot of the Fe* tracer in the North Atlantic Ocean with a remineralization rate ($R_{Fe:N}$) of $0.05 \text{ mmol mol}^{-1}$ from surface to 225 m depth. A contour line of 0 separates areas of negative Fe* from areas with positive Fe*. Positive values of Fe* imply there is enough iron to support complete consumption of NO_3^- when this water is brought to surface, and negative Fe* values imply a deficit. See text for details.

Principal Component Analysis (PCA) of the following variables: dissolved aluminum, particulate iron, MnO_2 , Gourain. The figure presented a transect from 50°W to 10°W at a depth of 0 to 200 m. The color scale corresponds to the Fe* concentration in nmol L⁻¹. The whole water mass is shown in grey (DSOW), the ENACW in yellow, the IrSPMW in blue, the Labrador Sea Water in green, the Mediterranean Sea Water in red, and the East Atlantic Deep Water in black. The multiple water masses (DFe) are plotted as a function of the first dimension of the PCA. The depth is represented in meters as a function of the second dimension of the PCA (PFe:MnO₂, mol).

Station	Date sampling DD/MM/YYYY	filtration μm	Latitude $^{\circ}\text{N}$	Longitude $^{\circ}\text{E}$	Z_m m	DFe (nmol L ⁻¹)		
						average	SD	n
1	19/05/2014	0.2	40.33	-10.04	25.8	1.07	± 0.12	1
2	21/05/2014	0.2	40.33	-9.46	22.5	1.01	± 0.04	1
4	21/05/2014	0.2	40.33	-9.77	24.2	0.73	± 0.03	1
11	23/05/2014	0.2	40.33	-12.22	31.3	0.20	± 0.11	2
13	24/05/2014	0.45	41.38	-13.89	18.8	0.23	± 0.02	1
15	28/05/2014	0.2	42.58	-15.46	34.2	0.22	± 0.03	2
17	29/05/2014	0.2	43.78	-17.03	36.2	0.17	± 0.01	1
19*	30/05/2014	0.45	45.05	-18.51	44.0	0.13	± 0.05	2
21	31/05/2014	0.2	46.54	-19.67	47.4	0.23	± 0.08	2
23*	02/06/2014	0.2	48.04	-20.85	69.5	0.21	± 0.05	6
25	03/06/2014	0.2	49.53	-22.02	34.3	0.17	± 0.04	2
26	04/06/2014	0.45	50.28	-22.60	43.8	0.17	± 0.03	2
29	06/06/2014	0.45	53.02	-24.75	23.8	0.17	± 0.02	1
32	07/06/2014	0.2	55.51	-26.71	34.8	0.59	± 0.08	2
34	09/06/2014	0.45	57.00	-27.88	25.6	NA	±	0
36	10/06/2014	0.45	58.21	-29.72	33.0	0.12	± 0.02	1
38	10/06/2014	0.45	58.84	-31.27	34.5	0.36	± 0.16	2
40	12/06/2014	0.45	59.10	-33.83	34.3	0.39	± 0.05	1
42	12/06/2014	0.45	59.36	-36.40	29.6	0.36	± 0.05	1
44	13/06/2014	0.2	59.62	-38.95	25.8	NA	±	0
49	15/06/2014	0.45	59.77	-41.30	60.3	0.30	± 0.05	2
53*	17/06/2014	0.45	59.90	-43.00	36.4	NA	±	0
56*	17/06/2014	0.45	59.82	-42.40	30.0	0.87	± 0.06	1
60*	17/06/2014	0.45	59.80	-42.00	36.6	0.24	± 0.02	2
61*	19/06/2014	0.45	59.75	-45.11	39.8	0.79	± 0.12	1
63*	19/06/2014	0.45	59.43	-45.67	86.7	0.40	± 0.03	1
64	20/06/2014	0.45	59.07	-46.09	33.9	0.27	± 0.06	2
68*	21/06/2014	0.45	56.91	-47.42	26.3	0.22	± 0.01	1
69*	22/06/2014	0.45	55.84	-48.09	17.5	0.24	± 0.02	1
71	24/06/2014	0.45	53.69	-49.43	36.7	0.32	± 0.04	2
77*	26/06/2014	0.45	53.00	-51.10	26.1	NA	±	0
78	27/06/2014	0.45	51.99	-53.82	13.4	0.79	± 0.05	1

Table 1: Station number, date of sampling (in the DD/MM/YYYY format), size pore used for filtration (μm), station location, mixed layer depth (m) and associated average dissolved iron (DFe) concentrations, standard deviation and number of samples during the GEOTRACES GA01 transect. Note that the asterisk next to station numbers refers to disturbed temperature and salinity profiles as opposed to uniform profiles.

Deleted:

Seawater used for calibration	SeaFAST-pico™ DFe values (nmol L ⁻¹)			reference or certified DFe values (nmol L ⁻¹)		
	Average	SD	n	Average	SD	
SAFe S	0.100	± 0.006	2	0.095	± 0.008	
GSP	0.16	± 0.04	15	NA	± NA	
NASS-7	6.7	± 1.7	12	6.3	± 0.5	

60

Table 2: SAFe S, GSP and NASS-7 dissolved iron concentrations (DFe, nmol L⁻¹) determined by the SeaFAST-pico™ and their consensus (SAFe S, GSP; <https://websites.pmc.ucsc.edu/~kbruland/GeotracesSaFe/kwbGeotracesSaFe.html>) and certified (NASS-7; https://www.nrc-cnrc.gc.ca/eng/solutions/advisory/crm/certificates/nass_7.html) DFe concentrations. Note that yet no consensual value is reported for the GSP seawater.

Deleted: Area

Formatted Table

Margins	Stations #	DFe:DAI (mol:mol)		PFe:PAI (mol:mol)		DFe:PFe (mol:mol)		n
		average	SD	average	SD	average	SD	
<i>Iberian Margin</i>	2 and 4	0.07	± 0.03	0.20	± 0.01	<u>0.13</u>	± <u>0.09</u>	10
<i>East Greenland Margin</i>	56 and 53	0.21	± 0.09	0.30	± 0.01	<u>0.12</u>	± <u>0.03</u>	6
<i>West Greenland Margin</i>	61	0.18	± 0.02	0.32	± 0.01	<u>0.14</u>	± <u>0.04</u>	3
<i>Newfoundland Margin</i>	78	1.1	± 0.41	0.31	± 0.01	<u>0.06</u>	± <u>0.02</u>	4

Table 3: Averaged DFe:DAI (Menzel Barraqueta et al., 2018) and PFe:PAI (Gourain et al., in prep.) ratios reported per margins. Note that to avoid phytoplankton uptake, only depth below 100 m depth are considered.

Deleted: Area

Formatted Table

Deleted:

Deleted: ⁻¹

Deleted:

Formatted Table

Deleted: ⁻¹

Deleted: 4